

CAMPIMETRY WITH OFFSET STIMULUS AND DYNAMIC FIXATION

by

Erkan Mutlukan, B.Sc., M.D.

(Hacettepe Univ. 1984, 1986)

A Thesis

Submitted for the Degree of Ph.D.

to

The University of Glasgow

on the basis of research conducted within

The Tennent Institute of Ophthalmology

University of Glasgow

38 Church Street, Glasgow G11 6NT

Submitted August 1994 & January 1995

Copyright ©E. Mutlukan

ProQuest Number: 13815559

All rights reserved

INFORMATION TO ALL USERS

The quality of this reproduction is dependent upon the quality of the copy submitted.

In the unlikely event that the author did not send a complete manuscript and there are missing pages, these will be noted. Also, if material had to be removed, a note will indicate the deletion.



ProQuest 13815559

Published by ProQuest LLC (2018). Copyright of the Dissertation is held by the Author.

All rights reserved.

This work is protected against unauthorized copying under Title 17, United States Code
Microform Edition © ProQuest LLC.

ProQuest LLC.
789 East Eisenhower Parkway
P.O. Box 1346
Ann Arbor, MI 48106 – 1346

Ther
10163
C971

This work is dedicated to

JAMES FINBARR CULLEN

a great tutor, a true friend

ACKNOWLEDGEMENT

I would like thank my former and latter supervisors Dr Bertil E. Damato and Professor Colin M. Kirkness for giving me the opportunity to work for the University of Glasgow and to contribute, for their supervision, encouragement and review of my progress. My research was possible with the support and help of my supervisors and also Professor William R. Lee and I am grateful to all of them.

Financial support for my work was provided by The International Glaucoma Association, The Royal National Institute for the Blind, The Ross Foundation for Prevention of Blindness, McCunn Trust, The Royal Society of Medicine and the University of Glasgow. I am indebted for their generous assistance.

I have greatly benefited from the expertise of Mr James McGarvie and Dr Aled Evans of Department of Biophysics and Clinical Engineering, Glasgow Health Board, who performed the code writing and development of the software in collaboration. I am thankful for their contribution which made most of the research work possible.

Dr Gordon Dutton and Dr David Keating were always willing to discuss my problems and generously gave their time to guide me. I thank them very much. I would like to express my sincere gratitude to all junior and senior ophthalmologists, optometry and orthoptic staff of the Tennent Institute of Ophthalmology, neuro-ophthalmology unit of the Southern General Hospital and optometry clinic of the Caledonian University. They enabled this work by allowing me to enroll the subjects from their clinics and performing some of the conventional perimetry as part of routine patient care. I always had access to photographic and technical help, and I thank to the paramedical staff of the Tennent Institute for their compassionate assistance. I am also grateful to the patients and volunteers who graciously agreed to participate.

PUBLICATIONS

Mutlukan, E., Damato, B.E. The dark perimetric stimulus. *British Journal of Ophthalmology*, 1992, 76:264-267.

Mutlukan, E., Damato, B.E., Jay, J. Clinical evaluation of a multi-fixation campimeter for the detection of glaucomatous visual field loss. *British Journal of Ophthalmology*, 1993, 77:332-338.

Mutlukan, E., Damato, B.E., Tavadia, S.M. Clustering of fixation targets in multifixation campimetry. *Eye*, 1993, 7:131-133.

Mutlukan, E. Computer assisted perimetry with static dark and bright stimuli. *Documenta Ophthalmologica* 1993, 84: 335-350.

Mutlukan, E. Glaucomatous optic neuropathy causes sensitivity loss to light offsets in the visual field. *Neuro-Report* 1993, 4 (10): 1159-1162.

Mutlukan, E., Damato, B.E. Computerized perimetry with moving and steady fixation in children. *Eye* 1993, 7: 554-561.

Mutlukan, E., Damato, B.E. (1993). The visibility threshold for dark perimetric stimulus. In: Mills, R. (ed) *Perimetry Update, 92/93*, Kugler Publications, Amsterdam, New York, pp:345-351.

Mutlukan, E., Keating, D., Damato, B.E. (1993). A touch screen multi-stimulus video campimeter. In, Mills, R. (ed) *Perimetry Update, 92/93*, Kugler Publications, Amsterdam, New York, pp: 589-595.

Damato, B.E., Mutlukan, E., McGarvie, J., Johnston, S., Keating, D., Evans, A. (1993). Computer assisted moving eye campimetry. In: Mills, R. (ed) *Perimetry Update, 92/93*, Kugler Publications, Amsterdam, New York, pp: 315-318.

Mutlukan, E. Comparison of automated static dark stimuli with the Humphrey STATPAC in glaucomatous visual field loss. *British Journal of Ophthalmology* 1994, 78: 175-184.

Mutlukan, E. The effect of refractive blur on the detection sensitivity to light offsets in the central visual field. *Acta Ophthalmol.* 1994, 72: 189-194.

Mutlukan, E. Detection sensitivity to light offsets is abnormal in glaucomatous visual field. *Doc. Ophthalmol.* 1994, 87: 245-264.

Mutlukan, E. Eccentricity compensated dark on bright stimuli in screening for neuro-ophthalmic visual field loss (in press).

Mutlukan, E. Topographical reproducibility of small scotoma using computerised dynamic fixation (in press).

Mutlukan, E. Topographical distribution of glaucomatous visual field defects to light offsets (submitted).

ESSAYS

Mutlukan, E. Dark stimulus perimetry: testing of pathway in glaucoma. Mary Hawthorne research award essay in ophthalmology, Glasgow University, 1991.

PAPER PRESENTATIONS

Mutlukan E. Visual field loss to light offset stimuli in primary open angle glaucoma. XIth International Perimetric Society Meeting, Washington D.C., U.S.A., July 1994.

Mutlukan E. Detection thresholds to light offsets in the visual field. XXVIIth International Congress of Ophthalmology, Toronto, Canada, June 1994.

Mutlukan E. Automated perimetry with dark and bright stimulus. University of Edinburgh, Princess Alexandra Eye Pavilion, Edinburgh, September, 1992.

Mutlukan, E. Visual field examination with single and multiple dark on bright stimuli in glaucoma. Glaucoma Group of the United Kingdom and Ireland; XIIIth Annual Meeting, November 1992, London.

Mutlukan, E. Computerized off pathway testing: the dark stimulus in diagnosis of visual dysfunction. The Rank Prize Funds Symposium on Ophthalmological Image Processing; June 1992, Grasmere.

Mutlukan, E., Damato, B.E. Visibility threshold for dark perimetric stimulus. Xth International Perimetric Society Meeting. Kyoto, Japan; October, 1992.

Mutlukan, E., Keating, D., Damato, B.E. A touch screen multistimulus video campimeter. Xth International Perimetric Society Meeting. Kyoto, Japan; October, 1992.

Mutlukan, E., Damato, B.E., McFadzean, R., McGarvie, J., Evans, A. Computer assisted moving eye campimeter (C.A.M.E.C.) in neuro-ophthalmology. IXth International Neuro-ophthalmology Symposium. Williamsburg, Virginia, USA, July, 1992.

Mutlukan, E., Damato, B.E., McFadzean, R., Evans, A., McGarvie, J. C.A.M.E.C. in the detection of neuro-ophthalmic visual field loss. IXth Congress of European Society of Ophthalmology. Brussels, Belgium; May, 1992.

Mutlukan, E., Damato, B.E. Evaluation of OKP glaucoma screening chart. Scottish Ophthalmological Club Meeting. Glasgow, United Kingdom; March, 1992.

Mutlukan, E., Damato, B.E. Testing visual fields with black stimuli. Scottish Ophthalmological Club Meeting. Sterling, United Kingdom; March, 1991.

Mutlukan, E., Stevenson, R.W., Damato, B.E. The oculo-kinetic perimeter in the screening of glaucoma. College of Ophthalmologists Annual Congress. Glasgow, United Kingdom; May, 1991.

Mutlukan, E. The detection of glaucoma with OKP (Oculo-Kinetic Perimetry): further studies. Glaucoma Group of the United Kingdom and Ireland. XIth Annual Meeting. London, November, 1990.

CONTENTS	Page
Title	i
Dedication	ii
Acknowledgement	iii
Publications	iv
Presentations	vi
Contents	viii
List of Contents	ix
List of Figures	xvi
List of Tables	xxi
Summary	xxiii
Abbreviations	xxvi
Glossary	xxvii
Part I. Introduction	1
Part II. Material and Methods	67
Part III. Results	95
Part IV. Discussion	118
References	153
Appendix (Tables & Figures)	189
Programme Diskette	pocket

LIST OF CONTENTS

Page #

Part 1. INTRODUCTION

1.1.	Visual Field and Its Measurement	1
1.1.1.	Description of The Visual Field	1
1.1.2.	Perimetry and Campimetry	1
1.2.	Basic Factors in Visual Field Measurement	2
1.2.1.	Fixation	2
	Static Fixation	2
	Dynamic (Moving Eye) Fixation	3
1.2.2.	Luminance and Contrast	5
	Stimulus Luminance	6
	Background Luminance	6
1.2.3.	Detection and Response Behavior	7
1.2.4.	Other Stimulus Factors	9
	Size (area)	9
	Duration	10
	Coordinates	11
	Focus	12
	Colour	12
	Mode of Presentation	12
1.2.5.	Other Observer Factors	13
	Patient Experience and Fatigue	13
	Pupil Size	13
	Troxler's Phenomenon	14
1.3.	Clinical Testing of Visual Field	15
1.3.1.	Isoptre and Scotoma	15
1.3.2.	Kinetic Perimetry	15
1.3.3.	Static Perimetry	16

1.3.4.	Representation of the test results (Cartography)	18
	Graphic Display	18
	Grey Scale (Symbols) Display	18
	Numeric Display	18
1.4.	Visual Field Test Instrumentation	20
1.4.1.	Bjerrum Screen Campimeter	20
1.4.2.	Goldmann Perimeter	20
1.4.3.	Tubingen (Harms-Aulhorn) Perimeter	21
1.4.4.	Friedmann Visual Field Analyzer	21
1.4.5.	Dicon Autoperimeter	22
1.4.6.	The Octopus Perimeter	23
1.4.7.	The Humphrey Visual Field Analyzer	23
	Threshold Strategies	24
	Suprathreshold Strategies	24
1.5.	Automated Visual Field Interpretation	26
1.5.1.	Reliability Indices (Catch - Trials)	26
	Fixation Losses	26
	False-Positive Responses	26
	False-Negative Responses	27
1.5.2.	Normal Reference Field	27
1.5.3.	Global Visual Field Indices	28
	Mean Sensitivity (MS)	29
	Mean Defect (MD)	29
	Loss Variance (LV)	30
	Short Term Fluctuation (STF)	30
	Corrected Loss Variance (CLV)	31
1.5.4.	Empiric Probability Maps	31
	The 'Total Deviation' Probability Map	32
	The 'Pattern Deviation' Probability Map	32

1.6.	Video Display Unit (VDU) and Video-Campimetry	34
1.6.1.	Cathode Ray Tube (CRT)	34
1.6.2.	Video-Campimetry	36
1.6.3.	Other Unconventional Perimetry	37
1.7.	Sensory Visual System	38
1.7.1.	Rods and Cones	38
	Colour Perimetry and Blue-on-Yellow Stimulus	39
1.7.2.	Bipolar Cells	41
1.7.3.	Modulator Cells and Receptive Fields	42
	Receptive Field Perimetry	43
1.7.4.	Ganglion Cells and ON / OFF Dichotomy	43
1.7.5.	Retino-Cortical Neural Visual Pathway	45
1.7.6.	Lateral Geniculate Nucleus and Parallel Pathways	47
	Magnocellular and Parvocellular Pathways	47
	On- and Off-Pathways	48
1.7.7.	Visual Cortex and Magnification Factor	49
1.8.	Offset (Decremental) Stimuli in Visual Testing	50
1.8.1.	Light Decrements (Offsets) versus Increments (Onsets) in Psychophysics	50
1.8.2.	The Offset (Dark-on-Bright) Stimulus in Clinical Testing	52
1.9.	Disease Process Causing Visual Field Loss	55
1.9.1.	Glaucoma	55
1.9.2.	Glaucomatous damage and the visual field	56
1.9.3.	Other causes of visual field loss	59
1.10.	Screening	60
1.10.1.	Medical Screening	60
1.10.2.	Glaucoma Screening	63
1.11.	Aim of the Thesis	66

Part 2. MATERIAL AND METHODS

2.1.	Light Offset Stimuli and Dynamic Fixation on Bjerrum Screen	67
2.1.1.	Meridional Hill of Vision to the Offset and Onset Stimuli	68
2.1.2.	The Effect of Variation in Illumination on Offset and Onset Stimuli	69
2.2.	Clinical Evaluation of Dynamic Fixation and Constantly Exposed Offset Stimuli for the Detection of Glaucomatous Visual Field Loss	70
2.2.1.	Constantly Exposed Offset Stimulus of 1.5 mm. Diameter	72
2.2.2.	Constantly Exposed Offset Stimulus of 3.0 mm. Diameter	72
2.3.	Constantly Exposed Offset Stimulus with Dynamic Fixation in Detection of the Blind Spot as a Model of Small Absolute Scotoma	73
2.4.	Computer-Assisted Moving-Eye Campimetry (CAMEC)	74
	Fixation Target	74
	Stimulus Factors	75
	CAMEC Modules	78
	CAMEC Test Programs	80
2.4.1.	Temporal Variation in CRT Background Luminance	81
2.4.2.	CRT Luminance Variation with Monitor 'Brightness' Setting	82
2.4.3.	Stimulus Brightness Selection on a CRT	83
2.4.4.	Topographical Variation in CRT Luminance and Image Contrast	83
2.4.5.	Temporal Variation in Stimulus Duration	83
2.5.	Fixation Control with Dynamic and Static Fixation in Children	85
2.6.	Dynamic Fixation with Single Intensity Static Offset Stimuli in Screening for Neuro-ophthalmic Visual Field Loss	86
2.7.	A Comparison of Single Intensity Static Offset Stimuli with the Onset Stimuli of Humphrey VFA in Glaucoma	88

2.7.1.	The Sensitivity and Specificity of Offset Stimuli in Glaucoma	89
2.7.2.	Detection Thresholds for Offset Stimuli in Glaucoma	89
2.8.	Detection Thresholds to Static Offset Stimulus and The Effect of Refractive Blur	90
2.9.	Topographical Reproducibility of Small Scotoma with Computerised Dynamic Fixation and Offset Stimuli	91
2.10.	Detection Thresholds to Light Offsets in Normals, Ocular Hypertension and Primary Open-Angle Glaucoma	92
Part 3.	RESULTS	
3.1.	Light Offset Stimuli and Dynamic Fixation on Bjerrum Screen	95
3.1.1.	Meridional Hill of Vision to the Offset and Onset Stimuli	95
3.1.2.	The Effect of Variation in Illumination on Offset and Onset Stimuli	95
3.2.	Clinical Evaluation of Dynamic Fixation and Constantly Exposed Offset Stimuli for the Detection of Glaucomatous Visual Field Loss	96
3.2.1.	Constantly Exposed Offset Stimulus of 1.5 mm. Diameter	96
3.2.2.	Constantly Exposed Offset Stimulus of 3.0 mm. Diameter	98
3.3.	Constantly Exposed Offset Stimulus with Dynamic Fixation in Detection of the Blind Spot as a Model of Small Absolute Scotoma	99
3.4.	Computer-Assisted Moving-Eye Campimetry (CAMEC)	100
3.4.1.	Temporal Variation in CRT Background Luminance	100
3.4.2.	CRT Luminance Variation with Monitor 'Brightness' Setting	100
3.4.3.	Stimulus Brightness Selection on a CRT	100
3.4.4.	Topographical Variation in CRT Luminance and Image Contrast	101
3.4.5.	Temporal Variation in Stimulus Duration	101

3.5.	Fixation Control with Dynamic and Static Fixation in Children	103
3.6.	Dynamic Fixation with Single Intensity Static Offset Stimuli in Screening for Neuro-ophthalmic Visual Field Loss	104
3.7.	A Comparison of Single Intensity Static Offset Stimuli with the Onset Stimuli of Humphrey VFA in Glaucoma	106
3.7.1.	The Sensitivity and Specificity of Offset Stimuli in Glaucoma	106
3.7.2.	Detection Thresholds for Offset Stimuli in Glaucoma	107
3.8.	Detection Thresholds to Static Offset Stimulus and The Effect of Refractive Blur	108
3.8.1.	The Effect of Eccentricity on Offset Threshold	108
3.8.2.	The Effect of Stimulus Size on Offset Threshold	108
3.8.3.	The Effect of Defocus on Offset Threshold	109
3.9.	Topographical Reproducibility of Small Scotoma with Computerised Dynamic Fixation and Offset Stimuli	110
3.10.	Detection Thresholds to Light Offsets in Normals, Ocular Hypertension and Primary Open-Angle Glaucoma	111
3.10.1.	Detection Thresholds in the Normal Central Visual Field	111
3.10.2.	Detection Thresholds in Glaucomatous Central Visual Field	112
3.10.3.	Detection Thresholds in the Central Visual Field of Ocular Hypertensives	113
3.10.4.	Topographical Distribution of the Defects to the Offset and Onset Stimuli	116
3.10.5.	Test Duration with Dynamic Fixation and Ascending Staircase Method	117
Part 4.	DISCUSSION	
4.1.	Light Offset Stimuli and Dynamic Fixation on Bjerrum Screen	118
4.1.1.	Meridional Hill of Vision to the Offset and Onset Stimuli	118
4.1.2.	The Effect of Variation in Illumination on Offset and Onset Stimuli	119

4.2.	Clinical Evaluation of Dynamic Fixation and Constantly Exposed Offset Stimuli for the Detection of Glaucomatous Visual Field Loss	120
4.3.	Constantly Exposed Offset Stimulus with Dynamic Fixation in Detection of the Blind Spot as a Model of Small Absolute Scotoma	128
4.4.	Computer-Assisted Moving-Eye Campimetry (CAMEC)	130
4.4.1.	Temporal Variation in CRT Background Luminance	130
4.4.2.	CRT Luminance Variation with Monitor 'Brightness' Setting	130
4.4.3.	Stimulus Brightness Selection on a CRT	130
4.4.4.	Topographical Variation in CRT Luminance and Image Contrast	131
4.4.5.	Temporal Variation in Stimulus Duration	131
4.5.	Fixation Control with Dynamic and Static Fixation in Children	133
4.6.	Dynamic Fixation with Offset Stimuli in Screening for Neuro-ophthalmic Visual Field Loss	134
4.7.	A Comparison of Single Intensity Static Offset Stimuli with the Onset Stimuli of Humphrey VFA in Glaucoma	136
4.7.1.	The Sensitivity and Specificity of Offset Stimuli in Glaucoma	136
4.7.2.	Detection Thresholds for Offset Stimuli in Glaucoma	137
4.8.	Detection Thresholds to Static Offset Stimulus and The Effect of Refractive Blur	139
4.9.	Topographical Reproducibility of Small Scotoma with Computerised Dynamic Fixation and Offset Stimuli	141
4.10.	Detection Thresholds to Light Offsets in Normals, Ocular Hypertension and Primary Open-Angle Glaucoma	143
4.11.	Final Remarks	149

LIST OF FIGURES

Figure 1: Schematic drawing of the principle of a CRT as utilised in video-display terminals

Figure 2: The retina transmits visual information into the optic nerve.

Figure 3: The retino-cortical neural visual pathway. LGN=Lateral Geniculate Nucleus.

Figure 4: The organisation of the retinal nerve fiber layer.

Figure 5: a. The optic chiasm, b. Hemianopic field loss in chiasmatic lesion.

Figure 6: Luminance profiles of light increments (onsets) and decrements (offsets) introduced by black and white stimuli on opposite as well as grey backgrounds.

Figure 7: The Oculo-Kinetic Campimetry Chart.

Figure 8: a. Oculo-Kinetic Campimetry Chart A; b. OKC Chart B.

Figure 9: The equipment used in Computer Assisted Moving Eye Campimeter (CAMEC).

Figure 10: Conversion of percentage and decibel contrast values for stimuli.

Figure 11: The test grid for CAMEC 26 Point Screening Program (Filled circles: Primary test locations; Empty circles: Secondary test locations).

Figure 12: Age distribution of the children tested with CAMEC and Dicon Autoperimeter Blind Spot Test Programs.

Figure 13: Test grids of the paediatric blind spot test programs of CAMEC and Dicon perimeter.

Figure 14: Primary test locations in the left visual field and secondary test locations added automatically in the abnormal right field.

Figure 15: The stimulus locations of CAMEC 76 Point Screening Test, showing double arcuate scotomas in a glaucomatous eye.

Figure 16: The offset stimuli test locations along the nasal horizontal meridian.

Figure 17: The blind spot test grid of CAMEC.

Figure 18: 'Hill of Vision' to black-on-white and white-on-black stimuli.

Figure 19: The effect of ambient illumination on black-on-white and white-on-black stimuli.

Figure 20: The effect of ambient illumination on black-on-grey and white-on-grey stimuli.

Figure 21: OKC positive result rate according to the stage of glaucomatous visual field loss.

Figure 22: OKC positive result rate according to the age of control cases.

Figure 23: OKC abnormality in glaucoma suspect eyes of various age groups.

Figure 24: Positive OKC result rate according to the level of visual acuity.

Figure 25: OKC results in different age groups.

Figure 26: Equivalent Friedman Analyser light sensitivity required for 50% detection of 1.5 mm diameter offset (black-on-white) stimulus of OKC.

Figure 27: OKC results above the age of 60 years.

Figure 28: The average luminance of the concentric zones on CRT surface against time.

Figure 29: The effect of various screen 'Brightness' settings on the luminosity.

Figure 30: Top: The average luminance of 64 shades of grey as uniform screen background. Bottom: The average luminance obtained with small grey patches (shades 1-40) as foreground on 10 cd/m² background.

Figure 31: The variation in CRT screen luminance at 36 locations (6x6) on the monitor used for tests (left). The topographical non-uniformity of the background applies equally to the stimulus intensity and provides stability to the stimulus contrast (right).

Figure 32: The scores obtained in each eye by the blind spot tests of CAMEC and Dicon Autoperimeters.

Figure 33: Left homonymous superior quadrantanopia to light offsets (top) and Goldmann perimeter (bottom) caused by a right intracranial temporo-parietal lobe tumor.

Figure 34: Positive (abnormal) result rate with CAMEC and Goldmann tests according to different visual acuity levels.

Figure 35: Regression analysis of CAMEC test duration (in seconds) versus patient age (in years) in bilaterally normal (top) and abnormal fields (bottom).

Figure 36: The frequency of abnormality at each test location on STATPAC Total Deviation (top) and Pattern Deviation (bottom) results.

Figure 37: A superior Bjerrum scotoma on STATPAC (top row) and CAMEC results with four different offset stimulus contrast (middle and bottom rows).

Figure 38: The nasal field loss on STATPAC result appeared more extensive when compared with lowest contrast (-10%) offset stimuli which also revealed double arcuate scotomas.

Figure 39: The true and false positive result rates with offset stimuli against STATPAC Pattern

Deviation results at all test points in three annuli eccentricity bands.

Figure 40: Equivalent Humphrey threshold levels required for the detection of light offsets on 10 cd/m² background.

Figure 41: Equivalent Humphrey threshold levels required for the detection of light offsets on 100 cd/m².

Figure 42: The effect of visual acuity on detection thresholds to light offsets.

Figure 43: Topographical reproducibility of blind spot mapping varied between 64% (top) to 80% (middle) with an average of 73% (bottom).

Figure 44: Mean±Standard Deviation offset detection sensitivity (in decibels) at each test location in the central visual field.

Figure 45: CAMEC and Humphrey VFA results in three glaucomatous eyes showing similar defects.

Figure 46: Global field indices obtained with offset and onset stimuli.

Figure 47: The field results from three ocular hypertensives.

Figure 48: Average global field indices obtained with onset and offset stimuli.

Figure 49: The regression analysis of the global visual field indices against the risk of developing visual field loss (RDVFL) in all eyes.

Figure 50: The regression analysis of the global visual field indices against the level of intra-ocular pressure (IOP) in all eyes.

Figure 51: The regression analysis of the global visual field indices against cup-to-disc ratio

(CDR) in all eyes.

Figure 52: Family history had no significant effect on average field scores.

Figure 53: Topographical distribution of visual field defects to onset stimuli of Humphrey perimeter in primary open angle glaucoma.

Figure 54: Topographical distribution of visual field defects to offset stimuli of CAMEC in primary open angle glaucoma.

Figure 55: Topographical distribution of visual field defects to offset stimuli of CAMEC in ocular hypertensives.

Figure 56: Normal visual fields of an 8 year-old to CAMEC and Humphrey tests.

Figure 57: Right homonymous supero-temporal partial quadrantanopia in a 5 1/2 year old girl who could be tested with CAMEC only.

Figure 58: Bitemporal hemianopia to the offset stimuli of CAMEC in pituitary adenoma.

Figure 59: Bitemporal hemianopia to the offset stimuli of CAMEC in craniopharyngioma.

LIST OF TABLES

Table 1: Negative contrast (offset) steps available in the ascending threshold program of CAMEC.

Table 2: The blind spot test parameters of Dicon Autoperimeter and CAMEC.

Table 3: The amount of plus sphere refraction required to achieve various visual acuity levels.

Table 4: Selection criteria for POAG, OHT and control cases.

Table 5: Detection of physiological blind spot according to the number of corresponding test stimuli in OKC method.

Table 6: Stimulus durations which can be obtained with CAMEC software program.

Table 7: The details of paediatric cases abandoned blind spot tests.

Table 8: Neuro-ophthalmic conditions of the patients included in the study.

Table 9: Test durations of CAMEC 26-point screening test in neuro-ophthalmology.

Table 10: Detection thresholds for single intensity offset stimuli on 10 cd/m² background.

Table 11: Detection thresholds for single intensity offset stimuli on 100 cd/m² background.

Table 12: Offset thresholds at various visual acuity levels.

Table 13: Offset stimuli spatial summation coefficient (k) values beyond 18 degrees eccentricity at various acuity levels.

Table 14: Global visual field indices obtained in POAG, OHT and control groups.

Table 15: Abnormal test result rates according to the global field indices and their prediction limits.

Table 16: The test durations (seconds) and total number of stimulus presentations with the light onset stimuli using bracketing (BT) technique and, with the light offset stimuli using ascending single-crossing (ASC) method.

SUMMARY

The dark-on-bright (negative contrast, light decremental, light offset) stimulus and dynamic fixation target are non-conventional and their usefulness in visual field examination has not been fully documented before. The utility of light offsets (i.e. offset stimuli) and dynamic fixation was investigated for kinetic and static perimetry on a tangent screen without or with automation and the results were compared to those from conventional bright-on-dark (positive contrast, light incremental, light onset) stimuli and static fixation.

The disappearance eccentricities of offset and onset stimuli of equal size were determined in eight normal eyes, using dynamic fixation technique at two different levels of surrounding illumination. Kinetic offset stimulus has a smaller "isoptre" than onset stimulus and, the variation of ambient illumination has less effect on the visibility of offset stimulus.

The Oculokinetic Campimetry (OKC) with a constantly exposed offset stimulus was performed in 366 glaucomatous eyes and 217 normal eyes. When a 1.5 mm stimulus was used, a true positive OKC result was obtained in 45% of eyes with relative scotomas and 81% of eyes with small absolute scotomas. A false positive result was obtained in 9% of patients aged 60-70 yrs and 13% of patients older than 70 yrs. When a 3 mm stimulus was used in the glaucomatous patients above the age of 60 yrs, the OKC test was positive in 33% of eyes with relative scotomas and 56% of eyes with small absolute scotomas while none of the control subjects produced a positive result. In 63% of the eyes, abnormal OKC results reflected smaller scotomas than those to the conventional visual field tests, suggesting underestimation of the topographical extent of the scotomas. Inside the absolute scotomas, constantly exposed offset stimulus was still detectable with 19% - 67% frequency between 5°-13° eccentricity. The OKC method may be useful to reveal moderate to advanced glaucomatous field defects when conventional methods are not available.

Two hundred and seventy two eyes were tested with a OKC having a constantly exposed stimulus and either one or two of the fixation targets corresponding to the physiological blind spot. The second fixation target increased the blind spot detection rate from 65 % to 85 %. The performance of multi-fixation targets in OKC is low if the stimulus is exposed constantly.

The usefulness of automated static offset stimuli combined with a dynamic fixation target was investigated further, using Computer Assisted Moving Eye Campimeter (CAMEC). CAMEC is capable of presenting automated light offset stimuli of specified luminance contrast, size, duration and coordinates in reference to a dynamic fixation target on a cathode ray tube.

Thirty-two children, aged 4-10 years, were examined with the blind spot test programs of both CAMEC and the Dicon Auto-Perimeter. Among those who completed both tests the blind spot was detected in 75% by the static fixation of Dicon Auto-Perimeter and, 100% by the dynamic fixation of CAMEC. The mean CAMEC score (61.0%) was significantly higher than the mean Dicon Auto-Perimeter score (26.6%). Joystick controlled dynamic fixation method allowed detection and quantification of scotomas in patients more than 4 years of age.

One hundred and sixty nine eyes were examined with both single intensity high contrast (i.e. black) static offset stimuli of CAMEC and standard Goldmann Perimetry in a neuro-ophthalmology clinic. Conventional perimetry revealed a visual field abnormality in 75 patients, and the offset stimuli had detection rate of 90 % , with good or fair topographical correlation in 82 % and poor correlation in 18 % of eyes. CAMEC produced a normal result in 87 % of normal eyes, allowing accurate diagnostic visual field examination in neuro-ophthalmic practice. Among the elderly, the efficiency of dynamic fixation method of CAMEC decreases because of difficulties related to joystick use.

Twenty-five glaucomatous eyes were examined with the Humphrey Visual Field Analyser Thresholding Program 30-2 and CAMEC, using single intensity static offset stimuli at various contrast levels. Dark-on-bright stimuli allowed the delineation between glaucomatous field defects and the normal regions in the central visual field. Offset stimuli of lower contrast provided higher abnormal point detection rates. Furthermore, visual field defects to the low contrast offset stimuli were more extensive than those to the luminous stimuli. Lower stimulus contrasts and higher background luminance level required higher retinal sensitivity for the detection of dark-on-bright stimuli.

Detection thresholds to offset stimuli of Goldmann size III and IV were determined along the nasal horizontal meridian of the central visual fields of 5 normal subjects. Detection sensitivity

diminished with increasing amounts of plus lens-induced refractive blur. The larger size decremental stimuli provided a wider dynamic range, less inter-individual variation in stimulus visibility and more resistance to refractive error than those obtained with the smaller size stimuli.

CAMEC with suprathreshold static light offset stimuli were used in mapping of the physiological blind spot in 10 healthy eyes. On repeat testing, an average topographical reproducibility rate of 73 % was achieved in mapping of the blind spot as a model of small absolute scotoma, with an average of 1.4 degrees and 0.6 degrees variability in the vertical and horizontal dimensions of the blind spot respectively. Dynamic fixation provides as good fixation maintenance as conventional static fixation method.

Twenty-one primary open angle glaucoma (POAG) patients, 21 ocular hypertensive (OHT) patients and, 13 normal individuals were tested with full threshold test program 24-2 of the Humphrey Visual Field Analyser. The same eyes were also tested with threshold offset stimuli and dynamic fixation. Test locations with decreased sensitivity outside the 95% CI were determined and global field indices of 'Mean Sensitivity', 'Mean Defect' and 'Loss Variance' were calculated for each eye. The offset stimuli had 95% sensitivity in the POAG group and 100% specificity in the control group. In the OHT group, offset stimuli indicated field abnormality in 57% - 62% of the eyes which tended to be the ones with higher risk of developing glaucoma. The topographical distribution of the field defects to light offset stimuli in the POAG and OHT groups was found to be of nerve fiber layer type and similar to that revealed by light onset stimuli in the POAG group, confirming that the abnormalities to offset stimuli indeed indicate optic nerve damage. Campimetry with offset stimulus and dynamic fixation had Positive Predictive value of 63% (20/32) and Negative Predictive value of 96% (22/23), against the conventional testing which, in turn, exhibited Postive Predictive value of 95% (20/21) and Negative Predictive value of 65% (22/34).

Although the clinical potential of light offset stimulus with conventional static fixation was not addressed by this research and remains to be investigated, the results from this work suggest that automated offset stimuli presented with dynamic fixation indicate normal and diseased visual fields in video-campimetry for screening and quantification of scotomas and also reveal visual field loss missed by the conventional onset stimulus.

Abbreviations:

C.A.M.E.C.	: Computer Assisted Moving Eye Campimeter
c.d.	: candela
C.D.R.	: Cup-to-Disc Ratio
C.L.V.	: Corrected Loss Variance
C.R.T.	: Cathode Ray Tube
d.B.	: Decibel
E.G.A.	: Enhanced Graphics Array
F.H.	: Family History
I.O.P.	: Intra-Ocular Pressure
L.V.	: Loss Variance
M.D.	: Mean Defect
M.S.	: Mean Sensitivity
O.H.T.	: Ocular Hyper-Tension
O.K.C.	: Oculo-Kinetic Campimetry
P.D.	: Pattern Deviation
P.O.A.G.	: Primary Open Angle Glaucoma
R.D.V.F.L.	: Risk of Developing Visual Field Loss
R.O.C.	: Receiver Operating Characteristics
S.T.F.	: Short Term Fluctuation
T.D.	: Total Deviation
T.I.	: Topographical Index
V.D.U.	: Video Display Unit
V.G.A.	: Video Graphics Array

Glossary of Terms and Concepts:

adaptation: final stage of the process in which the visual system becomes adjusted to different level of light or colour than it was exposed to during an immediately preceding period.

ambient lighting: lighting throughout an area that produces general illumination.

brightness: scale of measurable qualities of being bright, brilliant, dim or dark; often used when referring to the percept of subjective magnitude of light sensation.

candela (nit): the International System (SI) unit of brightness intensity. One candela is one lumen per steradian.

central visual field: area of surroundings within 30 degrees from the object of visual fixation.

contrast: the manifestation of differences in brightness or colour between objects or areas in space.

contrast sensitivity: the ability to detect the presence of minimal brightness or colour differences between objects

dynamic fixation: maintenance of visual fixation on a moving target with simultaneous and harmonious eye movements.

illuminance: the density of the luminous flux incident on a surface. It is measured in lumens per square meter (lm/m^2) or lux. see lumen (1 lux = 0.0929 footcandle) .

illumination: the act of illuminating or state of being illuminated; often used for the term 'illuminance'.

light: radiant energy that is capable of stimulating the retina and producing a visual sensation; the visible portion of the electromagnetic spectrum.

lumen: light flux emitted within a unit solid angle (one steradian) by a point source having a uniform light intensity of one candela.

luminance: photometric brightness of objects or areas in specifying the stimulus for vision; the light intensity per unit area of a surface (by emittance or reflection) in a given direction, measured in candelas per meter square ($\text{cd}/\text{m}^2=\text{nit}$). ($1 \text{ cd}/\text{m}^2 = 10000 \text{ stilb} = 0.318 \text{ apostilb} = 3180 \text{ lambert} = 3.426 \text{ footlambert}$).

luminance threshold: the minimum perceptible difference in luminance for a given state of visual adaptation.

lux: see illuminance and lumen.

mesopic vision: vision with fully adapted eyes at lumiance conditions between those of photopic (cone mediated) and scotopic (rod mediated) vision, that is, between about 3.4 and 0.034 candelas per meter square.

negative contrast: brightness difference created by dim objects or areas on a lighter surface; dark-on-bright pattern.

offset stimulus: visual field test stimulus formed by the offset of a given area of light on a defined background; light decremental stimulus (also see 'negative contrast').

onset stimulus: visual field test stimulus created by the onset of a given area of light on a defined background; light incremental stimulus (also see 'positive contrast').

pixel: unit graphic area on a cathode ray tube.

positive contrast: brightness difference created by light objects or areas on a dimmer surface; bright-on-dark pattern.

Snellen acuity: visual acuity as determined from testing with optotypes designed by Herman

Snellen in 1862.

static fixation: maintenance of visual fixation on a steady target with no eye movements.

tangent screen: flat surface

threshold: the value of a variable of a physical stimulus that permits the stimulus to be perceived a specific percentage of the time or at a specific accuracy level; perception accuracy 50% of the time or the value of the stimulus variable that just permits the sensation.

visual acuity: the measure of the smallest resolvable spatial detail.

Part 1. INTRODUCTION

Basic research is what I am doing when I do not know what I am doing.

[Werner von Braun]

1.1. Visual Field and Its Measurement

1.1.1. Description of The Visual Field

The visual field is the amount of surroundings that is visible to the eye at any one time.

1.1.2. Perimetry and Campimetry

Perimetry is the measurement of the visual field. It involves recording of the visual function of the eye at topographically defined loci in the visual field. In conventional visual field testing, the ability to discern a stimulus which is just perceptibly brighter than the background (i.e., differential light detection sensitivity) is determined. Therefore, the presentation of the stimulus in the field of vision is achieved with the onset of a light of a given area and brightness. The term campimetry is used for the measurement of central visual field that is up to 30 degree eccentricity from fixation and on a tangent screen. The term perimetry, although used interchangeably with campimetry, is referred when the whole visual field including the area beyond the 30 degree eccentricity is examined. Evolution of visual field testing is summarized elsewhere ^{1,2}.

1.2. Basic Factors in Visual Field Measurement

Reliable and meaningful measurements of visual fields are possible by specifying the testing conditions and standardizing the methods for application of these conditions. A common framework for measurement of the field of vision, which is ensured through specifications, would allow exchange and comparison of information obtained at different times in different patients and in different places. The fundamental standards for conventional visual field testing are described in detail elsewhere^{3,4} and the following is a brief overview of the established standards therein unless further referencing is provided.

1.2.1. Fixation

Static Fixation

The measurement of visual field is conducted in reference to the central gaze fixation point. Conventional perimetry is performed with a steady eye fixing at a steady target to maintain fixation during the test. In reference to the outside world, both the eye and the fixation target remain immobile since the visual field is described as the portion of the external environment of the observer wherein the steadily fixating eye can detect visual stimuli³. The accuracy of fixation has the key importance during the testing of the visual field as unstable fixation would increase the variability of measurements and shifted fixation would cause the displacement of the visual field defects on cartographic test results.

The human eye is not designed to be steady as evidenced by spontaneous continuous eye movements in a resting state. The background neuronal activity and the continuous interaction of balance between different gaze control systems such as saccadic, pursuit and cerebello-vestibular system interactions result in constant physiological involuntary

eye movements of small amplitude up to a few degrees⁵⁻⁸. Therefore, it is unphysiological to maintain a still fixation during visual field testing. Clinical trials support that fact, as 25% of individuals could not maintain steady fixation at all and the rest may fixate only within an area of 3 to 6 degree diameter with intermittent fixation losses^{9,10}. The situation becomes more pronounced with increase in the patient's age¹¹ and prolonged test durations, even if the subjects are well experienced in perimetry¹⁰. Visual field examination is often omitted in young children with ocular and neurological disease as conventional methods fail when young patients lose interest in the examination or are unable to keep their eye still throughout the procedure¹². Despite these shortcomings, children are tested with adaptations of conventional oculo-static perimetry¹³⁻²⁴.

Monitoring of fixation is necessary during the test to ensure reliability of the results. Monitoring may be self-monitoring by the patient by paying attention to the disappearance of a target in the physiological blind spot²⁵. The other methods are the observation of the eye by the practitioner directly as in Friedman Analyzer or indirectly using a telescope as in Goldmann, Tubingen perimeters, infrared scanning²⁶, stimulus presentations in the blind spot (Heijl-Krakau Method)²⁷ or electro-oculographic scanning²⁸.

Eye movements have also been exploited to register the detection of the stimuli in the visual field. In that form of eye movement perimetry, the patient is instructed to maintain a centrally located static fixation target and look towards the visual field test stimuli to signal their detection. The eye movements towards the stimulus are recorded either by a technician²⁸, by an infrared camera²⁹ or by recording the electro-oculographic potentials through an amplifying system^{30,31}.

Dynamic (Moving Eye) Fixation

History or exploitation of eye movements in detection of visual field defects goes back

to the discovery of physiological blind spots by Mariotte in 1666¹. Mariotte demonstrated his new discovery, physiological blind spot, to the King (of England and France), by asking the king to look at a sideways fixation point and showing that the head of another person, 20 feet away, became invisible. Nearly three centuries later the same method which involves the use of eye movements with a dynamic fixation target around a fixed stimulus to test various points in the visual field has been employed for the exploration of the central visual field in contemporary ophthalmology by Smith²⁵. It is possible to maintain a stable fixation while keeping the eye mobile simultaneously and in coordination with the fixation target. A practical analogy may be that one is standing still on a railroad carriage. The position of the standing person in reference to the carriage does not change regardless of whether or not the carriage is in motion. Stimuli of defined loci may be presented to the eye for testing purposes provided that the motion of the eye is under control and adjusted with the stimulus coordinates. As the visual sensitivity in the field of vision during slow (i.e., pursuit) eye movements is not suppressed in contrast to detection sensitivity loss during fast (i.e., saccadic) eye movements³², it may be possible to keep the eye mobile to perform reliable sensitivity measurements. Although strict stability of the retinal image of the stimulus is not a requirement for optimum resolution and slow eye movements are admissible^{33,34}, bringing the eye to a complete stop just before the stimulus presentation would further prevent any sensitivity distortion which might be introduced by the eye movement.

The 'Oculo-Kinetic (Eye Movement) Perimetry' ('OKP') chart designed by Damato is based on the same principles^{35,36} and also incorporates the black stimulus of Highman³⁷. This simple and inexpensive method of examining the visual field is performed with a white tangent screen made of a piece of white paper or cardboard and having a central black test stimulus and a series of numbered fixation targets located peripherally at desired coordinates. When the patient looks at each number in turn from the correct distance, the stimulus is accurately positioned at known points in the visual field. Numbers associated with disappearance of the stimulus are recorded by crossing out the same numbers on a miniature version of the chart so that a plot of defects is obtained.

At the end of the examination the record sheet is inverted so that the results are comparable with those obtained conventionally.

The computerized version of oculo-kinetic fixation method invented by Damato involves a randomly meandering fixation target on a video display unit (VDU), and the stimuli are presented in relation to the moving fixation target at preselected coordinates³⁸. That computerized moving eye fixation method called Computer Assisted Moving Eye Campimeter (CAMEC) was intended originally for children only and involved intermittent appearance of multiple fixation targets on a video display unit (VDU) at selected locations³⁹. Each fixation target consisted of a randomly meandering fixation spot and a circle which could be moved to track the fixation spot by the patient using a mouse. The stimuli were to be presented in relation to the moving fixation target at desired coordinates. The usefulness of the method was seriously hindered by the fact that the appearance of the fixation targets in defective field areas was not recognized by the patient. The system was basically a fixation monitoring software without any known, recognized, specified or calibrated stimuli and background³⁸⁻⁴⁰ (Williamson et al., unpublished paper submitted to 'Eye'). The CAMEC software was re-designed with code writing by Mr Jim McGarvie and Dr Aled Evans and contributions by Drs Damato, Keating and the author during the progress of this work.

1.2.2. Luminance and Contrast

Adequately stable and calibrated light intensity values are the essential components of any visual field testing device. The brightness of the background and test stimuli need to be specified photometrically. In conventional perimetry, the stimulus and the background are defined by their luminance as specified by the manufacturer. Luminance (L) is the luminous flux emitted by a surface per unit solid angle per unit projected area. The international unit of luminance is the candela (cd)/m² and other units are now regarded as obsolete. The conversion to other units can be made using the formulae

given in the Glossary. Illuminance is the amount of light per unit area falling on a surface from a distant source and represented with unit Lux.

Stimulus Luminance

The actual stimulus for visual excitation is the image on the retina and that is called the proximal stimulus. The strength of that stimulus is determined by the intensity of the distal stimulus (the image on the instrument) and pre-retinal factors such as pupil size and transparency of the cornea, lens and vitreous. The 'threshold' contrast is defined as the contrast level that will give a particular probability of detection of the stimuli. The amount of stimulus contrast required for its detection on a defined background is called the 'luminance difference threshold', also the 'differential light detection sensitivity'. Stimulus contrast for a small target on a large uniform background⁴¹ (such as a perimetric stimulus) is defined Weber's⁴² Luminance Contrast formula of $C = \frac{L_t - L_b}{L_b} = \frac{\Delta L}{L_b}$ where 'L_t' is the luminance of the test target and 'L_b' is the luminance of the background upon which the target is presented. The Weber fraction has been used widely in the visual literature and regarded as representative of perceptual effects of a stimulus⁴³. The stimulus contrast may be positive or negative; that is, the target may have a higher luminance (brighter) than the background (positive contrast) or a lower luminance (darker) than the background (negative contrast). The above given Weber's formula is used to describe both positive and negative contrasts. The Michelson contrast formula⁴⁴ of $C = \frac{L_t - L_b}{L_t + L_b}$, originally introduced to describe the visibility of interference fringes, is used for spatially⁴³ or temporally⁴¹ periodic stimuli, alternating large areas of dark and bright patterns such as checker-board or grating patterns⁴⁵.

Background Luminance

It is evident from the above described contrast formulae that the luminance of the background on which the stimulus is presented has a profound effect on the stimulus' contrast detection threshold. When the background adapting light intensity is low, very

little additional light (ΔL) must be added to reach threshold. As the background intensity increases, ΔL rises and the function of ΔL versus L_b over a broad range above threshold becomes a straight line. Because the line is straight, its slope is a constant (i.e. $\Delta L/L_b = \text{constant}$)⁴⁶. The constancy of this fraction is termed the "Weber-Fechner relation". The fraction remains constant over 3 logarithmic unit (i.e. 1000 times) background luminance change for cone function but, for routine office perimetry, it is recommended that a low photopic background luminance be chosen such that both rods and cones are functional while L_b still falls within a range over which the Weber's fraction remains constant. At and above a background level of 8 cd/m² (with a 4 mm pupil diameter) little change occurs in contrast threshold. It is recommended that for routine clinical tests, the background levels should not be less than 10 cd/m². This setting criterion is recommended because: a) This represents a so called mesopic level of adaptation at which both rods and cones contribute nearly equally to visual sensitivity⁴⁶, b) it requires less sensitive calibration of equipment, c) it is less sensitive to modest fluctuations in light source output, d) the result is less dependent upon modest variations in eye pupil size, e) visual functions are tested at clearly defined photopic level, and f) fixation control is easier than at lower adaptation levels. It is necessary that the patient be adapted to the luminance of the background field for a few minutes before the start of the visual field test.

1.2.3. Detection and Response Behavior

There is no single level of stimulus contrast below which it will never be detected and above which it will always be detected. The probability of stimulus detection varies in a range between 0 to 100 percent. The probability of detection of a stimulus is increased with increase in contrast for a given size or, increase in size for a given contrast. Usually the threshold is the contrast level with the stimulus detection probability of 50 percent. That means at this stimulus contrast level half of the stimulus presentations would be detected and half of them would be missed by the observer.

When a faint (i.e., low contrast) stimulus is presented to an observer, the contrast of the stimulus and the patient's willingness to say "yes" determine together whether the patient will detect it. The threshold level, for instance, would vary if the observer wanted to be sure about the presentation resulting in a higher threshold than that of a subject who is willing to say "yes" whenever they have the slightest idea that a target had been present. In addition to the patient's conscious willingness for detection of the stimulus, the patient's internal sensations contribute to the responses. Two main types of internal sensations occur either in the absence of the target or in the presence of the target, each encouraging the patient to respond for the contrary. During visual field testing, the observer should decide for each stimulus presentation whether or not the internal sensation is in agreement with a real life situation. Decision making is easiest when the stimulus is at its highest contrast and becomes more difficult with the decrease in contrast as the internal sensations start to conflict. Because of the time limitation for testing in the clinical environment, the threshold is defined as the average of the lowest contrast detected and the highest contrast missed during successive presentations of ascending staircase (increasing steps) or descending staircase (decreasing steps) of contrast.

The time required for an observer to signal the detection of visual stimulus is the reaction time and that changes as a function of the presentation coordinates in the visual field. The patient's level of vigilance, psycho-motor state, dark adaptation, whether the stimulus is static or kinetic, the speed of the kinetic stimulus and the presence of visual field defect mutually determine the reaction time.

A signal or cue which are often auditory preceding a stimulus may influence the probability of a "yes" response because of conditioning. The visual field test should be performed in a room where unnecessary noise and distractions are avoided and lighting conditions are under complete control.

1.2.4. Other Stimulus Factors

In addition to stimulus luminance contrast, the other important stimulus variables which altogether determine the visibility of the stimulus against a uniform background at a given retinal locus are its size (area), the duration of the stimulus exposure, the coordinates of the stimulus in the field, the stimulus image sharpness on the retina, difference in chromaticity between the stimulus and background and the mode of stimulus presentation.

Size (Area)

The angular size of a presented stimulus at a given coordinate is calculated as the arc-tangent of the ratio of stimulus diameter in millimeters to the test distance between the background and the pupil in millimeters. In conventional perimetry, the stimulus shape is circular. Thresholds determined with oval or rectangular stimuli differ negligibly from those determined with circular stimuli provided that the same surface area is maintained. In general, there is an inverse relationship between light detection threshold and the area of an incremental stimulus and the exact mathematical nature of the relationship is determined by the retinal locus, the duration of exposure and background luminance as well as the stimulus dimensions. The light incremental threshold-stimulus size relationship constitutes the spatial summation (Ricco's Law); that is $\Delta L \times A^k = \text{critical value to reach threshold (i.e. constant)}$. The 'A' equals the area of the stimulus and exponent 'k' is referred to as the summation coefficient (the slope of the function) which equals one (ie, $k=1$) in Ricco's Law. One can estimate 'k' for a given part of the visual field measuring the contrast threshold for two targets that differ in area by a known amount. The successive targets of the Goldmann perimeter (for example size III versus IV) vary in area by a factor of four. Exponent 'k' can then be estimated by⁴:

$$k = \frac{\log \Delta L_2 - \log \Delta L_1}{\log A_1 - \log A_2}$$

The 'k' is not constant and varies with the eccentricity in the field, background adapting luminance, stimulus duration, patient age and the presence of field abnormality. Thus,

Piper's Law refers to $k=0.5$ while Pieron's Law corresponds to $k=0.33$. Goldmann concluded that $k=0.8$ was a close approximation for different 'k' values at different eccentricities. Sloan's detailed experiments with Goldmann perimeter⁴⁷ indicated 'k' coefficient values of 0.55 at the fovea and 0.9 at 45 degrees nasally under photopic conditions with augmentation of summation in dark adaptation as demonstrated by Fankhauser and Schmidt. A detailed review in English of the above non-English literature is available⁴⁸. A recent study using Humphrey Visual Field Analyzer found mean $k=0.5$ at 10 degree, $k=0.7$ at 30 degree and $k=0.8$ at 50 degree eccentricity⁴⁹.

Duration

The importance of stimulus duration is two-fold. Firstly, the stimulus should be presented for long enough to enable the completion of temporal (time-related) processing in the human visual system.

The visual system responds to the presentation of a stimulus according to its duration of exposure. The critical stimulus duration is the exposure period in which the visual response is built up and the temporal summation of the visual signal is completed. The frequency of detection of a stimulus in the field of vision increases with longer presentation times and reaches to a plateau in less than 0.1 seconds^{4,50}. The temporal processing can also be described as the eye-visual cortex transmission time and takes an average of 0.075 second for both light onset (positive contrast) and offset (negative contrast) stimuli with no statistically significant difference as determined by Visual Evoked Cortical Potential latency measurements⁵¹. The temporal summation of the visual response also varies with several factors including the stimulus eccentricity in the field, the stimulus size, colour, background light intensity and presence of pathology in the field. For stimulus exposures shorter than the critical duration, ΔL (threshold intensity) \times T (duration of exposure) = constant (Bloch's Law). For exposures longer than 0.5 seconds, ΔL = constant, indicating no effect of duration on detectability of the stimulus⁴⁸.

Broca-Sulzer effect produces the seeming paradox of a short flash appearing subjectively brighter than a longer flash of the same luminance.

Secondly, longer stimulus durations encourage the patient to look away from the fixation target, resulting in fixation losses and false positive responses (stimulus seen when not supposed to be seen). If the duration of exposures exceeds the latency for fast (i.e. saccadic) eye movements which is on average 0.3 seconds, there may be a tendency for some individuals to give up the fixation to look at the peripheral stimulus ⁴⁸. The stimulus duration values of 0.2-0.4 seconds are generally acceptable.

If the stimulus is moved in case of kinetic perimetry, the rate of movement should be kept sufficiently low and stable to enable completion of temporal summation. There is not a strict definition of the ideal rate of speed for stimulus movement in kinetic perimetry. The stimulus may be moved from non-seeing to seeing as preferred in routine clinical testing. The opposite, which is the movement from seeing to non-seeing may also be used to fit specific needs.

Coordinates

The angular position of a stimulus in the visual field is specified relative to the centre of the entrance pupil of the eye in the primary line of sight. The entrance pupil is the image of the centre of the iris aperture as seen through the cornea. The primary line of sight connects the point of fixation and the centre of the pupil. In the specified coordinates of stimulus presentation in the field of vision, the zero degree half-meridian is defined as the horizontal line to the right of the fixation point of the patient and should be located at the same height as the interpupillary line. The half-meridian angle is then measured counter-clockwise relative to the zero-degree meridian. The 180 degree half-meridian is to the patient's left. The eccentricity of the stimulus is represented with degrees which is the arctangent of the ratio of the distance between the centre of the fixation target and the stimulus to the test distance between the eye and fixation target.

Focus

The blur of the retinal image of the test stimulus results in change in both its perceived size and its contrast. The most frequent causes for stimulus blur are uncorrected refractive error and the opacities of optical media of the eye such as corneal, lenticular or vitreal opacification. To perform reliable visual sensitivity evaluation, blur of the retinal image must be minimized with proper refractive correction for the test distance, especially for small test stimulus sizes. As refractive error diminishes detection sensitivity mostly within the central visual field, appropriate refractive correction for the test distance is mandatory for campimetry. Beyond 30 degree eccentricity from the fovea, no significant effect of target blur on detection exists in conventional perimetry^{47,52} although motion detection is suppressed by refractive error as far as 80 degrees in the peripheral visual field^{53,54}.

Colour

It is desirable that the stimulus and background wave-length composition (spectrum or colour) should be specified along with their luminance since even white light sources may have different spectral compositions and the thresholds would be different to different colours. The exact definition of the wave-length of the stimulus light is more important when colour fields are measured.

Mode of Presentation

The vast majority of clinically used conventional equipment present a single stimulus at a time. A few portable and semi-automated tangent screen campimeters operating with multiple stimuli such as Herrington-Flock Screener⁵⁵, Friedman⁵⁶ and Henson Analyzers⁵⁷ have been described. The subtle differences between response properties to single and multiple static stimuli are discussed in detail elsewhere⁵⁸.

1.2.5. Other Observer Factors

Patient Experience and Fatigue

A high number of abnormal points may occur in the periphery of the field during the first visual field test of an inexperienced normal person, especially when static threshold method is used. These false abnormal points tend to improve with repeated testing as the patient develops experience⁵⁹. Similar defective test locations may occur in mid-periphery of the visual fields of ocular hypertensives and with increased experience, the number of depressed points, the total defect and the intra-test variability decrease⁶⁰. In glaucoma patients with previous experience in kinetic perimetry, repeat threshold static perimetry does not display any further training or experience effect⁶¹.

The field results tend to deteriorate with continuous testing for longer than a few minutes as a result of patient fatigue and the fatigue effect becomes more obvious during the testing of the second eye leading to less gain from experience^{62,63}.

Pupil Size

The luminance (measured at the centre of the entrance pupil of the eye) and the pupil area provides an estimate of retinal illuminance. The retinal illuminance (in Trolands) is the stimulus luminance (cd/m^2) multiplied by pupillary area (mm^2). With smaller pupil sizes, the retinal representation of the stimulus becomes weaker. Pupil size changes also alter the level of retinal light adaptation. With large pupil size the directional sensitivity of the retina changes as the far peripheral pupillary zones are less effective in stimulating a response than the central pupillary area in the normal individual at photopic levels (the Stiles-Crawford effect). This factor is generally overlooked in clinical work. As it is impractical to control pupil size or define retinal illuminance for each eye tested in routine practice, only the stimulus luminance is mentioned. Pupil size alters the retinal adaptation state by changing retinal illuminance. The use of

cycloplegics and miotics may alter retinal adaptation levels by nearly 2 logarithmic units (i.e., 100 times) through pupil diameter changes⁶⁴. Additionally, peripheral ocular aberrations become more pronounced with dilated pupil causing visual blur and an apparent reduction in the visual field. Miotic agent induced pupil constriction also results in stimulus blur due to increased accommodation. Pupil sizes of 3 mm to 6 mm are regarded as the normal range with no detrimental effect on the stimulus detection.

Troxler's Phenomenon (Neurogenic fast local light adaptation)

A non-moving stimulus stabilized on the retina will fade and disappear after a few seconds if the fixation is maintained very still. In the peripheral field, the disappearance of the stimulus takes place even if the fixation is not steady. Blinking, periodical stimulus presentation and slight eye movements return the stimulus to detection. Troxler's phenomenon is considered independent of photochemical mechanism and the site of origin is probably at lateral geniculate nucleus⁶⁵.

1.3. Clinical Testing of Visual Field

The goal of conventional clinical visual field testing is to measure detection sensitivity to a white light onset stimulus in different regions of the field at low photopic background luminance levels with an attempt to identify normal and abnormal ('scotomatous') areas showing sensitivity loss. Two general techniques for visual field assessment are manual kinetic and automated static perimetry.

1.3.1. Isoptre and Scotoma

The highest sensitivity is normally found in the fovea which is the centre of the visual field and sensitivity progressively decreases towards the periphery. The test locations in the visual field that have the same sensitivity for a stimulus of fixed size, contrast and exposure duration on a fixed background brightness is named an "isoptre". A topographic map of the visual field may be obtained with a series of isoptres formed by lines or grey tones, each representing a particular level of contrast sensitivity.

A "relative scotoma" is a partial visual deficit in a given isoptre area of visual field in which sensitivity decreased (contrast threshold is elevated) beyond normal variation. Nonetheless, maximum intensity or maximum size stimulus is still detectable in a relative scotoma. An "absolute scotoma" implies total loss of vision in a given field area in which the maximum stimulus contrast (the largest or most intense stimulus available) is not detected inside an isoptre.

1.3.2. Kinetic Perimetry

In manual kinetic perimetry, a stimulus of fixed size and contrast on a defined background is moved from non-seeing to seeing or vice versa until the appearance or

disappearance of the stimulus is detected by the patient. This procedure is repeated along several meridians. The lines connecting all the detection and disappearance loci defines the isoptres and field abnormalities to that particular stimulus-background combination. A number of isoptres may be determined and the quantification of the visual field defect may be achieved by altering the stimulus intensity and/or size. Kinetic perimetry enables more speedy field examination, but sometimes lacks reliability because of its dependence on patient's reaction time and the speed of target movement. In kinetic perimetry, the stimulus is continuously exposed and the motion of the stimulus also contributes to its detection (Riddoch Phenomenon).

1.3.3. Static Perimetry

If visual field testing is performed with non-moving stimuli, the technique is "static"⁶⁶. Static stimuli can be presented at selected locations to perform spot checks inside the isoptres in combination with manual kinetic testing with Goldmann or Tubingen perimeters. The ascending method which presents increasing intensity stimuli until detection is the preferred one in manual static perimetry. Purely static examination with manual perimetry is time-consuming and used in a limited scale. During 1970s, static perimetry became computerized with the work of Lynn and Tate⁶⁷ and gained a rapid acceptance in the form of Octopus⁶⁸ and Competer⁶⁹ Perimeters. Automated (computer-assisted) static perimetry which involves presentations of non-moving stimuli at selected locations briefly under computer control is the more scientifically rigorous, although manual kinetic perimetry has its advantages in certain situations. The latest design of a series of different types of computerized static perimeters is Humphrey Visual Field Analyzer⁷⁰ which is now the most widely used automated perimeter.

In automated static perimetry the stimulus is kept fixed in size and retinal location, and it is presented for a controlled exposure duration in the visual field. The test sequence follows a staircase procedure to estimate the threshold. The contrast of the stimulus is

either increased (ascending) or decreased (descending) by the computer until the stimulus is detected or missed by the observer. After the reversal of patient responses occurred, stimulus intensity may be altered in opposite direction with smaller steps. The staircase procedure in current practice terminates after crossing the threshold once or twice and that design is considered closest to ideal⁷¹. It is customary to define the stimulus intensity of a computerized perimeter and the determined threshold results in decibel (dB) units. The brightest stimuli have the intensity of 0 dB and increasing sensitivity (the ability to see dimmer stimuli) is denoted by higher dB values. The stimulus contrast may be changed as little as one decibel (i.e., 0.1 log-unit steps) with each presentation after the determination of contrast at a selected locus. The stimulus is moved to a different retinal position randomly after each presentation during the threshold measurement procedure with staircase method.

A series of contrast threshold determinations may be performed in the overall field to obtain the 'hill of vision' or along a selected meridian to represent a sensitivity profile across the visual field. The random order of stimuli presentations across the field of vision and accurate registry of patient responses without the need for a perimetrist facilitated the examination substantially by decreasing the test time and eliminating the operator variability. As the goal of clinical perimetry is to assess detection sensitivity in the visual field, automated static perimetry comes closest to a rigorous definition of sensitivity.

Before commencing a computer-assisted static visual field measurement, the following instructions should be given: "Watch the fixation target at all times without looking around to see the stimuli. Push the button as soon as you think that you see a spot in the side vision. If you are not sure, but if you think that you saw a spot, press the button anyway. Do not push the button if you don't think that there is a spot. Don't worry if you think that you don't see spots for a while, this is normal. You may blink normally during the test. Please do not talk during the test. But, if you feel uncomfortable or need some rest or if you lose concentration, ask for a break."

In computerized supra-threshold static perimetry, stimuli stronger than the expected threshold values are presented at each test location. If the first stimulus intensity is detected, no further presentations are made at this location. This method is used for screening for abnormalities without any quantification, saving time at the cost of reduced information.

1.3.4. Representation of the test results (Cartography)

Graphic Display

In manual kinetic perimetry, stimulus locations where the detection occurred are outlined with a pen by the examiner to identify isopters to particular stimulus settings at the end of the examination. Similarly, in manual static visual field testing with Friedman Analyzer, stimulus detection is recorded manually with symbols.

Grey Scale (Symbols) Display

The most common visual graphic representation of the automated visual field test results is the grey scale plot. The sensitivity values obtained from the examination are assigned different sized or shaded symbols on the printout of the test result. Generally, the larger or darker the symbol, the lower the sensitivity. The symbols may appear only at the tested locations or, the spaces between the tested locations are also interpolated such that the visual field appears in various shades of grey as the periphery of visual field has lower sensitivity than the centre. The grey scale plot, therefore, becomes darker towards the periphery of the field.

Numeric Display

That simply reflects the dB threshold values at tested locations on automated perimeters

such as Humphrey VFA. The determination of depressed numeric threshold values in a given test result may be achieved by comparing the each threshold value to the surrounding locations⁷²⁻⁷⁴. Comparison of threshold values between the mirror image test locations in both eyes of the same individual⁷⁵ or across the horizontal⁷⁶⁻⁷⁸ and vertical⁷⁹ meridian of each field also identifies sensitivity loss. A few test points with significantly reduced sensitivity may occur easily by chance alone. Such false-abnormalities are, however, scattered randomly in the field as they occur independently. Clusters of depressed points of two or more are regarded as true defects⁸⁰.

1.4. Visual Field Test Instrumentation

1.4.1. Bjerrum Screen Campimeter

A white or colored disc at the end of a wand is presented against a black or grey cloth background. A self-luminant stimulus is also described for the same technique⁸¹. The stimulus contrast is determined by the reflectance of the disc and the background. Because contrast is fixed, the size of the target must be varied in order to change stimulus detectability. Isoptres measured with the Bjerrum screen are for the stimuli of different angular size but of constant contrast. In contrast, the projection perimetry such as Goldmann uses targets of different contrast but constant angular size. The Bjerrum screen is usually illuminated by a light source from above and that results in lower screen luminance at the bottom than that at the top, and that induces different levels of retinal adaptive state in different parts of the visual field. Subsequently the visibility of the same size and contrast stimulus may be different at the top or bottom of the screen. A way of getting around this problem is keeping the stimulus fixed on the screen and having the eye fixed at the end of a wand²⁵. By moving the wand and the eye in different directions, the visibility of the stimulus may be measured.

1.4.2. Goldmann Perimeter

This device has a hemispheric bowl background which has a radius of 30 cm and which is set at a luminance of 10 cd/m². Six different sizes of stimuli varying from 1/16 mm² (i.e. Size 0) to 64 mm² (i.e. Size V) may be presented on the background through a projection system. The stimulus sizes are arranged in a way that each stimulus is of four times the area of the previous one. Through different filter settings the brightness of each stimulus may be varied with 0.5 log-units (filters 1 to 4). Further 0.1 log-units steps are achieved with additional five steps of filters (i.e., a,b,c,d,e). The maximum

stimulus intensities obtained with filter settings for 'e' (that is, 318.3 cd/m² or 1,000 apostilb). Filter combination '1-a' has the lowest luminance, measuring 13 apostilb. In addition to kinetic presentation, static spot checks may be performed in desired locations within any isoptre using a shutter mechanism. A telescope is used to monitor eye movements.

1.4.3. Tubingen (Harms-Aulhorn) Perimeter

This device is similar to but more versatile than the Goldmann perimeter and comes with a hemisphere of 33 cm. radius. The background intensity may be varied from 3.183 to 3.183 x 10⁻⁶ cd/m² in 5 log-unit steps. The stimuli may be presented in circular or rectangular shape, ranging in diameter from 7 to 114 minutes. The luminance of the test stimuli may be varied from 318.3 to 3.183 x 10⁻⁸ cd/m² in 0.1 log-unit steps. A precise shutter allows exposure durations of 0.1 second or more. Both kinetic isoptre plotting and static spot checks can be performed. Fixation monitoring is provided by a technician, using a telescopic viewer.

1.4.4. Friedman Visual Field Analyzer

The Friedman Analyzer consists of a strobe light that flashes for about 0.5 msec. and evenly illuminates a translucent screen (a diffuser). The diffuser is used as the test surface and the light emitted by the strobe light forms multiple stimuli on that screen. A pair of opaque black plates with 98 holes sits in front of the screen as the patient sees it. An underlying rotary plate with holes on it can be placed in 31 positions (A to Z) with a lever. The superimposing holes on two overlying plates form groups of stimuli of 2 to 4 every time the strobe is flashed. The holes are larger towards the edge of the plate and smaller near fixation. The size gradient is adjusted for the hill of vision so that when a given stimulus intensity is determined to be at suprathreshold for a certain

amount at one location, the other locations would be equally suprathreshold. The intensity of the flashes can be attenuated from the maximum intensity of 1000 apostilbs by filters in two decibels (0.2 log-unit steps). An external light source illuminates the front plate surface and presents the background illumination. The Friedman Mark-II table-top instrument offers two strategies for examining the inner 25 degrees of the visual field: a standard program of 60 points in 18 patterns, and an extended program of 98 points in 31 patterns, each pattern formed by a set of stimuli of 2 to 4. The protocol for the standard test program sets the initial brightness level of simultaneous patterns of 2, 3 or 4 points to coincide with the patient's age-expected-level; generally as 0.2 log-units above the age-normative threshold value. Any missed points are retested at increased luminance obtained by reducing the amount of neutral density filter in increments of 0.2 log-units until a positive response (that is, detection) is achieved. Thus, it is possible to quantify the detection sensitivity at each test location as normal or either a relative or absolute defect. The principles of Friedman Analyzer combined with semi-automation were made available in Henson Analyzer.

1.4.5. Dicon Auto-Perimeter

Dicon Automated Perimeter uses light emitting diode (LED) stimuli which produce yellow-green light with a peak wave-length emission of 570 nm. The Dicon AP 3000 Perimeter has 512 LEDs distributed on a hemispheric bowl of 33 cm radius. The background intensity may be set to 0, 10, 31.5 or 45 apostilbs (asb.) by the user. LED stimulus size is equivalent to Goldmann I target (i.e, 0.25 mm²). The actual brightness of each LED may go to a maximum of 10 000 asb. and may be reduced to 1 000 asb. with a diffuser mounted in front of LEDs. The device may perform suprathreshold or threshold related screening as well as full thresholding. The results may be printed in numeric and grey-scale plots as well as meridional profiles. The Dicon AP 3000 has 379 of the LEDs within the central 30 degrees with 2.5 degrees separations. A video-fixation monitor, dual disc drives, CRT user screen, a touch-light pen and thermal dot-

matrix printer are standard equipment. Fixation monitoring is achieved with intermittent blind spot checks (Heijl-Krakau method) under software control in the Dicon Perimeter.

At the beginning of a test, 21 closely spaced points centred at the normal location of the physiological blind spot are tested. The computer locates the centre of the blind spot defined by the missed points. In the normal mode of operation of the monitor during field testing, a stimulus is presented at the centre of the blind spot every 7-10 seconds. If the patient responds to that stimulus a fixation loss is recorded. The number of fixation losses serves as an index of fixation quality.

1.4.6. The Octopus Perimeter

A number of perimeters have been marketed as part of the 'Octopus' family. They are hemispheric (i.e., bowl) perimeters presenting the light stimulus with a projection system in standard Goldmann stimulus sizes, providing a number of suprathreshold and threshold strategies and various test grids. Fixation monitoring is achieved with an infra-red camera which synchronizes the stimulus presentations according to the maintenance of fixation. In general, the Octopus perimeter is the European counterpart of the Humphrey Visual Field Analyzer (VFA). The Octopus perimeter comes with a statistical interpretation software, the 'Octo-soft Program'. The full details of the Octopus system are available elsewhere ^{73,82-84}.

1.4.7. The Humphrey Visual Field Analyzer

The Humphrey VFA is a computerized automatic projection perimeter, capable of producing Goldmann standard sizes of test stimuli and 1 dB precision in stimulus brightness levels. The decibel (dB) notation indicates filtering in stimulus brightness. For instance, 0 dB means no attenuation in stimulus brightness and the maximum intensity of 10 000 apostilb whereas 10 dB and 20 dB indicate 10 and 100 times

decrease in stimulus brightness (i.e. down to 1000 and 100 apostilb) respectively. A hemispherical bowl background, a customized built-in computer, user CRT monitor fitted with a light pen and a printer are housed in a single cabinet. Among a range of different models, the most developed one includes hard and floppy disc drives, a video-monitor for fixation check and a cartridge backup. Test commands are chosen from a series of menus that appear on the CRT monitor. Full details of the setting and operation of the Humphrey VFA are described in the manual that accompanies the device⁸⁵. Humphrey test software enables both full thresholding and suprathreshold screening tests.

Threshold Strategies

They are designed to quantify the visual threshold at every test location in the test pattern. In addition to the standard 'Full Threshold' mode, other methods such as the 'Full Threshold from Prior Data' and 'Fast Threshold' strategies are available. The latter two save time as they use the previous test results of the patient as the baseline, but in turn do not allow statistical evaluation with the interpretation software 'STATPAC' or 'FASTPAC'. Among a number of full threshold test grids available, the most frequently used ones are 30-2 and 24-2 programs which test 76 or 54 test locations with 6 degree resolution in the central 30 degree and 24 degree visual field respectively. The test grids which provide 6-degree resolution between the test locations of these two programs avoid vertical and horizontal meridians allowing better assessment of the correspondence of detected scotomas to those meridians in neuro-ophthalmology and glaucoma.

Suprathreshold Strategies

Several screening test grids are available for the central field, involving 40 to 166 test points and also for peripheral field and full field. Four screening strategies available are single intensity, threshold related, three-zone and quantify-defects programs.

Single intensity screening strategy: A particular stimulus is chosen and the visual field is screened with that stimulus. The default stimulus intensity is 24 decibels and can be altered. The limitation of this program is that when a single target intensity is used to screen the entire visual field it will be markedly suprathreshold near the centre, but may be close to threshold or even infrathreshold near the periphery. Shallow relative defects may therefore be missed near the centre, while normal points may be screened as abnormal near the periphery.

Threshold related screening strategy: The threshold is actually determined at four points around the fixation in the visual field before the screening portion of the test is begun. Using the threshold values obtained in each quadrant, the computer automatically constructs a theoretical hill of vision and estimates the expected threshold at each test location in the screening test pattern. The screening test stimuli are presented as six decibels brighter than the estimated thresholds in the rest of the visual field. Any defect deeper than six decibels should therefore be detected.

Three-zone strategy: Defects detected with the 6 dB suprathreshold target is retested with a very bright or maximal luminance stimulus of 10,000 Asb (i.e., zero decibel). This allows the screening test to distinguish relative and absolute scotomas.

Quantify-Defects strategy: In that program the actual threshold is measured at any point found to be abnormal on screening with the six decibel suprathreshold target. The main purpose of screening visual field examination programs of Humphrey VFA are to establish the presence or absence of a visual field defect and indicate the boundaries of the scotomas. They are particularly useful among those patients who have not had previous visual field examinations. They are not suitable for quantification of field defects or careful follow-up of patients to determine the progression of the disease or the effectiveness of the treatment. Central 76 point screening grid is identical to that of threshold program 30-2.

1.5. Automated Visual Field Interpretation

1.5.1. Reliability Indices (Catch - Trials)

Fixation Losses

The frequency of fixation losses is used to assess the patient's cooperation for steady fixation during the test. In the Humphrey visual field analyzer, the ratio of number of fixation losses to the total number of stimulus presentations in the physiological blindspot is recorded. More than 20% fixation losses is regarded as a sign of low patient cooperation. During the first threshold test, 45% of glaucomatous and 30% of the normal subjects produce unreliable results because of difficulty in maintaining a stationary fixation as well as too many false negative responses in glaucoma cases⁸⁶. Among ocular hypertensives, low test reliability mainly due to fixation instability was found in 35% of cases on initial testing, decreasing to 25% with experience⁸⁷. In several repeat testing, 4% of normals and 8-9% of ocular hypertensive and glaucoma patients consistently fail to produce reliable results with lack of reliability being almost exclusively due to fixation losses^{87,88}. Although lack of accurate fixation does not cause false field defects in normal eyes, they lead to underestimation of the existing defects in glaucomatous eyes⁸⁹.

False-Positive Responses

The number of occasions in which the response button is pressed without a stimulus being presented represents the patient's over-willingness to see in the field of vision. If the number of false positives are greater than 33% of attempts, the result is unreliable. High number of false positive responses causes underestimation of existing field defects.

False-Negative Responses

Occasionally, an easily detectable (too bright stimulus) is presented and the patient is expected to press the button. The number of 'no' responses to such bright stimuli should normally be less than 33% of the total attempts to qualify as a reliable result. Abnormally high numbers of false negatives indicate the patient's lack of attention to the stimulus presentations during the test. High false negative rates lead to apparently abnormal fields in normal subjects and overestimate the existing glaucomatous field defects for about 9 dBs⁸⁹.

Factors such as age, pupil diameter and visual acuity do not influence the reliability parameters⁸⁶.

1.5.2. Normal Reference Field

The sensitivity in the visual field decreases with eccentricity and age^{90,91}. The detection sensitivity to static light stimuli declines for 0.14 - 0.26 dB with each degree of eccentricity. An average of 0.5-0.6 dB depression in sensitivity occurs within the central visual fields in each decade of life. The linear decline in detection sensitivity to light with increasing age at all test locations^{17,92,93} make it necessary to define the limits of normal for test locations to enable comparisons between the results from same or different individuals.

According to LeBlanc, a sensitivity depression of 5 dB or more in reference to age-expected normal sensitivity at any given test location is abnormal⁷⁵. That, however, was based on the assumption that the threshold variability with age or between the individuals had a normal distribution at each test point and the variability was constant with a uniform standard deviation of 2.4 dB⁹⁴. Heijl and co-workers found that the threshold values did not have a normal distribution at any test point and the variability

in threshold was not constant at different locations⁹⁵. In other words, what is normal in one test location may be significantly abnormal in another. The significance limits (i.e. confidence intervals) should, therefore, be defined at each test location individually.

The significance of the differences between the measured and age-expected threshold values⁹⁶ at different test locations are represented in empiric probability maps^{95,97} and deviation maps⁹⁶. Such maps are easier and more accurate to interpret than the grey and numeric scale maps.

1.5.3. Global Visual Field Indices

The statistical software packages, OCTOSOFT and STATPAC, incorporated in Octopus and Humphrey Visual Field Analyzers respectively, perform comparisons between the individual test results and age-expected normal visual field threshold values stored in the computer data-bank. They facilitate the recognition and analysis of the defects on a single visual field test by calculating the global visual field indices and statistical significance of sensitivity deviations (i.e., 'Probability Maps'). A series of repeat tests can be processed and compared by this software package also.

A more recently designed statistical software package, FASTPAC, of Humphrey VFA serves to the same purposes. The difference between STATPAC and FASTPAC is simply the method of threshold determination at test locations. The decibel values used in STATPAC are obtained with double crossing of the threshold with ascending and descending steps in the stimulus brightness with 4 dB and 2 dB steps respectively as opposed to FASTPAC results which represent threshold crossing only once with 3 decibel steps⁹⁸.

Global visual field indices are intended to summarize clinically important features in the visual field by using conventional statistical methods such as means and standard

deviations. The calculation of the global field indices is possible only when the age expected normal threshold values are known for each of the individual test locations in different age groups.

Mean Sensitivity (MS)

The MS reflects the mean of the decibel threshold values measured at all test locations.

$$MS = \frac{\sum_{i=1}^m x_i}{m}$$

(x_i = measured sensitivity of test location i ; m =number of test locations tested, 52 for the test grid employed in the study).

That index is sensitive to a diffuse change in the visual field and insensitive to small localized changes. It is also affected by media opacities, refractive errors and small pupil size. Since it is not corrected for age, the mean sensitivity should decrease with age in all individuals.

Mean Defect

The mean of the differences between the measured and age expected threshold values represent the total damage and named 'Mean Defect'.

$$MD = \frac{\sum_{i=1}^m (z_i - x_i)}{m}$$

(z_i = age expected sensitivity of test location i)

MD was introduced by Flammer⁹⁹ and is mostly influenced by diffuse damage and also by pre-retinal factors such as pupil size, refractive error, and media opacity. It is not sensitive to small localized areas of field loss⁵⁵. Unlike the 'Mean Sensitivity', 'Mean

'Defect' should not increase with age in a normal individual. 'Mean Deviation' is the reciprocal of 'Mean Defect' in the Humphrey VFA.

Loss Variance (LV)

The 'Loss Variance' is an index of irregularity in the shape of the hill of vision. It is intended to be sensitive to localized damage in the field of vision¹⁰⁰. The square root of the LV is used in the Humphrey VFA and is named 'Pattern Standard Deviation' (PSD). LV is calculated by:

$$LV = \frac{\sum_{i=1}^m (x_i + MD - z_i)^2}{m-1}$$

Short Term Fluctuation (STF)

This index reflects the variability in the individual threshold values with repeated testing during the test (i.e. intra-test and intra-individual variability). Ten randomly selected stimulus locations were measured twice during the test session and the average variability in the repeat threshold values obtained from both locations is first calculated. The square-root of the mean variance of all tested locations is taken as the short term fluctuation.

The STF may be 3 dB in a single threshold determination and is reduced to 2 dB as a result of two subsequent determinations^{101,102}. STF less than 2 dB is normal. When the short term fluctuation is higher, it may represent low level of patient cooperation and vigilance, especially in the presence of other abnormal reliability indices. When the other reliability indices are within normal limits, a high STF may be the first sign of visual field disturbance, such as in glaucoma^{103,104}. Therefore, STF is also a global field index (see below). Patient fatigue may also increase the STF.

The variability of the threshold results from the same individual on different test occasions (Inter-test variability) is 'Long Term Fluctuation (LTF)'. LTF seems to be dependent of the presence of visual field abnormalities and is greater in patients with deteriorating fields, although it is unrelated to age or eccentricity ¹⁰⁵. Long term fluctuation remains one of the major challenges in automated threshold visual field testing.

Corrected Loss Variance (CLV)

The 'corrected loss variance' is the 'loss variance' adjusted for 'short term fluctuation'. It is derived by:

$$CLV = LV - STF^2$$

CLV is analogous to the 'corrected pattern standard deviation (CPSD)' index in Humphrey VFA. CLV provides a more accurate estimate of localized damage since both STF and/or localized damage can cause an elevated Loss Variance. The CLV filters out the intra-test variability component and leaves the true localized defect in the visual field.

The calculation of global field indices are performed in the same way in STATPAC and FASTPAC .

1.5.4. Empiric Probability Maps

It is impossible to define the minimum normal threshold with a single decibel value for all test points. It is therefore necessary to determine the significance limits for threshold deviations for each individual test point location. As a result these significance limits were implemented in graphical display of probability maps showing the statistical

significance of deviations obtained at the individual test locations in a patient. STATPAC of the Humphrey VFA calculates and prints out 'Total Deviation' and 'Pattern Deviation' empiric probability maps to assist interpretation.

The 'Total Deviation' Probability Map

For each individual point of C30-2 grid except those two in the blind spot (ie. 74 locations):

- i) the difference between the observed and age expected dB threshold is calculated,
 - ii) the deviation is compared to the confidence limits which are empirically determined and stored in the data-bank of the computer,
 - iii) the highest significance reached, $p < 5\%$, $p < 2\%$, $p < 1\%$ and $p < 0.5\%$, is determined,
 - iv) a symbol is plotted at the corresponding location for the highest significance p value.
- The total deviation in an individual test point is the sum of the deviation caused by diffuse (generalized, homogenous) reduction in sensitivity plus localized reduction in sensitivity.

The 'Pattern Deviation' Probability Map

To filter out the diffuse loss component and reflect localized 'pattern' loss only, it is assumed that the most sensitive points in the field are outside any existing localized defects. Therefore:

- i) The differences between the observed and age-expected threshold values are ordered from the most negative (lowest sensitivity) to the most positive (highest sensitivity) excluding the test points in the outermost ring of the test grid (C30-2) and the one below the physiological blind spot,
- ii) The 85th percentile lower limit of the deviations from all 51 test location is determined and considered as the estimate of the diffuse component,
- iii) The diffuse component is subtracted from each of the individual differences between the observed and age-expected thresholds. The final numeric value is the dB pattern

deviation at each test point.

iv) The significance (p value) reached by each of these differences is displayed with a symbol on the 'Pattern Deviation' map.

Thus, the 'Pattern Deviation' map shows only the localized component of the field loss.

The empiric probability maps indicate even the most shallow significant deviation from normal and also help categorize the abnormal points according the depth and statistical significance of the defects. Test point significance on an empiric probability map indicates only how often a particular threshold value occurs in the normal population. Its significance level does not mean that the chances of a given amount of deviation being normal. The probability maps are accepted as aid for clinical interpretation ¹⁰⁶⁻¹⁰⁸ and have also been used for research ¹⁰⁹⁻¹¹¹.

1.6. Video Display Unit (VDU) and Video-Campimetry

1.6.1. Cathode Ray Tube (CRT)

One way of presenting visual field test stimuli is to use a cathode ray tube (CRT) and its screen as the background. In a color CRT, three beams of electrons are emitted from the cathode guns, formed into a beam (cathode ray) by the anodes, and accelerated towards the front surface of the tube (Figure 1). The intensity and direction of the beam may be varied by magnetic coils. The phosphor material covering the inner layer of the front surface of the CRT transforms the kinetic energy of the electrons forming the cathode rays into red, green and blue light and a pattern or an image. Variation in the intensity of each beam results in different colour hue combinations. Different white light intensity levels can also be obtained by varying the red, green, blue phosphor emissions simultaneously and equally. The cathode ray tube emits several electromagnetic radiation and field types, but that radiation has no adverse effect on human health¹¹².

A video display unit is a system controlling the operation of a CRT according to the input coming from an external signal source, such as a video camera, television, broadcast transmission or a computer. To accurately focus the beams on the appropriate colour phosphor, the electron beams are passed through an aperture referred to as a shadow mask. The CRT screen is divided into cells, i.e. pixels, each pixel being formed by a group of three colors of phosphors. Pixels are the smallest unit area on the screen. A pixel's physical size depends on the size of CRT and its screen resolution. The screen resolution (clarity of detail) becomes higher with smaller pixel size. The combination of pixels form the foreground and background of an image by providing contrast between the pixel groups.

A video display unit monitor under computer control turns any pixel on or off independently on the screen. Each pixel has defined coordinates horizontally (i.e., X-

axis) and vertically (i.e., Y-axis) on the screen. The internal controller of the video display unit lets the computer software determine the resolution of the screen. In an 'Enhanced Graphics Array' (EGA) video system, the screen resolution is 640 x 350 pixels, on X and Y axis respectively. In video graphics array (VGA), the screen resolution is 640 x 480 pixels. The size of each pixel can be calculated simply by dividing the horizontal and vertical dimensions of the CRT by the number of pixels on each axis.

In a non-interlaced CRT display, the electron beam scans sequentially across each horizontal line of the display starting from the top. At the end of each horizontal scan, the electron beam flies back to the beginning of the subsequent horizontal scan of the next lower line. The completion of scanning the all screen until the bottom line is formed takes a fraction of a second. The vertical refresh frequency of a display expresses the number of complete scans and appearances of an image per second¹¹³. The IBM 8512 video-display unit used in this study had the vertical refresh rate of 70 Hz., per image taking 14 milliseconds to complete. Because of the refresh rate, the display screen will appear to flicker in some conditions.

The flicker sensation can be decreased by increasing the refresh rate of the monitor, by decreasing the number of lines on the display, alternately refreshing the odd and even-numbered display lines (interlace) and increasing the persistence of the phosphor, with each having its own perceptual and technical trade offs¹¹⁴. The flicker sensation is also dependent on the luminance of the screen, becoming more perceptible with increasing screen brightness. On 10 cd/m² background the flicker sensation does not happen as the screen vertical refresh rate (70 Hz) exceeds the critical flicker frequency (i.e., CCF; 20-50 Hz) on a range of varying background intensity levels¹¹⁴⁻¹¹⁶.

The electron beam velocity, the rate at which the electron beam is modulated (i.e., video bandwidth), the velocity of horizontal fly back and the vertical velocity of the beam all place constraints on the distance between addressable pixels (i.e., display addressability)

and the way a single pixel appears on the screen (i.e. display resolution). The cathode ray tubes are available with a number of different phosphor types and phosphor decay times. The phosphor decay of current CRTs vary from fractions of one millisecond to a few milliseconds¹¹⁷. There are three different ways in which different colors of phosphors are arranged in a pixel; vertical lines, vertical slots or, as in the IBM monitor used in the study, triplet points.

Different color combinations, hue and saturation can be obtained by changing the intensity of each of the three beams. The luminosity of a CRT is determined by the type of the phosphor used, its refresh rate and the cathode voltage¹¹⁸. The screen radiance in the CRT is mainly the result of the beam current which is controlled mainly by the control voltage of the cathode guns. As a result, the screen radiance has a positive linear relationship to the beam current¹¹⁹. The spectral composition (colour) of the chromatic CRT brightness is dependent on the regulation of the voltage and is potentially variable with voltage fluctuation. Any irregularities in the screen voltage of the CRT may result in a change in the radiance of one color beam without affecting the others. When the intensities of three guns are kept equal, different levels of achromatic luminance, varying from black and dark grey to white, are achieved. In monochrome CRTs, the screen intensity is determined by one beam which forms only tones of grey for each pixel available, forming achromatic patterns¹²⁰. The coordinates of the pixel by pixel stimuli area on the background are determined by the VDU zoom-scroll circuitry. A detailed technical description of CRT operation is available elsewhere^{119,121}.

1.6.2. Video-Campimetry

The use of computer graphics and video-display units was first described in the analysis of visual fields with the conventional light stimulus by Accernero¹²² and found a rapid acceptance in several forms of testing such as Colour Contrast Perimetry^{123,124}, Ring Perimetry¹²⁵, Motion Detection Test¹²⁶, Fine Matrix Perimetry¹²⁷⁻¹²⁹ and Noise-field

Campimetry¹³⁰ involving personal computers and conventional "oculo-static" fixation with an adequate method of monitoring the patient's fixation either with intermittent blind spot checks or additional attachment for infrared eye movement detection. Suprathreshold strategies with single¹³¹ and multiple^{132,133} conventional light incremental (onset) stimuli combined with voice activated response registry were reported in video-campimetry. Also, single intensity kinetic high-contrast offset (i.e. black) stimulus is experimented in video-campimetry^{134,135}. None of the previously described methods are configured to perform threshold or suprathreshold visual field examination with static light offset (dark-on-bright=negative contrast=decremental) stimuli conforming with the established perimetric standards. Computer Assisted Touch Screen (CATS) Campimeter was developed to offer single and multiple static light offset stimuli with novel touch-screen as well as mouse-emulated patient interface and optional forced-choice fixation monitoring in both screening and threshold modes¹³⁶. Computer-Assisted Moving Eye Campimeter (CAMEC) also accommodates the single stimulus characteristics of CATS in combination with dynamic fixation maintenance which allows excursion of the eye during the test.

1.6.3. Other Unconventional Perimetry

Visual field examination with different types of stimuli, fixation control and response registry methods have been described. The broad reviews of other novel computerized perimetric techniques such as Flicker and Temporal Modulation Perimetry, Pattern Discrimination Perimetry, Scanning Laser Ophthalmoscopic Perimetry, The Whole-field Scotopic Perimetry, Layer-by-Layer Perimetry, Acuity Perimetry, High-Pass Resolution (Ring) Perimetry, Peripheral Displacement (Motion Detection) Perimetry, as well as other psychophysical and electrophysiological methods such as Spatial and Temporal Contrast Sensitivity Testing, Pattern Electoretinograms and Pseudo-random Binary Pattern Stimulation which are experimented in visual field assessment are available elsewhere¹³⁷⁻¹⁴¹.

1.7. Sensory Visual System

The retina is the visual sensory end organ of the central nervous system and forms the inner layer of the eye globe. It consists of a layer of photo-receptor cells (rods and cones) whose axons synapse with other modulator neuronal cells (bipolar, horizontal and amacrine cells) which process the response (Figure 2). These modulator cells in turn synapse with retinal ganglion cells. The axons of ganglion cells form the nerve fiber layer which forms the top layer of the retina and the optic nerve at the disc. The neural signals initiated by the ganglion cells are transmitted to the occipital visual cortex of the brain via the optic nerves, optic tracts, lateral geniculate nuclei and the optic radiation¹⁴²(Figure 3).

1.7.1. Rods and Cones

'Visual Gain' is defined as the ratio of the magnitude of the physiological response to the stimulus magnitude, forming the balance and physiological sensitivity in the visual system. The photoreceptors constitute the first step in the visual system in which visual gain is established at different light adaptation levels for different retinal eccentricity and target sizes ^{143,144}.

There are an average of 57.4 million rods and 3.3 million cones in the human retina¹⁴⁵. The number of photo-receptor cells is dependent on the size of retinal surface area and optic disc. The photo-receptors in the fovea centralis which is the centre of the visual field, are exclusively cones. In the same area, the rods are virtually absent. The cones are responsible for photopic and color vision. The cones contain three different photopigments to have a maximum absorption at about 440 nm (short wave length sensitive; blue), 535 nm (middle wave length sensitive; green) and 570 nm (long wave length sensitive; red). The cones are also scattered in the peripheral retina where rods are the main photoreceptors. The rods function at low levels of illumination forming

scotopic vision. The optic disc has no photoreceptors and is a blind spot in the field of vision¹⁴⁶.

The fovea centralis contains approximately 200 000 cones/mm². The remaining retina contains about 5 000 cones/mm² which decline in intensity towards the periphery. The rod density has its peak at 3 mm (20 degrees) from the fovea centralis with 150 000 rods/mm² and that decreases less abruptly than the cone population to about 35 000 rods/mm² at the periphery¹⁴⁷. In result, the distribution of the optic nerve fibers to the ganglion cells and photo-receptors is not uniform. In the foveola, approximately 150 000 cones are connected to twice that many ganglion cells, each cone connecting to two ganglion cells. In the far periphery, there may be as many as 10 000 rods connected in clusters to a single nerve fiber with considerable overlapping so that a point light stimulus excites several clusters at once¹⁴⁶. The resolution sensitivity of the photoreceptors as a result varies with eccentricity, background luminous saturation and the representation of the retina in the visual cortex¹⁴⁸.

The sensitivity of the eye for the detection of a stimulus varies with the level of adaptation to dark and light backgrounds. The light and dark adaptation have two mechanisms, namely a neural process that is completed in about 0.5 seconds and a slower photochemical process involving molecular changes in visual pigment that occurs in about one minute for light adaptation and 45 minutes for dark adaptation⁴⁶. Above the retinal illuminance level of 3.2×10^{-3} cd/m², cones start to contribute to visual sensitivity along with the rods (mesopic level)⁴. Traditionally, rods are taken to be saturated about 3 cd/m², but above this level, rods still contribute to colour vision and pupil size⁴¹. Nonetheless, the conventional adapting luminance used with the Goldmann perimeter which is 10 cd/m² is regarded as representative of the mesopic level⁴⁶.

Colour Perimetry and Blue-on-Yellow Stimulus

As some retinal diseases influence rod or cone function differentially and more

selectively, specific rod or cone anomalies may be missed with white luminous stimuli because of rod response contribution at modest photopic background levels of conventional perimeters¹⁴⁹. The threshold to positive contrast (incremental) stimulus may be measured for one wave-length while the background is illuminated using a different wave length composition to increase the sensitivity of the test for cone disease. For instance, a strong yellow adapting background selectively reduces the sensitivity of the red and green cones, but only minimally influence the blue cone sensitivity. When a blue test target is presented on the yellow background, the visibility of the stimulus reflects the functionality of the blue cone system¹⁵⁰.

Visual field testing with blue stimuli on yellow background generates larger glaucomatous scotomas than conventional white-on-white light stimuli¹⁵¹. Neither red nor blue stimuli embedded in white surround of identical luminance of 10 ft-lambert (i.e. approx. 3 cd/m²)¹²⁴, however, found defects which could not be detected by conventional automated perimetry in optic nerve disease¹⁵². Similarly, when the same technique was used in manifest glaucoma and glaucoma suspect patients, all visual field defects found by blue stimuli could be detected by incremental static light stimuli¹²³. No advantage of blue-on-yellow perimetry could be found over conventional automated perimetry in discriminating diseased fields from normals using receiver operating characteristics (ROC) analysis using standard stimulus/background parameters¹⁵¹. Increasing absorption/filtering of blue light in the aging lens and consequent necessity for 'lens density index' and 'age correction factor' calculations for each tested eye hinder the practicality of the method^{153,154}. Even when these factors were taken into consideration, the lengthy examinations with blue-on-yellow perimetry indicated a significant difference in glaucoma suspect eyes in comparison to normal controls only in the supero-nasal field with high false positive rates against the white light stimuli¹⁵⁵. The perception of blue color was more impaired in high-tension glaucoma than the low-tension glaucoma¹⁵⁶ and the field defects to the blue stimuli were wider and deeper¹⁵⁷. The blue stimulus perimetry has recently been re-emphasized as a 'more sensitive' method in glaucoma¹³⁷ despite previous controversy and become an optional mode in

Humphrey Visual Field Analyzer. In that mode, static blue stimuli of Goldmann size V are presented against a high luminance 200 cd/m^2 yellow adapting background which saturates the red and green sensitive cones and isolates the blue (short-wave) sensitive cones. The prospective follow-up of glaucoma and ocular hypertension patients with Goldmann Size V stimulus over a five-year period indicated that the visual field defects to the blue stimuli could be more extensive and more progressive than those to the conventional white stimuli¹⁵⁸, early field deficits with blue stimuli converting to the visual field defects to the conventional light stimuli with the progression of the disease¹⁵⁹. The lengthy dark adaptation period (minimum 15 minutes) and lens density index calculation requirements before each test together with poor test specificity of blue-on-yellow perimetry restrict its clinical efficiency and usefulness.

1.7.2. Bipolar Cells

The photoreceptor cells of the retina connect to the ganglion cells through bipolar cells which transfer the visual information¹⁶⁰ as fully described elsewhere¹⁶¹. The bipolar cells respond to either increments (on-type) or decrements in light (off-type)¹⁶²⁻¹⁶⁴. The connection patterns of rods and cones are not uniform, resulting in low-spatial frequency (large size) contrast sensitivity for rod vision and high spatial frequency (smaller size) sensitivity to cone vision at different levels of retinal light adaptation¹⁶⁵⁻¹⁶⁷. Bipolar cells connecting to rods are 'on' type, and those connecting to cones are both 'on' and 'off' type¹⁶⁸⁻¹⁷⁴. Consequently, bipolar cells can use independently the full sampling capacity of cone array¹⁷⁵. Inputs into both on and off type bipolar cells come from cones in photopic adaptation levels as the rods are considered practically saturated. One 'on-type' and one 'off-type' bipolar cells converge onto each given ganglion cell¹⁷⁶, 'on' bipolar exciting the 'on' ganglion cell or inhibiting the 'off' ganglion cell and vice versa¹⁷⁷. Bipolar cells also provide lateral connections to horizontal¹⁷⁸, amacrine and interplexiform cells¹⁷⁹. In human retina, three types of horizontal cells were identified. Some of them contact all cones and rods (Type H1) whereas the others contact only

either short-wave sensitive (Type H2) or middle and long-wave sensitive cones (Type H3) without rod sampling¹⁷⁸. A comprehensive updated review of retinal morphology with extensive referencing is already available elsewhere¹⁸⁰.

1.7.3. Modulator Cells and Receptive Fields

In the fovea, each cone connects to two ganglion cells, one 'on' and one 'off' type¹⁸¹ via bipolar cells. With increasing eccentricity from the fovea, gradually more photoreceptors converge on single bipolar and retinal ganglion cells because of decrease in the number of retinal ganglion cells towards the periphery¹⁸¹⁻¹⁸⁶. As a result of this architecture, the unit retinal area, receptive field¹⁸⁷, over which light has some effect is formed. The receptive field of a neuron is the retinal area in which a visual stimulus causes a change in the activity of a neuron. It is suggested that the density of ganglion cell receptive fields in human eye is 30 000 receptive fields per degree in the central retina¹⁸¹.

The increasing photoreceptor-ganglion cell convergence ratio with eccentricity results in enlargement of the receptive field sizes^{148,186,188,189}. In photopic conditions the size of the 'on' type receptive field centre is 4.5'-9' at fovea, increasing to 60'-90' at 10-15 degrees from fovea and 120'-200' at 60-70 degrees from fovea. Similar to that inverse relationship between the receptive field size and ganglion cell density, the number of overlapping receptive field centres at a given retinal point decreases towards the periphery also¹⁹⁰, from 32 at 10 degree eccentricity to 13 at 70 degree eccentricity¹⁹¹. As a result visual sensitivity decreases gradually further away from the fovea^{192,193}. Retinal ganglion cell quantity, like photoreceptors, decreases with ageing¹⁹⁴ along with neuronal loss in the visual cortex of the brain¹⁹⁵. As indicated by the visual sensitivity decrease with ageing¹⁹⁶, the overlap and/or size of the receptive fields therefore may also be age dependent although no report on this exists yet.

The centre and the surround of a receptive field can be treated as two distinct response mechanisms, each having its own summing area and generating its response

contribution. The amount of response (total integrated gain) is determined by the area of receptive field covered by the stimulus, being largest in the centre and lower in the surround (Gaussian distribution)^{197,198}. The end result is that stimulation occurs according to the balance in the amount of light falling into the excitatory centre and inhibitory surround fields¹⁹⁹⁻²⁰¹. Optimum response is obtained if the stimulus just covers the receptive field centre and as the spot size increases, the stimulation fades with the inhibition by antagonistic surround^{202,203}. With dark adaptation, the receptive field surround becomes almost ineffective and the centre enlarges by about 25% of the photopic size¹⁹¹.

Receptive Field Perimetry

A psychophysical procedure that measures the properties of retinal ganglion cell receptive fields is described by Westheimer^{204,205} and was later adapted as a clinical test by Enoch^{206,207}. In that, a small constant diameter test field is maintained at a constant suprathreshold brightness at the visual field location to be tested. This field is kept flashing at the rate of one per second and is easily detectible on the fixed background hemispheric field of a perimeter. A continuously presented (non-flashing) field is then centred on the flashing field. The diameter of the superimposed continuous field is varied in steps from almost equal to the flashing spot to several times larger in diameter. At each diameter the luminance needed in that field in order to make the small flashing field disappear and reappear is measured. With this procedure it is possible to calculate the area of the on-centre and the surround of the ganglion cell receptive field. It was suggested that the abnormalities of the inner and outer retina can be distinguished by studying the centre surround ratio changes.

1.7.4. Ganglion Cells and ON / OFF Dichotomy

There are at least 11 different classes of retinal ganglion cells²⁰⁸. An average of 85% of

total one million retinal ganglion cells have concentrically organized receptive fields with two antagonistic regions, an 'on-centre' or an 'off-centre' with an opposite sign inhibitory surround²⁰¹. In the remaining 15% of the ganglion cells, there is no inhibitory surround mechanism and the receptive field is 'non-concentric'. The diameter of the excitatory receptive field centre is equal to the dendritic distribution field size of the ganglion cell it belongs in the retina^{200,209,210}.

The 'on-centre' receptive field is activated by light falling in its centre area and inhibited by illumination in the 'surround' area. Conversely, the off-centre receptive field activates the ganglion cell with decrement of the light falling inside the receptive field centre and inhibits it with a light decrement in the surround area¹⁹⁹.

As the detection sensitivity to a perimetric stimulus is determined by the number²¹¹⁻²¹⁶ and the size^{217,218} of overlapping receptive fields at a given visual field location, it is important to realize that the visibility of a light increment or decrement is the product of the excitatory receptive field centre²¹⁹, not of the surround. A neuro-transmitter analogue 2-amino-4-phosphonobutyrate (APB)²²⁰ paralyzes selectively retinal on-type bipolars, amacrine and ganglion cells as well as lateral geniculate nucleus and visual cortical on-type neurons with no effect on off-type cells. Following APB application, both the centre and the surround responses of on-centre cells were blocked, incremental stimuli becoming invisible while the responses to the decremental stimuli remained virtually unchanged²²¹. It is concluded that i) the surround area of a receptive field, which has an inhibitory filtering function only, is formed by the horizontal and amacrine cells and not by interactions between the 'on' and 'off' ganglion cells; ii) the 'on' and 'off' retino-geniculo-striate pathways remain segregated up to the visual cortex until converging on single cortical neurons; iii) on- and off-pathways are not stimulated simultaneously with a given bright or dark stimuli; and iv) cortical receptive field organization is likely the product of intracortical circuitry, not that of the convergence of the 'on' and 'off' pathways^{168,200,209,221,222}.

Administration of 2-amino-4-phosphonovaleric acid (APV) or APB in mammalian retina does not only cease the function of on-type cells, but enhances the discharges from off-type ganglion cells²²³. It was suggested that the increase in 'off' activity might be explained with blockage of inhibitory inputs from 'on' bipolars into the 'off' ganglion cells. If that is true for human eye, the detection sensitivity to light decrements should be higher against a dim background and become less with increasing adapting (background) luminance. Similar pharmacological asymmetries exist with administration of serotonin which blocks 'on' cells²²⁴ and dimethyltryptamine²²⁴ and baclofen²²⁵ which block 'off' cells only.

The quantity of off-centre retinal ganglion cells is 1/3 to 2/3 of the on-centre cells depending on the eccentricity^{197,208,226-238}. The average size of the receptive fields of the off-centre cells is larger than the on-centre cells^{233,239}, as expected from a smaller number of 'off' type cells and consequent higher photoreceptor to ganglion cell convergence. Although the morpho-physiological data come from monkey eyes, it may still reflect a highly accurate model of human visual system²⁴⁰.

The retinal ganglion cells display initial functional lamination in the retina and the stratification sequence proceeding from the vitread (near to vitreous of the eye; inner) surface is On-centre P cells, Off-centre P cells, On-centre M cells and Off-centre M cells¹⁹⁰. The dendritic trees of these ganglion cells branch and connect to bipolar cells with similar stratification in the 'inner plexiform' layer of the retina, the connections of On-centres being more vitread than the Off-centres¹⁷⁶.

1.7.5. Retino-Cortical Neural Visual Pathway

Visual information originating from the retinal ganglion cells is transmitted through the optic nerve which is formed at the optic disc by the retinal nerve fiber layer. The retinal nerve fiber layer which consists of approximately 1.2 million axons does not show

laminar segregation of different calibers of axons coming from different classes of ganglion cells²⁴¹. The retinal nerve fiber layer can be divided into three topographical sectors, namely i) papillo-macular bundle which leads to a central scotoma with its pathology, ii) arcuate bundles which cause nasal steps with respect to the horizontal meridian and arcuate scotomas in the superior and inferior hemifields and iii) nasal radial bundle which form wedge shaped sectorial defects in the temporal aspect of the blind spot when damaged (Figure 4).

The optic nerve leaves the eye at lamina cribrosa of the disc and meets the fellow optic nerve intracranially at the optic chiasm where the optic nerve fibres coming from the nasal hemi-retina cross to the other side and join to the temporal hemiretinal fibers from the fellow eye (Figure 5). Lesions of the optic chiasm lead to bitemporal complete or incomplete hemianopia with respect to the vertical meridian.

Behind the optic chiasm, axons form the optic tract which further synapse in the Lateral Geniculate Nucleus (LGN), a relay station and processing centre before the visual cortex. LGN ganglion cells project their impulses on the visual cortical neurons via the optic radiation.

Lesions affecting the optic tract, lateral geniculate nucleus, optic radiation and visual cortex produce hemifield defects (hemianopia) that are "homonymous", that is occupying the same side of the visual fields in both eyes, with respect to the vertical meridian. In other words, a nasal hemianopia in the right eye together with a temporal hemianopia in the left eye produces a left homonymous hemianopia. Detailed anatomophysiological and schematic reviews of the visual pathway in reference to the visual fields are available elsewhere^{142,242}.

1.7.6. Lateral Geniculate Nucleus and Parallel Pathways

Magnocellular and Parvocellular Pathways

According to the morphology and response characteristics, retinal ganglion cells are also classified as P-type (also P-Beta), for those projecting to the Parvocellular layers (Layers 3-6) of Lateral Geniculate Nucleus (LGN) of the brain and M-type (also P-alpha), for those projecting to the Magnocellular layers (Layers 1 & 2) of LGN^{186,243}.

LGN layers 1,4,6 take their inputs from the contra-lateral eye and layers 2,3,5 belong to the ipsilateral eye in either LGN²⁴⁴. The vast majority of cones providing input to the centre and surround of magnocellular cells are red and green type and only some appear to receive signals from blue cones¹⁹⁸. The signals from blue (short - wavelength sensitive) cones are transmitted via P cells and almost exclusively via the On-pathway^{227,245,246}. Parvocellular (P) retinal ganglion cells have small receptive field diameter, small somal and axonal caliber whereas Magnocellular (M) retinal ganglion cells have large receptive fields (nearly 6 times), large cell bodies and axons^{188,247}. In accordance with their smaller receptive fields, P cells have higher spatial resolution^{197,233,248}. The conduction velocity of the visual signal is higher in magnocellular cells, as expected from their large axons^{236,243}. M-type ganglion cells are 3-10 times less numerous than the P-type^{210,247}. The centre-surround mechanism of M cells is more sensitive to achromatic luminance contrast as opposed to the dominant feature of colour-opponency in 80% of P-type receptive field components^{236,238}. The sensitivity of M cells to achromatic contrast becomes most pronounced at short stimulus exposure durations^{197,236} as they respond to the visual stimuli transiently²⁰⁰, at lower stimulus contrasts (below 15% contrast)²⁴⁹ and at lower levels of adapting background luminance²⁵⁰.

In monkey eyes, selective lesions of parvocellular system impair visual acuity, colour vision, high-spatial frequency (i.e. small size) and low-temporal frequency (i.e. slow-

flicker) contrast sensitivity, brightness discrimination, pattern (shape and texture) discrimination and stereopsis, whereas magnocellular lesions distort low-spatial frequency contrast sensitivity, fast flicker as well as low-contrast fast motion perception²⁵¹⁻²⁵³. In humans, parvocellular system is affected by optic neuritis²⁵⁴ and magnocellular system is damaged preferentially in glaucoma^{255,256}. Visual information on motion perception which decreases in glaucoma²⁵⁷ is mediated and integrated by both On and Off pathways²⁵⁸ within the magnocellular system²⁵⁹.

On- and Off-Pathways

On and Off pathways remain morphologically segregated in the LGN also. On-centre ganglion cells are concentrated in layers 5 and 6 and off-centre cells are concentrated in layers 3 and 4 of parvocellular LGN^{236,260}. The magnocellular layers 1 and 2 have mixture of both type cells. Cytochrome-oxidase (CO) staining of the mitochondria reflect the metabolic activity rate of retinal and LGN ganglion cells²⁶¹. In monkey experiments, metabolic activity in magnocellular and On-centre cell groups was found to be higher than the parvocellular and off-centre counterparts, as indicated by the higher optical and electron microscopic densities of CO-reacted neurons in these groups²³⁷.

Objective asymmetries in human On and Off visual pathways are documented electrophysiologically also. Visual evoked cortical potentials (VECPs) to light decremental and incremental fast pattern reversal stimuli revealed lower contrast sensitivity to small size stimulus patterns (coarser 'spatial tuning') in Off pathway than the On pathway²⁶², as expected from the larger receptive field sizes of Off-type ganglion cells. VECPs to pattern offsets (light decrements) were of lower amplitude than those to pattern onsets (increments) with no significant difference between the latency of responses to onsets and offsets⁵¹ and these findings were attributed to the smaller quantity of off-type cells and consequent larger receptive fields and less receptive field overlap in Off-pathway.

On and Off pathways yield equal sensitivity and rapid information transfer for both light increments and decrements and facilitate high contrast sensitivity¹⁶⁸ which is processed mainly by magnocellular system. On and Off pathways for sensing brightness are important contributors to colour contrast perception which is mediated mainly by parvocellular pathway²⁶³.

1.7.7. Visual Cortex and Magnification Factor

The mapping of the visual field onto the striate cortex is eccentricity dependent; fovea occupying a large area and the periphery claiming a small portion of the visual cortex both in monkey²⁶⁴ and human brain²⁶⁵⁻²⁶⁷. Holmes suggested that the central 15 degree visual field occupied 25% of the visual cortex²⁶⁵ but the recent advances in neuro-imaging revealed that the central 10 degrees was represented by at least 60% of the occipital cortex^{266,267}. The cortical magnification factor (M) indicates the amount of cortex associated with each degree of visual field and is represented with $M^2 = \text{mm}^2 \text{cortex/degree}^{268-270}$. The cortical magnification factor simply represents the variation of retinal ganglion cell density (D) with the M^2 varying 4000 times with eccentricity between the fovea and the peripheral visual field²⁷¹. Signals transmitted by the parallel pathways blend together generally after the first synapse in the visual cortex of the brain and the detailed reviews of retino-cortical pathways^{229,272}, the connections of the Magnocellular, Parvocellular^{203,273} and On and Off pathways^{274,275} into the visual cortex are available elsewhere.

1.8. Offset (Decremental) Stimuli in Visual Testing

1.8.1. Light Decrements (Offsets) versus Increments (Onsets) in Psychophysics

Above described objective asymmetries between the On and Off pathways in morphological, physiological, pharmacological and electrophysiological domains also exist psychophysically. A bright target on a dark background is perceived larger than a dark target with identical geometry on opposite background²⁷⁶⁻²⁷⁹.

Stimulus detection rates and reaction times differ in the foveal vision for increments and decrements^{278,280}. The time to detect the offset of light was found to be shorter than that needed to detect its onset. When the nasal horizontal meridian up to 50 degree eccentricity was tested with a stimulus of 1-degree diameter and 3 dB incremental or decremental steps in light intensity in two observers, the threshold critical duration for stimulus detection was the same for both onsets and offsets in the macula within 10 degree field. Beyond 10 degrees from the fovea and against the photopic background, light decrements were detectable at shorter (up to 5 milliseconds difference) durations of presentation. Against a scotopic background, the critical stimulus duration thresholds were equal. The average duration required for the detection of 50% of the stimulus presentations (i.e., 'time threshold') was less than 40 milliseconds in photopic vision and longer but less than 100 milliseconds in scotopic vision at all eccentricities²⁸¹. The technical reliability of 5 milliseconds difference and the statistical significance of that subtle difference in two observers are not certain, although the time threshold differences for onsets and offsets were attributed to a likely activity difference of undetermined nature between the on- and off-pathways.

A one-degree diameter foveal circular field of white light was presented with increment or decrements in its luminance for stimulus durations of up to 2 seconds. There was no difference found in the onset and offset thresholds in the foveal vision and the critical

duration for detection of both type stimuli was less than 0.1 second at various adapting background intensity levels. The critical duration for stimulus detection was less in higher background intensities²⁸². Similarly, foveal incremental and decremental stimuli of 1-degree rectangular size were equally detectable with no difference between the threshold values²⁸³.

Luminance increment and decrement detection thresholds were established in macular 10 degree diameter field, using a full field size stimulus. The detection of decrements in the light intensity of the 10 degree-size stimulus was easier (lower thresholds) by 0.5 to 1.5 decibels in two subjects²⁸⁴. Stimulation of the macular 7 degree field with grating patterns made of alternate dark and bright bars and average luminance of 13 cd/m² in 4 observers provided opposite results, light increments being more detectable than the light decrements in mid-spatial frequencies (i.e., size of bars; 1-2 cycles/degree = 2-4 bars/degree). That finding also supported the view that the smaller sizes of on-type receptive fields provided higher contrast sensitivity to light increments, bright bars appearing wider than the dark bars²⁸⁵.

Comparison of onsets and offsets with a one degree diameter stimulus presented for 0.1 second at 15 degree eccentricity in the nasal field suggested easier detectability of light offsets. The thresholds to offsets were lower than those to onsets by 0.1-4.0 dBs with 3 dB intra-individual (intra-test) variability in 5 subjects²⁸⁶. Interestingly, in this experiment, the subjects presented the stimuli to themselves using a trigger and also reported whether or not they were visible. When two observers presented the stimuli to themselves using a potentiometer and signalled their detection, the incremental detection thresholds were consistently higher than the decremental thresholds, suggesting easier detectability of offsets than onsets also²⁸⁷. The stimuli were presented at 7 degree eccentricity from the fovea in the inferior nasal quadrant with various stimulus sizes and the durations and the experiment took two hours for each subject. Like the other reports described above, an artificial pupil of 2 mm diameter was used. The easier detectability of offsets than the onsets was interpreted as a sign of off-type cells being more sensitive

than the on-type cells²⁸⁸.

With the stimulation of 3-degree foveal field, the detection threshold contrast for offsets was slightly lower than increments in 7 subjects, suggesting easier detectability of offsets. Light decrements, however, required longer reaction times to the stimuli by the patients²⁸⁰.

The central 3-degree foveal field was also tested with random dot pattern stimuli, creating random onsets and offsets of black dots at various locations. The detection of both type of stimuli became more difficult with immediately preceding presentation of opposite type stimuli at the same locations²⁸⁹. It was interpreted that the negative interference between the opposite type stimuli in their detection is a sign of the inhibitory interaction between the on and off-type cells, the detection being easier for light onsets. The 5-degree macular contrast sensitivity to grating patterns created with sudden light offset was found to be 50-65% lower than the contrast sensitivity to sudden light onsets especially at lower spatial frequencies (larger size bars)²⁹⁰. Light onsets were 10% more visible than the light offsets in a similar study with bar patterns²⁹¹. These findings are consistent with smaller amount of cells in the off-pathway and consequent lower contrast sensitivity.

1.8.2. The Offset (Dark-on-Bright) Stimulus in Clinical Testing

Visual field examination is universally performed with luminous stimuli on a relatively dim background. The luminous stimulus has remained in routine perimetric practice for over a century, probably due to the historical assumption that the eye fundamentally is a light sensor. While the advancements in static test techniques and the incorporation of custom-built and personal computers elaborated the conventional approach of differential light sensitivity determination across the field of vision, it appeared that the visual system also had 'differential dark sensitivity' due to parallel pathways.

Whereas conventional perimetry with light increments tests on-pathway and mainly on-centre receptive fields at various locations across the retina, there may be advantages in testing the off-pathway with the offset (dark-on-bright) stimuli because of the asymmetries between both systems and possibility that the field defects that are missed with a conventional light onset stimulus might be detected by the offset stimulus in certain conditions, such as glaucoma, retinal and intracranial disorders affecting the visual system. It was shown in animal eye that on- and off-centre ganglion cells behaved differently in stress^{292,293}. There is also evidence in the literature to suggest that off -pathway may be affected differentially by a disease process and cerebral palsy is such a condition^{294,295}.

In addition to the psychophysical experimentation described above, the high contrast black stimulus has previously been described for blind spot detection and fixation monitoring on a hand-held tangent screen test chart³⁷. Crick suggested that the black stimulus might reveal glaucomatous visual field loss, although no actual clinical result was reported²⁹⁶. The low, intermediate and high contrast kinetic dark stimuli have been experimented on a white Bjerrum screen in the diagnosis of cone dysfunction²⁹⁷. Computerized suprathreshold testing with kinetic black (single intensity) stimulus on a video-display unit^{134,135} and 'delay campimetry' which involved recording patient reaction times to a static black stimulus at a number of locations in the visual field^{298,299} were suggested to yield additional clinical information especially in retinal inflammatory disorders and inflammatory/demyelinating optic neuropathies respectively. Delayed stimulus perception was found only with light offsets in some patients and only with light onsets in others. Furthermore, single intensity grey and white high-pass spatial frequency targets³⁰⁰ which present areas of light onset and offset simultaneously as a ring-shaped static opto-type were employed on a video-display unit under computer control and gave similar results to conventional methods³⁰¹. Scanning laser ophthalmoscope and incorporation of computer control enabled direct presentation of kinetic single intensity suprathreshold light offset stimuli of various contrasts onto the retina through a dilated pupil³⁰² and proved useful in mapping visual deficits in retinal

degenerative disorders^{303,304}. Computerized suprathreshold and threshold testing for detection sensitivity to static offset stimuli which conform to conventional perimetric standards, however, have not been reported before.

1.9. Disease Process Causing Visual Field Loss

1.9.1. Glaucoma

Glaucoma is the most common cause of visual field loss and preventable eventual blindness in the developed countries^{305,306}. Glaucoma is a form of optic neuropathy in which slowly progressive loss of visual field occurs without the individual's awareness.

Glaucoma patients may be sub-categorized according to the level of intra-ocular pressure (i.e., high- or low-tension glaucoma) or the rate of onset (i.e., acute versus chronic) or the aetiology (i.e., primary or secondary and open-angle or angle-closure glaucoma)^{307,308}. Chronic primary open angle glaucoma (POAG) accounts for 90% of the cases. In POAG, there may be increased resistance to aqueous outflow from the eye at the trabecular meshwork due to microscopic degeneration of the trabeculum, which is situated at the angle between the root of the iris and the cornea³⁰⁹.

The prevalence of glaucomas is between 1 - 2% in the British population³¹⁰. In the United States, the prevalence of glaucomas is 1.7% among whites and 5.6% among blacks³¹¹. A further 0.2% of the population develop glaucoma each year. It is estimated that over 11% of all blindness and 9% of visits to ophthalmologist are due to glaucoma³⁰⁶. The magnitude of the problem increases with age and becomes five to 10 times more frequent beyond age 70³¹². The risk of developing glaucoma is increased in individuals with positive family history, myopia over -5 dioptries and diabetes³¹³.

Glaucomatous optic neuropathy is generally regarded as due to an intraocular pressure sufficiently raised to a level beyond the individual tolerance limit of the morpho-vascular structures of the optic nerve head³¹³⁻³¹⁵. Although intra-ocular pressure rise is neither necessary nor adequate to cause glaucomatous optic neuropathy in all cases³¹⁶, intraocular pressure mediated mechanical damage to the axons and/or decrease

in the vascular supply to the optic nerve³¹⁷ at the level of lamina cribrosa^{318,319} may be responsible for neuronal damage with local blockage of axonal transport³²⁰. As the most common cause of preventable blindness in developed countries, glaucoma progresses with axonal damage at the optic nerve head leading to cupping³²¹, descending and ascending neural loss in the retinal nerve fibre layer¹⁰⁷, retinal ganglion cells^{322,323}, photoreceptors³²⁴, optic nerve fibres³²⁵ and magnocellular layers of the lateral geniculate nucleus^{255,256}.

1.9.2. Glaucomatous damage and the visual field

Initially, glaucomatous visual field defects are 'relative' (detectable with sub-maximal stimulus brightness) and fluctuate in severity, but later becomes 'absolute' and irreversible^{140,326,327}. The visual field loss may occur both in a diffuse or a localized (pattern) fashion. Generalized (diffuse) visual field loss may be attributed to glaucoma if there is no media opacity or small pupil size. The presence of generalized visual field loss found with Goldmann perimetry in Primary Open Angle Glaucoma (POAG)³²⁸⁻³³² was not observed in all patients^{333,334}. The only study claiming the absence of diffuse loss in POAG using automated perimetry (Competer) did not compare the visual fields of glaucomatous patients to the true age-corrected normal threshold values³³⁵. Purely diffuse loss in the absence of other causes has been documented in POAG, using the STATPAC empiric probability maps of Total Deviation and Pattern Deviation of Humphrey Visual Field Analyzer in 3 eyes only³³⁶. Therefore, the occurrence of generalized or diffuse visual field depression in Primary Open Angle Glaucoma (POAG), in contrast with the presence of characteristic localized defects, remained controversial.

The topographical selectivity of glaucomatous visual field loss has previously been reported for manual and automated conventional perimetric techniques^{328,337-347}. Localized (pattern) visual field defects in open angle glaucoma, by virtue of their shape

and location, are nerve fiber layer type, that is small scotomata at about 15 degrees from fixation mostly in supero-temporal quadrant, gradually developing an arcuate shape and eventually respecting to horizontal meridian especially nasally, causing a 'nasal step'. Only 10% of glaucomatous defects occur outside the central visual field beyond 30 degrees from fixation^{77,348}.

Although some studies suggested differences in the distribution of the field deficits in low and high-pressure glaucomas, the defects being closer to the fixation and more diffuse in low tension glaucoma^{331,349-353}, there is not conclusive evidence or universal agreement on whether different types of glaucomas produce different patterns of visual field defects³⁵⁴⁻³⁵⁷.

It has been realized that the optic nerve head (disc) changes in glaucoma occur prior to detectable visual field loss to conventional light stimuli^{319,358-360}. The disc change involves the enlargement of the central cup of the disc, which reflects the decrease in the number of neuronal axonal fibers in the optic nerve head where the optic nerve is formed. At the level of retrobulbar optic nerve, the nerve fibers are killed throughout the nerve³⁶¹ but, the ganglion cell axonal fibers of the superior and inferior quadrants seem to be lost earlier and 2 - 3 times more extensively than the fibers of the lateral quadrants, with an overall decrease in the number of all fibers resulting in cupping of the disc^{323,362}. The standard method of estimating optic disc cupping is to describe the ratio of cup diameter to the disc diameter in vertical axis. The vertical cup-to-disc ratio of 0.6 or larger may be indicative of glaucomatous damage. Since the superior and inferior portions of the optic nerve are formed by the axons of the arcuate area ganglion cells above and below the macula, the glaucomatous field defects are seen more frequently in arcuate areas, but later than the onset of the damage and cupping in the optic nerve. Clinical examination of the nerve fiber layer of the retina in red-free (green) light also demonstrates gaps in the integrity of the layer since the early stages of glaucomatous neural damage and these defects also occur prior to demonstrable visual field loss with conventional perimetry³⁶³⁻³⁶⁶. Therefore, a number of patients who have

been found to have high intraocular pressures and normal visual fields (i.e., ocular hypertensives) but suspicious optic disc signs such as asymmetric cups, vertical elongation of the cup, notching of the neuro-retinal rim around the disc and peripapillary nerve fiber layer defects, constitute an intermediate group, glaucoma suspects^{329,330,367-369}. As a substantial portion of the optic nerve may well be atrophic before the detection of field loss^{321,323}, the absence of detectable visual field loss in these glaucoma suspects raises the question about the sensitivity of conventional perimetry and indicates the need for more sensitive test procedures for optic nerve damage.

Glaucoma is known to damage selectively retinal ganglion cells with large somal diameter both in monkey³²⁵ and human eyes^{322,361,370,371}. It is possible that larger axons have less resistance to compression and ischaemia produced by intraocular pressure because of smaller surface-to-volume ratio³⁷². Magnocellular²⁴⁷ cells, blue (short wavelength) sensitive on-centre ganglion cells²²⁷ and off-centre ganglion cells¹⁷⁴ have larger somal and axonal diameters. Thus, the new diagnostic tests for detection of early glaucomatous visual loss must have affinity to larger sized ganglion cells.

Visual field testing with conventional light onset stimuli of Goldmann kinetic perimeter can document the early glaucomatous visual deficit reproducibly only after 50% of the optic nerve axons are lost^{107,321,323}. The comparison of retinal ganglion cell density and threshold to automated perimetric stimuli at 109 locations in 3 glaucomatous eyes indicates that, on average, a 5 dB loss requires 20% ganglion cell death and a 10 dB loss represents a 40% loss²¹⁶. Up to 10 degree eccentricity in the field, 5 dB loss is equivalent to 50% ganglion cell death in the retina. In human glaucomatous eyes, 3%-36% of the ganglion cells still existed when 0 dB sensitivity was found. That was explained with either damaged non-functioning cells still being present in the retina or not being tested with conventional light stimulus intensity. It was concluded that 0 dB sensitivity occurred when receptive field centres of adjoining ganglion cells no longer overlapped²¹⁶. It has been suggested that there could be little point in diagnosing glaucomatous visual loss at an early stage as patients tend to go blind despite

treatment³⁷³. There is increasing evidence, however, that visual loss can be retarded, arrested or even reversed with proper treatment^{313,316,374-376}. Therefore, it is crucial to detect the ongoing glaucomatous disease process in the optic nerve at its earliest level to achieve best prognosis.

1.9.3. Other causes of visual field loss

In general, organic lesions leading to visual field loss along the neuro-visual pathway may be grouped as inflammatory, degenerative, ischaemic, traumatic, neoplastic or compressive in nature and may occur at pre-retinal level (e.g., ptosis, uncorrected refractive error, miosis, media opacity involving cornea, lens or vitreous), retinal level (e.g., detachment, dystrophy, degenerative disorders, chorioretinitis, diabetic or other retinopathy, tumor, ischaemia), at the optic disc (e.g., ischaemic optic neuropathy, papillitis, chronic papilloedema, coloboma), optic nerve (e.g., inflammation, ischaemia, tumour, compression, trauma), optic chiasm and tracts (e.g., tumor, inflammation, infarct, vascular or infiltrating lesions) or beyond in lateral geniculate nucleus, optic radiation and visual cortex (infarct, arterio-venous malformation, tumor). The pattern of the visual field loss is usually indicative of the site of the lesion as briefly described above (see 1.7.6.). A detailed review of such lesions and their typical visual field consequences are available elsewhere³⁷⁷.

1.10. Screening

1.10.1. Medical Screening

Medical screening is the detection of occult disease or organic defect by the application of tests, examinations and other procedures which can be applied rapidly. The primary purpose of medical screening is to sort out apparently well persons who may have a disease or defect from those who do not have the same condition without any attempt to entertain a definite diagnosis. In situations in which the abnormal (positive) results of the screening test lead to medical treatment of the condition, the term 'prescriptive screening' is used³⁷⁸.

When the application of medical screening procedures are applied economically to large groups of apparently well individuals, the investigation procedure is called 'mass screening'³⁷⁹. Mass screening can be either 'monophasic' or 'multiphasic'. In 'monophasic' medical screening, either a single or a battery of tests are performed towards the detection of an individual disease or defect. In such circumstances, screening procedures are usually confined to those people who are at special risk of having the condition³⁸⁰. Multiphasic screening aims at the detection of more than one occult diseases or defects in large groups of apparently well persons using multiple screening tests. For instance, if a visual field screening test procedure is performed, either on its own or in combination with tonometry and ophthalmoscopy, to reveal either the absence or presence of a visual field defect and/or the presence of glaucoma, the procedure is monophasic screening. If the field screening test is combined with a battery of other tests to perform differential diagnosis and document the exact nature and aetiology (e.g., glaucoma, ischemic optic neuropathy, pseudotumor cerebri, cerebral infarct or tumor, etc.) underneath the detected abnormality, screening is multiphasic.

Ideally, a screening test should be sensitive enough to bring to attention all those with the disease in the group, and specific enough to exclude only those without the

condition being sought for. If the result of a screening test is abnormal in a person who really has the disease, the result is 'true positive' (TP). When the test result is normal in a healthy individual without the disease then the result is 'true negative' (TN). Having an abnormal and normal test result in a normal and diseased individual are described as 'false positive' (FP) and 'false negative' (FN) results, respectively. The sensitivity of a screening test is the conditional probability of a positive test result, given that the patient has the disease which is proven by a "gold standard" method ($TP/(FN+TP)$). The test specificity is the conditional probability of a negative test result, given the patient does not have the disease ($TN/(TN + FP)$)³⁸¹. Predictive value of a positive test result is the ratio of number of those with the disease and detected by the test to the total number of individuals with abnormal test result ($TP/(TP+FP)$). Similarly, predictive value of a negative test is represented by the ratio of those with normal result and no disease to the total number of normal results in the group screened ($TN/(TN+FN)$). It has recently been suggested that repeated visual field testing of the same individuals with a screening method may also give reliable results to establish the sensitivity and specificity of the new technique in the absence of an external 'gold standard'³⁸². This new approach is based on the observation that the true and false positive result rates obtained with initial testing decrease to their square with repeat testing, improving the specificity and reducing the sensitivity with each repeat test. The validity and applicability of this new approach, however, is still to be investigated in full.

A good screening test is one where both sensitivity and specificity are high. Although a 100% discrimination between the diseased and healthy populations is desired as a result of a screening procedure, there is always, to some extent, an associated error rate in the screening measurements that exists, simply because no information or its interpretation is free of error. The frequency distributions of test scores from the two populations of normals and diseased will overlap³⁸³. Increasing the sensitivity of a screening test usually requires sacrifice from the specificity and vice versa.

The benefits and cost of testing (e.g., financial, time of testing, discomfort to the patient, etc.) determine together the level of trade off between the sensitivity and the specificity of the screening test³⁸⁴.

The criteria set by Wilson brings the following principles of screening in medicine³⁸⁵:

1. The condition sought should be an important problem.
2. There should be a recognized latent or early symptomatic stage.
3. The natural history of the condition, including its development from the latent to declared disease, should be adequately understood.
4. There should be an accepted treatment for the disease.
5. There should be a suitable test or examination.
6. The test or examination should be acceptable to the population.
7. Facilities for diagnosis and treatment should be available.
8. There should be an agreed policy on whom to treat as patients.
9. The cost of screening (including diagnosis and subsequent treatment of patients) should be economically balanced in relation to the possible expenditure on medical care as a whole.
10. Case finding should be a continuous process and not a once for all project.

In general, "Wilson's Criteria" are regarded as difficult to meet. Glaucoma and other neuro-ophthalmic conditions causing visual field defects seem to comply with the above principles and ideally suited³⁸⁶⁻³⁸⁸ to purpose of visual field screening towards the diagnosis and treatment of such conditions.

During visual field screening, the examination of a large number of points throughout the visual field would be ideal, in theory, but is impracticable because such a strategy would be too time-consuming and exhausting for the patient. When screening for visual field loss, it is therefore necessary to examine a small number of points, which are carefully selected according to known patterns of visual field loss in glaucoma and other important diseases³⁸⁹. If speed and economy can be achieved with acceptable sacrifice

from sensitivity and specificity, then visual field screening might become a routine in the community, where it could be administered in combination with other types of examination for the detection of disease.

1.10.2. Glaucoma Screening

The detection of glaucoma in the community is an unresolved problem. It is one of the leading causes of blindness in the developed world. Undetected glaucoma accounts for approximately 50% of the cases in the community and the vast majority of those hidden cases are recognized only when end-stage visual field loss or even late legal blindness have occurred^{367,390-392}. Early diagnosis of glaucomatous neural damage is of critical importance in achieving the best prognosis in treatment and effective blindness prevention in the community³⁰⁵.

As it is usually possible to arrest the progress of the glaucomatous visual loss, if detected at an early stage, the screening for glaucoma, especially in general practice, is frequently emphasized³⁹²⁻³⁹⁶. In current practice, most people referred with suspected glaucoma do not have this disease^{397,398}. And yet, most glaucoma sufferers are recognized only when advanced visual field loss, or even legal blindness, have occurred³⁹⁰. This unsatisfactory situation exists because of the limitations of tonometry^{373,399,400} and ophthalmoscopy⁴⁰¹⁻⁴⁰⁴. Tonometry alone would yield 53% false negative and 45% false positive errors if 21 mm Hg is accepted as the maximum limit of normal intraocular pressure. This is because 5 - 10% of the population have an abnormally high intraocular pressure, but less than 1% of 'ocular hypertensive' individuals develop detectable optic nerve damage each year. To make it even more complicated, nearly half of all glaucoma sufferers have a normal intraocular pressure reading at any one time. Similarly, if glaucoma referrals were made on the basis of cup to disc ratio of 0.7 or greater, the screening decision would have a sensitivity of only 33% and a specificity of 80%. Problems with cup to disc ratio arise because of the

variation of the optic disc size in the population, which cannot be assessed accurately by direct ophthalmoscopy. Other glaucomatous ophthalmoscopic findings e.g., narrowing of the pink neuroretinal rim area of the optic disc, splinter disc hemorrhages or nerve fiber layer defects, require a high level of expertise which is not available at primary care settings i.e. optometric practice. As a result, only one in three referrals for suspected glaucoma gets confirmation of the disease⁴⁰⁵. For these reasons, intraocular pressure measurements and ophthalmoscopy performed for glaucoma screening should be combined with visual field testing. Thus, effective and efficient visual field screening is highly desirable in order to identify individuals who are in the early stage of this disease³⁹²⁻³⁹⁶. It was suggested that the frequency of visual field screening should be adjusted according to the age as twice in each decade of life up to age of 50 years, once every two to three years up to age 70 and once a year thereafter³¹³. Early detection and prevention of blindness through effective visual field screening may help decrease the financial burden of the condition to the community as well as improve individual well-being of the detected patients³⁸⁶.

Despite its invaluable importance in confirming the visual loss and presence of glaucoma and other optic pathway disorders, visual field testing is usually omitted as a first line investigation in combination with tonometry and ophthalmoscopy for screening in optometric practice⁴⁰⁶. Although visual field examination is a well established method of screening for glaucoma⁴⁰⁷ it is usually omitted because conventional techniques are difficult for both the patient and the examiner, time consuming and expensive^{87,408,409}. The dependence of perimetry on costly equipment and technical personnel further restricts its availability in the community. The need for a skillful examiner or a computerized monitoring system, both increase further the cost of the examination. As a result, perimetry is usually omitted as a first line investigation in the community even when a glaucoma suspect is to be referred to an ophthalmologist^{405,406,410}. Among 704 referred glaucoma suspect patients, it was found that a mere 47% had been tested by the optometrist with a field screener⁴¹⁰. Although perimetric equipment is widely available in optometric practice, only 6% of the patients

have visual field test. Only 10% of individuals over age 40 years are examined with any form of perimetry³⁹¹. At least 20% of primary examiners, optometrists, virtually never use a field screener⁴⁰⁶.

For the same reasons, perimetry is an under-utilized tool in ophthalmic clinics, despite the fact that no ophthalmic examination can be regarded complete without perimetry. In addition to glaucoma and a number of other eye diseases such as retinal detachment, tumor, infarct and degenerative disorders which cause visual field loss, brain disorders also give visual field manifestations^{411,412}. There has been no practical and satisfactorily informative visual field test instrument available to non-ophthalmic clinicians such as neurologists, neuro-surgeons, paediatricians, internists or general practitioners although the population receiving services from those disciplines are at higher risk of having visual field loss³⁹⁴.

1.11. Aim of the Thesis

The objective of this work was to establish the usefulness of dynamic (i.e., moving eye) fixation target and light decremental (i.e., offset) stimuli in clinical testing of the central visual field. That required the investigation of:

- I. Dynamic fixation method combined with either continuous or intermittent (brief) stimulus presentations in the central visual field examination; and,
- II. Various contrasts of light offset stimulus in screening and quantification of normal and abnormal central visual fields.

In connection with the above, computerized single-intensity and threshold static light offset stimuli of perimetric standardization were devised in video-campimetry. The development and performance testing of light onset stimuli in video-campimetry and comparative evaluation of equal and opposite amount of light changes on CRT were not addressed.

The following hypotheses were studied:

1. Isoptres to continuously exposed offset and onset stimuli presented with dynamic fixation may differ and the isoptres may vary with changes in ambient illumination.
2. Dynamic fixation and constantly exposed static offset stimuli used in 'oculo-kinetic perimetry' may have different informative value in various stages of visual field loss and in different age groups.
3. Clustering of fixation targets may influence the test sensitivity in oculo-kinetic campimetry.
4. Video-campimetric dynamic fixation and conventional static fixation methods may provide different levels of fixation control in children.
5. Diagnostic screening potential of CAMEC strategies with offset stimuli and dynamic fixation may differ from that of conventional perimetry in terms of sensitivity, specificity and efficiency.
6. Refractive blur may influence the detection sensitivity to offset stimuli.
7. The results from dynamic fixation and offset stimuli may vary on repeat testing.

Part 2. MATERIAL AND METHODS

Good judgement comes from experience; and experience, well, that comes from bad judgement.

[Anonymous]

2.1. Light Offset Stimuli and Dynamic Fixation on Bjerrum Screen

The presentation of a dark-on-bright (offset) stimulus on a white tangent screen is difficult, as it would require a white wand which would lead to confusion by casting a dark shadow. This technical difficulty is overcome by using a novel campimetry technique which does not require the stimulus to be moved on the screen, because it is the patient's eye which moves instead²⁵.

The aim of the study was to describe 'the hill of vision' to the offset stimuli on a tangent screen, identify differences between responses to offset and onset type campimetric stimuli in the central visual field by dynamic fixation technique and to determine how these responses vary with changes in ambient illumination. The study involved the assessment of the visual fields of the right eyes of eight volunteers, six of whom were male and two female. Their visual acuities were all 6/5, and the pupil sized ranged between 3 and 5 mm. in 150 lux room illumination. All eyes were normal. The experiments were performed with three different types of tangent screen: black, white, and grey, having a light reflectance (albedo) of 5%, 95%, and 50% respectively. Each test stimulus consisted of a disc attached on to the screen which had a light reflectance of either 5% (black, offset) or 95% (white, onset) creating equal and opposite luminance changes (i.e. $\pm\Delta L$) on white, black or grey background at a given illuminance level (Figure 6). Neither Weber's nor Michelson's formula alone (Chapter 1.2.2) could represent that stimulus opponence on all stimulus-background combinations:

Stimulus	Weber's Contrast	Michelson's Contrast
White-on-Black	$0.95-0.05 / 0.05 = +18.0$	$0.95-0.05/0.95+0.05= +0.90$
Black-on-White	$0.05-0.95 / 0.95 = -0.95$	$0.05-0.95/0.05+0.95= -0.90$
White-on-Grey	$0.95-0.50 / 0.50 = +0.90$	$0.95-0.50/0.95+0.50= +0.31$
Black-on-Grey	$0.05-0.50 / 0.50 = -0.90$	$0.05-0.50/0.05+0.50= -0.82$

The tangent screen was illuminated with a white light halogen lamp fitted with a diffuser and a dimmer switch which was positioned at 2 meters from the screen. The illumination of the screen was measured and adjusted with a luxmeter (Solex SL100). No spectrophotometry was performed.

The fixation target consisted of a pointer, which was moved across the screen superotemporally by the examiner, so that the pursuit movements of the subject's eye induced a relative shift of the stimulus along the 225 degree (inferonasal) meridian in the central visual field. The eccentricity from fixation at which the stimulus was no longer seen was recorded. This procedure was repeated five times for each target and illuminance level, and a mean value was taken as the final result.

Every time the ambient illumination was altered, 3 minutes were allowed to elapse before the examination was begun so as to ensure the subject's retinal light adaptation had taken place. The subject was seated, with the head resting on a chin rest so that the right eye was 150 cm. from the screen. The left eye was covered with an occluder. All perimetric examination were performed by the same individual, and all tests for each subject were completed on the same day.

2.1.1. Meridional Hill of Vision to the Offset and Onset Stimuli

Four volunteers (two males and two females; mean age 30 years, range 28-31 years) were tested with each of five sizes of offset stimuli (1,2,3,4, and 5/1500 mm.) against a white background, and also with onset targets of the same size on a black background. The peripheral visibility of both stimulus types on the 225 degree meridian was compared.

2.1.2. The Effect of Variation in Illumination on Offset and Onset Stimuli

The effect of variation in ambient illumination on the eccentric visibility of offset and onset stimuli on the 225 degree meridian was examined at two levels of illumination, which were 13 and 400 lux (that is, a difference of 1.5 log units). The colour temperature of the various light levels were not determined and it is possible that variations may have occurred.

Eight volunteers (mean age 30 years, range 25-39) were tested with each of the following four stimulus-background combinations in a random order: white-on-black, black-on-white, white-on-grey, and black-on-grey. The grey background was employed in order to neutralize the difference in retinal light adaptation levels to different backgrounds, and to establish whether the results were due to the stimulus or the background. In each case a 1/1500 mm. (2.5 minutes arc) stimulus visibility with change in illumination was calculated with the formula $[(I-i) / i] \times 100$ where 'I' is the isoptre at 400 lux and 'i' is the isoptre at 13 lux. The percentage change in the isoptre of the offset stimulus was compared with that of the onset stimulus by non-parametric sign test for paired data.

2.2. Clinical Evaluation of Dynamic Fixation and Constantly Exposed Offset Stimuli for the Detection of Glaucomatous Visual Field Loss

A hand-held Oculo-kinetic Campimetry chart which consisted of a white card (29.5 cm x 42.0 cm), with multiple fixation targets numbered 1-26 on each side, was used for the examination of the left or right eyes (Figure 7). A black eye-occluder fitted to the lateral edge of the card by means of a rigid side-arm ensured that the correct side of the card was presented to the eye and that the card was held at the proper distance (40 cm). The first fixation target consisted of the letter 'L' or 'R' , depending on the eye being examined, and tested the left or right blind-spot respectively. The 26 numbered fixation targets spiralled towards the centre of the chart to examine the field at 12.5 degrees superiorly, 15 degrees nasally and inferiorly, and at additional points more centrally. These fixation targets were coloured light-blue so that the patient would not confuse them with the central black test stimulus.

The aim of this work was to establish the screening value of oculo-kinetic campimetry chart and constantly exposed offset stimuli in different stages of glaucomatous field loss and in various age groups. The oculo-kinetic campimetry was performed under good illumination (photopic level, 100 - 150 lux with 0.2 log unit variation). During the test, the right eye was examined first, with appropriate correction for presbyopia, if necessary. If the edge of the bifocal segment interfered with the examination, the patient was advised to tilt the head backwards or forwards to move the chart into the central part of the near segment. All examinations were performed under supervision, with the stimulus left constantly exposed. The patient was asked to look at each fixation target for about one second. If any numbers were reported by the patient to be associated with disappearance of the stimulus, these were deleted on the record sheet by the examiner and the eye was re-examined. This was done without comment by the examiner so as to avoid bias. Reproducibly missed test stimuli at one or more test locations constituted an abnormal (i.e. positive) result. Suprathreshold conventional perimetry was performed with three zone quantification (normal, relative or absolute

field loss) before or after the oculo-kinetic perimetry, by optometrists as part of routine patient care, using either the Friedman Visual Field Analyzer, Dicon 3000 Autoperimeter or Tubingen Perimeter and in some of the control subjects, with Henson Visual Field Analyzer. These perimeters have the same maximum stimulus brightness (1000 Apostilb) and the criteria of a relative or absolute defect is uniform between different devices. Despite the fact that suprathreshold static perimetry with single and multiple stimuli and suprathreshold kinetic perimetry represent different types of testing with major instrument design differences and non-identical response properties, they all give similar results in the detection of visual field loss⁴¹³⁻⁴¹⁵. The depth of all detected glaucomatous visual field defects is the same with similar topographical distribution when quantified with single kinetic and multiple static stimuli^{416,417}. The results of the conventional perimetry were categorized independently according to the Aulhorn-Karmeyer Classification⁴¹⁸ by three ophthalmologists and an optometrist without knowledge of the OKC results and a mean score was calculated for each eye. Although the Aulhorn-Karmeyer Classification which categorizes defects as 'relative only' (Stage 1), 'small absolute scotoma separate from blind spot' (Stage 2), 'larger absolute scotoma connected to blind spot' (Stage 3) and 'hemifield loss' (Stage 4), originally referred to kinetic perimetry, it can also be applied to static perimetry because of the above described similarities between results from both methods.

The perimetrically experienced patients were selected from a hospital glaucoma clinic. The controls consisted of hospital workers, spouses and friends escorting the patients to the glaucoma clinic of Tennent Institute (OKC and conventional tests performed by the author) as well as patients attending a nearby refraction clinic where Dr R. Stevenson and his undergraduate students performed the tests on 100 controls (as part of an undergraduate dissertation submitted to Caledonian University School of Optometry, 1991). In the control group, only the results from the right eye was included. In both groups, individuals were excluded if they appeared to be very frail and eyes were tested only if the visual acuity was 6/18 or better and if there was no other ocular disease.

2.2.1. Constantly Exposed Offset Stimulus of 1.5 mm. Diameter

In the first part of the study, the test object was a 1.5 mm diameter (1.8 mm²) black spot creating a high contrast light offset stimulus. This subtended a visual angle of 0.2 degrees, and provides a normal isoptre of approximately 20 degrees in keeping with recommendations for the detection of glaucoma using a white stimulus on a black tangent screen⁴¹⁹.

Oculo-kinetic campimetry with 1.5 mm offset stimulus was performed on 222 eyes (116 right, 106 left) of 126 individuals (68 male, 58 female; aged 16 - 91 yrs, mean 66.4 yrs) attending the glaucoma clinic with known or suspected glaucoma in one or both eyes. A total of 189 controls (83 male, 106 female; aged 19-86) were examined also.

2.2.2. Constantly Exposed Offset Stimulus of 3.0 mm. Diameter

In the second phase of the study, the OKC test with a 3.0 mm diameter offset stimulus (7.1 mm²) stimulus which subtended a visual angle of 0.4-degrees, was performed on 144 glaucoma eyes (73 right, 71 left) of 88 patients (35 female, 53 male; aged 60 - 85 yrs, mean 70 yrs), and 31 right eyes of 31 normal individuals (15 female, 16 male; aged 60 - 85 years, mean 70 yrs). The patients and healthy volunteers for controls in this part of the study were different from those examined with a 1.5 mm stimulus.

2.3. Constantly Exposed Offset Stimulus with Dynamic Fixation in Detection of the Blind Spot as a Model of Small Absolute Scotoma

The aim of this work was to establish the influence of clustering of fixation targets on test detection sensitivity in oculo-kinetic campimetry. Two different oculokinetic campimetry charts were used (i.e. Chart A and Chart B), which had either one or two fixation targets corresponding to the physiological blind spot (Figure 8). Subjects with a visual acuity of 6/12 or better and without any known ocular or systemic disease were selected randomly from hospital personnel and persons escorting patients to our hospital clinic. Two hundred and seventy two eyes (136 right, 136 left) of 139 perimetrically naive individuals (66 male, 73 female; age range 21-78 yrs, mean 45 yrs) were included in the study.

Sixty nine individuals were tested with Chart A and seventy individuals were tested with chart B by the author and an undergraduate medical student, S.M. Tavadia. All patients were examined with a high contrast offset (black-on-white) 1.5/400 mm stimulus. The OKC was performed under indoor normal lighting conditions (100-150 Lux). The right eye was tested first. Presbyopic and ametropic individuals were fitted with an appropriate optical correction. The same examination protocol was followed in each patient. The subject was asked to look at the first fixation target (ie number '1') and to say whether or not the stimulus was visible. Next, the subject was asked to read each number aloud and to report any numbers that were associated with disappearance of the stimulus. The results were recorded by the examiner without comment so as not to cause any bias. After examining the fellow eye, both eyes were examined a second time. If the test stimulus disappeared on both examinations when the patient looked at the number or numbers corresponding to the blind spot, the result was regarded as 'non-fluctuating positive'. If the blind spot was detected during one of the two consecutive examinations, the result was categorized as 'fluctuating positive'. If the blind spot was not detected on both examinations, the result was categorized as 'false negative'.

2.4. Computer-Assisted Moving-Eye Campimetry (CAMEC)

CAMEC operates on an IBM PS/2-286 personal computer with a VGA or EGA colour graphics card, a 14-inch VGA colour monitor (IBM 8512), a sound card (Audiocard 330E, RS Components Ltd, Corby, England) with loudspeaker, a joystick (Suncom Technologies Ltd.) and an IBM dot matrix printer. In addition, an adjustable head-rest is attached to the top of the computer monitor with a Velcro strap (Figure 9) .

To function, the CAMEC software requires two commercial programs to be installed. The Audiocard software controls the speech card so that CAMEC can give auditory or "spoken" commands and comments to the patient. The Microsoft Works spreadsheet is used to adjust test variables and to design examination strategies. The new CAMEC software code was written by Mr J. McGarvie and Dr A. Evans with design contribution by Drs Damato, Keating and the author. Various spreadsheets with different examination strategies were composed solely by the author (see Diskette).

Fixation Target

The dynamic fixation target consists of a spot and a circle. As the computerized version of moving eye method was originally intended primarily for children, the circle is added to mimic a computer game to maintain the patient's interest and attention. The test is designed to prevent loss of fixation by means of a constantly moving fixation target which is a disc shaped spot on the monitor and which must be held within the circle by the patient using a joystick. This task forces the patient to look at the spot and the circle so that the direction of gaze is controlled by the computer. As the capability of different children and adults to perform visual tests vary widely, the speed of the fixation target and hence the difficulty of the tracking procedure is adjusted automatically according to the patient's competence. Stimuli are presented successively in the central visual field as long as the patient satisfactorily maintains the moving fixation target in the circle. If the patient allows the fixation target to escape from the circle, the computer

bleeps repeatedly until cooperation is regained, and CAMEC issues "spoken" commands (with a female voice), such as "Please move the circle over the spot". This strategy ensures that the patient's fixation is well maintained when stimuli are presented.

The colour of the fixation target and the circle can independently be adjusted using the spreadsheet. The radius of the fixation target can be varied from 0.4 mm to 5.9 mm (0.07-1.12 degrees), with a default of 1.6 mm (0.3 degrees), and the radius of the circle can independently be varied from 1.2 mm to 7.8 mm (0.22 - 1.40 degrees), with a default of 7.0 mm (1.34 degrees).

The speed of the fixation target can be altered, using the spreadsheet, but automatically varies during a preliminary test program according to the patient's ability to maintain the circle over the moving spot. In addition, during the examination proper, CAMEC checks the patient's ability to keep the circle over the spot, because this may improve with experience or deteriorate with fatigue. The amount by which the fixation target accelerates or decelerates, and the proportion of time for which the fixation target must lie outside the circle before there is any change in the speed of the fixation target can each be adjusted separately using the spreadsheet.

Stimulus Factors

Presentation: Test stimuli are presented silently, one at a time. Although to the patient they seem to occur at random locations, the order of their presentation is pre-determined using the spreadsheet so as to reduce the fixation inadequacies. The eccentricity and meridian of each stimulus in relation to the patient's direction of gaze are calculated by the computer according to the distance between the eye and the screen, the location of the fixation target and the location of the test stimulus. Because the fixation target moves to the edges of the computer screen, the visual field is examined to an eccentricity of 29 degrees when the working distance is 30 cm. The fixation target stops moving when the stimulus is presented.

Detection: Awareness of the stimulus is signalled by the patient pressing a button on the joystick. If the button is pressed during the stimulus presentation or during a pre-selected time period immediately afterwards (i.e. during the response time), the computer emits a rewarding bleep and after a delay varying from 0.8 to 5.0 seconds, another stimulus is presented at a different location. The time between two stimulus presentations depends on the spatial distance between the two stimuli, the tortuosity of the path followed by the fixation target and the ability of the patient to keep the spot within the circle.

If the patient does not press the button when a stimulus appears, the stimulus is presented a second time, unless the blind-spot is being examined. If any one of these two stimulus presentations are detected, the stimulus is recorded as seen. Non-reproducible missed stimuli (i.e. one out of two) are recorded as false negatives. If neither of the two stimuli are seen, a stronger stimulus can be presented, which has more contrast, or a larger radius, or both.

If the patient attempts to cheat by pressing the button at random, the computer emits phrases such a "Please don't guess" or "Don't guess" and delays the presentation of further stimuli for approximately one or two seconds. In addition, such guesses are recorded on the final printout as false positive results.

The response period ('delay') allowed after each stimulus presentation can be the same for all patients and adjusted using the spreadsheet or it can be varied automatically according to each patient's response time as measured during a preliminary test (See below). In the latter case, the response period allowed after each stimulus presentation is a specified percentage of the patient's measured response time. The "response delay" setting of the CAMEC programs used in this research was kept constant at 1.0 seconds.

Size: The size of each rectangular stimulus can be varied in twelve steps from 1 x 1 pixels to 13 x 13 pixels on a 24.1 cm x 18.05 cm CRT screen, therefore, corresponding

to 0.14 mm² to 24.4 mm² in Video Graphics Array (VGA, 640x480 pixels) resolution (1 pixel measures 0.38 mm x 0.38 mm) or 0.20 mm² to 33.4 mm² in Enhanced Graphics Array (EGA, 640x350 pixels) resolution (1 pixel measures 0.38 mm x 0.52 mm). These stimuli are selected for the working distance of 30 cm.

Intensity: The stimulus intensity is entered in the test program spreadsheet which is used as the look-up table by the personal computer. The intensity of the background is adjustable in the same way. The luminance intensity on the test CRT monitor which have a range of 64 levels of brightness can be varied independently for both the background and each stimulus. It is therefore possible to examine differential detection sensitivity by presenting light offset (decremental, negative contrast) static stimuli on a selected background.

The contrast (C) value of the offset stimuli on 10 cd/m² background of the monitor is calculated using the "Weber's Luminance Contrast" formula⁴² which is acceptable for a small target on large uniform background⁴²⁰ such as CRT⁴³ and recommended for perimetric stimulus definition purposes by the International Council of Ophthalmology³:

$\text{Contrast}_{\text{Weber}}(C_w) = \frac{\text{Stimulus Luminance} - \text{Background Luminance}}{\text{Background Luminance}}$

and that can also be converted to decibel (DB) contrast ⁴²¹ (Figure 10):

$$C_{\text{DB}} = 20 \text{ Log } (-C_w)$$

Rectangular stimuli with sharp borders (square-wave) can be presented either as single contrast (intensity) or a minimum contrast (-4% = 28 dB) light grey followed by increasingly higher contrasts of static dark-on-bright (offset) stimuli until the stimulus is detected by the patient (single crossing threshold examination) at each test location.

In order to achieve a reliable stimulus detection, the following factors are observed during testing with CAMEC as with conventional automated perimetry: 1) Selection of the appropriate trial lens; 2) Placing the patient in front of the monitor adjusting the height of the seat and the screen, ensuring good patient comfort; 3) Maintaining the right test distance; 4) Occluding the fellow eye; 5) Locating the perimeter in a darkened and quiet room.

Duration: CAMEC stimulus duration can be varied from 0.1 seconds to 10 seconds with 0.1 second steps.

Coordinates: The CAMEC stimulus presentation coordinates on the Cathode Ray Tube (CRT) are entered into the test spreadsheet as degree meridian (ie 0 - 359 degrees) and degree eccentricity (i.e. up to 29 degrees). During the test, the eccentricity (∞) values are transposed to pixel coordinates on the CRT automatically by the computer by:

Pixel distance from fixation = Test distance (mm) x Tangent ∞ / Pixel size (mm)

In order to achieve maximum coordinate precision, that transposition is conducted in reference to the central pixel of the moving fixation dot.

CAMEC Modules

The Logo module: When CAMEC is not in use, the screen shows a picture of an eye, with the written instruction to press the button on the joystick to commence the examination.

The Setup module: By means of written and auditory commands, the patient is instructed to keep the head straight and still, to cover the left eye and to press the button on the joystick when he or she is ready to start the examination.

The Response module: The patient is asked to press the button on the joystick as soon as a number of large black spots on the screen are seen. This test is performed three

times and the average of the last two response times is calculated. This module may be activated optionally and was kept inactive during the research work described herein.

The Training module: A spot and a circle are displayed on different parts of the screen and the patient is asked to move the circle over the spot, using the joystick. When this task is successfully accomplished, the patient is reassured with the words "Well done!" and instructed to keep the circle over the spot as the latter meanders across the screen in an unpredictable fashion. Initially, the movement of the spot may be fast for the average person, but then slows down until the patient successfully maintains the circle over the spot for a specified proportion of the time. Once the speed of the fixation target is adjusted according to the patient's ability, the patient is advised to press the button when the stimulus appears. Four successive stimuli are presented, one in each quadrant. If any stimulus is correctly identified, the patient is reassured with the message "Well done!" and the examination begins. However, if the patient fails to position and maintain the circle over the moving fixation target or if none of the four stimuli are seen the test is aborted and the patient is advised to seek assistance. This module is compulsory and cannot be shut off at present. It lasts approximately 2.5 minutes.

The Calibration module: In CAMEC, different levels of stimulus brightness are obtained by selecting grey shades among the 64 available tones in VGA resolution. The calibration module allows the user to choose suitable colours or grey shades for the fixation point and circle, the background, and for each stimulus. The calibration software generates disc patterns on the screen with the ability to change the brightness or the colour of the disc pattern or the background by varying the intensity of each colour gun independently at 64 levels. Filled circles having a chosen radius are shown against the selected background. Calibration of various shades of grey can be achieved using a suitable photometer.

The Symbol module: The user can define up to 16 symbols for recording on the hard copy output the awareness of the various test stimuli. Each symbol has an array of 13

x 13 pixels and is designed using the computer mouse.

The Result module: Results can be viewed on screen, saved on disc and printed, with the results of both eyes on a single sheet. Additional information includes patient details, test duration, number of false positive and false negative responses, and a table showing the meaning of the symbols.

Audit module: The duration of each test and the time taken to complete the various parts of the test are automatically stored together with a summary of the examination results for subsequent analysis of the machine's performance.

CAMEC Test Programs

The test modules can be designed by the user by means of the spreadsheet and these can subsequently be modified. The following were designed for the investigative work solely by the author:

The 26-Point Screening Test: Twenty-six single-intensity stimuli are distributed throughout the central field (primary test locations), with additional four stimuli in the region of the normal blind-spot. If any stimulus other than one corresponding to the normal blind-spot is missed, it is presented a second time. Whenever non-blindspot stimuli are missed more than once, additional (secondary) points are examined, which are located between seen and unseen primary stimuli (Figure 11). This strategy is designed to reduce the number of points examined in scotomatous areas whilst increasing the number of points examined at the margins of any detected defects, while minimizing the false alarm rate. The static dark stimuli were presented for 0.4 seconds and had the luminance intensity of 8 Apostilb (Asb) on a brighter background of 32 Asb (10 cd/m^2), therefore creating a Weber's Contrast of -76%. The stimulus size is eccentricity compensated, becoming larger towards the periphery, with a rectangular surface area of 1.8 mm^2 up to 10 degrees, 3.1 mm^2 between 10 and 20 degrees and 4.9

mm² beyond 20 degrees from the fixation. The 26 point examination is completed in 4 minutes if all stimuli are seen. When a visual field defect is present, an additional 4-5 seconds are necessary for the re-test of each primary stimulus or the addition of a secondary stimulus, provided that the patient has good dexterity.

The 76-Point and 54-Point Screening Tests: These two programs had identical test grids to Humphrey Visual Field Analyzer (VFA) C30-2 and C24-2 programs respectively. Additional 4 stimuli were presented within the physiological blind spot. No secondary stimuli were employed. The stimulus sizes were eccentricity compensated, measuring 1.8 mm² up to 10 degrees, 3.1 mm² between 10 and 20 degrees and 4.9 mm² beyond 20 degrees from the fixation. Four stimulus contrasts of -76% (2.4 dB), -37% (8.6 dB), -22% (13.2 dB) and -10% (20 dB) on 10 cd/m², and also two stimulus contrasts of -76% and -22 % on 100 cd/m² were selected, using EGA graphics, each being available as a single stimulus intensity for either test grid.

The 54-Point Threshold Test: The retinal sensitivity at 54 primary points (Program 24-2 test grid of Humphrey VFA) in the central field is measured with increasing contrast levels of offset stimuli. An ascending staircase single-crossing threshold strategy with approximately 2-decibel steps are used. In that strategy, the test starts with the lowest contrast (lightest grey) stimulus and the contrast is increased after reproducible miss of each intensity until the stimulus is either seen or the highest contrast (black) stimulus is missed (Table 1).

2.4.1. Temporal variation in CRT Background Luminance

For calibration, the luminance of the CRT surface was measured at 36 (6 x 6) locations using a photometer (Minolta nt-1), using CAMEC Calibration Module. The VDU used in the study did not have any additional voltage regulator and the spectral composition (colour temperature) of the gray tones used in the study was not measured. Although

it is possible to maintain a fixed level of light intensity on a CRT from day to day automatically using an electronic feed-back circuitry attached to a lightmeter⁴²², the screen background intensity adjustment was made manually every time the monitor was switched on.

Measurements were made immediately after switching the CRT mains on, within the first few minutes, on grey shade number 40. Measurements were repeated in 1/2 hour and 1, 2, 3, 4 and 6 hours later. To provide standardization, monitor 'Brightness' and 'Contrast' adjustments were always kept at the same level. The luminance values and their variation were evaluated according to the locations on the screen where the measurements were performed. These locations were grouped in 4 concentric zones, namely the centre, inner, intermediate and outer zones.

2.4.2. CRT Luminance Variation with Monitor 'Brightness' Setting

The standardization of stimulus intensity for the same patient or between the patients on repeat examination is possible only by generating same amount of brightness on different test occasions using a given grey shade. The 'Brightness' and 'Contrast' settings of a CRT monitor are of crucial importance in attaining a selected brightness level. The effects of these settings were investigated in the monitor used for the clinical testing of the patients.

Luminance measurements were made at 36 locations for each of the 64 shades (numbers 0-63) of grey available. The mean value is calculated for each grey shade at brightness settings of minimum, medium (half-way) and maximum. The 'contrast' setting was always kept at its minimum.

2.4.3. Stimulus Brightness Selection on a CRT

Theoretically, a small patch of any grey shade presented on another shade should maintain the same amount of luminance indicated in the curve. Does any dark grey shade presented on a brighter shade, or vice versa, really produce the expected luminance? In order to answer the question, grey shades 0 - 40 were presented as 1.5 cm diameter disc patterns on a bright background (shade #37; 10 cd/m²) and also on a dark background (shade #1; 0.3 cd/m²), using the calibration module (see Chapter 2.4). The brightness of the same numbers of grey shades was measured against two different backgrounds.

2.4.4. Topographical Variation in CRT Luminance and Image Contrast

The photometric measurements of the CRT employed in clinical testing were made in a 6 x 6 grid of circular grey patterns of 1.5 cm diameter on a three different and seemingly uniform brighter backgrounds of 3 cd/m², 10 cd/m² and 100 cd/m². A total of six points were measured around each disc and averaged as the background intensity. Also the luminance inside each disc was recorded as the stimulus intensity.

2.4.5. Temporal Variation in Stimulus Duration

Of critical importance in any computer-based CRT display system is the accuracy of the input display timing obtained¹¹⁷. The stimulus duration is controlled by an 'internal timer' in the computer. As the computer's 'internal timer' has an operating frequency of 18.2 Hz, the precision of the stimulus durations is expected to be limited to +/- 0.055 seconds. During the test, the software program loops while moving the fixation target, the elapsed time is checked and if it is found greater than the preset duration then the stimulus presentation is postponed. That initiates a new loop in attempt to re-generate

the cancelled stimulus with more accurate timing. In that way, homogeneity and standardization are achieved at least partially in stimulus duration.

The real-time accuracy of stimulus durations was tested using an additional software program to record the 'internal timer' operation and the time periods in which stimulus presentations took place. The internal timer operation duration of 100 consecutive stimuli were recorded by for four different preset desired 'stimulus duration' values; 0.1 second, 0.2 second, 0.4 second and 0.6 second, using the software by Mr J McGarvie. No actual physical measurements of stimulus durations were made on the CRT screen.

2.5. Fixation Control with Dynamic and Static Fixation in Children

The aim of this study was to evaluate the ability of the dynamic fixation and offset stimuli of CAMEC to detect the physiological blind spot and to maintain fixation in children.

A total of 32 normal eyes (19 right, 13 left) of 32 consecutive patients (15 boys, 17 girls) aged 4-10 years (mean 5.8+/-1.5 years) who were attending the Orthoptic Clinic were included in this study (Figure 12). All eyes had a visual acuity of 6/9 or better. Each eye was examined by both the Dicon Autoperimeter fitted with a video fixation monitor (Cooper-Vision Inc., USA) and CAMEC. Each patient was tested with both the 'Blind Spot Program' of DICON, which presents 13 stimuli in a 5x7 degree area at the blind spot location and an additional eight stimuli in the surrounding periphery (i.e., total 21 stimuli), and a similar CAMEC 'Blind Spot Test Program' which presents 14 stimuli in the blind spot (Figure 13). The parameters of both techniques used in the study are given in Table 2.

The order of the two tests were selected randomly for all cases. Sixteen eyes were tested with Dicon first and 16 eyes were tested with CAMEC first. Both tests were operated by the author in the presence of at least one parent. All patients were initially given the demonstration program of each method during which they were also reminded repeatedly to look at the fixation target only. Once the child was familiar with the requirements of the test procedure, the examination was performed without any further intervention.

The percentage ratio of the number of missed stimuli to the total number of stimulus presentations in the blind spot area was the test score for each technique. The scores from the two field test methods were compared using the Wilcoxon signed-rank test (Statistical advice was provided by Dr D.Keating).

2.6. Dynamic Fixation with Single Intensity Static Offset Stimuli in Screening for Neuro-ophthalmic Visual Field Loss

The usefulness of CAMEC and single intensity high contrast static offset stimuli in the recognition of neuro-ophthalmic visual field defects have been investigated and the test sensitivity, specificity and efficiency were determined against standard Goldmann Perimetry. The visual fields of 107 patients (52 females and 46 males), aged 9-78 years (mean 42 years) with corrected visual acuity better than 6/36 (<+/- 7.00 dioptre spherical equivalent) were tested using routine Goldmann perimetry and the CAMEC 26-Point Screening Program with -76% contrast single intensity offset stimuli in the neuro-ophthalmology clinic. The spatially adaptive test grid for eccentricity compensated offset stimuli consisted of 26 primary test locations and four additional stimuli are presented to locate the physiological blind spot (Figure 14). According to the patient responses (push-button registry) to the primary stimuli, the secondary stimuli whose coordinates are pre-registered in the test program spreadsheet are selected and added automatically by the computer in between the 'seen' and reproducibly 'missed' primary stimuli to define the borders of the detected abnormality in an economical manner. The order of the two examinations was selected randomly. The technician (author) remained in the room while the CAMEC test is in progress and monitored the patient's fixation also. Occasional reminders to maintain fixation were also provided.

Goldmann Perimetry was performed, as part of routine patient care, by qualified optometrists on all patients, using standard kinetic stimuli (size I = 0.25 mm²) and filter combinations of 2e (100 Asb), 3e (320 Asb) and 4e (1000 Asb, maximum intensity) with additional static spot-checks inside the isoptres. A rest interval of 10-15 minutes was allowed between the Goldmann and CAMEC tests to minimize patient fatigue. The results with two or more reproducibly 'missed' adjacent single intensity offset stimulus locations were regarded as abnormal^{413,423}. The Goldmann perimetry findings were evaluated and the abnormalities defined in the clinic by various neuro-ophthalmology staff who were unaware of the field status to the offset stimuli. A comparison was made

between the results from both types of tests to determine the sensitivity and specificity of the offset stimulus design later. The efficiency (time requirement) of CAMEC test was evaluated also.

2.7. A Comparison of Single Intensity Static Offset Stimuli with the Onset Stimuli of Humphrey VFA in Glaucoma

In this study, the scotoma detection sensitivity and specificity of single intensity offset perimetric stimuli of varying contrast on a cathode ray tube are compared with conventional light onset stimuli of the Humphrey Visual Field Analyzer in glaucomatous eyes, using the STATPAC empirical probability maps as the gold standard. The detection thresholds in terms of Humphrey Visual Field Analyzer decibel values have also been established for different contrasts of offset stimulus.

Twenty-five glaucomatous eyes (17 right and 8 left) of 25 perimetrically experienced primary open angle glaucoma (POAG) patients (13 male and 12 female), aged between 35 - 82 years (Mean 68 years) were included in the study. All eyes had 6/6, N5 or better visual acuity with correction less than ± 7.00 dioptres spherical equivalent, no media opacities and normal (3-6 mm) pupils. None of the patients suffered from non-glaucomatous ocular disorders or systemic disease. Four offset stimulus contrasts of -76% (n=25 eyes), -37% (n=14 eyes), -22% (n=25 eyes) and -10% (n=9 eyes) on 10 cd/m² and also two stimulus contrasts of -76% (n=10 eyes) and -22% (n=10 eyes) on 100 cd/m² were selected for single intensity testing. These were the only suitable gray tones of the EGA graphics software of CAMEC in giving a useful stimulus range. These offset stimulus contrasts were presented on a 10 cd/m² background for 0.2 seconds. Tests were performed with single intensity stimuli as separate examinations in a random order, using CAMEC 76-Point Screening Test (Figure 15) and either before or after the Humphrey 30-2 threshold test. Both CAMEC and Humphrey VFA tests were administered by the author. All patients had prior demonstration / training which involved the recognition of the offset stimuli for each test. Patient fatigue was minimized with ample rest periods during and between the test sessions. All tests for each individual were performed with full aperture near correction at a 30 cm test distance and completed on the same day.

2.7.1. The Sensitivity and Specificity of Offset Stimuli in Glaucoma

The Humphrey STATPAC 'empiric probability (p) values' as well as the offset stimulus detection status, ('seen' or 'missed') for each contrast at the corresponding test locations were compared at eccentricity annuli bands of 4-9 degrees, 10-20 degrees and 20-28 degrees using the 'Minitab' statistical software package. The sensitivity and specificity of the different offset stimulus contrasts were studied by performing point-by-point comparisons between the Humphrey 'Total Deviation' (TD), 'Pattern Deviation' (PD) plots and CAMEC results, except the test locations above and below the physiological blind spot. The threshold results showing significant depression in 'TD' and 'PD' plots beyond 95% confidence interval (shown with STATPAC symbols representing $p < 5\%$, 2%, 1% and 0.5%) were categorized as representing the visual field abnormality and the remaining locations (inside 95% confidence interval, $p > 5\%$) were considered healthy parts of the visual field.

2.7.2. Detection Thresholds for Offset Stimuli in Glaucoma

The decibel threshold values on the numeric map of Humphrey VFA and the offset stimulus detection status ('seen' or 'missed') for each contrast at the corresponding test locations were compared at three eccentricity annuli bands of 4-9 degrees, 10-20 degrees and 20-28 degrees, excluding the test locations above and below the physiological blind spot.

The retinal sensitivity levels in terms of Humphrey decibels have been determined for all contrasts and sizes of offset stimuli as the detection thresholds above which 70% of the 'seen' and below which 70% of the reproducible 'missed' responses were recorded by CAMEC.

2.8. Detection Thresholds to Static Offset Stimulus and The Effect of Refractive Blur

The normal detection threshold values to light decrements on a CRT monitor are defined at different eccentricities along the nasal horizontal meridian of the normal central visual field and the effect of refractive blur on the visual sensitivity to various sizes of offset stimuli is described.

The right eyes of five perimetrically experienced healthy male individuals (mean age 28.8 yrs.; range: min. 25 yrs., max. 33 yrs.) were included in the study. All eyes had at least 6/5, N5 visual acuity with correction, normal pupils (3.5 - 5 mm in diameter) and normal visual fields with Humphrey Visual Field Analyzer Threshold Program 24-2.

The detection thresholds were determined at 6°, 12°, 18°, 24° and 30° eccentricity from fixation along the nasal horizontal meridian. At each eccentricity, the stimuli were presented at two locations above and below the nasal horizontal meridian with 4° vertical separation (Figure 16). Therefore, the final detection sensitivity at each eccentricity was represented by the average of two threshold crossings. Measurements were repeated with rectangular stimuli sizes of both 4 mm² and 16 mm² (Goldmann equivalent sizes III and IV respectively) at four different Snellen near visual acuities of 6/6, 6/12, 6/24, 6/60 (measured with 'Rosenbaum Pocket Vision Screener', Cleveland, Ohio) in 30 cm. test distance with full aperture correction. The average amount of full aperture corrections required to achieve visual blur and various acuity levels have been shown in Table 3. Each threshold test took 3 - 4 minutes. All 8 tests were completed on the same day with a few minutes of rest intervals between the sessions for each subject.

2.9. Topographical Reproducibility of Small Scotoma with Computerized Dynamic Fixation and Offset Stimuli

The dimensions of the physiological blind spot as a model of small scotoma to light offsets and the topographical reproducibility of detected scotomas on repeat examination using computerized dynamic fixation method are investigated.

The normal right eyes of 10 perimetrically experienced healthy individuals, 8 male, 2 female, mean age 30.6 yrs. (range: min. 23 yrs., max. 44 yrs.), were included in the study. All eyes had at least 6/5, N5 visual acuity with correction ($< \pm 7.00$ spherical equivalent).

The offset test stimulus has been adjusted to present Weber's contrast polarity of -15% (i.e., 17 dB) contrast on 10 cd/m^2 background intensity. That stimulus contrast is suprathreshold in the normal central visual field and its non-detection indicates abnormally low sensitivity. The stimuli were presented in the each 'blind spot test program grid' with 1 degree resolution (Figure 17). Each eye was tested twice to document the fluctuation of the results. Each 'blind spot test' takes 11-15 minutes to complete, depending on the size of the blind spot and the individual level of dexterity in joystick manipulation. Tests were completed on the same day with adequate rest intervals during and between the tests to minimize patient fatigue.

2.10. Detection Thresholds to Light Offsets in Normals, Ocular Hypertension and Primary Open-Angle Glaucoma

Threshold evaluations were performed in the central visual field using offset stimuli with dynamic fixation and onset stimuli with static fixation to establish the sensitivity and specificity of each method against the other. The differential detection thresholds to light onsets and offsets were measured using the Humphrey Visual Field Analyzer and CAMEC respectively. The results from the equal sizes and durations of static threshold light onset and offset stimuli in the central visual fields of normal, glaucomatous and ocular hypertensive eyes were compared. The relationship between visual sensitivity to both types of stimuli was established in both normal and glaucomatous abnormal visual fields as well as ocular hypertensive eyes.

The conventional perimetry was performed using the full threshold test program 24-2 of the Humphrey Visual Field Analyzer (Humphrey Instruments, San Leandro, CA). The threshold determinations to the offsets were performed with CAMEC 24-2 threshold program. Since the joystick use significantly prolongs the duration of CAMEC examination among the elderly (see Chapter 3.6.) and the attention required for the maintenance of that central visual-motor task may influence the peripheral detection thresholds in all age groups, in this study, the joystick was manipulated and the fixation was monitored by the operator (author) in order to prevent any attenuating influence of joystick use on patient vigilance required for the detection of light offsets. Threshold examinations with light offsets and onsets were performed using identical test grids (Program 24-2, 54 locations), stimulus size (Goldmann-IV equivalent=16 mm²) and duration (0.2 second). All subjects had prior demonstration involving the recognition of the light 'onsets' and 'offsets'. Both tests were administered by the author in a random order and completed on the same day. Patient fatigue was minimized by several rest intervals during and between the tests.

Twenty-one patients with primary open angle glaucoma (POAG) and 21 patients with

ocular hypertension (OHT) attending the glaucoma clinic, and 13 age-matched normal individuals (hospital workers and the patients' friends) were tested with both techniques. The eyes constituting the diseased and control groups were included in the study according to the selection criteria given in Table 4. If both eyes of the subjects satisfied the criteria, only one eye was selected randomly. In the presence of asymmetrical cupping between the two eyes of ocular hypertensive subjects, the eyes with higher cup to disc ratio were enrolled. None of the subjects suffered from non-glaucomatous ocular disorders or any systemic disease. Highest IOP recording without treatment was used for assessments. To prevent bias, cup-to-disc ratio was determined for each eye by independent clinicians as part of routine patient care at clinic before the tests. More than 6 decibels (dB) sensitivity loss at two or more adjacent test points, or at least 10 dB sensitivity loss at one test location on the results from the Humphrey STATPAC were regarded as representative of visual field abnormality⁴²⁴. The following logistic regression model formulated by Hart et. al.⁴²⁵ and which uses a weighted combination of patient age, intraocular pressure (IOP), cup to disc ratio (CDR) and family history (FH) for glaucoma to estimate the 'risk of developing visual field loss' (RDVFL) was used to calculate the glaucoma risk for each individual included in the study.

$$\text{RDVFL} = \frac{1}{1 + e^{(\text{Factors})}}$$

$$\text{Factors} = [14.64 + (-1.48 \times \text{FH}) + (-12.20 \times \text{CDR}) + (-0.16 \times \text{IOP}) + (-0.07 \times \text{AGE})]$$

The tests were performed with full aperture near correction for 30 cm test distance. The visual field threshold results were printed-out automatically by the computer at the end of each test.

The visual field test results from each method were evaluated according to the individual test points as well as the global visual field indices. Firstly, 95% confidence intervals (CI) of the decibel (dB) threshold values were calculated for each of the 52

test points constituting the test grid (excluding the two test locations above and below the physiological blind spot) in the control population, using a commercially available statistical software package (Minitab). 'Non-parametric sign test for median' was used for CI calculations. The threshold values below the lower 95% CI limit for each test point were regarded as abnormal locations in the visual fields of control, OHT and POAG populations.

Secondly, global visual field scores for both 'onset' and 'offset' stimuli were calculated for each eye according to the global visual field index formulas of 'Mean Sensitivity' (MS), 'Mean Defect' (MD) and 'Loss Variance' (LV)⁹⁹. The age expected threshold values used in the formulas for global field indices were determined using regression analysis of threshold results against the patient age for all of the individual test points in the control group.

The 95%, 98% and 99.9% CI were also established for 'MD' and 'LV' in the control group, using non-parametric sign test for median. The global field index values below the lower confidence limits are regarded abnormal. Statistical comparisons of the results were made with Mann-Whitney Test.

Part 3. RESULTS

The fewer the facts the stronger the opinion.
[Andy Warhol]

3.1. Light Offset Stimuli and Dynamic Fixation on Bjerrum Screen

3.1.1. Meridional Hill of Vision to the Offset and Onset Stimuli

The disappearance eccentricities of the offset stimuli in the meridian tested were significantly smaller than those of the onset stimuli of equal size (Non-parametric Sign Test for paired data, $p < 0.05$) (Figure 18).

3.1.2. The Effect of Variation in Illumination on Offset and Onset Stimuli

The percentage increase in white-on-black onset stimulus disappearance eccentricity was significantly more than that of black-on-white offset stimulus (Non-parametric Sign Test for paired data, $p = 0.0156$). Increasing the ambient illumination from 13 lux to 400 lux increased the isoptre of the onset stimulus by 59% and the isoptre of offset stimulus by 36% (Figure 19).

Similarly, the eccentric visibility change due to illuminance variation was significantly more for the white-on-grey onset stimulus than that the black-on-grey offset stimulus ($p = 0.0078$). At the higher ambient illumination, the offset and onset stimuli disappearance eccentricities increased by 75% and 117% respectively (Figure 20). Isoptre increases of offset stimulus and onset stimulus on grey background were significantly more pronounced than those of offset stimulus on white background ($p = 0.0156$) and onset stimulus on black background ($p = 0.0078$).

3.2. Clinical Evaluation of Dynamic Fixation and Constantly Exposed Offset Stimuli in the Detection of Glaucomatous Visual Field Loss

3.2.1. Constantly Exposed Offset Stimulus of 1.5 mm. Diameter

All patients were able to complete the test. At least one test location causing reproducible disappearance of the stimulus was required to consider the test result abnormal (i.e. positive). The OKC test was positive in 45% of eyes with only relative visual field loss (Stage 1), 81% of eyes with small absolute scotomas separate from the blind spot (Stage 2) and 100% of eyes with more extensive absolute visual field defects connected to the blind spot (Stages 3 and 4). When the results were categorized according to the severity of field loss in the worse eye, the OKC result was positive in 51% of patients with only relative field loss, 86% of patients with small absolute defects and 100% of patients with large absolute defects extending to the blind spot (Figure 21).

Three control subjects were found to have unequivocal visual field loss on conventional perimetry and were excluded from the study. The results were considered according to age groups and are summarized in Figure 22. The false positive result rate was 1% in patients under the age of 60 yrs, 9% between the ages of 60 - 70 yrs and 13% over the age of 70 yrs.

A sub-group of 95 eyes of 66 patients attending the glaucoma clinic had no evidence of glaucomatous visual field loss in one or both eyes on conventional perimetry. These eyes had ocular hypertension and/or abnormal optic disc appearances or definite glaucoma in the fellow eye. In this group, an abnormal OKC result occurred in 24% of eyes and was more common in patients older than 60 yrs of age (8% v.s. 30%; $p < 0.01$, chi-square test)(Figure 23) and in eyes with a visual acuity of less than 6/6 (6.4% v.s. 41.7% ; $p < 0.01$, chi-square test) (Figure 24). The OKC positive result rate is shown according to age in Figure 25.

There were 38 eyes (30%) with a glaucomatous visual field defect which was missed with OKC. In four eyes the depth of the relative scotoma was less than 5 decibels(dB) and would not universally be regarded as unequivocal field loss^{409,426}. In 26 eyes the field loss was relative and deeper than 4 dB in the central 15 degrees. Two eyes had small absolute scotomas within the 15 degrees, which were missed because they were situated in between the points examined by the OKC chart. In a further six eyes, the visual field defects were more than 15 degrees from fixation.

The cartographic results of the glaucomatous eyes showing visual field loss to conventional perimeters were compared topographically to those from OKC among those who produced a true positive OKC result (n=89 eyes), using transparent overlays of OKC test coordinates. The ratio of the number of OKC test locations producing an abnormality to the total number of OKC locations falling inside the scotomas on conventional results was calculated for each eye and named 'topographical index' (T.I.). The OKC abnormalities were more widespread (T.I.>1.0) than the conventional scotomas in 17% (15/89) of the eyes. The OKC and conventional field defects were of equal size (T.I.=1) in 20% (18/89) of the true positive OKC results. In the remainder 63% (56/89) of the eyes, abnormal OKC results reflected smaller scotomas (TI<1) than those to the conventional visual field tests, suggesting underestimation of the topographical extent of the scotomas.

The Friedman Analyzer test results from glaucomatous eyes which also gave OKC abnormality (n=47) were used to further determine the equivalent light sensitivity required for non-detection of 1.5/400 offset stimulus on OKC chart. In that, transparent overlays with OKC coordinates were used to tally missed and seen OKC test locations in relation to Friedman cartograph in each eye. The percentage missed offset stimuli was plotted against each retinal light sensitivity value on Friedman result ('frequency of seeing' curve) for eccentricity bands of 13° (OKC Points 1 - 17), 9° (OKC Points 18 - 22) and 5° (OKC Points 23 - 26). Inside the absolute scotomas, the offset stimulus of OKC was missed with 81% frequency at 13°, with 40% frequency at 9° and with 33%

frequency at 5° eccentricity. The equivalent light sensitivity required for 50% non-detection of black stimulus could be identified only at 13° and that was 0.8 - 1.0 log unit (100 - 159 Apostilb) (Figure 26).

3.2.2. Constantly Exposed Offset Stimulus of 3.0 mm Diameter

In the second phase of the study, the OKC test was performed with a 3 mm stimulus to determine whether the specificity could be improved without a significant reduction in sensitivity above 60 years of age.

In the sample of abnormal eyes, the OKC test result was positive in 33% of eyes with relative defects only (Stage 1), 56 % of eyes with absolute scotomas separate from the blind-spot (Stage 2), 80% of eyes with arcuate defects extending to the blindspot (Stage 3) and all eyes with altitudinal defects (Stage 4) (Figure 27). None of the 13 'glaucoma suspect' eyes of 13 patients produced an abnormal OKC result. None of the control cases produced a false positive OKC test result.

3.3. Constantly Exposed Offset Stimulus with Dynamic Fixation in Detection of the Blind Spot as a Model of Small Absolute Scotoma

With Chart A, which had one fixation target corresponding to the blind spot, a non-fluctuating positive result was obtained in 75/138 eyes (54%); a fluctuating positive result occurred with 14/138 eyes (10 %); and a false negative result occurred with 49/138 eyes (36 %).

With Chart B, which had two fixation targets corresponding to the blind spot, a non-fluctuating positive result with one or both targets was obtained with 102/134 eyes (76 %); A non-fluctuating positive result occurred with one target only in 20/102 eyes (20 %) and with both fixation targets in 82/102 eyes (80%). With 12 eyes (9 %), a fluctuating positive result only was obtained with one or both fixation targets. A false negative result occurred with 20/134 eyes (15 %) (Table 5).

3.4. Computer-Assisted Moving-Eye Campimetry (CAMEC)

3.4.1. Temporal Variation in CRT Background Luminance

With repeated luminance measurements over time, the average CRT screen luminance within five minutes after switching on was 10 cd/m². The luminance rapidly increased within the first 30 minutes at all zones, reaching to 11.8 cd/m², the 97% of the final average level. There was little increase in the luminance afterwards, measuring a mean of 12.0 cd/m² (98% of final) in 1 hour and 12.2 cd/m² (100%) in 2 hours. The average luminance remained steady thereafter. It appeared that the average screen luminance was highest at the centre, decreasing gradually towards the edges of the screen (Figure 28). Repeat measurements performed on different days produced similar results.

3.4.2. CRT Luminance Variation with Monitor 'Brightness' Setting

The overall screen luminance increased gradually with lighter grey shades. The luminance curve displayed a shift to higher levels and became more linear with increasing 'brightness' setting. That change affects the amount of the light differences (steps) between the grey shade levels at different settings, having a direct impact on stimulus and background compositions and their contrast values (Figure29). The same experiment was repeated further at minimum level of 'brightness' and various levels of 'contrast' settings. A similar variation in luminance curve was noted.

3.4.3. Stimulus Brightness Selection on a CRT

When the grey shades 0 - 40 were presented as 1.5 cm diameter disc patterns on a bright background of 10 cd/m², the luminance values became higher than expected

(Figure 30). When the background was 0.3 cd/m^2 , the brightness of each grey shade became less than expected.

3.4.4. Topographical Variation in CRT Luminance and Image Contrast

Background measurements revealed topographical luminance irregularities, reaching -11% to +16% of the mean screen luminance of 10 cd/m^2 . When the measurements were repeated for higher and lower background levels, topographical luminance irregularities were -17% to +15% of the 100 cd/m^2 background and -8% to +17% of the 3 cd/m^2 background. At three different background levels, the pattern of irregularity was constant. Identical variations were observed for the stimulus luminance.

The stimulus and background intensities varied equally from one location to another across the CRT surface. That indicates that the stimulus to background luminance ratio remained constant at different locations, therefore, protecting the Weber's contrast and visibility of the stimuli (Weber's Law) irrespective of topographical fluctuations in CRT brightness (Figure 31).

3.4.5. Temporal Variation in Stimulus Duration

The average stimulus duration determined by registering the internal clock response was found to be longer than those preset values entered in the test spreadsheet. The amount of prolongation in the stimulus period varied according to the preset value. For the shortest preset value of 0.1 second, the average stimulus duration was 66% longer. The prolongation in the mean duration became less obvious with higher preset values and was +42% for 0.2 second, +20% for 0.4 second, and +10% for 0.6 second. (Table 6). These values represent the temporal variation in stimulus duration as a matter of internal clock response registry rather than a physical measurement of the actual stimulus

durations on the screen which may also be influenced by the phosphor persistence/decay time of the individual CRT used.

3.5. Fixation Control with Dynamic and Static Fixation in Children

Twenty-four of the 32 children performed and completed both tests successfully. The details of the patients who could not cooperate sufficiently on either test and the number of abandoned tests are given in Table 7.

Among the 24 patients who successfully completed both tests, the blind spot was detected in 18 eyes (75%) by the Dicon Auto-Perimeter and in 24 eyes (100%) by CAMEC. The full scores from all patients are shown in Figure 32.

The blind spot detection scores were significantly higher with CAMEC (mean 61.0%, SD 22.5%, range 14-100%) than with the Dicon Autoperimeter (mean 26.6%, SD 24.1%, range 0-77%)(Wilcoxon test, $p < 0.001$).

3.6. Dynamic Fixation with Single Intensity Static Offset Stimuli in Screening for Neuro-ophthalmic Visual Field Loss

One hundred and sixty nine eyes (87 right and 82 left) from 98 patients who completed both the Goldmann and CAMEC screening tests were included in the evaluation. The 26-point test had to be abandoned in the remaining 9 patients (8%) due to lack of cooperation, and these patients were excluded from the analysis. Six patients (6%) could complete the screening test only with continuous assistance with the joystick; however, the results from these patients were included in the study.

Goldmann perimetry revealed visual field abnormalities in 110 eyes (57 right, 53 left) of 75 patients, but interpreted within the normal range in 59 eyes (30 right, 29 left). Neuro-ophthalmic conditions of the patients are listed in Table 8. The field defects indicated by Goldmann perimetry were quadrantanopia in 21 eyes, hemianopia in 27 eyes, constriction (partial/generalized) in 54 eyes, altitudinal defect in 4 eyes and arcuate and paracentral defects in 4 eyes.

The 26-point test produced normal results in 87% (26/30) and 86% (25/29) of the right and left eyes respectively with normal Goldmann perimetry results (true negative rate=specificity). The offset stimuli also revealed the Goldmann visual field defect in 88% (50/57) and 91% (48/53) of the right and left eyes respectively (true positive rate=sensitivity) (Figure 33). The distribution of the abnormal results from both offset and onset stimuli according to visual acuity were similar, suggesting no apparent discrepancy in the influence of low visual acuity on high contrast (i.e. black) offset stimuli and conventional light stimuli (Figure 34).

In order to document the topographical correspondence between visual field defects shown by both type of stimuli, those defects identical in location and extent in the central visual field were categorized as a 'good' correlation. If the location or the size of the defects differed slightly in the two tests, the correlation was 'fair'. A discrepancy

in both the location and extent of the defects indicated a 'poor' correlation. The subjective comparative evaluation of the results showed a good or fair degree of topographical correlation between the defects in 49 % and 33 % of the eyes respectively. For example, an inferotemporal partial quadrantanopia in the right and normal visual field in the left eye of a 66 year old male who had craniopharyngioma excision several years ago were revealed by CAMEC (Figure 14). The field loss to the offset stimuli extends to the superotemporal quadrant along the vertical meridian, causing 'fair' degree of correspondence to that obtained by the luminous stimuli of Goldmann perimeter. Only 17% of the results from the offset stimuli indicated a 'poor' correlation and in one case, there was no correlation between the recorded abnormalities.

The duration (efficiency) of the 26-point screening test was studied further using a statistical software program (Minitab Inc, USA) and Pearson's product moment correlation (parametric) test and linear regression analysis. The data used satisfied the criteria of normal distribution⁴²⁷ and met the conditions for a linear relationship between the parameters^{428,429} including the random distribution of y residuals⁴³⁰. In unilaterally and bilaterally tested individuals with normal visual field, the average test duration under computerized dynamic fixation monitoring was 550 seconds and 695 seconds respectively. When a visual field defect was present in one or both eyes, the average duration was longer with a mean value of 751 seconds and 1170 seconds respectively (Table 9). The duration of the 26-point screening test also extended with increasing patient age, both with bilaterally normal (n = 22, r = 0.45, p = 0.037) and abnormal (n = 36, r = 0.45, p=0.005) visual fields (Figure 35). Regression analysis predicts the estimated test duration (T.D.) for bilaterally normal fields as T.D. (Seconds) = 577 + (3.35 x AGE) and for bilaterally abnormal fields as T.D. (Seconds) = 828 + (9.46 x AGE).

3.7. A Comparison of Single Intensity Static Offset Stimuli with the Onset Stimuli of Humphrey VFA in Glaucoma

3.7.1. The Sensitivity and Specificity of Offset Stimuli in Glaucoma

STATPAC evaluation of the decibel threshold values revealed relative scotomas in 11 eyes (Aulhorn-Karmeyer Classification, Stage 1), small isolated absolute scotomas in 10 eyes (Stage 2) and absolute scotomas connected to the blind spot in 4 eyes (Stage 3) with the mean global visual field indices of -5.2 dB Mean Defect (MD); 6.1 dB Pattern Standard Deviation (PSD); 5.4 dB Corrected Pattern Standard Deviation (CPSD); and 2.2 dB Short Term Fluctuation (STF). The reliability indices from all Humphrey threshold results were within the normal range (i.e. fixation losses < 20%, false answers < 33% of total attempts). The cumulative frequency of involvement of the test locations in the 'Total Deviation' and 'Pattern Deviation' plots is shown in Figure 36.

All four contrasts of static offset stimuli indicated the abnormal areas in the central visual fields of one glaucomatous eye as shown in Figure 37. In general, lower contrasts of offset stimuli delineated more extensive visual field abnormalities and displayed abnormal areas which were not detected by the light stimulus and STATPAC (Figure 38). The highest contrast (-76%, black) stimuli and the lowest contrast (-10%, light grey) stimuli identified the normal and abnormal points respectively with the best accuracy at all eccentricity bands. For instance, the black (-76% contrast) stimulus identified 93% of the normal locations (true negative rate=specificity) in 'PD' plots as such with a false positive rate of 7% within 10 degrees from fixation; however, its true positive rate (detection of abnormality=sensitivity) for glaucomatous loss was only 49% in the same area. Both the true and false positive rates increased with increase in eccentricity. The true positive rate improved with lowering offset stimulus contrast and reached to 86% at -10% contrast with a higher 'false positive' rate of 35% within 10 degree eccentricity. That relationship between the offset stimulus contrast and the detection rates was evident at all eccentricities (Figure 39).

3.7.2. Detection Thresholds for Offset Stimulus in Glaucoma

The full results from 10 cd/m² and 100 cd/m² are given on Tables 10 and 11. The retinal sensitivity levels required for the detection of all four contrasts of offset stimuli in the selected sizes were lower than the normal retinal sensitivity values for the mean age of the study group⁹⁰ and, therefore, designed offset stimuli were supra-threshold (Figure 40). Lower contrasts of offset stimuli required higher retinal sensitivity for their detection. Decreasing the stimulus contrast to -10% from -76% on 10 cd/m² background caused an increase in the offset stimulus detection threshold for 2.6-3.5 Humphrey decibels (dB) (at 6 and 28 degree eccentricity respectively). Increasing the background luminance to 100 cd/m² caused a significant elevation in the detection threshold for -22% offset stimuli in all eccentricities (Mean difference: +0.82±0.36 dB, p=0.0068; paired t-test) without any effect on the threshold for -76 % stimuli (Mean difference: -0.06±0.4 dB, p=0.76) (Figure 41).

3.8. Detection Thresholds to Static Offset Stimulus and the Effect of Refractive Blur

The full results from each stimulus size and test location at various visual acuity levels are shown in Table 12.

3.8.1. The Effect of Eccentricity on Offset Threshold

The detection sensitivity to light offsets was greater near the fixation, gradually decreasing towards the periphery of the central visual field, for both size III and size IV stimuli. When the 4 mm² offset stimuli were employed in the absence of refractive blur, the average reduction in sensitivity with increasing eccentricity was 0.22 decibels/degree. At lower visual acuity levels (i.e. <6/6) that inverse relationship between the sensitivity and the eccentricity was also present, with an average of 0.21 dB/degree (range 0.19 - 0.22 dB/degree).

3.8.2. The Effect of Stimulus Size on Offset Threshold

Quadruplication in the area of the offset stimulus resulted in reduced detection thresholds and easier detectability along the horizontal meridian. The spatial summation coefficient (k) values for offsets could not be determined accurately at 6 and 12-degree eccentricity at all acuity levels as well as at 18-degree at 6/6 acuity since even the lowest contrast (i.e. 23 dB) stimuli were suprathreshold and detectable in the fields tested. The coefficient k values were calculated between 18 to 30 degrees from fixation at various acuity levels and these are shown in Table 13. The spatial summation (k value) fluctuated with eccentricity, reaching to a maximum of 0.5 in the central field.

3.8.3. The Effect of Defocus on Offset Thresholds

The average of threshold recordings from all ten test locations in each eye has been used as the 'Mean Sensitivity' to light offsets in evaluation of the effect of the visual blur which was introduced by plus lenses (Table 3). With 4 mm² stimuli, 1 log unit decrease in visual acuity (i.e. to 6/60) resulted in an average of 3.84 dB depression in the 'mean sensitivity' (R²=76.4%). The effect of the refractive blur on the visual sensitivity to 16 mm² stimulus was less pronounced, reducing the 'mean sensitivity' by an average of 0.92 dB (R²=55.5%). The full results from each acuity level are shown in Figure 42.

3.9. Topographical Reproducibility of Small Scotoma with Computerized Dynamic Fixation and Offset Stimuli

The average (mean & SD) horizontal diameter (width) of the physiological blind spot measured 5.8 ± 1.2 degrees (range: 5.0 - 8.0) and 5.6 ± 0.7 degrees (range 5.0 - 7.0) on the first and second test results respectively (Wilcoxon test; $p=1.00$). The vertical diameter (height) of the blind spot on two consecutive testing was 6.2 ± 0.9 degrees (range: 5.0 - 9.0) and 6.6 ± 1.3 degrees (range: 5.0 - 9.0) (Wilcoxon test; $p=1.00$). The mean intra-individual variation in the diameters of the scotomas with repeated testing (topographical long-term fluctuation) was 1.4 degrees (range 0.0 - 3.0 degrees) vertically and 0.6 degrees (range 0.0 - 2.0 degrees) horizontally.

The number of abnormal test points representing the blind spot on the test results were 23 ± 5 (min 16, max 32) for the first test and 24 ± 5 (min 16, max 39) for the second test. The slight increase in the number of missed test locations on the second test results was not significant (Wilcoxon sign test; $p=1.00$) and was not correlated to the results of the first test ($r=0.59$, $R^2=34.9\%$, $p=0.07$).

The percentage reproducibility of the blind spot mapping on re-testing of the visual field was further investigated by calculating the ratio of the number of repeatedly missed locations to the total number of missed locations on both tests. The average number of repeatedly missed test stimulus locations in the physiological blind spot was 17 ± 4 (range: 13-25). The overall reproducibility of the map of the scotomas on re-testing was $73\% \pm 5\%$ (range 64% - 80%) (Figure 43). Regression analysis of the results showed no relationship between the repeatability of the blind spot test results and the patient age ($r=-0.007$, $R^2<0.01\%$, $p=0.984$).

3.10. Detection Thresholds to Light Offsets in Normals, Ocular Hypertension and Primary Open-Angle Glaucoma

There was no significant difference between the average ages of the POAG group (62.7 ± 8.8 years; range 37 - 76 yr), the OHT group (60.7 ± 10.2 years; range 39 - 75 yr) and the control group (59.8 ± 13.5 years; range 40 - 84 yr) ($p > 0.61$). The spectacle corrections required for the best near vision in the POAG group ($+2.96 \pm 2.58$; range -3.50 - +6.50 dioptres spherical equivalent = D.sph.eq.), the OHT group ($+3.25 \pm 2.39$; range -3.00 - +6.75 D.sph.eq.) and the control group ($+2.50 \pm 2.36$; range -2.00 - +5.50 D.sph.eq.) were not significantly different ($p > 0.46$). No significant difference existed between the average pupil diameters of glaucomatous (3.91 ± 0.49 , range 3 - 5 mm), hypertensive (3.93 ± 0.59 , range 3 - 5.5 mm) and normal eyes (4.04 ± 0.43 , range 3.5 - 5 mm) ($p > 0.42$). Reliability indices from the Humphrey Visual Field Analyzer were within the acceptable range (i.e. fixation losses $< 20\%$, false positive and negatives $< 33\%$ of total attempts). The full results of global field indices from the POAG, OHT and control groups are given in Table 14.

3.10.1. Detection Thresholds in the Normal Central Visual Field

Average detection thresholds to light offsets at individual test locations in the normal central visual fields of control eyes are shown in Figure 44. In normal eyes, the MS score had negative correlation with age, decreasing in older patients, for both offset stimulus ($r = -0.709$, $p = 0.007$) and onset stimulus ($r = -0.734$, $p = 0.004$). The regression formulas for the offsets and onsets were " $MS_{\text{off}} = 22.9 - (0.0354 \times \text{age})$ " and " $MS_{\text{on}} = 34.8 - (0.0681 \times \text{age})$ " respectively, suggesting an average sensitivity decline of 0.4 dB/decade for offsets and 0.7 dB/decade for onsets.

Using 95% CI for individual test points, none of the control eyes had abnormal test points to either stimuli, producing 100% specificity for the offset stimuli against the

conventional stimuli in the normal central visual field. The onset stimuli of Humphrey VFA also did not produce abnormal threshold values at adjacent test locations in all control as well as OHT eyes.

The specificity (detection of normal field) and the sensitivity (detection of field abnormality) rates of both the 'onset' and the 'offset' stimuli were evaluated further using the prediction limits of 95% (i.e. $p=0.05$), 98% (i.e. $p=0.02$) and 99.9% (i.e. $p=0.001$) for the MD and LV scores from the control group (Table 15). All individual MD and LV scores with the 'onset' and 'offset' stimuli provided equal specificity rates in the control group, reaching to 100% according to the 99.9% prediction limit.

3.10.2. Detection Thresholds in the Glaucomatous Central Visual Field

Light offsets revealed visual field defects comparable to those shown by the conventional threshold testing in glaucomatous eyes (Figure 45). In one eye with POAG, there were four non-adjacent (scattered) abnormal test locations to offset stimuli, therefore, qualifying as a false negative result. At least 3 or more adjacent abnormal test locations to offset stimuli were present in the remaining 20 of the POAG eyes, giving sensitivity rate of 95.2% against the Humphrey stimulus:

Adjacent Locations	≥ 3	≥ 5	≥ 10	≥ 20	≥ 30	≥ 40
% Abnormal	95.2% (20/21)	90.5% (19/21)	85.7% (18/21)	61.9% (13/21)	38.1% (8/21)	19.1% (4/21)

The average 'MD' and 'LV' scores with both the 'onset' and 'offset' stimuli from the POAG group were significantly higher than those from the OHT and control groups ($p<0.0001$).

In the POAG group, the individual MD_{on} and LV_{on} scores obtained with the onset stimuli were below the 99.9% prediction limit and, therefore, qualified as significantly abnormal (p<0.001) in 86% (18/21) and 100% (21/21) of the eyes respectively (Figure 46).

When the 99.9% prediction limit was regarded as the cut-off point for abnormality, the global field indices from the 'offset' stimuli, MD_{off} and LV_{off} provided sensitivity rates of 86% (18/21) and 91% (19/21) respectively in glaucomatous eyes. The sensitivity rates improved to 91% (19/21) with MD_{off} and 95% (20/21) with LV_{off} along with a reduction in specificity to 77% (10/13) when the 95% prediction limit (i.e. p=0.05) was taken as the normal range (Table 15).

3.10.3. Detection Thresholds in the Central Visual Field of Ocular Hypertensives

Light offsets produced abnormal results in some of the glaucoma suspect eyes in the presence of full and normal fields to light onsets (Figure 47).

The offset stimuli revealed at least 3 adjacent abnormal test locations in 57% (12/21) of the OHT eyes (Specificity=43%). The abnormality rate to offset stimulus according to the number of significantly abnormal adjacent test locations was analyzed further in the OHT group:

Adjacent Location	≥ 3	≥ 5	≥ 6	≥ 8	≥ 10	≥ 15	≥ 20
Abnormal %	57.1% (12/21)	47.6% (10/21)	42.9% (9/21)	38.1% (8/21)	33.3% (7/21)	19.0% (4/21)	9.5% (2/21)

Although the average 'MD_{off}' score from the OHT group was higher than that of the control group, the difference was not statistically significant (p=0.096). The average 'LV_{off}' score of the OHT group was, however, significantly higher than that of the control group (p=0.005). The average visual field scores with the 'onset' stimuli did not differ significantly between the OHT and the control groups ('MD_{on}' p=0.97; LV_{on} p=0.78)(Figure 48).

In the OHT group, MD_{on} and LV_{on} indicated a field abnormality in 5% (1/21) and 14% (3/21) of the eyes respectively. The abnormal result rates with the offset stimuli were higher in the ocular hypertensive eyes, 43% (9/21) with MD_{off} and 62% (13/21) with LV_{off}.

Among the eyes with abnormal visual field scores to the 'offset' stimuli, 7 out of 9 eyes with abnormal MD_{off} and 8 out of 13 eyes with abnormal LV_{off} scores had asymmetrically higher cup-to-disc ratios than their fellow eyes. Only one out of a total of 8 eyes with such asymmetrical cupping in the ocular hypertension group produced visual field abnormality to the 'onset' stimuli.

The relationship between the visual field scores and the risk factors, namely IOP, CDR and RDVFL, was investigated further in the whole study group (n=55) using non-parametric Spearman rank order correlation test⁴³¹, using a statistical software program (Systat Inc, USA). Since the field scores and the data reflecting the above clinical risk factors (except CDR) did not have normal distribution in the study population as determined by testing their probability density function⁴²⁷, Spearman's test was preferred over Pearson's product moment correlation (a parametric test). Linear regression analysis was not performed for the same reason although the data otherwise satisfied the straight line fit criteria^{428,429} including the distribution of their y residuals⁴³⁰. Field scores from both 'onset' and 'offset' stimuli tended to increase with the RDVFL, IOP and CDR, showing positive correlation with increasing risk of having glaucoma (n=55):

Field Score	RDVFL	IOP	CDR
MD _{off}	r=0.648	r=0.373	r=0.522
LV _{off}	r=0.706	r=0.443	r=0.518
MD _{on}	r=0.489	r=0.241	r=0.387
LV _{on}	r=0.501	r=0.268	r=0.359

As shown above, that increase in the quantity of the field defects with increase in glaucoma risk parameters was more pronounced (i.e. higher r value) with the 'offset' stimuli than with the 'onset' stimuli. Positive correlations observed with the visual field indices from both types of stimuli are also evident on the full results with RDVFL (Figure 49), IOP (Figure 50) and CDR (Figure 51). Interestingly, MD and LV scores with both stimuli were further found to have a stronger positive correlation with the increasing CD than the level of IOP. Family history of glaucoma had no significant effect on the average visual field scores (Figure 52).

When the field scores and the clinical parameters were analyzed separately within the OHT group (n=21) using Spearman's test, it was found that the scores from offset stimuli also had stronger positive correlation with increasing CDR and RDVFL than those from onset stimuli:

Field Score	RDVFL	IOP	CDR
MD _{off}	r=0.454	r=0.230	r=0.633
LV _{off}	r=0.447	r=0.054	r=0.556
MD _{on}	r=0.176	r=-0.150	r=0.254
LV _{on}	r=0.270	r=-0.102	r=0.120

Interestingly, IOP was found to have the least if not meaningless bearing on the field scores in the OHT group.

When offset stimulus was compared to onset stimulus as the gold standard in all three groups of individuals tested (n=55), CAMEC threshold test had the Positive Predictive Rate of 63% (20/32) and Negative Predictive Rate of 96% (22/23).

When the results from onset stimulus of the Humphrey VFA was compared to those from CAMEC as the gold standard, the light onset stimuli had the sensitivity of 63% (20/32) and the specificity of 96% (22/23) against the offset stimulus, giving Positive Predictive Rate of 95% (20/21) and Negative Predictive Rate of 65% (22/34).

3.10.4. Topographical Distribution of the Defects to the Offset and Onset Stimuli

The frequency of abnormal threshold results at each individual test location in the central visual field was calculated for both onset and offset stimuli in POAG and OHT groups. That was achieved by determining the ratio of total number of abnormal threshold recordings (i.e below lower 95% prediction limit) to the total number of eyes tested for each individual test point in the visual fields of each group, giving the pointwise cumulative distribution of involvement. The onset stimuli of Humphrey VFA gave abnormal results in POAG group most frequently in the superior Bjerrum area between 10-20 degree eccentricity from fixation and supero-nasal field beyond the 15 degree eccentricity, to a lesser degree in the inferonasal field and least frequently in the inferior Bjerrum area (Figure 53). The offset stimuli of CAMEC revealed visual field abnormalities with the same topographical pattern with higher frequency of involvement in these areas in both POAG (Figure 54) and OHT groups (Figure 55).

The pointwise cumulative frequency of involvement of test locations to onsets and offsets was compared between the results from different study groups with OHT or

POAG. The frequency of abnormality to one stimulus type (x axis) was compared to those from the other (y axis) between subjects. Pearson's product moment correlation and regression tests were performed for that purpose as the data used satisfied the necessary conditions⁴²⁷⁻⁴³⁰.

The correlation between the topographical distribution of visual field abnormalities to onsets and offsets was significant in the POAG group ($r=0.42$, $p=0.002$).

The offset stimuli indicated abnormal visual field areas in the OHT group also. The topographical distribution of the scotomas to CAMEC with light offsets in ocular hypertensive eyes were significantly correlated to those shown by the conventional onset stimuli in the POAG group ($r = 0.31$, $p=0.028$).

The frequency distribution of scotomas to the offset and onset stimuli of 16 mm² (Goldmann size IV) were also compared to the distribution of glaucomatous loss to 4 mm² onset stimuli (Goldmann size III) in an independent glaucoma patient population which was described in Chapter 3.7 (Figure 36). A highly significant agreement was found for both the onset stimuli ($r=0.67$, $p=0.001$) and offset stimuli ($r=0.49$, $p<0.001$) in the POAG group and also for the offset stimuli in the OHT group ($r=0.38$, $p=0.005$).

3.10.5. The Test Duration with Dynamic Fixation and Ascending Staircase Method

The average test time for an eye with normal visual field was approximately 11 minutes with either stimulus. The efficiency of the ascending single crossing technique decreased with the prolongation of the test durations by approximately 22% in ocular hypertensive and by 83% in glaucomatous eyes in parallel to an increase in the number of stimulus presentations in the abnormal visual field areas. The average Humphrey test durations were equal in both normal and ocular hypertensive eyes, but prolonged only by 14% in glaucomatous eyes (Table 16).

Part 4. DISCUSSION

The smallest fact is a window through which the infinite may be seen.
[Aldous Huxley]

4.1. Light Offset Stimuli and Dynamic Fixation on Bjerrum Screen

4.1.1. Meridional Hill of Vision to the Offset and Onset Stimuli

The campimetry was performed by a dynamic fixation technique so as to be able to use a fixed test stimulus, thereby eliminating the need for manually moving the stimulus using a wand which would have caused a shadow on the background and which could also have resulted in tilting of the stimulus. A moving fixation target²⁵ was used instead of several printed numbers on the screen³⁵ so as to prevent bias caused by the patient memorizing the numbers associated with disappearance of the stimulus. Contrary to routine conventional practice, the stimulus moved centrifugally. Although it is well known that isoptres may differ when the direction of stimulus movement is from seen-to-unseen compared with unseen-to-seen, variability was avoided by standardizing the direction of movement in all subjects.

One of the principal findings of this study was that the eccentric visibility of offset stimuli was less than that of onset stimuli of equivalent size, depending on the definition of the contrast used. There are several possible explanations for this phenomenon. Firstly, light scatter from the bright surface into the adjacent dark surface on the campimeter may have caused changes in the perceived sizes and contrasts of the stimuli, the apparent size and contrast of the offset stimulus being smaller compared with the onset stimulus as expected from "point spread function". Secondly, the onset stimuli moved through relatively dark adapted and correspondingly more sensitive parts of the visual field than the offset stimuli which were presented to bleached parts of the retina. This explanation is implausible in view of the fact that the offset stimulus was less visible than the onset stimulus even on a grey background. Furthermore, the phenomenon was observed under photopic conditions. An alternative explanation for the reduced visibility of the offset stimulus may be the fact that it depended mainly on off-centre ganglion cells and was influenced by the differences between the on and off

channels.

4.1.2. The Effect of Variation in Illumination on Offset and Onset Stimuli

The visibility of the offset stimulus was perceived by the subjects as being more constant under varying lighting conditions than that of the onset stimulus. This difference was observed even when the same grey background was used for both stimuli. As both type of stimuli introduced equal and opposite amount of light changes onto the retina at each illuminance level, the explanation of that finding may be that on and off systems may behave differently with changing levels of ambient illumination. The practical significance of this difference is that standardization of the ambient illumination may be less important when Bjerrum Screen Campimetry is performed with dark stimuli on a bright background than vice versa. This would render the offset perimetric stimulus superior to the conventional light onset stimulus when tangent screen visual field examination is performed in the community and in other situations where it is difficult to maintain standardized and constant lighting conditions. The visibility of the black stimulus was almost unchanged despite changes in the background at a given level of ambient illumination (Figure 19, 20) and that can be explained with the fact that both black-on-white target (i.e. 95% Weber's and 90% Michelson's Contrast) and black-on-grey target (i.e. 90% Weber's and 82% Michelson's Contrast) attained similar high contrast stimulus strength.

In conclusion, this study has shown that the offset perimetric stimulus is less visible and more stable under variable lighting conditions than the onset stimulus when used on a tangent screen in combination with dynamic fixation maintenance.

4.2. Clinical Evaluation of Dynamic Fixation and Constantly Exposed Offset Stimuli for the Detection of Glaucomatous Visual Field Loss

The OKC procedure has appeal in its cost effectiveness and simplicity as well as its screening potential in large populations with restricted access to medical care. The improvements needed to overcome some of its deficiencies and to make it a more effective clinical screening tool have been indicated as a result of this work.

The results of initial clinical trials of the OKC screening were over-optimistic, suggesting identical results from the screening chart to those from conventional Goldmann kinetic and Humphrey static perimeters⁴³².

The first oculokinetic campimetry instrument was a wall mounted tangent screen with one hundred numbers (100-Point Chart) which were distributed up to a 25 degree eccentricity from fixation, and were arranged in 16 meridians at 2.5 to 5 degree intervals. Alvarez et al tested 64 eyes of 37 selected glaucoma patients with unequivocal field loss, using the 100-Point Chart and either Dicon 3000 Autoperimeter or Tubingen Oculus kinetic perimetry⁴³³. The average patient age was 65 years. The centrally located black test stimulus of OKC chart was 2 mm in diameter. The fixation numbers, which made the black spot disappear, were regarded as abnormal and to represent glaucomatous visual field loss. All patients produced OKC abnormalities in all tested eyes. When the abnormal areas on conventional test results and OKP recordings were compared, the results were identical in 88% of the eyes and at identical locations but with different extent in 6% of the eyes. Although no descriptive selection criteria were given for abnormal fields and control subjects, it was concluded that OKP technique could produce results comparable with those obtained with conventional perimetry, regardless of the severity of the field defect, and identical defects could be established in 94% of the abnormal eyes. Only in four eyes (6%) there was no recognizable similarity between the conventional and OKC visual field test results. That finding was attributed to the patient's fatigue. Despite the simplicity of that chart and highly accurate

results, it was not considered suitable for screening purposes because it was considered to be too laborious, taking about seven minutes per eye (Damato, personal communication).

The same equipment, also called 'General Purpose Chart', which tests a hundred points in the central 25 degree field was further studied in 51 eyes with glaucomatous visual field defects and 51 non-glaucomatous eyes of age-matched individuals. The mean age of the study group was 57 years old. Black spots of 2 mm, 3 mm and 5 mm were used as OKC stimuli. Among patients with glaucoma, 32 eyes (63%) had relative defects only and 19 eyes (37%) had small absolute scotomas. At one meter test distance, the 3 mm black stimulus achieved 92% sensitivity in detection of visual field defects revealed by other conventional perimeters, either the Friedman Visual Field Analyzer Mark II, Dicon 3000 Autoperimeter, or Tübingen Oculus Perimeter. Only 5% of the control eyes produced abnormal OKP results. The distribution of the abnormal OKP results suggested that the most informative points in the visual field were located at 12 to 15 degrees from fixation, especially in the superior and inferior nasal parts of the field ⁴³⁴.

Based on the results of the previous studies, a hand-held OKC chart has been designed. The new version had only 23 numbered fixation points located at eccentricities where glaucomatous involvement was found to be most frequent. Ninety-eight eyes of 54 glaucoma patients with a mean age of 64 years, and 116 eyes of 68 age-matched controls with presumably normal visual fields (without verification with conventional perimetry) were included in this study. The black stimulus diameter of the new prototype OKC field screener was 1.5 mm, and the chart was held at 40 cm from the eye during the test. A ribbon fitted with an eye occluder and attached to the chart at the side was used to cover the fellow eye and maintain the correct distance during the test. The OKC black stimulus was missed at a minimum of one fixation point, giving positive test results in 93% of 27 eyes with glaucomatous visual field loss, 69% of 32 eyes with equivocal field loss and 41% of 39 eyes with suspicion of glaucoma, but no

previous glaucomatous field defect. Only 9% of 116 control eyes had field defects to OKC. When two or more missed locations on OKC Chart were regarded a field defect, an average of 73% of glaucomatous and 7% of control eyes were classified as abnormal⁴³⁵. It was also noted that problems arose when a ribbon was used to maintain the correct chart-eye distance. In addition, some patients tended to read the numbers too quickly, so that their field defects remained undiscovered.

These problems were remedied by: 1) attaching an eye occluder to the chart by means of a rigid side arm; 2) increasing the number of fixation targets to 26 in order to slow down the eye movements; and 3) considering the test results to be positive only if any number was consistently associated with disappearance of the stimulus on repeated examination.

Felius et.al. compared the frequency of the observed OKC test spot to thresholds on the 'Humphrey Visual Field Analyzer (HVFA) 30-2 threshold program', in 33 eyes with glaucoma or ocular hypertension. Their findings indicated that the 50% and 95% frequency of the undetected OKC stimulus were on the average equivalent to approximately 15 and 20 decibel stimuli on the HVFA respectively⁴³⁶. They concluded that the OKC test was somewhat insensitive and the precise relationship of OKC test results to Humphrey field analyzer values could not be derived. The insensitivity of OKC was attributed to unavoidable fixation errors and Troxler's phenomenon during the OKC test procedure.

Vernon and Quigley compared the 26 point OKC glaucoma screening chart to a Humphrey 30-2 program in 27 glaucomatous eyes and 32 ocular hypertensive eyes. The sensitivity and specificity of the OKC chart in comparison to Humphrey threshold testing were 71% and 81%, respectively, when 9 decibel elevation in Humphrey threshold was regarded to represent a visual field abnormality. The sensitivity and specificity of OKC were 100% and 70% respectively, when a Humphrey threshold elevation was 21 decibels. This amount of visual field loss is categorized as relative

scotoma according to Humphrey visual field analyzer specifications^{90,437}. The mean light sensitivity required for the visibility of 1.5 mm black OKC stimulus was 6 decibels lower than the expected retinal sensitivity of the studied age group. That amount of sensitivity loss is known to be beyond the lower limit of 95% confidence interval for light threshold in normal population and indicates too high suprathreshold value of the black stimulus. Indeed, the mean light sensitivity values causing disappearance of OKC stimulus was 16 decibels lower than the age normals. Interestingly, it was noted that all patients who failed the OKC had involvement of the first 17 fixation targets. As the fixation targets 18 to 26 are in the central 10 degrees from fixation, they concluded that the new version of the chart should have only 22 fixation targets, extending more peripherally, nasally and inferiorly⁴³⁸.

Wishart studied the OKC chart against Humphrey threshold program 24-1 or 24-2 in 56 glaucomatous or glaucoma suspect patients with good reliability on previous automated perimetry. The OKC indicated glaucomatous visual field loss in 61% of the patients with abnormal Humphrey test results. Among glaucoma suspect eyes with ocular hypertension and/or optic disc abnormality and normal Humphrey results, OKC indicated visual field abnormality in 38% of patients, therefore yielding 62% specificity against light threshold determination⁴³⁹. Further analysis of true positive OKC results indicated that the disappearance of black OKC test stimulus corresponded to an average of 21 decibels elevation in retinal light threshold on Humphrey analyzer. In half of those true positive cases OKC did not document the full extent of Humphrey scotomas and were partially normal in another quadrant of the field displaying an average of 20 decibels elevation on threshold to light. The author concluded that the OKC chart was unsuitable for glaucoma screening due to its low sensitivity and specificity. That conclusion is however unsubstantiated as firstly, the author did not use age-matched normal controls to establish the correct specificity and secondly, did not analyze the OKC results according to the type, namely the relative or absolute nature of scotomas to a Humphrey field analyzer. This issue is also applicable to the former reports on OKC trials which are summarized before.

Independent clinical trials of 26-point OKC glaucoma screener also indicated 0% to less than 50% sensitivity in early relative scotomas in glaucoma^{440,441}. Similarly, the OKC glaucoma screener was capable of revealing all eyes with Stage III (absolute scotomas connected to blind spot) and more advanced glaucomatous defects.

When testing the visual field, the examination should always be as sensitive as possible. However, it is important to adapt the examination strategy and the sensitivity according to circumstances such as the patient's level of cooperation, the time available and the expertise of the examiner. When, for example, a highly cooperative glaucoma suspect with a raised intraocular pressure is being examined for glaucomatous visual field loss, it would be ideal if automated threshold static perimetry was performed. However, when examining an inexperienced patient or when large numbers of apparently healthy individuals are being screened randomly in the community, such exquisite sensitivity cannot be achieved. This is because the automated threshold perimetry would be too difficult and laborious for many patients and too time consuming and expensive for the examiner^{74,76,78,442,443}. Additionally, highly sensitive perimetry would detect many people with subtle defects caused by various conditions such as refractive errors, media opacities, and such individuals would unnecessarily be referred for specialist opinion. Without deviating from the fundamental principle of striving for maximum sensitivity, it is, therefore, necessary to make compromises if screening for glaucomatous visual field loss is to become more widely available. Despite the availability of tonometry and ophthalmoscopy, there is evidence that many, perhaps most, glaucoma sufferers are still not being detected until they have developed dense visual field defects extending close to fixation^{376,390,397,398}. Further research is required to establish whether or not such individuals could be detected sooner than at present and with greater cost efficiency by the large scale application of simple visual field tests that are designed to detect only dense visual field loss. Such studies have hitherto been hampered by the lack of perimetric methods that could widely be used by non-specialists.

The purpose of the OKC chart has been defined as to enable visual field examination

for the presence of glaucomatous visual field loss in situations where conventional tests are not available. The findings of the present study suggest that when a 1.5 mm stimulus is used, the 26 number OKC chart does indeed detect large areas of dense visual field loss within the central 15 degree field, with a false positive result of about 10% in apparently healthy individuals in the seventh decade of life. The specificity rate of 90% found in this study is similar to those predicted in previous studies^{434,435}. The false positive rate diminishes to a low level of approximately 1% when the diameter of the stimulus is increased to 3 mm, but at the cost of missing eyes with only relative glaucomatous visual field defects. There are two main conclusions to be drawn from such results. Firstly, the OKC chart should be used only in combination with ophthalmoscopy, and tonometry, if possible, and not as a substitute for these tests. Secondly, it would seem useful to vary the size of the stimulus according to the eccentricity, age and visual acuity of the patient. Whether or not the test is universally useful cannot be concluded from the present investigation and will depend on the circumstances in which it is applied and the way in which patients are managed when a positive result is obtained. Additionally, oculo-kinetic visual field screening is user-dependent despite its simplicity, so that the results vary according to the examination technique. Further studies are therefore indicated in a variety of situations.

The topographical extent of the field defects to oculokinetic campimeter and its light offset stimuli was smaller than those to the conventional oculo-static instruments (i.e. Topographical Index < 1.0) in the vast majority of the glaucomatous eyes. It also appeared that the false negative results from individual OKC test locations corresponding to absolute scotomas became rather pronounced in inner eccentricities, towards the centre of the OKC chart. The frequency of non-detection of continuously exposed offset stimuli with dynamic fixation never reached to the expected 100% in the absolute scotoma areas and was, at best, 35% in the inner eccentricity and 80% in the outer eccentricity. These findings can be attributed to fixation losses during oculo-kinetic testing with continuous stimulus exposure.

This study suggests a number of revisions in the design of the OKC chart. These include interchangeable stimuli which perhaps could be 1 mm, 2 mm and 3 mm in diameter, and which could be selected according to the visual acuity and the age of the patient in order to improve the sensitivity and specificity. As the visibility of a high contrast light offset stimulus on a bright background is more constant under variable lighting conditions than a reflective light onset stimulus on a dark background, a black stimulus is preferable for the OKC glaucoma test, which is intended for use in the community, where standardization of the ambient illumination is impractical. It is tempting to vary the contrast instead of the size in order to manipulate the sensitivity and specificity, but as with white stimuli, lower contrast offset (grey) stimuli would require the illumination to be more carefully standardized.

In the present study, the discrepancy between the results of the OKC glaucoma test and conventional perimetry in the glaucoma suspect eyes may partly be due the false negative results with the conventional manual perimetry and false positive results with the OKC caused by reduced visual acuity. Such problems may not have occurred if automated threshold perimetry had been used instead of automated and manual suprathreshold perimetry. However, this would have resulted in a biased sample of patients, because it is known that many individuals are not cooperative enough for automated threshold perimetry. In any case, the OKC chart under investigation was designed to detect dense visual field loss which was readily identified with the conventional perimeters used in the study.

The average equivalent 50% detection threshold of 0.8 - 1.0 log unit for the light offset stimulus indicate that the suprathreshold value of OKC chart at 13° eccentricity is 0.2 - 0.4 log unit in the 70 year age group^{444,445}. This also supports that the increasing false alarm rate with age in OKC testing is due to relatively lower suprathreshold value of the 1.5 mm black stimulus.

The introduction of interchangeable stimuli should allow the full central visual field (30

degrees) to be examined with the hand-held chart. This change inevitably increases the number of fixation targets but has the advantage of making the hand-held chart useful not only for glaucoma detection but also for neuro-ophthalmic assessment. In the new version of the chart, the sequence of the numbers may be reversed, so that they spiral outward instead of inward, thereby making it easier for the examiner to decide whether to examine only the central 15 degrees or the central 30 degrees of the visual field from fixation.

In the present study, the result was considered abnormal only if any points were consistently missed when the examination was repeated⁴⁴⁶. It is shown that such criteria results in small defects being missed by OKC; a better method of confirming the presence of a defect might be to cover and uncover the test stimulus as described for portable visual field screeners^{447,448}. Implementation of a shutter mechanism as described would also solve the problems of fixation losses and Troxler phenomenon. It has been suggested that OKC may give spurious results because of the Troxler phenomenon⁶⁵ when the stimulus is left constantly exposed⁴³⁶. Although this should not happen when the patient looks at each number for only one second, as currently recommended, the possibility of false positive results is reduced even further when the stimulus is made to appear and disappear, so that this precaution should be taken routinely when an abnormal result is suspected. In conclusion, this study gives an indication of the results that can be expected in different age groups with the 26 number OKC glaucoma screening chart. The investigation has also enabled several revisions for the chart to be made, which should increase the scope of the test in situations where conventional perimetry is not possible.

4.3. Constantly Exposed Offset Stimulus with Dynamic Fixation in Detection of the Blind Spot as a Model of Small Absolute Scotoma

Contrary to conventional methods, oculokinetic campimetry is performed with continuous exposure of the test stimulus and the patient says when the stimulus appears and disappears. Constant stimulus exposure was hoped to enable the performance of the field examination more rapidly. There have been patients, however, who tended to rush the examination so as to have increased the probability of missing small defects⁴³⁵.

In this study, the psychophysical accuracy of continuous light offset stimulus exposure in OKC and the effect of clustering fixation targets on test sensitivity have been investigated, using the physiological blindspot as an absolute scotoma model.

Conventionally, a scotoma is regarded as clinically significant if it is at least three degrees in diameter³⁸⁹. The physiological blind spot, with constant diameters of 5.5 degrees by 7.5 degrees, was ideally suited for the purposes of this study. Each subject was examined with either Chart A, Chart B, but not both, so as to avoid bias from a learning effect.

It appears that 46% individuals can not reliably detect visual field defects with constantly exposed stimulus of oculokinetic method. At least two fixation points which correspond to the absolute scotoma are required to identify 3 out of 4 defects, as the addition of a second fixation target in the scotoma area increased the non-fluctuating positivity rate from 54% to 76%. This finding suggests that, the constant exposure of the offset stimulus is not desirable due to high false-negative result rate and the greater the number of points examined within a scotoma, the greater is the probability of detecting the defect. For this reason, future OKC charts should have a shutter mechanism and additional fixation targets which would slow down the eye movements and intensify the grid in the most vulnerable parts of the visual field.

At present, a test result is considered positive only if the stimulus consistently disappears when the examination repeated. The results of this study suggest that, for a given location, such a strategy causes a fluctuation rate of 10% at the test location and also severely reduces the sensitivity of the examination. When an inconsistent or fluctuating positive response occurs, the result should be regarded as inconclusive and selected points re-examined with an intermittently presented stimulus. In other words, the patient should look continuously at a number and say when the stimulus appears and disappears, while the examiner uncovers and covers the stimulus with a white card or ideally with a shutter mechanism^{447,448}. The results suggest that intermittent stimulus exposure may provide better sensitivity in visual field screening.

The current strategy for testing, the blindspot is designed to help the patient to position the chart correctly, to understand the principle of the examination and in addition, to help the examiner to assess the patient's reliability. Another efficient method of achieving these objectives on OKC, however, might be for the blindspot to be discovered by the patient in exactly the same way as abnormal scotomas are detected, using numbered fixation targets. This strategy makes it easier for the examiner to decide whether it is safe to leave the stimulus constantly exposed or whether to cover and uncover the stimulus with the patient indicating when the stimulus appears and disappears.

In conclusion, this study establishes the sensitivity of oculo-kinetic continuous stimulus exposure in detection of absolute scotomas, confirms the value of clustering fixation targets, re-indicates the need for cover / uncover of stimuli for brief presentations to improve sensitivity, suggests an alternative method of interpreting inconsistent results, and identifies the need for repeated testing of the blind spot during the examination.

4.4. Computer-Assisted Moving-Eye Campimetry (CAMEC)

4.4.1. Temporal Variation in CRT Background Luminance

The repeated luminance measurements over time indicated that the screen luminance of the CRT used for this research was uneven. The luminance of the monitor increases for two hours after power supply. That increase is most rapid during the first half hour and gradually reaches a plateau afterwards. Temporal variation in CRT screen brightness with time is confirmed for the monitor used in CAMEC test. Conclusions drawn from the experiment was that a 'heating' period of at least 30 minutes should be allowed for the CRT before any visual field testing was performed, in order to maintain the same light adaptation state of the eye.

4.4.2. CRT Luminance Variation with Monitor 'Brightness' Setting

In order to achieve a background luminance level of 10 cd/m^2 and a suitable range of grey shades for the offset stimuli on that background, the 'brightness' and 'contrast' settings have to be kept at their minimum in the CAMEC CRT monitor. Grey shade number 37 produced the desired background brightness of 10 cd/m^2 which is employed in conventional Goldmann and Humphrey perimeters. The luminance curve obtained with that setting (Figure 30) was used for the calibration of the offset stimuli.

4.4.3. Stimulus Brightness Selection on a CRT

When presented on a lighter background, using the calibration module (Chapter 2.4) that generates 6x6 disc grid pattern on CRT (Chapter 2.4.1), the brightness of a small dark pattern becomes higher probably due to light scatter from the background. Similarly,

when a dark grey was selected as the background, small areas of brighter grey shades measured darker than the expected, probably due to some masking by the background. These findings suggest that the selection and calibration of the stimulus shades should be performed in small patches against the desired background level for the clinical tests, since the final stimulus contrast and visibility would otherwise be different from what is predicted by the uniform screen measurements.

4.4.4. Topographical Variation in CRT Luminance and Image Contrast

Uneven phosphor distribution on the CRT screen and the alignment of the electron guns may explain the brightness irregularities. Stimulus contrasts intended for CAMEC should be checked and if necessary recalibrated for a given monitor before it is employed in testing of the patients. Achieving a white background uniformity on a CRT has always been difficult and digital electronic methods developed to overcome the problem in TV sets⁴⁴⁹ may become available for computerized video-campimetry in the future. At its present form, the screen luminance irregularities on the CAMEC monitor may not cause uneven retinal light adaptation levels as the fixation location constantly varies. Additionally, stimulus contrast is maintained steadily at different locations on the screen, enabling reliable contrast sensitivity measurement.

4.4.5. Temporal Variation in Stimulus Duration

As the processing of visual information is regarded as complete by 0.1 seconds following its onset, some computerized perimeters such as Octopus maintain 0.1 second default duration. It appears that even the minimum CAMEC stimulus duration remains above 0.1 second, thereby avoiding incomplete perception of the stimuli by the visual system and the likelihood of false negative patient responses. As the variation in the stimulus duration does not affect the fluctuation in the test results with automated

perimetry⁴⁵⁰, slight irregularities in the CAMEC stimulus duration should not cause any adverse effect on the test result.

4.5. Fixation Control with Dynamic and Static Fixation in Children

The moving fixation target and tracking method of CAMEC controls the patient's direction of gaze, thus enabling the child to perform successfully. In children with sufficient cooperation for static fixation, CAMEC with offset stimuli may also successfully indicate normal status of the visual fields as shown by the suprathreshold screening programs of the Humphrey Visual Field Analyzer and CAMEC showing full and normal visual field test results from an 8-year-old child with good cooperation (Figure 56). This study reveals that dynamic fixation can be used by most children above the age 5 years when motor development is sufficient to use a joystick effectively, and that visual field defects can be detected in patients who can not be assessed properly using conventional methods. Additionally, the higher scores with CAMEC than Dicon confirm that fixation is maintained better with a moving fixation target than a stationery target. For instance, dynamic fixation method and light offsets revealed a right homonymous superotemporal partial quadrantanopia in a 5.5 year old girl with an intracranial (left temporal lobe) pathology who could not be examined with conventional perimetric methods (Figure 57). This further suggests that in the paediatric age group, a moving eye fixation method disguised as a video-game should allow more accuracy in quantification of visual field abnormalities than conventional static fixation methods. In summary, computerized moving fixation method was found to be a useful way of examining the visual field in children aged 5 years or more.

4.6. Dynamic Fixation with Offset Stimuli in Screening for Neuro-ophthalmic Visual Field Loss

Although Goldmann perimetry is the preferred method for visual field assessment in neuro-ophthalmology⁴⁵¹, automated perimetry is also valuable in the diagnosis of visual neural pathway disorders. The usefulness of automated perimetry is often restricted by patient-related factors such as experience and cooperation especially in full threshold examination^{87,409,452,453}. Automated screening with single intensity suprathreshold stimuli, therefore, is more satisfactory because of greater speed and reliability^{74,78,413,414,423,454}. Such screening programs should have the ability both to map precisely and selectively the topographical extent of an abnormality and to take account of the normal decrease in visual sensitivity with increasing distance from fixation⁴⁵⁵.

The results with eccentricity compensated stimulus sizes and computer-aided selective topographical adaptive strategy suggest that the sensitivity and specificity of single intensity high contrast (-76%) offset stimuli compare favorably with the results of other investigators using conventional automated single intensity suprathreshold screening programs with onset stimuli, identifying 9 out of 10 abnormal and normal visual fields correctly by either method^{74,78,414}. Interestingly, some of our patients observed more extensive visual field defects with -76% contrast dark stimuli compared with conventional luminous stimuli. For example, a residual bitemporal partial quadrantanopia to Goldmann perimetry was much more extensive and a near-complete hemianopic loss bitemporally in a 50 year old male with 6/5, N5 acuity, who had transsphenoidal surgery for a pituitary adenoma in the past (Figure 58).

Also a bitemporal hemianopia due to previously removed craniopharyngioma in a 71 old female with 6/18 visual acuity in both eyes appeared only as a temporal constriction in the right eye when tested with Goldmann Perimeter (Figure 59).

The moving-eye screening test program provides satisfactory spatial adaptation and

higher grid resolution in suspicious parts of the visual field only, without unnecessary prolongation of the test. The existing stimulus grid and topographically adaptive strategy appear to recognize scotomas which respect the vertical and horizontal meridians, a major localizing feature in neuro-ophthalmological diagnosis. Physiological rotations of the eye, which may be up to 7 degrees around the optical axis during fixational eye movements, may explain some of the cases with a low level of topographical correlation between the results obtained with moving and steady fixation techniques⁴⁵⁶.

The test duration of CAMEC 26-Point Screening test became prolonged with increasing patient age for both normal and abnormal fields, probably due to difficulty with joystick manipulation in the elderly. The duration of a psychophysical test reflects its efficiency. The efficiency of computerized moving fixation technique is less among elderly patients. Changes in manual dexterity, reaction time, ability to concentrate and fixate with increasing patient age may explain this finding. For patients who display inadequate dexterity, auto-locking of the tracking system and a simple push-button response strategy may shorten the test duration. Alternatively, different interaction methods such as screening with multiple offset stimuli presentations and touch-screen recording of stimulus awareness may be preferable¹³⁶.

A personal computer based back propagation neural network developed for the 26-Point stimulus test grid may, in the future, be incorporated to CAMEC to enable automated interpretation and recognition of neuro-ophthalmic and glaucomatous scotoma patterns in visual field screening and in situations where perimetric expertise is not readily available^{457,458}.

The results of this study suggest that static offset stimuli on a cathode ray tube can be employed reliably in the clinical investigation of the central visual field. In conclusion, dark-on-bright perimetric stimuli may be useful in neuro-ophthalmology as an adjunct to the existing visual field screening techniques.

4.7. A Comparison of Single Intensity Static Offset Stimuli with the Onset Stimuli of Humphrey VFA in Glaucoma

4.7.1. The Sensitivity and Specificity of Offset Stimuli in Glaucoma

The lower true positive detection rates with higher contrast offset stimuli provide further evidence that the offset stimulus becomes more suprathreshold with increasing contrast. However, lower contrasts of suprathreshold offset stimuli have been missed more frequently in the apparently normal parts of the glaucomatous visual fields, causing higher 'false positive' rates. The R.O.C. curve (Figure 39) suggests that the optimum sensitivity and specificity for the stimulus sizes used in this study would have been provided by 30% contrast stimuli with 70% true and 30% false positive rates. The high incidence of false positive results with low contrast stimuli also suggests more extensive visual field involvement to offset stimuli in glaucoma, and may represent false negative (defect remained undetected) results from conventional onset stimuli. Slightly higher (an average of 3-6%) false positive rates against the 'PD' results suggest that the detection of the offset stimuli, like the onset stimuli, is influenced by the diffuse sensitivity loss in the visual field.

Offset stimuli of low contrast were frequently missed in apparently normal parts of the glaucomatous visual fields, especially at the outer eccentricities. This is partly due to the negative effect of the peripheral stimuli locations on patient attentiveness⁴⁵³ as well as the possible decrease in the suprathreshold values of the selected offset stimulus sizes in glaucomatous visual fields. The true negative rate of 71% from the lightest grey (-10%) offset stimuli within 10 degree eccentricity provides evidence that even the lowest negative contrast value employed in this study was at least 4 dB above the equivalent light threshold in the central visual field. Therefore, seemingly false positive results from offset stimuli also suggest that negative contrast may indicate glaucomatous visual field defects which were not present to the onset (positive contrast) stimuli of the

Humphrey Visual Field Analyzer.

4.7.2. Detection Threshold for Offset Stimulus in Glaucoma:

The visibility of offset perimetric stimulus, like that of conventional luminous stimulus, is dependent on stimulus parameters such as size, contrast and level of background luminance. Selecting progressively larger stimuli towards the periphery of the visual field (eccentricity compensation) caused the detection thresholds for offset stimuli to follow the slope of normal hill of vision at all contrast levels.

Lower contrasts of offset perimetric stimulus functioned as weaker stimuli and required higher retinal sensitivity for their detection in the visual field. Therefore, it seems possible that the visual field may be evaluated by presenting successive offset stimuli with increasing or decreasing contrast. An average of 3.14 Humphrey dB change in the offset stimulus detection threshold in response to varying the stimulus contrast from -76% to -10% represents the small dynamic range of the stimulus sizes used in this study. The dynamic range, however, may be varied by altering the stimulus area.

Employing a high background luminance with offset stimulus may provide several advantages over luminous stimuli on a dim background. First of all, the field can be tested under ordinary ambient illumination conditions without needing adaptation periods. Secondly, the inadvertent reflections and glare on the glass surface of CRT, as well as the after-image following brief stimulus presentations, become less of a problem. With higher background intensity, however, screen flicker, dirt on the screen and the awareness of vitreous floaters may impose negative effect on the test. Additionally, increasing the background luminance seem to necessitate higher retinal sensitivity for the detection of low contrast offset stimuli on CRT.

Several alternative explanations may be suggested for that observation. Although the

stimulus contrasts were calibrated separately for different backgrounds, it was not possible, because of technical limitations, to measure the luminance of a spot smaller than approximately 1.5 cm in diameter. It is likely that the actual contrast and perceived size of the offset stimuli were reduced due to increased light scatter into the small stimulus area especially when the background is brighter. Intraocular light scatter and glare may also interfere with the visibility of lower contrasts by changing the contrast value of the stimulus falling on the retina. Therefore, actual stimulus contrasts on the retina may be different than those determined with measurements on the CRT screen. An alternative explanation might be the decrease in the ratio of the retinal receptive field excitatory centre area to the inhibitory surround area under higher luminance, and the consequent lower contrast gain and stimulus visibility²¹⁹. Therefore, the effect of background onto the visibility of offset stimulus should be taken into consideration in the design and application of tests for different clinical situations.

4.8. Detection Thresholds to Static Offset Stimulus and the Effect of Refractive Blur

In this study, detection sensitivity to offset test stimuli which are just perceptibly darker than the background have been determined along the nasal horizontal meridian of the normal central visual field using CAMEC. Similar to the conventional onset test stimuli^{66,90,144,459}, negative threshold gradient with increasing eccentricity also exists for decremental stimuli. Furthermore, visual field thresholds to the larger offset stimuli were lower in the normal visual field, suggesting that detection threshold to light offset stimuli, similar to light onset stimuli, is subject to spatial summation. The summation coefficient for offsets, like onsets, changes with eccentricity, being lower near fixation and higher in periphery. The spatial summation was not complete (i.e., $k < 1.0$) at any eccentricity or acuity level and reached a maximum of $k=0.5$. It appears that offset stimulus size of 16 mm^2 provides wider dynamic contrast range (available steps between the detection contrast and maximum contrast) for decremental stimuli as a result of spatial summation and increased detection sensitivity to light offsets, and may be more useful in clinical test purposes.

Refractive blur caused depression in detection sensitivity to both sizes of negative contrast stimuli, an effect observed also in Ring Perimetry which combines light and dark components in a stimulus^{460,461}. The detrimental effect of refractive error, however, was more pronounced with small sizes of light offsets at all eccentricities. Increasing amounts of blur also caused more variation in the normal threshold results as indicated by larger standard deviations from the small size offset stimuli than those from the larger stimuli (Figure 42). These findings are in agreement with the previous reports on conventional onset stimuli and the effect of defocus on detection thresholds which raised with blur more significantly when the onset stimulus size was equal or smaller than 4 mm^2 ^{462,463}. In conclusion, dark-on-bright stimulus of Goldmann size IV equivalent may be more useful when employed in routine visual field testing because of its higher

resistance to refractive blur, better dynamic range and less inter-individual variation in its visibility especially in the absence of optimal refractive correction.

4.9. Topographical Reproducibility of Small Scotoma with Computerized Dynamic Fixation and Offset Stimuli

The main aspects of field testing are the detection of true defects, and the documentation of the field changes over time. This task, however, is more complex than automated screening for field abnormalities since the clinically significant true topographical changes in the existing defects frequently require to be distinguished from confounding long-term fluctuation (intertest variability) of the results.

The physiological blind spot, with constant diameters of 5.5° by 7.5° , was used as a paradigm of a small scotoma and represented a clinically significant defect in normal persons for the purpose of this study. The topographical reproducibility of the scotoma mapping with the dynamic fixation method and single intensity suprathreshold offset stimuli was an average of 73% with a maximum of $\pm 2^{\circ}$ - 3° fluctuation in the dimensions of the defects over repeated testing, providing satisfactory topographical reliability for monitoring of the extent of scotomas with repeat examination.

The physiological blind spot consists of an absolute component in the centre formed by the optic nerve head and a surrounding relative scotoma formed by peripapillary scleral ring (zone alpha) or peripapillary chorioretinal irregular pigmentation / atrophy (zone beta) which may be caused by glaucoma when tested with light onsets⁴⁶⁴. The difference between the physiological blind spot and a true pathological scotoma such as a glaucomatous absolute defect is that the blind spot has a steeper border formed by the relative defect around it⁴⁶⁵. Increased 'short term fluctuation' seen in the relative scotoma component around the borders is otherwise observed both in glaucomatous and physiologic scotomas^{465,466}.

The delimitation of the blind spot depends on the size of the onset stimulus as the scotoma is absolute to small sizes and gradually becomes completely relative with larger sizes, using full thresholding⁴⁶⁷. This is attributed to the easier detectability of larger

stimuli caused by the increased stray light scattered from the larger area to the periphery on the retinal plane^{467,468}. Stray light contamination in scotoma measurement may not be relevant to the detectability and not hinder the usefulness of large size light offset stimuli such as the one used in this study. Further studies with more than one size offset stimuli would be useful to reach a conclusion. The Goldmann IV equivalent rectangular stimuli used in the study has a diagonal diameter of 65 minutes of arc (1.1 degrees) which is five times smaller than the horizontal diameter of the physiological absolute scotoma. The diameters of the physiological blind spot established with the suprathreshold offset stimulus intensity are in complete agreement with its already known size, suggesting no underestimation by the offset stimuli employed. Therefore, the variability in the measurements by dynamic fixation and offset stimuli is due to the quality of fixation, not the underestimation of the scotoma. Additionally, the higher threshold fluctuation reported to exist in the surrounding relative scotoma component may have contributed to the variability to some extent although the measurements were made with suprathreshold stimuli instead of full thresholding method.

The mean distance of actual fixation from the original intended target of fixation measures 0.2 degrees and total fixation instability with spontaneous eye movements is about 1.2 degrees in normal eyes, using scanning laser ophthalmoscopically controlled fundus perimetry⁴⁶⁴. The reproducibility rates in the blind spot diameter obtained with dynamic fixation and light offsets are in full agreement with the fixational instability observed with the conventional onset stimulus and static fixation. This suggests that computerized dynamic fixation method provides as good stable fixation as conventional steady fixation with good reliability, although it may still be affected by the spontaneous eye movements. The results suggest that the offset stimuli and moving fixation method can be employed in the assessment of the blind spot, a procedure which may be necessary for neuro-ophthalmologic conditions such as papilloedema and peripapillitis^{451,469-472} as well as in fixation monitoring with Heijl-Krakau method.

4.10. Detection Thresholds to Light Offsets in Normals, Ocular Hypertension and Primary Open-Angle Glaucoma

In this study, the threshold visual sensitivity to light decrements in the central visual field was investigated in patients with POAG and OHT, combined with age-matched normal individuals, with an attempt to demonstrate the presence of visual loss secondary to glaucomatous optic nerve damage. It has been found that the brief exposures of static light offset stimuli combined with dynamic fixation on a VDU could indicate normal threshold sensitivity in the central visual field with 100% specificity and as similar to the conventional light onset stimuli and steady fixation. The normal visual sensitivity to the offset stimuli appears to be age dependent, like that of the onset stimuli, and decreases with age presumably due to decreased optical clarity and depletion of neural reserves⁴⁷³. That finding indicates that the evaluation of visual fields to offset stimuli should be made according to the age of the individual patient.

The offset stimuli of CAMEC could also document the glaucomatous visual field abnormalities with an accuracy of 95% if the same defects were also detectable by the conventional light onset stimuli of Humphrey VFA.

It has emerged from this study that the conventional visual field indices of MD and LV can be calculated satisfactorily for threshold examination using the offset stimuli.

Global visual field indices obtained with the offset stimuli achieved a sensitivity of 91-95% for MD and LV respectively. The specificity of the global indices estimated with the offset thresholds was equal to those obtained with the onset stimulus of Humphrey VFA ranging from 77% to 100% according to 95% and 99.9% confidence limits respectively. The sensitivity and specificity of the offset stimuli global indices in glaucomatous visual field loss were comparable to those of conventional automated onset stimuli, which is 87-88% sensitive and 77-85% specific, as determined by the Octosoft statistical program of Octopus perimeter⁴⁷⁴.

Only one glaucomatous eye with small but significant topographical field abnormality to the 'onset' stimuli yielded normal LV_{off} score ($p>0.05$) and no cluster of abnormal test locations to offset stimuli. That may be due to low patient cooperation / fixation instability at the central reference target during the test rather than a genuine underestimation of the visual defect by the offset stimuli.

In ocular hypertensive eyes with apparently no field loss to the onset stimuli, there were abnormal areas in 57% of the visual field results to the offset stimuli. The MD and LV scores to light offsets in the OHT group were defective more frequently (43% - 62%) relative to those in the control group (0%) as well as relative to those to light onsets (5% - 14%) ($p<0.0001$). The comparison of global field indices from the 'offset' and 'onset' stimuli suggests that in eyes with ocular hypertension and the suspicion of early optic neuropathy, off-pathway examination may produce significant visual field abnormalities which are not obvious with the conventional on-pathway testing. The correlation between the visual field scores against the RDVFL and CDR confirm that those ocular hypertensive eyes with higher risk of glaucomatous visual loss tend to exhibit more pronounced defects to 'offset' stimuli despite the normal sensitivity to light onsets. Asymmetrical cupping of the optic nerve head is regarded as being highly suggestive of early glaucomatous neuropathy and 8 eyes within the OHT group had that condition. The LV_{on} scores were in the normal range in 88% (7/8) of these eyes. Interestingly, 100% (8/8) of those eyes with asymmetrically enlarged cup-to-disc ratios in the OHT group produced abnormal LV_{off} scores, suggesting non-detection of glaucomatous damage by the 'onset' stimuli. Additionally, more pronounced positive correlation between the glaucoma risk factors and the global indices from the offset stimuli further confirm that glaucomatous visual sensitivity loss to the light offsets is more extensive than that to the light onsets. Indeed, the topographical distribution of the visual field defects to the offset stimuli in the OHT group and the correlation of these defects to those in two independent POAG groups provide further evidence that the offset stimuli may be indicating the damage that the onsets do not. These findings can

be explained with the fact that threshold offset stimuli may be stimulating the 'off-pathway' which is formed by the 'off-centre' retinal ganglion cells. These cells are of larger somal diameter than their 'on-centre' counterparts¹⁷⁴ and are more vulnerable to glaucomatous damage which preferentially affects large ganglion cells^{322,370} and their large calibre axons^{325,361}. Additionally, the smaller quantity (reserves) of retinal ganglion cells in 'off' than 'on' system^{208,226-229} and the magnocellular contribution for the visibility of low contrast stimuli on low photopic background^{249,250} may explain the visual field defects to 'offset' stimuli in the absence of any visual deficit to the 'onset' stimuli.

When the results of the onset stimuli of Humphrey VFA were compared in a reverse fashion to those from the offsets as the gold standard (n=55), the onsets had good specificity (i.e. 96%) but poor sensitivity (i.e. 63%) which also supports the above interpretation. It appears that both types of stimuli may be complementary to each other as suggested by the high positive (95%) and low negative (65%) predictive rates with onsets and high negative (96%) and low positive (63%) predictive rates with offsets. The implication of the above predictive rates is that the offsets may indicate defects when they do not exist to onset stimuli and also a normal field to offsets will also be normal to onsets.

The correlation between the quantity of glaucomatous visual field defects to the offset stimulus and the clinical parameters (the intraocular pressure, cup-to-disc ratio and risk of developing visual field loss) was stronger (i.e. higher r value) than the correlation observed with the defects to the onsets.

It is conceivable that the results of the comparison of light onsets and offsets in this study are not completely free from confounding factors. Firstly, the offset stimuli were presented with a moving fixation target while the onset stimuli were presented with steady fixation. For an ideal comparison of light onsets and offsets, one might argue on the necessity of conventional static fixation for both stimuli. As evidenced by the topographical reproducibility study described previously (Chapter 4.9) no confounding

effect is expected to be introduced by dynamic fixation. Although the visual detection sensitivity in the field of vision during the slow pursuit eye movements remain the same as the sensitivity of a static eye³², the complete stop of the fixation target of CAMEC at the time of stimulus appearance further eliminates the likelihood of any blur which may be introduced by dynamic fixation. The mode in which the CAMEC test is administered with joystick interface may lead to the detection of different types of neural deficits, such as lack of attention especially in elderly. The evidence for this comes from 'Useful Field of View' test which registers central and peripheral selective attention tasks^{475,476}. In some elderly individuals who have normal conventional visual fields, attentional and information processing deficits rather than the sensory ones may be present. The joystick mediated fixation monitoring system of CAMEC imposes a dual-task selective attention paradigm with central (tracking) and peripheral (detection) tasks whereas the static fixation method of Humphrey VFA has only the peripheral detection task. As most of the elderly individuals were previously noted to have difficulties with the joystick use, resulting in prolongation of the CAMEC test and patient fatigue (Chapter 4.6), that additional burden was eliminated by using the joystick by the operator (author). That modification is expected to eliminate the occurrence of visual attentional deficits during testing with the offset stimuli of CAMEC. Although it is not entirely possible to filter out any attentional deficit component in the explanation of field defects to light offsets in the OHT group, the correlation between the defects and glaucomatous clinical parameters as well as the 100% specificity in age matched control group suggest that any attentional deficits because of dynamic fixation technique were unlikely.

In this study, the threshold determinations with the offset stimuli could be performed only with the ascending single-crossing technique rather than a double-crossing bracketing strategy (i.e. STATPAC) of Humphrey Visual Field Analyzer, due to the design of CAMEC software. The thresholding strategy of CAMEC is similar to that of the new FASTPAC procedure of Humphrey VFA. Recent studies have demonstrated that the FASTPAC procedure had greater within-subject variability (short-term

fluctuation=STF) in threshold estimates^{477,478} which is included in the LV score. Corrected loss variance (CLV) calculation is the method of filtering out that STF component, but that was not possible because of lack of repeat threshold measurements in CAMEC test. Instead, LV was implemented on Humphrey results. It is known that increased STF may be the first sign of early visual field loss in glaucoma^{103,104}. As a result, the existing defects to the offset stimuli in OHT group, at least to some extent, may be the result of higher STF component in the visual field. At the same time, FASTPAC threshold determination is known to cause underestimation of glaucomatous visual field defects^{477,479}. That makes it more unlikely for the FASTPAC-like strategy and inherent higher STF to be the explanation for the significant field loss to the offset stimuli in the OHT group of this study. Besides, the frequency of involvement at the individual test points in the POAG group was higher, and the field defects were more pronounced with the offset stimuli and single-crossing strategy than those with the STATPAC of conventional perimeter. Furthermore, the distribution of the visual field defects to the offset stimuli both in glaucomatous and ocular hypertensive eyes are remarkably similar to those to the conventional onset stimuli in two different groups of glaucomatous eyes, confirming the true nature of the glaucomatous visual deficits to light offsets.

Ideally, the monitor size should have been large enough to cover the full extent of the central field. Nonetheless, the calculation of normative values for each test location with the same equipment and test algorithm cancels out any effect that small monitor size and resulting light adaptation irregularities may introduce. Secondly, eye movements reduce the possibility of topographical luminance irregularities on the retina implemented by the monitor screen uneven brightness. As the onset and offset stimuli were generated on two different media, namely a CRT monitor and a projection bowl respectively, stimulus perception properties were most likely different. The onsets and offsets could not be produced with satisfactory calibration to present equal and opposite amount of light changes as part of two separate CAMEC tests because of the limited dynamic range and non-linear luminance curve of the 64 shades of grey available and

the nature of the hardware. The final comprehensive psychophysical comparative evaluation of the light offsets and light onsets should be possible in the future with the ability of creating equal but opposite amounts of light changes on a CRT. Unless such a work is performed with a suitable software and CRT, perhaps using 256 or more shades of grey in normal and abnormal fields, the clinical evidence with strong statistics described here on the superiority of offsets over onsets may not be fully conclusive. The prospective long-term follow up of those ocular hypertensive eyes with field defects only to the offset stimuli and the documentation of conversion of the conventional field results from normal to abnormal will support the findings of this cross-sectional study.

The usefulness of dynamic fixation and the light offset stimulus in day-to-day perimetric practice depends not only on its sensitivity and specificity to visual defects but also the efficiency (time requirement) of the test mode in which it is employed. Long test durations with the ascending 2 dB offset stimulus steps in the abnormal visual fields restrict the usefulness of the current technique in the quantification and follow up of visual field abnormalities. The implementation of a double-crossing bracketing technique in CAMEC should be expected to result in longer test times and further sacrifice in the efficiency of the current design of dynamic fixation method. No negative effect from long test durations with the ascending method on the reliability of the results from glaucomatous eyes in this study, however, is suspected because of ample rest periods provided during the tests.

4.11. Final Remarks

Too many fixation losses, false negative and positive responses render a field test result unreliable^{88,89,480}. Glaucoma patients usually give consistently unreliable results due to false negatives on repeat testing^{86,480} whereas normals, ocular hypertensives and glaucomatous individuals produce unreliable results almost exclusively due to fixation instability regardless of experience^{86,87,480}. Loss of fixation is, therefore, one of the severe limitations of conventional "oculo-static" perimetry, which prevents many patients from being examined^{409,452}. One method of overcoming this problem is to test the blindspot several times during an examination, but this may be unreliable in the presence of extensive visual field loss.

The fixation method used in CAMEC, the first automated dynamic fixation instrument, successfully holds fixation only if the difficulty of the tracking procedure is well adjusted to the patient's level of ability. If the task is too easy, then some uncooperative patients will look away from the target and search for the stimulus, whereas if the task is too difficult, then the examination will be slow, tiring and even impossible for the elderly. CAMEC therefore measures the patient's ability to track the fixation target, first of all, during a preliminary examination, and then intermittently during the examination proper. The moving fixation target undoubtedly slows down the examination, but this is not important if the only other alternative is not to perform any perimetry at all. For experienced patients who are so trustworthy that monitoring of fixation is unnecessary, the tracking process can be made easier or completely shut off so that the examination can be performed more quickly. Indeed, Dicon Autoperimeter has recently integrated a projected moving fixation light to maintain patient interest and that does not require any tracking.

The moving fixation target may not cause problems in patients with strabismus, because one eye is covered and because it is possible for such patients to turn the head instead of the eye. CAMEC has not yet been assessed in patients with severe ophthalmoplegia,

gaze paresis or nystagmus, who may have difficulty with the examination.

Some individuals, especially if elderly, are unable to manipulate the joystick, resulting in progressive prolongation of the test with age or complete non-compliance. With such patients, the tracking procedure can either be simplified or the joystick can be manipulated by an examiner, with the patient telling the examiner when the stimulus is seen. Optionally, in future versions of CAMEC, the tracking may be made automatic. In such situations, the examiner would, of course, need to monitor fixation as with non-automated forms of perimetry.

Automated visual field examination in both screening and quantification of visual defects has been achieved for the first time using static light offset (decremental=dark-on-bright) stimuli conforming to international standards. Initial results suggest that light offsets may reveal defects as well or better than the conventional onset stimuli. Further studies are required to establish the specificity of the offset stimulus to 'off-pathway' and 'magnocellular' system. Offset stimuli prevent the problem caused by persistent phosphorescence on the computer screen after an onset stimulus on a dim background has been switched off. Bright background also minimizes screen reflections. The flicker sensation also becomes more perceptible with increasing background luminance. Excessive screen flicker may interfere the perception of very low contrast stimuli inadvertently and therefore, for testing with high background luminance, the vertical refresh rate of the VGA computer monitor may need to be increased from standard 70 Hz. to 100 Hz. with accessory graphic cards.

In addition to the need for a suitable bracketing strategy for more efficient thresholding with the light offset stimuli, the current dynamic range of the offset stimulus intensities on video displays require to be improved and refined further. The Goldmann stimulus size IV was selected for clinical testing with light offsets because of its wider dynamic range, higher resistance to optical blur and lower inter-individual detection variability. In the lower end of contrast spectrum where small luminance changes correspond larger

decibel values, more precise quantification may be achieved with additional steps between 22-28 dB (-10% to -4%) contrast especially within 15 degrees from the fixation. For that purpose, either improved video graphics with larger selection of grey shades or monitors with suitable screen luminance dynamics may prove useful.

Because of the low cost of personal computers, CAMEC can be useful in non-ophthalmic clinics where the demand for visual field examination is not enough to justify a financial investment in more expensive equipment. In addition, CAMEC may be useful for reserve purposes in the event of an over-demand for the conventional perimetry or a breakdown of such equipment in ophthalmic clinics.

The monitoring of glaucoma patients by sequential perimetry is currently limited by severe logistical problems, which make it necessary to reduce the frequency of visual field examination to six or twelve monthly. The recognition of progressive visual field deterioration can therefore be delayed considerably. In selected cases, CAMEC may allow more frequent visual field examination, either using equipment installed in the patient's home or at a hospital or community clinic on a non-appointment basis. If a statistical program such as regression analysis of the global field sensitivity or individual thresholds at different test location is incorporated that would bring more reliability in the recognition of significant visual field loss changes over time. So that, even the frequency of routine hospital visits by patients with glaucoma may safely be reduced by performing home follow-up with personal computers. Such a strategy would, however, need to be rigorously evaluated, before any recommendation can be made.

CAMEC is a visual field analyzer which attempts to train the patient how to perform the examination, using auditory and other commands and instructions. As the adjustment of test variables and storage of results are also fully automated, CAMEC may be useful for screening purposes in the community using portable or fixed equipment. A problem with visual field examination in non-specialized clinics is the interpretation of the results. For this reason, a diagnostic facility for CAMEC, which is based on automated

pattern-recognition with a neural network, has been described.

Future research work is required to define the effect of dynamic fixation in control of fixation losses, false positive and negative responses in comparison to conventional static fixation during clinical testing. The optimum stimulus parameters for a threshold strategy using offsets, including various stimulus sizes, decibel steps and bracketing strategies, should be investigated further. The effect of media opacities, especially cataract, on offset thresholds should be defined. Short term fluctuation and inter-test (long-term) variability of offset thresholds should also be established with further work using improved test software programs. Finally, threshold testing with offset stimuli should also be experimented in other disease categories such as retinopathies or optic neuropathies other than glaucoma to expand its clinical scope.

By using a moving fixation target and offset stimuli on standard personal computers, automated visual field examination may, in the future, become a routine procedure in a wide variety of situations where the usefulness of other forms of perimetry is limited.

REFERENCES

Whenever I hear the word culture, I reach for my revolver.
[Herman Goring]

- 1 Griffin JR. Historical summary of visual fields methods. *J Am Optom Assoc* 1980; **51**: 833-835.
- 2 Verriest G. Modern Trends in Perimetry. *Brit J Physiol Opt* 1975; **33** (3): 19-31.
- 3 Research Group - International Perimetric Society. *Perimetric standards and perimetric glossary*. The Hague, Boston, London: Dr W Junk bv Publishers, 1979: 3-14.
- 4 NAS-NRC Committee on Vision. First interprofessional standard for visual field testing: report of working group 39. *Adv Ophthal* 1980; **40**: 173-224.
- 5 Jung R, Kornhuber HH. Results of electronystagmography in man: The value of optokinetic, vestibular and spontaneous nystagmus for neurologic diagnosis and research. In: Bender MB, ed. *The oculomotor system*. New York: Harper and Row, Hoeber Medical Division, 1964; 428-482.
- 6 Winterson BJ, Collewign H. Microsaccades during finely guided visuo-motor tasks. *Vision Res* 1976; **16**: 1387-1390.
- 7 Dell'Osso LF, Abel LA, Daroff RB. Inverse latent macro square-wave jerks and macro-saccadic oscillations. *Ann Neurol* 1977; **2**: 57-60.
- 8 Herishanu YO, Sharpe JA. Normal square-wave jerks. *Invest Ophthalmol Vis Sci* 1981; **20**: 268-272.
- 9 Eizenman M, Trope GE, Fortinsky M, Murphy PH. Stability of fixation in healthy subjects during automated perimetry. *Can J Ophthalmol* 1992; **27**: 336-340.
- 10 Demirel S, Vingrys AJ. Eye movements during perimetry and the effect that fixational instability has on perimetric outcomes. *J Glaucoma* 1994; **3**: 28-35.
- 11 Kosnik W, Fikre J, Sekuler R. Visual stability in older adults. *Invest Ophthalmol Vis Sci* 1986; **27**: 1720-1725..
- 12 Simon JW, Mehta N, Simmons ST, Catalano RA, Lininger LL. Glaucoma after pediatric lensectomy/vitreotomy. *Ophthalmology* 1991; **98**: 670-674.
- 13 Fausset TM, Enoch JM. A rapid technique for kinetic visual field determination in young children and adults with central retinal lesions. In: Greve EL, Heijl A, eds. *Doc.Ophthalmol.Proc.Ser.: Seventh International Visual Field Symposium, Amsterdam, September 1986*. Dordrecht: Dr W.Junk Publishers, 1987; 495-501.
- 14 van Hof-van Duin J, Heersama DJ, Groenendaal F, Baerts W, Fetter WPF. Visual field and grating acuity development in low risk preterm infants during the first 2 1/2

years after term. *Behav Brain Res* 1992; **49**: 115-122.

15 Spafford C, Grosser GS. Retinal differences in light sensitivity between dyslexic and proficient reading children: new prospects for optometric input in diagnosing dyslexia. *J Am Optom Assoc* 1991; **62**: 610-615.

16 Cummings MF, van Hof van Duin J, Mayer DL, Hansen RM, Fulton AB. Visual fields of young children. *Behav Brain Res* 1988; **29**: 7-16.

17 Mayer DL, Fulton AB, Cummings MF. Visual fields of infants assessed with a new perimetric technique. *Invest Ophthalmol Vis Sci* 1988; **29**: 452-459.

18 Fausset TM. A rapid technique for kinetic visual field determination in young children and adults with central retinal lesions. *Doc Ophthalmol Proc Ser* 1986; **49**: 495-501.

19 Barnard NAS. Kinetic outline perimetry as a technique for examining the visual fields of young children (letter). *Ophthalmic Physiol Opt* 1988; **8**: 463-464.

20 Bowering ER, Maurer D, Lewis TL, Bren HP. Sensitivity in the nasal and temporal hemifield in children treated for cataract. *Invest Ophthalmol Vis Sci* 1993; **34**: 3501-3509.

21 Fetter WPF, van Hof-van Duin J, Baerts W, Heersema DJ, Wildervanck M. Visual acuity and visual field development after cryocoagulation in infants with retinopathy of prematurity. *Acta Paediatr* 1992; **81**: 25-28.

22 Takayama S, Tachibana H, Yamamoto M. Changes in the visual field after photocoagulation or cryotherapy in children with retinopathy of prematurity. *J Pediatr Ophthalmol Strabismus* 1991; **28**: 96-100.

23 Wilson M, Quinn G, Dobson V, Breton M. Normative values for visual fields in 4- to 12-year-old children using kinetic perimetry. *J Pediatr Ophthalmol Strabismus* 1991; **28**: 151-153.

24 Quinn GE, Fea AM, Minguini N. Visual fields in 4- to 10-year-old children using Goldmann and double-arc perimeters. *J Pediatr Ophthalmol Strabismus* 1991; **28**: 314-319.

25 Smith JV. New technique in campimetry. *Br J Ophthalmol* 1958; **42**: 251-254.

26 Eizenman M, Frecker RC, Hallett PE. Precise non-contacting measurement of eye movements using the corneal reflex. *Vision Res* 1984; **24**: 167-174.

27 Heijl A, Krakau CE. A note of fixation during perimetry. *Acta Ophthalmol (Copenh)* 1977; **55**: 854-861.

- 28 Trope GE, Eizenman M, Coyle E. Eye movement perimetry in glaucoma. *Can J Ophthalmol* 1989; **24**: 197-199.
- 29 Nagata S, Kani K. A new perimetry based on eye movement. In: Heijl A, ed. *Perimetry Update 88/89*. Amsterdam, Berkeley, Milano: Kugler & Ghedini, 1989; 337-340.
- 30 Armon H, Weinman A, Peleg A, Ticho U, Zauberman H, Mallek D. Automatic testing of the visual field using electro-oculographic potentials. *Doc Ophthalmol* 1977; **43**: 51-63.
- 31 Ticho U, Zauberman H, Faibish E, Armon H, Weinman J. Oculographic automatic perimetry in glaucoma visual field screening: a clinical study--preliminary results in glaucoma patients. *Doc Ophthalmol* 1979; **47**: 5-12.
- 32 Starr A, Angel R, Yeates H. Visual suppression during smooth following and saccadic eye movements. *Vision Res* 1969; **9**: 195-197.
- 33 Keesey UT. Effects of involuntary eye movements on visual acuity. *J Opt Soc Am* 1960; **50**: 769-773.
- 34 Westheimer G, McKee SP. Visual acuity in the presence of retinal-image motion. *J Opt Soc Am* 1975; **65**: 847-853.
- 35 Damato BE. Oculokinetic perimetry: a simple visual field test for use in the community. *Br J Ophthalmol* 1985; **69**: 927-931.
- 36 Damato BE. Assessment of the visual field by anyone, anywhere and at any time. *Trans Ophthalmol Soc U K* 1985; **104**: 681-685.
- 37 Highman VN. Examination of the central visual field at a reading distance. *Br J Ophthalmol* 1968; **52**: 408-414.
- 38 Damato BE. & University of Glasgow, *United States Patent Publication, No: 4,995,717*. US Patent Office, 1991.
- 39 Johnston SC, Damato BE, Evans AL, Allan D. Computerised visual field test for children using multiple moving fixation targets. *Med & Biol Eng & Comput* 1989; **27**: 612-616.
- 40 Megens JH. *CAMEC: Computer Assisted Moving Eye Campimetry; a clinical evaluation*. Dissertation; Submitted to the Catholic University, Nijmegen, Netherlands, 1989.

- 41 Rea MS. Some basic concepts and field applications for lighting, color and vision. In: Nadler PM, Miller D, Nadler DJ, eds. *Glare and contrast sensitivity for clinicians*. New York, Berlin: Springer-Verlag, 1990; 120-138.
- 42 Weber EH. [De pulsu, reseptione, auditu et tactu annotationes anatomicae et physiologicae, Leipzig 1834]. In: Boring EH, ed. *The history of experimental psychology*. New York: Appleton-Century-Crofts, 1950.
- 43 Westheimer G. The oscilloscopic view: Retinal illuminance and contrast of point and line targets. *Vision Res* 1985; **25**: 1097-1103.
- 44 Michelson AA. On the application of interference methods to spectroscopic measurements. *I Phil Mag Ser V* 1891; **31**: 338-348.
- 45 Lempert P. Standards for contrast acuity/sensitivity and glare testing. In: Nadler MP, Miller D, Nadler DJ, eds. *Glare and contrast sensitivity for clinicians*. New York: Springer-Verlag, 1990; 113-119.
- 46 Hart WM. Visual adaptation. In: *Adler's physiology of the eye*. St. Louis: Mosby Year Book., 1992; 9th edn. 502-529.
- 47 Sloan LL. Area and luminance of test objects as variables in examination of the visual field by projection perimetry. *Vision Res* 1961; **1**: 121-138.
- 48 Tate GW. The physiological basis for perimetry. In: Drance SM, Anderson DR, eds. *Automatic perimetry in glaucoma: A practical guide*. Orlando: Grune & Stratton, 1985; 1-28.
- 49 Kasai N, Takahashi G, Koyama N, Kitahara K. An analysis of spatial summation using Humphrey Field Analyser. In: Mills RP, ed. *Perimetry Update 92/93*. Amsterdam-New York: Kugler-Ghedini, 1993; 557-562.
- 50 Hart WM. The temporal responsiveness of vision. In: Hart WM, ed. *Adler's Physiology of the Eye, Clinical Application*. St. Louis: Mosby Year Book, 1992; 9th edn. 548-578.
- 51 Mutlukan E, Bradnam M, Keating D, Damato BE. Visual evoked cortical potentials from transient dark and bright stimuli: Selective 'on' and 'off' pathway testing? *Doc Ophthalmol* 1992; **80**: 171-181.
- 52 Ogle KN. Foveal contrast thresholds with blurring of retinal image and increasing size of test stimulus. *J Opt Soc Am* 1961; **51**: 862-869.
- 53 Leibowitz HW, Johnson CA, Isabelle E. Peripheral motion and refractive error.

Science 1972; 177: 1207-1208.

54 Johnson CA, Leibowitz HW. Practice, refractive error and feedback as factors influencing peripheral motion thresholds. *Perception & Psychophysics* 1974; 1514: 276-280.

55 Harrington DO, Drake MV. In: *The visual fields: Text and atlas of clinical perimetry*. St. Louis: The C.V. Mosby Co., 1990; 6th edn. 51-55.

56 de Boer RW, van den Berg TJ, Beintema MR, Greve EL, Hoppener J, Verduin WM. The Friedmann Visual Field Analyser Mark II--technical evaluation and clinical results. *Doc Ophthalmol* 1982; 53: 331-342.

57 Henson DB, Chauhan BC, Hopley A. Screening for glaucomatous visual field defects: the relationship between sensitivity, specificity and the number of test locations. *Ophthalmic Physiol Opt* 1988; 8: 123-127.

58 Greve EL. Single and multiple stimulus static perimetry in glaucoma; the two phases of perimetry. Thesis. *Doc Ophthalmol* 1973; 36: 1-355.

59 Heijl A, Lindgren G, Olsson J. The effect of perimetric experience in normal subjects. *Arch Ophthalmol* 1989; 107: 81-86.

60 Werner EB, Krupin T, Adelson A, Feitl ME. Effect of patient experience on the results of automated perimetry in glaucoma suspect patients. *Ophthalmology* 1990; 97: 44-48.

61 Werner EB, Adelson A, Krupin T. Effect of patient experience on the results of automated perimetry in clinically stable glaucoma patients. *Ophthalmology* 1988; 95: 764-767.

62 Wild JM, Searle AE, Dengler Harles M, O'Neill EC. Long-term follow-up of baseline learning and fatigue effects in the automated perimetry of glaucoma and ocular hypertensive patients. *Acta Ophthalmol* 1991, 69: 210-216.

63 Lachenmayr BJ, Drance SM, Chauhan BC, House PH, Lalani S. [Diffuse and localized glaucomatous visual field changes in light sense, flicker and visual acuity perimetry. Evidence of pressure damage]. *Fortschr Ophthalmol* 1991; 88: 530-537.

64 deGroot SG, Gebhard JW. Pupil size as determined by adapting luminance. *J Opt Soc North Am* 1952; 42: 492-495.

65 Clarke FJ, Belcher SJ. On the localization of the Troxler's effect in the visual pathway. *Vision Res* 1962; 2: 53-63.

- 66 Sloan L. Instruments and techniques for the clinical testing of the light sense. III. an apparatus studying regional differences in light sense. *Arch Ophthalmol* 1939; **22**: 233-251.
- 67 Tate GW, Lynn JR. . In: *Principles of quantitative perimetry: Testing and interpreting the visual field*. New York: Grune & Stratton, 1977; 270-287.
- 68 Spahr J. Zur automatisierung der perimetrie: I. Die anwendung eines computergesteuerten perimeters. *Graefes Arch Clin Exp Ophthalmol* 1973; **188**: 323-338.
- 69 Heijl A, Krakau CE. An automatic perimeter for glaucoma visual field screening and control. Construction and clinical cases. *Albrecht Von Graefes Arch Klin Exp Ophthalmol* 1975; **197**: 13-23.
- 70 Heijl A. The Humphrey Field Analyser: Concepts and clinical results. *Doc Ophthalmol Proc Ser* 1985; **43**: 55-64.
- 71 Johnson CA, Chauhan B, Shapiro LR. Properties of staircase procedures for estimating thresholds in automated perimetry. *Invest Ophthalmol Vis Sci* 1992; **33**: 2966-2974.
- 72 Werner EB, Drance SM. Early visual field disturbances in glaucoma. *Arch Ophthalmol* 1977; **95**: 1173-1175.
- 73 Li SG, Spaeth GL, Scimeca HA, Schatz NJ, Savino PJ. Clinical experiences with the use of an automated perimeter (Octopus) in the diagnosis and management of patients with glaucoma and neurological disease. *Ophthalmology* 1979; **86**: 1302-1312.
- 74 Heijl A, Drance SM. A clinical comparison of three computerised automatic perimeters in the detection of glaucoma defects. *Arch Ophthalmol* 1981; **99**: 832-836.
- 75 LeBlanc RP. Abnormal values in computerised perimetry. In: Whalen WR, Spaeth GL, eds. *Computerised visual fields: What they are and how to use them*. Thorofare: Slack Inc, 1994; 165-193.
- 76 Duggan C, Sommer A, Auer C, Burkhard K. Automated differential threshold perimetry for detecting glaucomatous visual field loss. *Am J Ophthalmol* 1985; **100**: 420-423.
- 77 Caprioli J, Spaeth GL. Static threshold examination of the peripheral nasal visual field in glaucoma. *Arch Ophthalmol* 1985; **103**: 1150-1154.
- 78 Heijl A, Drance SM, Douglas GR. Automatic perimetry (Competer); ability to detect early glaucomatous field defects. *Arch Ophthalmol* 1980; **98**: 1560-1563.

- 79 Bynke H, Krakau CET. A modified computerised perimeter and its use in neuro-ophthalmic patients. *Neuro-ophthalmology* 1981; **2**: 105-115.
- 80 Lieberman MF and Drake MV. *A simplified guide to computerised perimetry*. Thorofare: Slack Inc., 1987: 103-127.
- 81 Cohn T, Perolman J. The diodewand: A device for tangent screen perimetry. *Am J Optom Physiol Opt* 1974; **51**: 913-997.
- 82 Schmied U. Automatic (Octopus) and manual (Goldmann) perimetry in glaucoma. *Albrecht Von Graefes Arch Klin Exp Ophthalmol* 1980; **213**: 239-244.
- 83 Brenton RS, Argus WA. Fluctuations on the Humphrey and Octopus perimeters. *Invest Ophthalmol Vis Sci* 1987; **28**: 767-771.
- 84 Fankhauser F, Bebie H, Flammer J. Threshold fluctuations in the Humphrey Field Analyzer and in the Octopus automated perimeter. *Invest Ophthalmol Vis Sci* 1988; **29**: 1466.
- 85 *STATPAC User's Guide*. San Laendro, California: Allergan-Humphrey, 1987:
- 86 Katz J, Sommer A. Reliability indexes of automated perimetric tests. *Arch Ophthalmol* 1988; **106**: 1252-1254.
- 87 Bickler Bluth M, Trick GL, Kolker AE, Cooper DG. Assessing the utility of reliability indices for automated visual fields. Testing ocular hypertensives. *Ophthalmology* 1989; **96**: 616-619.
- 88 Katz J, Sommer A, Witt K. Reliability of visual field results over repeated testing. *Ophthalmology* 1991; **98**: 70-75.
- 89 Katz J, Sommer A. Screening for glaucomatous visual field loss. The effect of patient reliability. *Ophthalmology* 1990; **97**: 1032-1037.
- 90 Brenton RS, Phelps CD. The normal visual field on the Humphrey Field Analyser. *Ophthalmologica* 1986; **193**: 56-74.
- 91 Katz J and Sommer A. Asymmetry and variation in the normal hill of vision. *Archives of Ophthalmology*, **1986**; **104**: 65-68.
- 92 Holmin C, Krakau CET. Visual field decay in normal subjects and in cases of chronic glaucoma. *Graefes Arch Clin Exp Ophthalmol* 1980; **213**: 291-298.

- 93 Heijl A, Lindgren G, Olsson J. Perimetric threshold variability and age. *Arch Ophthalmol* 1988; **106**: 450-452.
- 94 Schwartz B, Nagin P. Probability maps for evaluating automated visual fields. *Doc Ophthalmol Proc Ser* 1985; **42**: 39-48.
- 95 Heijl A, Lindgren G, Olsson J, Asman P. Visual field interpretation with empiric probability maps. *Arch Ophthalmol* 1989; **107**: 204-208.
- 96 Bebie H. Computerised techniques of visual field analysis. In: Drance SM, Anderson D, eds. *Automatic perimetry in glaucoma: a practical guide*. New York: Grune & Stratton, 1985; 147-160.
- 97 Flammer J, Bebie H. Influence of age on quantitative perimetry. *Arch Ophthalmol* 1987; **105**: 24.
- 98 Mills RP, Barnebey HS, Migliazzo CV, Li Y. Does saving time using FASTPAC or suprathreshold testing reduce quality of visual fields? *Ophthalmology* 1994; **101**: 1596-1603.
- 99 Flammer J, Drance SM, Augustiny L, Funkhouser A. Quantification of glaucomatous visual field defects with automated perimetry. *Invest Ophthalmol Vis Sci* 1985; **26**: 176-181.
- 100 Flammer J. The concept of visual field indices. *Graefes Arch Clin Exp Ophthalmol* 1986; **224**: 389-392.
- 101 Bebie H, Fankhauser F, Spahr L. Static perimetry: Accuracy and fluctuations. *Acta Ophthalmol* 1976; **54**: 339-348.
- 102 Fankhauser F, Bebie H. Threshold fluctuations, interpolations and spatial resolution in perimetry. *Doc Ophthalmol Proc Ser* 1979; **19**: 295-309.
- 103 Flammer J, Drance SM, Fankhauser F, Augustiny L. Differential light threshold in automated static perimetry. Factors influencing short-term fluctuation. *Arch Ophthalmol* 1984; **102**: 876-879.
- 104 Flammer J, Drance SM, Zulauf M. Differential light threshold: Short and long-term fluctuation in patients with glaucoma, normal controls, and patients with suspected glaucoma. *Arch Ophthalmol* 1984; **102**: 704-706.
- 105 Boeglin RJ, Caprioli J, Zulauf M. Long-term fluctuation of the visual field in glaucoma. *Am J Ophthalmol* 1992; **113**: 396-400.

- 106 Lieberman MF, Ewing RH. Reassessing split fixation in advanced glaucoma. In: Mills RP, Heijl A, eds. *Perimetry Update 1990/91*. Amsterdam: Kugler & Ghedini, 1991; 473-489.
- 107 Sommer A, Katz J, Quigley HA, et al. Clinically detectable nerve fiber atrophy precedes the onset of glaucomatous field loss. *Arch Ophthalmol* 1991; **109**: 77-83.
- 108 Anderson DR. *Automatic static perimetry*. St.Louis: Mosby Year Book, 1992: 91-161.
- 109 Zamber R, Mills RP. Peripheral vs central confirmatory testing. In: Heijl A, ed. *Perimetry Update 1988/89*. Amsterdam: Kugler & Ghedini, 1989; 409-416.
- 110 Katz J, Sommer A, Gaasterland DE, Anderson DR. Comparison of analytic algorithms for detecting glaucomatous visual field loss. *Arch Ophthalmol* 1991; **109**: 1684-1689.
- 111 Suzumura H, Endo N, Harasawa K, Suzuki H, Murao T. A new screening program with the Kowa automated perimeter: a peripheral isoptometry and central three-zone program. In: Mills R, ed. *Perimetry Update 1992/93*. Amsterdam: Kugler & Ghedini, 1993; 331-338.
- 112 Bergqvist U. Health-Related Aspects of VDT Use. In: Roufs JAJ, ed. *The man-machine interface*. London: MacMillan Press, 1991; 1-6.
- 113 Reed AV. Microcomputer display timing: Problems and solutions. *Behav Res Meth Instr* 1979; **11**: 572-576.
- 114 Farrell JE, Casson EJ, Haynie CR, Benson BL. Designing flicker-free video display terminals. *Displays* 1988; **9**: 115-122.
- 115 Farrell JE, Benson BL, Haynie CR. Predicting flicker thresholds for video display terminals. *Proc Soc Info Disp* 1987; **28**: 449-453.
- 116 Eriksson S, Backstrom L. Temporal and spatial stability in visual displays. In: Knave B, Wideback PG, eds. *Work with Display Units*. North-Holland: Elsevier Science Publishers BV, 1987; 461-473.
- 117 Mayzner MS. The research potential of a computer-based cathode-ray tube display system. *Behav Res Meth Instr* 1968; **1**: 41-43.
- 118 Sperling G. The description and luminous calibration of cathode ray oscilloscope visual displays. *Behav Res Meth Instr* 1971; **3**: 148-153.

- 119 Rodieck RW. Raster-based colour stimulators. In: Mollon JD, Sharpe LT, eds. *Colour Vision; Physiology and psychophysics*. London: Academic Press, 1983; 131-144.
- 120 Wunk DF, Freeman JA. An electronically controlled visual stimulus generator for quantitative mapping of visual receptive fields. *Vision Res* 1979; **19**: 599-602.
- 121 Cowan WB. Discreteness artifacts in raster display systems. In: Mollon JD, Sharpe LT, eds. *Colour vision; Physiology and psychophysics*. London: Academic Press, 1983; 145-153.
- 122 Accornero N, Berardelli A, Cruccu G, Manfredi M. Computerized video screen perimetry. *Arch Ophthalmol* 1984; **102**: 40-41.
- 123 Hart WM,Jr., Gordon MO. Color perimetry of glaucomatous visual field defects. *Ophthalmology* 1984; **91**: 338-346.
- 124 Hart WM,Jr., Hartz RK, Hagen RW, Clark KW. Color contrast perimetry. *Invest Ophthalmol Vis Sci* 1984; **25**: 400-413.
- 125 Frisen L. A computer graphics visual screener using high pass spatial frequency resolution targets and multiple feed-back devices. *Ibid* 1986; Series **49**: 441-446.
- 126 Fitzke FW, Poinosawmy D, Ernst W, Hitchings RA. Peripheral displacement thresholds in normals, ocular hypertensives and glaucoma. In: Greve EL, Heijl A, eds. *VIIth International Visual Field Symposium*. Dr W.Junk Publishers: Doc.Ophthalmol.Proc.Ser., 1987; 447-452.
- 127 Fitzke FW, Chuang EL, Holden A, et al. Fine matrix perimetry. *Invest Ophth Vis Sci (Suppl)* 1987; **28**: 113.
- 128 Fitzke FW. Visual psychophysics with a video-display controlled by a micro-computer(Abstract). *J Physiol (Lond)* 1984; **351**: 6P.
- 129 Chen JC, Fitzke FW, Pauleikhoff D, Bird AC. Functional loss in age related Bruch's membrane change with choroidal perfusion defect. *Invest Ophthalmol Vis Sci* 1992; **33**: 334-340.
- 130 Aulhorn E, Kost G. Noise-field Campimetry: a new perimetric method. In: Heijl A, ed. *Perimetry Update 1988-89*. Amsterdam: Kugler-Ghedini, 1989; 331-336.
- 131 Vinuesa MJ, Rodrigues de Cunha AJ, Rodriguez Sanches J, Hernandez-Galilea E, Barahona JM. Comparative evaluation of Hipocampus and Goldmann Perimeters in measuring visual fields of patients with simple chronic glaucoma. *Chibret Int J Ophthalmol* 1990; **7**: 23-28.

- 132 Postaire JG, Hache JC, Diaf M. Fully automated screening procedure for early detection of visual field deficits. *J Biomed Eng* 1986; 8: 156-161.
- 133 Hache JC. A new multistimulus supraliminal technique for the early detection of glaucomatous scotomata. *Chibret Int J Ophthalmol* 1990; 7: 29-32.
- 134 Brunsmann J, Brunsmann F, Krastel H. Prototyp eines programmgesteuerten Video-Kampimeters (Prototype of a microcomputer-based video campimeter). *Fortschr Ophthalmol* 1985; 82: 578-580.
- 135 Krastel H, Meyer Josten C, Brunsmann J, Brunsmann F. Hochauflösende kontrolle des zentralen gesichtfeldes mit dem video-kampimeter (High resolution central visual field evaluation by videocampimetry). *Fortschr Ophthalmol* 1988; 85: 750-755.
- 136 Mutlukan E, Keating D, Damato BE. A Touch-Screen Multi-Stimulus Video Campimeter. In: Mills R, ed. *Perimetry Update 92/93*. New York, Amsterdam: Kugler-Ghedini, 1993; 589-595.
- 137 Johnson CA. Modern developments in clinical perimetry. *Current Opinion in Ophthalmology* 1993; 4: 7-13.
- 138 Arden GB. Comparison of new psychophysics and perimetry with electrophysiological techniques in the diagnosis of glaucoma. *Current Opinion in Ophthalmology* 1993; 4: 14-21.
- 139 Fitzke FW. Clinical psychophysics. *Eye* 1988; 2 Suppl: S233-S241.
- 140 Stamper RL. Psychophysical changes in glaucoma. *Surv Ophthalmol* 1989; 33 Suppl: 309-318.
- 141 Bodis-Wollner I. Electrophysiological and psychophysical testing of vision in glaucoma. *Surv Ophthalmol* 1989; 33: 301-307.
- 142 Horton JC. The central visual pathways. In: Hart WM, ed. *Adler's physiology of the eye: Clinical application*. St.Louis: Mosby Year Book, 1994; 728-771.
- 143 Buck S. Cone-Rod interaction over time and space. *Vision Res* 1985; 25: 907-916.
- 144 Drum B. Relation of brightness to threshold for light adapted and dark adapted rods and cones: effects of retinal eccentricity and target size. *Perception* 1980; 9: 633-650.
- 145 Panda-Jonas S, Jonas JB, Jacobczyk M, Schneider U. Retinal photoreceptor count, retinal surface area, and optic disc size in normal human eyes. *Ophthalmology* 1994; 101:

519-523.

146 Newell F. Physiology and biochemistry of the eye. In: *Ophthalmology, principles and concepts*. St. Louis: Mosby Year Book, 1992; 7th edn. 71-98.

147 Newell FW. Sensory Retina. In: *Ophthalmology, Principles, Concepts*. St.Louis: Mosby Year Book, 1992; 24-26.

148 Rovamo J, Raninen A. Cortical acuity and the luminous flux collected by retinal ganglion cells at various eccentricities in human rod and cone vision. *Vision Res* 1990; **30**: 11-21.

149 Sloan LL, Brown DJ. Progressive retinal degeneration with selective involvement of the cone mechanism. *Am J Ophthalmol* 1962; **54**: 629-641.

150 Hansen E. The color receptors studied by increment threshold measurement during chromatic adaptation in the Goldmann perimeter. *Acta Ophthalmol* 1974; **52**: 490-500.

151 Hart WM,Jr., Silverman SE, Trick GL, Neshor R, Gordon MO. Glaucomatous visual field damage. Luminance and color-contrast sensitivities. *Invest Ophthalmol Vis Sci* 1990; **31**: 359-367.

152 Hart WM, Burde RM. Color contrast perimetry: The spatial distribution of color defects in optic nerve and retinal disease. *Ophthalmology* 1985; **92**: 768-776.

153 Sample PA, Esterson FD, Weinreb RN, Boynton RM. The aging lens: In vivo assessment of light absorbtion in 84 human eyes. *Invest Ophthalmol Vis Sci* 1988; **29**: 1306-1311.

154 Johnston CA, Adams AJ, Twelker JD, Quig JM. Age related changes in of the central visual field for short wavelenght sensitive (SWS) pathways.(Abstract). *J Opt Soc Am* 1988; **5**: 2131.

155 Sample PA, Weinreb RN. Color perimetry for assessment of primary open-angle glaucoma. *Invest Ophthalmol Vis Sci* 1990; **31**: 1869-1875.

156 Yamazaki Y, Lakowski R, Drance SM. A comparison of the blue mechanism in high and low-tension glaucoma. *Ophthalmology* 1989; **96**: 12-15.

157 De Jong LA, Snepvangers CE, van den Berg TJ, Langerhorst CT. Blue-yellow perimetry in the detection of early glaucomatous damage. *Doc Ophthalmol* 1990; **75**: 303-314.

158 Johnson CA, Adams AJ, Casson EJ, Brandt JD. Progression of early glaucomatous

visual field loss as detected by blue-on-yellow and standard white-on-white automated perimetry. *Arch Ophthalmol* 1993; **111**: 651-656.

159 Johnson CA, Adams AJ, Casson EJ, Brandt JD. Blue-on yellow perimetry can predict the development of glaucomatous visual field loss. *Arch Ophthalmol* 1993; **111**: 645-650.

160 Saito T. Physiological and morphological differences between On- and Off-center bipolar cells in the vertebrate retina. *Vision Res* 1987; **27**: 135-142.

161 Dowling JE, Dubin MW. The vertebrate retina. In: Darian-Smith I, ed. *Handbook of Physiology*. Bethesda, MD: American Physiological Society, 1984; 317-339.

162 Stell WK, Ishida AT, Lightfoot DD. Structural basis for on- and off-centre responses in retinal bipolar cells. *Science* 1978; **198**: 1269-1271.

163 Saito T, Kujiraoka T, Toyoda J. Electrical and morphological properties of off-center bipolar cells in the carp retina. *J Comp Neurol* 1984; **222**: 200-208.

164 Saito T, Kaneko A. Ionic mechanisms underlying the responses of off-center bipolar cells in the carp retina. I. Studies on responses evoked by light. *J Gen Physiol* 1983; **81**: 589-601.

165 D'Zmura M, Lennie P. Shared pathways for rod and cone vision. *Vision Res* 1986; **26**: 1273-1280.

166 Williams DR. Seeing through the photoreceptor mosaic. *TINS* 1986; **May**: 193-198.

167 Richards W. Why rods and cones? *Biol Cybern* 1979; **33**: 125-135.

168 Schiller PH, Sandell JH, Maunsell JH. Functions of the ON and OFF channels of the visual system. *Nature* 1986; **322**: 824-825.

169 Muller F, Wassle H, Voigt T. Pharmacological manipulation of the rod pathway in the cat retina. *J Neurophysiol* 1988; **59**: 1657-1672.

170 Daw NW, Jensen RJ, Brunken WJ. Rod pathways in mammalian retinae. *Trends Neurosci* 1990; **13**: 110-115.

171 Hensley S, Xiong-Li Y, Wu SM. Relative contribution of rod and cone inputs to bipolar cells and ganglion cells in the tiger salamander retina. *J Neurophysiol* 1993; **69**: 2086-2098.

172 Smith EL, Harwerth RS, Crawford MLJ, Duncan GC. Contribution of the retinal On

- channels to scotopic and photopic spectral sensitivity. *Vis Neurosci* 1989; 3: 225-239.
- 173 Gouras P, Evers HU. The neurocircuitry of primate retina. In: Gallego A, ed. *Neurocircuitry of the retina*. New York: Elsevier, 1985; 233-244.
- 174 Famiglietti EV, Kolb H. Structural basis for On and Off-Center responses in retinal ganglion cells. *Science* 1976; **194**: 193-195.
- 175 Wassle H. Sampling of visual space by retinal ganglion cells. *Invest Ophth Vis Sci (Suppl)* 1988; **29**: 117.
- 176 Nelson R, Famiglietti EV, Kolb H. Intracellular staining reveals different levels of stratification for on- and off-center ganglion cells in cat retina. *J Neurophysiol* 1978; **41**: 472-483.
- 177 Breitmeyer BG. Metacontrast with black and white stimuli: evidence for inhibition of on- and off-sustained activity by either on- or off-transient activity. *Vision Res* 1978; **18**: 1443-1448.
- 178 Kolb H. Organisation of the outer plexiform layer of the primate retina: Electron microscopy of the Golgi-impregnated cells. *Phil Trans R Soc Lond [Bio]* 1970; **258**: 261-283.
- 179 Masland RH. The functional architecture of the retina. *Scientific American* 1986; **254**: 102-111.
- 180 Rowe MH. Functional organisation of the retina. In: Dreher B, Robinson SR, eds. *Neuroanatomy of the visual pathways and their development*. London: MacMillan Press, 1991; 1-68.
- 181 Drasdo N. Receptive field densities of the ganglion cells of the human retina. *Vision Res* 1989; **29**: 985-988.
- 182 Dawson WW, Maida TM. Relations between the human retinal cone and ganglion cell distribution. *Ophthalmologica* 1984; **188**: 216-221.
- 183 Curcio CA, Allen KA. Topography of ganglion cells in human retina. *J Comp Neurol* 1990; **300**: 5-25.
- 184 Drasdo N. The neural representation of visual space. *Nature* 1977; **266**: 554-556.
- 185 Perry VH, Cowey A. Retinal ganglion cells that project to the superior colliculus and pretectum in the macaque monkey. *Neuroscience* 1984; **12**: 1125-1137.

- 186 Perry VH, Oehler R, Cowey A. Retinal ganglion cells that project to the dorsal lateral geniculate nucleus in the macaque monkey. *Neuroscience* 1984; **12**: 1101-1123.
- 187 Glezer VD. The receptive fields of the retina. *Vision Res* 1965; **5**: 497-525.
- 188 de Monasterio FM. Center and surround mechanisms of opponent-color X and Y ganglion cells of retina of macaques. *J Neurophysiol* 1978; **41**: 1418-1434.
- 189 Spillmann L, Ransom-Hogg A, Oehler R. A comparison of perceptive and receptive fields in man and monkey. *Human Neurobiol* 1987; **6**: 51-62.
- 190 Perry VH, Silveira LC. Functional lamination in the ganglion cell layer of the macaque's retina. *Neuroscience* 1988; **25**: 217-223.
- 191 Ransom-Hogg A; Spillmann L. Perceptive field size in fovea and periphery of the light and dark adapted retina. *Vision Res* 1980; **20**: 221-228.
- 192 Crook JM, Lange-Malecki B, Lee BB, Valberg A. Visual resolution of macaque retinal ganglion cells. *Journal of Physiology* 1988; **396**: 205-224.
- 193 Hiltz R, Cavonius R. Functional organisation of the peripheral retina: Sensitivity to periodic stimuli. *Vision Res* 1974; **14**: 1333-1337.
- 194 Gao H, Hollyfield JG. Aging of human retina. *Invest Ophthalmol Vis Sci* 1992; **33**: 1-17.
- 195 Devaney KD, Johnson HA. Neuron loss in the aging visual cortex of man. *J Gerontol* 1980; **35**: 836-839.
- 196 Derefeld G, Lennerstrand G, Lundh B. Age variations in normal human contrast sensitivity. *Acta Ophthalmol* 1979; **57**: 679-683.
- 197 Derrington AM, Lennie P. Spatial and temporal contrast sensitivities of neurones in lateral geniculate nucleus of macaque. *J Physiol (Lond)* 1984; **357**: 219-240.
- 198 Derrington AM, Krauskopf J, Lennie P. Chromatic mechanisms in lateral geniculate nucleus of macaque. *J Physiol (Lond)* 1984; **357**: 241-265.
- 199 Wagner HG, MacNichol EF, Wolbarsht ML. Functional basis for on-center and off-center receptive fields in the retina. *J Opt Soc Am* 1963; **53**: 66-70.
- 200 Perry VH, Cowey A. The morphological correlates of X- and Y-like retinal ganglion cells in the retina of monkeys. *Exp Brain Res* 1981; **43**: 226-228.

- 201 Bishop PO. Processing of visual information within the retinostriate system. In: Darian-Smith I, ed. *Handbook of Physiology*. Bethesda, MD: American Physiological Society, 1984; 341-423.
- 202 Hammon RW, Scobey RP. The luminance and response range of monkey retinal ganglion cells to white light. *Vision Res* 1982; **22**: 271-277.
- 203 Sclar G, Maunsell JHR, Lennie P. Coding of image contrast in central visual pathways of the macaque monkey. *Vision Res* 1990; **30**: 1-10.
- 204 Westheimer G. Spatial interaction in the human retina during scotopic vision. *J Physiol (Lond)* 1965; **181**: 881-894.
- 205 Westheimer G. Spatial interaction in human cone vision. *J Physiol (Lond)* 1967; **190**: 139-154.
- 206 Enoch JM, Junga RM, Bachmann E. Static perimetric technique believed to test receptive field properties. *Am J Ophthalmol* 1970; **70**: 113-126.
- 207 Enoch JM. Quantitative layer-by-layer perimetry: An update. *Am J Optom Physiol Opt* 1982; **59**: 952-953.
- 208 Gouras P, Zrenner E. Color coding in primate retina. *Vision Res* 1981; **21**: 1591-1598.
- 209 Dawson H. *Physiology of the eye*. 5th edn., Churchill & Livingston, London, 1990.
- 210 Silveira LC, Perry VH. The topography of magnocellular projecting ganglion cells (M-ganglion cells) in the primate retina. *Neuroscience* 1991; **40**: 217-237.
- 211 Midena E. Psychophysics and visual aging. *Metab Pediatr Syst Ophthalmol* 1989; **12**: 28-31.
- 212 Nagata S, Takashima M, Inui T, Kani K. Estimation of receptive field area and density of human retina using computer simulation. In: Mills RP, ed. *Perimetry Update 92/93*. Amsterdam, New York: Kugler-Ghedini, 1993; 533-535.
- 213 Takashima M, Nagata S, Kani K. Examination of receptive fields using an automatic perimeter. In: Mills RP, ed. *Perimetry Update 92/93*. Amsterdam-New York: Kugler-Ghedini, 1993; 537-541.
- 214 Frisen L. Visual Fields. In: Kennard C, Rose FC, eds. *Physiological aspects of clinical neuro-ophthalmology*. London: Chapman and Hall, 1988; 16-26.

- 215 Drance SM and Anderson DR. *Automatic perimetry in glaucoma*. Orlando: Grune-Stratton, 1985.
- 216 Quigley HA, Dunkelberger GR, Green WR. Retinal ganglion cell atrophy correlated with automated perimetry in human eyes with glaucoma. *Am J Ophthalmol* 1989; **107**: 453-464.
- 217 Mimura O, Kani K, Inui T. Spatial summation in the foveal and parafoveal region. *Doc Ophthalmol Proc Ser* 1981; **26**: 139-146.
- 218 Mimura O, Inui T, Kani K, Ohmi E. Retinal sensitivity and spatial summation in ambliopia. *Jpn J Ophthalmol* 1984; **28**: 389-400.
- 219 Shapley R, Enroth-Cugell C. Visual adaptation and retinal gain controls. In: Osborn N, Chader G, eds. *Progress in retinal research. Vol. 3*. Oxford: Pergamon, 1984; 263-346.
- 220 Slaughter MM; Miller RF. 2-amino-4-phosphonobutyric acid: a new pharmacological tool for retina research. *Science* 1981; **211**: 182-184.
- 221 Schiller PH. The connections of the retinal On and Off Pathways to the lateral geniculate nucleus of the monkey. *Vision Res* 1984; **24**: 923-932.
- 222 Schiller PH. The On and Off channels of the visual system. In: Cohen B, Bodis-Wollner I, eds. *Vision and the Brain, The organisation of the central visual system*. New York: Raven Press, 1990; 35-41.
- 223 Bolz J, Wassle H, Thier P. Pharmacological modulation of on and off ganglion cells in the cat retina. *Neuroscience* 1984; **12**: 875-885.
- 224 Thier P, Wassle H. Indoleamine-mediated reciprocal modulation of on-centre and off-centre ganglion cell activity in the retina of the cat. *J Physiol Lond* 1984; **351**: 613-630.
- 225 Ikeda H, Hankins MW, Kay CD. Actions of baclofen and phaclofen upon ON- and OFF-ganglion cells in the cat retina. *Eur J Pharmacol* 1990; **190**: 1-9.
- 226 de Monasterio FM, Gouras P. Functional properties of ganglion cells of the Rhesus monkey retina. *Journal of Physiology* 1975; **251**: 167-195.
- 227 de Monasterio FM. Asymmetry of On and Off pathways of blue sensitive cones of the retina of macaques. *Brain Res* 1979; **166**: 39-49.
- 228 Zrenner E. Neurophysiological aspects of colour mechanisms in the primate retina. In: Mollon J, Sharpe LT, eds. *Color Vision: Physiology and Psychophysics*. New York:

Academic Press, 1983; 195-210.

229 Schiller PH. The Central Visual System. *Vision Res* 1986; **26**: 1351-1388.

230 Malpeli J, Schiller P. Lack of blue off-center cells in the visual system of the monkey. *Brain Res* 1978; **141**: 385-389.

231 de Monasterio FM. Properties of ganglion cells with atypical receptive-field organisation in the retina of macaques. *Journal of Neurophysiology* 1978; **41**: 1435-1449.

232 de Monasterio FM. Properties of concentrically organised X and Y ganglion cells of macaque retina. *J Neurophysiol* 1978; **41**: 1394-1417.

233 Wiesel TN, Hubel DH. Spatial and Chromatic interactions in the lateral geniculate body of the rhesus monkey. *J Neurophysiol* 1966; **29**: 1115-1156.

234 de Monasterio FM, Gouras P, Tolhurst DJ. Trichromatic colour opponency in ganglion cells of the rhesus monkey retina. *J Physiol (Lond)* 1975; **251**: 197-216.

235 de Monasterio FM, Gouras P, Tolhurst DJ. Concealed colour opponency in ganglion cells of the rhesus monkey retina. *J Physiol (Lond)* 1975; **251**: 217-229.

236 Schiller PH, Colby CL. The response of single cells in the Lateral Geniculate Nucleus (LGN) of the rhesus monkey to colour and luminance contrast. *Vision Res* 1983; **23**: 1631-1641.

237 Liu S, Wong Riley M. Quantitative light- and electron-microscopic analysis of cytochrome-oxidase distribution in neurons of the lateral geniculate nucleus of the adult monkey. *Vis Neurosci* 1990; **4**: 269-287.

238 Schiller PH, Malpeli JG. Functional specificity of lateral geniculate nucleus laminae of the rhesus monkey. *Journal of Neurophysiology* 1978; **41**: 788-797.

239 Hammond P. Cat retinal ganglion cells: size and shape of receptive field centers. *J Physiol (Lond)* 1974; **242**: 99-118.

240 Harwerth RS, Smith EL. Rhesus monkey as a model for normal vision of humans. *Am J Optom Physiol Opt* 1985; **62**: 633-641.

241 Ogden TE. Nerve fiber layer of primate retina: morphometric analysis. *Invest Ophthalmol Vis Sci* 1984; **25**: 19-29.

242 Trobe JD, Glaser JS. The neural visual pathway. In: *The visual fields manual: a practical guide to testing and interpretation*. Gainesville,Fl.: Triad Publishing Co., 1983;

29-62.

243 Kaplan E, Shapley RM. X and Y cells in the lateral geniculate nucleus of macaque monkeys. *J Physiol (Lond)* 1982; **330**: 125-143.

244 Clark WEL, Penman GG. The projection of the retina in the lateral geniculate body. *Proc Roy Soc ,Ser B* 1934; **114**: 291-313.

245 Evers HU, Gouras P. Three cone mechanisms in the primate electroretinogram: two with, one without off-center bipolar responses. *Vision Res* 1986; **2**: 245-254.

246 Wheeler TG. Retinal On and Off responses convey different chromatic information to the CNS. *Brain Res* 1979; **160**: 145-149.

247 Shapley R, Perry VH. Cat and monkey retinal ganglion cells and their visual functional roles. *TINS* 1986; **May**: 229-235.

248 Perry VH, Silveira LC, Cowey A. Pathways mediating resolution in the primate retina. *Ciba Found Symp* 1990; **155**: 5-14.

249 Brannan JR, Bodis-Wollner I. Evidence for two systems mediating perceived contrast. *Vis Neurosci* 1991; **6**: 587-592.

250 Purpura K, Kaplan E, Shapley RM. Background light and the contrast gain of primate P and M retinal ganglion cells. *Proc Natl Acad Sci U S A* 1988; **85**: 4534-4537.

251 Merigan W, Katz LM, Maunsell JHR. The effects of parvocellular lateral geniculate lesions on the acuity and contrast sensitivity of macaque monkeys. *J Neurosci* 1991; **11**: 994-1001.

252 Schiller PH, Logothetis NK, Charles ER. Role of the color-opponent and broad-band channels in vision. *Vis Neurosci* 1990; **5**: 321-346.

253 Schiller PH, Logothetis NK, Charles ER. Functions of the colour-opponent and broad-band channels of the visual system. *Nature* 1990; **343**: 68-70.

254 Wall M. Loss of P retinal ganglion cell function in resolved optic neuritis. *Neurology* 1990; **40**: 649-653.

255 Dandona L, Hendrickson A, Quigley HA. Selective effects of experimental glaucoma on axonal transport by retinal ganglion cells to the dorsal lateral geniculate nucleus. *Invest Ophthalmol Vis Sci* 1991; **32**: 1593-1599.

256 Chaturvedi N, Hedley-Whyte ED, Dreyer EB. Lateral geniculate nucleus in

glaucoma. *Am J Ophthalmol* 1993; **116**: 182-188.

257 Silverman SE, Trick GL, Hart WM, Jr.. Motion perception is abnormal in primary open-angle glaucoma and ocular hypertension. *Invest Ophthalmol Vis Sci* 1990; **31**: 722-729.

258 Shechter S, Hochstein S. On and off pathway contributions to apparent motion perception. *Vision Res* 1990; **30**: 1189-1204.

259 Merigan WH, Byrne CE, Maunsell JH. Does primate motion perception depend on the magnocellular pathway? *J Neurosci* 1991; **11**: 3422-3429.

260 Michael CR. Retinal afferent arborization patterns, dendritic field orientations, and the segregation of function in the lateral geniculate nucleus of the monkey. *Proc Natl Acad Sci U.S A* 1988; **85**: 4914-4918.

261 Kageyama GH, Wong Riley MT. The histochemical localization of cytochrome oxidase in the retina and lateral geniculate nucleus of the ferret, cat, and monkey, with particular reference to retinal mosaics and ON/OFF-center visual channels. *J Neurosci* 1984; **4**: 2445-2459.

262 Zemon V, Gordon J, Welch J. Asymmetries in ON and OFF visual pathways of humans revealed using contrast-evoked cortical potentials. *Vis Neurosci* 1988; **1**: 145-150.

263 Kolb H. Anatomical pathways for color vision in the human retina. *Vis Neurosci* 1991; **7**: 61-74.

264 Van Essen DC, Newsome WT, Maunsell HR. The visual field representation in striate cortex of the macaque monkey: asymmetries, anisotropies, and individual variability. *Vision Res* 1984; **24**: 429-448.

265 Holmes G. Disturbances of vision by cerebral lesions. *Br J Ophthalmol* 1918; **2**: 353-384.

266 Horton JC, Hoyt WF. The representation of the visual field in human striate cortex: a revision of classical Holmes map. *Arch Ophthalmol* 1991; **109**: 816-824.

267 McFadzean R, Brosnahan D, Hadley D, Mutlukan E. The representation of the visual field in the occipital striate cortex. *Br J Ophthalmol* 1994; **78**: 185-190.

268 Rovamo J, Virsu V, Nasanen R. Cortical magnification factor predicts the photopic contrast sensitivity of peripheral vision. *Nature* 1978; **271**: 54-56.

269 Virsu V, Nasanen R, Osmovita K. Cortical magnification and peripheral vision. *J*

Opt Soc Am 1987; **4**: 1568-1578.

270 Wood JM, Wild JM, Drasdo N, Crews SJ. Perimetric profiles and cortical representation. *Ophthalmic Res* 1986; **18**: 301-308.

271 Wassle H, Boycott BB. Functional architecture of the mammalian retina. *Physiol Rev* 1991; **71**: 447-480.

272 Lennie P. Parallel visual pathways: a review. *Vision Res* 1980; **20**: 561-594.

273 Livingstone MS, Hubel DH. Do the relative mapping densities of the magno- and parvocellular systems vary with eccentricity? *J Neurosci* 1988; **8**: 4334-4339.

274 Norton TT, Rager G, Kretz R. On and Off regions in layer IV of striate cortex. *Brain Res* 1985; **327**: 319-323.

275 Kretz R, Rager G, Norton TT. Laminar organization of ON and OFF regions and ocular dominance in the striate cortex of the tree shrew (*Tupaia belangeri*). *J Comp Neurol* 1986; **251**: 135-145.

276 Weale RA. Apparent size and contrast. *Vision Res* 1975; **15**: 949-955.

277 De Valois KK. Independence of black and white: Phase-specific adaptation. *Vision Res* 1977; **17**: 209-215.

278 White TW, Irvin GE, Williams MC. Asymmetry in the brightness and darkness Broca-Sulzer effects. *Vision Res* 1980; **20**: 723-726.

279 Burton GJ, Nagshineh S, Ruddock KH. Processing by the human visual system of the light and dark contrast components of the retinal image. *Biol Cybernetics* 1977; **27**: 189-197.

280 Rea MS, Ouellette MJ. Visual performance using reaction times. *Lighting Res Technol* 1988; **20**: 139-153.

281 Ehrenstein WH, Spillmann L. Time thresholds for increments and decrements in luminance. *J Opt Soc Am* 1983; **73**: 419-426.

282 Herrick RM. Foveal luminance discrimination as a function of duration of the decrement and increment in luminance. *J Comp Physiol Psychol* 1956; **49**: 437-443.

283 Roufs JAJ. Dynamic properties of vision-IV; Thresholds of decremental flashes, incremental flashes and doublets in relation to flicker fusion. *Vision Res* 1974; **14**: 831-851.

- 284 Krauskopf J. Discrimination and detection of changes in luminance. *Vision Res* 1980; **20**: 671-677.
- 285 Tyler CW, Chan H, Liu L. Different spatial tunings for ON and OFF pathway stimulation. *Ophthalm Physiol Opt* 1992; **12**: 233-240.
- 286 Short AD. Decremental and incremental visual thresholds. *J Physiol (Lond)* 1966; **185**: 646-654.
- 287 Patel AS, Jones RW. Increment and decrement visual thresholds. *J Opt Soc Am* 1968; **58**: 696-699.
- 288 Cohn TE. A new hypothesis to explain why the increment threshold exceeds the decrement threshold. *Vision Res* 1974; **14**: 1277-1279.
- 289 Phillips WA, Singer W. Function and interaction of On and Off transients in vision; I. Psychophysics. *Exp Brain Res* 1974; **19**: 493-506.
- 290 Breitmeyer B, Julesz B. The role of On and Off transients in determining the psychophysical spatial frequency response. *Vision Res* 1974; **15**: 411-415.
- 291 Stromeyer CF, Zeevi YY, Klein S. Response of visual mechanisms to stimulus onsets and offsets. *J Opt Soc Am* 1979; **69**: 1350-1354.
- 292 Grehn F, Grusser OJ, Stange D. Effect of short-term intraocular pressure increase on cat retinal ganglion cell activity. *Behav Brain Res* 1984; **14**: 109-121.
- 293 Grusser OJ, Grusser-Cornehls U, Schreier U. Responses of cat retinal ganglion cells to eye-ball deformation: a neurophysiological basis for pressure phosphenes. *Doc Ophthalmol Proc Ser* 1981; **30**: 36.
- 294 Marozas DS, May DC. Effects of figure-ground reversal on the visual-perceptual and visuo-motor performances of cerebral palsied and normal children. *Perceptual and Motor Skills* 1985; **60**: 591-598.
- 295 Uhlin DM, Dickson JD. The effect of figure-ground reversal in the H-T-P drawings of spastic cerebral palsied children. *J Clin Psychol* 1970; **26**: 87-88.
- 296 Crick PR and Crick JCP. Apparatus for detecting visual field defects of the eye. *British Patent Application*. GB 2 031 607 A. London: UK Patent Office, 1978.
- 297 Elenius V. Rod saturation perimetry; Testing the cone function with achromatic objects. *Arch Ophthalmol* 1985; **103**: 519-523.

- 298 Heron JR, Regan D, Milner B. Delay in visual perception in unilateral optic atrophy after retrobulbar neuritis. *Brain* 1974; **97**: 83-92.
- 299 Regan D, Milner BA, Heron JR. Delayed visual perception and delayed visual evoked potentials in the spinal form of multiple sclerosis and retrobulbar neuritis. *Brain* 1976; **99**: 43-66.
- 300 Howland B, Ginsburg A, Campbell F. High-pass spatial frequency letters as clinical optotypes. *Vision Res* 1978; **18**: 1063-1066.
- 301 Frisen L. High-pass resolution targets in peripheral vision. *Ophthalmology* 1987; **94**: 1104-1108.
- 302 Timberlake GT, Mainster MA, Peli E, Augliere RE, Essock EA, Arrend LA. Reading with a macular scotoma. I. Retinal location of scotoma and fixation area. *Invest Ophthalmol Vis Sci* 1986; **27**: 1137-1147.
- 303 Acosta F, Lashkari K, Reynaud X, Jalkh AE, Van de Velde F, Chedid N. Characterisation of functional changes in macular holes and cysts. *Ophthalmology* 1991; **98**: 1820-1823.
- 304 Sjaarda RN, Frank DA, Glaser BM, Thompson JT, Murphy RP. Resolution of an absolute scotoma and improvement of relative scotomata after successful macular hole surgery. *Am J Ophthalmol* 1993; **116**: 129-139.
- 305 Hitchings RA. Glaucoma screening. *Br J Ophthalmol* 1993; **77**: 326.
- 306 Leske MC. The epidemiology of open angle glaucoma: A review. *Am J Epidemiol* 1983; **118**: 166-191.
- 307 Van Buskirk EM, Cioffi GA. Glaucomatous optic neuropathy. *Am J Ophthalmol* 1992; **113**: 447-452.
- 308 Drance SM. Glaucoma-Changing Concepts; Bowman lecture. *Eye* 1992; **6**: 337-345.
- 309 Grierson I. What is open angle glaucoma? *Eye* 1987; **1**: 15-28.
- 310 Crick RP. Computerised clinical database for glaucoma-ten years experience. *Res & Clin Forums* 1980; **2**: 29-39.
- 311 Wilson MR. Primary Open Angle Glaucoma: Magnitude of the problem in the United States. *J Glaucoma* 1992; **1**: 64-67.

- 312 Phelps CD. Glaucoma. *Primary Care* 1982; **9**: 729-741.
- 313 Anderson DR. Glaucoma: The damage caused by pressure. *Am J Ophthalmol* 1989; **108**: 485-495.
- 314 Morrison JC, Dorman-Pease ME, Dunkelberger GR, Quigley HA. Optic nerve head extracellular matrix in primary optic atrophy and experimental glaucoma. *Arch Ophthalmol* 1990; **108**: 1020-1024.
- 315 Hoyng PF, de Jong N, Oosting H, Stilma J. Platelet aggregation, disc haemorrhage and progressive loss of visual fields in glaucoma. A seven year follow-up study on glaucoma. *Int Ophthalmol* 1992; **16**: 65-73.
- 316 Schumer RA, Podos SM. The nerve of glaucoma. *Arch Ophthalmol* 1994; **112**: 37-44.
- 317 James B. Bloodflow in the pathogenesis of glaucoma. *Current Opinion in Ophthalmology* 1993; **4**: 65-72.
- 318 Gaasterland D, Tanishima T, Kuwabara T. Axoplasmic flow during chronic experimental glaucoma. 1. Light and electron microscopic studies of the monkey optic nervehead during development of glaucomatous cupping. *Invest Ophthalmol Vis Sci* 1978; **17**: 838-846.
- 319 Quigley HA, Addicks EM, Green WR, Maumenee AE. Optic nerve damage in human glaucoma: II. The site of injury and susceptibility to damage. *Arch Ophthalmol* 1981; **99**: 635-649.
- 320 Quigley HA. Reappraisal of the mechanisms of glaucomatous optic nerve damage. *Eye* 1987; **1**: 318-322.
- 321 Quigley HA, Hohman RM, Addicks EM, Massof RW, Green WR. Morphologic changes in the lamina cribrosa correlated with neural loss in open-angle glaucoma. *Am J Ophthalmol* 1983; **95**: 673-691.
- 322 Asai T, Katsumori N, Mizokami K. [Retinal ganglion cell damage in human glaucoma: 1. Studies on somal diameter]. *Folia Ophthalmol Jpn* 1987; **38**: 701-709.
- 323 Quigley HA, Addicks EM, Green WR. Optic nerve damage in human glaucoma. III. Quantitative correlation of nerve fiber loss and visual field defect in glaucoma, ischemic neuropathy, disc edema, and toxic neuropathy. *Arch Ophthalmol* 1982; **100**: 135-146.
- 324 Panda S, Jonas JB. Decreased photoreceptor count in human eyes with secondary angle-closure glaucoma. *Invest Ophthalmol Vis Sci* 1992; **33**: 2532-2536.

- 325 Quigley HA, Sanchez RM, Dunkelberger GR, L'Hernault NL, Baginski TA. Chronic glaucoma selectively damages large optic nerve fibers. *Invest Ophthalmol Vis Sci* 1987; **28**: 913-920.
- 326 Feuer WJ, Anderson DR. Static threshold asymmetry in early glaucomatous visual field loss. *Ophthalmology* 1989; **96**: 1285-1297.
- 327 Caprioli J. Automated perimetry in glaucoma. *Am J Ophthalmol* 1991; **111**: 235-239.
- 328 Aulhorn E, Harms H. Early visual field defects in glaucoma. In: *Glaucoma Symposium*. Basel: Karger, 1967; 151-186.
- 329 Armaly MF. The visual field defect and ocular pressure level in open angle glaucoma. *Invest Ophthalmol* 1969; **8**: 105-124.
- 330 Armaly MF. Ocular pressure and visual fields: A 10-year follow-up study. *Arch Ophthalmol* 1969; **81**: 25-40.
- 331 Drance SM, Douglas GR, Airaksinen PJ, Schulzer M, Hitchings RA. Diffuse visual field loss in chronic open-angle and low-tension glaucoma. *Am J Ophthalmol* 1987; **104**: 577-580.
- 332 Anctil JL, Anderson DR. Early foveal involvement and generalised depression of the visual field in glaucoma. *Arch Ophthalmol* 1984; **102**: 363-370.
- 333 Werner EB, Saheb N, Patel S. Lack of generalised constiction of affected visual field in glaucoma patients with visual field defects in one eye. *Can J Ophthalmol* 1982; **17**: 53-55.
- 334 Langerhorst CT, van den Berg TJ, Greve EL. Is there general reduction of sensitivity in glaucoma? *Int Ophthalmol* 1989; **13**: 31-35.
- 335 Heijl A. Lack of diffuse loss of differential light sensitivity in early glaucoma. *Acta Ophthalmol (Copenh)* 1989; **67**: 353-360.
- 336 Drance SM. Diffuse visual field loss in open-angle glaucoma. *Ophthalmology* 1991; **98**: 1533-1538.
- 337 Drance SM. The early field defects in glaucoma. *Invest Ophthalmol* 1969; **8**: 84-91.
- 338 Drance SM. The glaucomatous visual field. *Invest Ophthalmol Vis Sci* 1972; **11**: 85-97.
- 339 Greve EL, Verduin WM. Detection of early glaucomatous damage; Part 1: Visual

- field examination. *Doc Ophthalmol Proc Ser* 1977; **14**: 103-114.
- 340 Rabin S, Kolesar P. Mathematical optimization of glaucoma visual field screening protocols. *Doc Ophthalmol* 1978; **45**: 361-380.
- 341 Kosaki H. The earliest visual field defect (IIa stage) in glaucoma by kinetic perimetry. *Doc Ophthalmol Proc Ser* 1979; **19**: 255-259.
- 342 Fruno F, Matsuo H. Early stage progression in glaucomatous visual field changes. *Doc Ophthalmol Proc Ser* 1979; **19**: 247-243.
- 343 Coughlan M, Friedman AI. The frequency distribution of early visual field defects in glaucoma. *Doc Ophthalmol Proc Ser* 1981; **26**: 345-349.
- 344 Krieglstein GK, Schems W, Gramer E, Leydhecker W. Detectability of early glaucomatous field defects. *Doc Ophthalmol Proc Ser* 1981; **26**: 19-24.
- 345 Hart WM, Jr., Becker B. The onset and evolution of glaucomatous visual field defects. *Ophthalmology* 1982; **89**: 268-279.
- 346 Heijl A, Lundqvist L. The frequency distribution of earliest glaucomatous visual field defects documented by automatic perimetry. *Acta Ophthalmol (Copenh)* 1984; **62**: 658-664.
- 347 Henson DB, Chauhan BC. Informational content of visual field location in glaucoma. *Doc Ophthalmol* 1985; **59**: 341-352.
- 348 Stewart WC, Shields MB. The peripheral visual field in glaucoma: re-evaluation in the age of automated perimetry. *Surv Ophthalmol* 1991; **36**: 59-69.
- 349 Caprioli J, Spaeth GL. Comparison of visual field defects in the low-tension glaucomas with those in the high-tension glaucomas. *Am J Ophthalmol* 1984; **97**: 730-737.
- 350 Levene RZ. Low tension glaucoma: A critical review and new material. *Surv Ophthalmol* 1980; **24**: 621-624.
- 351 Anderton S, Hitchings RA. A comparative study of visual fields of patients with low-tension glaucoma and those with chronic simple glaucoma. *Doc Ophthalmol Proc Ser* 1983; **35**: 97-99.
- 352 Lachenmayr BJ, Drance SM, Chauhan BC, House PH, Lalani S. Diffuse and localized glaucomatous field loss in light-sense, flicker and resolution perimetry. *Graefes Arch Clin Exp Ophthalmol* 1991; **229**: 267-273.

- 353 Chauhan BC, Drance SM, Douglas GR, Johnson CA. Visual field damage in normal-tension and high-tension glaucoma. *Am J Ophthalmol* 1989; **108**: 636-642.
- 354 Greve EL, Geijssen C. Comparison of glaucomatous visual field defects in patients with high and low intraocular pressures. In: Greve EL, Heijl A, eds. *Fifth international visual field symposium*. The Hague: Dr.W.Junk Publishers, 1983; 101-105.
- 355 Motolko M, Drance SM, Douglas GR. Visual field defects in low-tension glaucoma. Comparison of defects in low-tension glaucoma and chronic open angle glaucoma. *Arch Ophthalmol* 1982; **100**: 1074-1077.
- 356 King D, Drance SM, Douglas G, Schulzer M, Wijsman K. Comparison of visual field defects in normal tension and high tension glaucoma. *Am J Ophthalmol* 1986; **101**: 204-207.
- 357 Phelps CD, Hayreh SS, Montaque PR. Visual field in low tension glaucoma, primary open angle glaucoma, and anterior ischemic optic neuropathy. *Doc Ophthalmol Proc Ser* 1983; **35**: 113-124.
- 358 Chandler PA and Grant WM. *Lectures on Glaucoma*. Philadelphia: Lee & Febiger, 1965: 14-16.
- 359 Read RM, Spaeth GL. The practical appraisal of the disc in glaucoma: The natural history of cup progression and some specific disc-field correlations. *Trans Am Acad Ophthalmol Otolaryngol* 1974; **78**: 255-274.
- 360 Gloster J. Vertical ovalness of glaucomatous cupping. *Br J Ophthalmol* 1959; **59**: 721-724.
- 361 Quigley HA, Dunkelberger GR, Green WR. Chronic human glaucoma causing selectively greater loss of large optic nerve fibers. *Ophthalmology* 1988; **95**: 357-363.
- 362 Quigley HA, Green WR. The histology of human glaucoma cupping and optic nerve damage: clinicopathologic correlation in 21 eyes. *Ophthalmology* 1979; **86**: 1803-1830.
- 363 Sommer A, Miller NR, Pollack I, Maumenee AE, George T. The nerve fiber layer in the diagnosis of glaucoma. *Arch Ophthalmol* 1977; **95**: 2149-2156.
- 364 Hitchings RA, Spaeth GL. The optic disc in glaucoma. *Br J Ophthalmol* 1976; **60**: 778-785.
- 365 Quigley HA, Miller NR, George T. Clinical evaluation of nerve fiber layer atrophy as an indicator of glaucomatous optic nerve damage. *Arch Ophthalmol* 1980; **98**:

1564-1571.

366 Sommer A, Quigley HA, Robin AL, Miller NR, Katz J, Arkel S. Evaluation of nerve fiber layer assessment. *Arch Ophthalmol* 1984; **102**: 1766-1771.

367 Hollows FC, Graham PA. Intraocular pressure, glaucoma and glaucoma suspects in a defined population. *Br J Ophthalmol* 1966; **50**: 570-586.

368 Graham PA. The definition of pre-glaucoma: A prospective study. *Trans Ophthalmol Soc U K* 1968; **88**: 153-165.

369 Perkins ES. The Bedford glaucoma survey: I. Long-term follow-up of borderline cases. *Br J Ophthalmol* 1973; **57**: 179-185.

370 Glovinsky Y, Quigley HA, Dunkelberger GR. Retinal ganglion cell loss is size dependent in experimental glaucoma. *Invest Ophthalmol Vis Sci* 1991; **32**: 484-491.

371 Asai T, Katsumori N, Mizokami K. [Retinal ganglion cell damage in human glaucoma. 2. Studies on damage pattern]. *Nippon Ganka Gakkai Zasshi* 1987; **91**: 1204-1213.

372 Radius RL. Anatomy of the optic nerve head and glaucomatous optic neuropathy. *Surv Ophthalmol* 1987; **32**: 35.

373 Eddy DM, Sanders LE, Eddy JF. The value of screening for glaucoma with tonometry. *Surv Ophthalmol* 1983; **28**: 194-205.

374 Katz LJ, Spaeth GL, Cantor LB, Poryzees EM, Steinmann WC. Reversible optic disk cupping and visual field improvement in adults with glaucoma. *Am J Ophthalmol* 1989; **107**: 485-492.

375 Niesel P, Flammer J. Correlations between intraocular pressure, visual field and visual acuity, based on 11 years of observations of treated chronic glaucomas. *Int Ophthalmol* 1980; **3**: 31-37.

376 Jay JL, Allan D. The benefit of early trabeculectomy versus conventional management in primary open angle glaucoma relative to severity of disease. *Eye* 1989; **3**: 528-535.

377 Bajandas F, Kline LB. Visual Fields. In: *Neuro-ophthalmology review manual*. 3rd edn. Thorofare: Slack Inc, 1988:1-42.

378 Hart CR. *Screening in General Practice*. Edinburgh, London, New York: Livingston, Churchill, 1975.

- 379 Pollack I. Glaucoma Screening. *J All-India Ophthalmol Soc* 1966; **14**: 1-5.
- 380 Tudor J, Hart CR. Screening in primary care. In: Hart CR, ed. *Screening in general practice*. Edinburgh, London, New York.: Livingston, Churchill., 1975; 17-30.
- 381 Aspinall P. Clinical inferences and decisions: I. Diagnosis and Bayes' Theorem. *Ophthal Physiol Opt* 1983; **3**: 295-304.
- 382 Schulzer M, Anderson DR, Drance SM. Sensitivity and specificity of a diagnostic test determined by repeated observations in the absence of an external standard. *J Clin Epidemiol* 1991; **44**: 1167-1179.
- 383 Teeling-Smith G. The economics of screening. In: Hart CR, ed. *Screening in general practice*. Edinburgh, London, New York: Livingston, Churchill., 1975; 31-40.
- 384 Trobe JD, Krischer JP. Cost-benefit analysis in screening. Unexplained visual loss. *Surv Ophthalmol* 1983; **28**: 189-193.
- 385 Hart CR. The history of screening. In: Hart CR, ed. *Screening in general practice*. Edinburgh, London, New York: Livingston, Churchill, 1975; 3-16.
- 386 Gottlieb LG, Schwartz B, Pauker SG. Glaucoma screening. A cost-effectiveness analysis. *Surv Ophthalmol* 1983; **28**: 206-228.
- 387 Greve EL, Verduin WM. Mass visual field investigation in 1834 persons with supposedly normal eyes. *Albrecht Von Graefes Arch Klin Exp Ophthalmol* 1972; **183**: 286-293.
- 388 Keltner JL, Johnson CA. Mass visual field screening in a driving population. *Ophthalmology* 1980; **87**: 785-792.
- 389 Anderson DR. *Perimetry with or without automation*. 2nd edn. St. Louis, Washington D.C., Toronto: The C.V. Mosby Company., 1987.
- 390 Elkington AR, Lewry J, MacKean J, Sargent P. A collaborative hospital glaucoma survey. *Res & Clin Forums* 1982; **4**: 31-40.
- 391 Vernon SA, Henry DJ, Cater L, Jones SJ. Screening for glaucoma in the community by non-trained staff using semi-automated equipment. *Eye* 1990; **4**: 89-97.
- 392 Sommer A, Tielsch JM, Katz J, et al. Relationship between intraocular pressure and primary open angle glaucoma in white and black Americans. *Arch Ophthalmol* 1991; **109**: 1090-1095.

- 393 Acers T. Glaucoma detection in general medical practice. *OSMA Journal* 1965; **58**: 397-398.
- 394 Steinmann WC, Licht L, Siegler JE, Nichols CW. Screening for glaucoma by general medicine residents. *Arch Intern Med* 1982; **142**: 785-786.
- 395 Ader OL, Callahan SE, McCotter MB. Glaucoma screening in a local health department. *The sight saving review* 1969; **39**: 145-151.
- 396 Ross AK. The organisation of glaucoma screening in general practice. *J Roy Coll Gen Practit* 1968; **15**: 358-362.
- 397 Harrison JR, Wild JM, Hopley AJ. Referral patterns to an ophthalmic outpatient clinic by general practitioners and ophthalmic opticians and the role of these professionals in screening for ocular disease. *BMJ* 1988; **297**: 1162-1167.
- 398 Clearkin L, Harcourt B. Referral pattern of true and suspected glaucoma to an ophthalmic outpatient clinic. *Eye* 1983; **103**: 284-287.
- 399 Levi L, Schwartz B. Glaucoma screening in the health care settings. *Surv Ophthalmol* 1983; **28**: 164-174.
- 400 Sponsel WE. Tonometry in question: can visual screening tests play a more decisive role in glaucoma diagnosis and management? *Surv Ophthalmol* 1989; **33** Suppl: 291-300.
- 401 Bengtsson B. The variation and co-variation of cup and disc diameters. *Acta Ophthalmol* 1976; **54**: 804-818.
- 402 Bengtsson B. The alteration and asymmetry of cup and disc diameters. *Acta Ophthalmol* 1980; **58**: 726-732.
- 403 Klein BE, Moss SE, Magli YL, Klein R, Johnson JC, Roth H. Optic disc cupping as clinically estimated from photographs. *Ophthalmology* 1987; **94**: 1481-1483.
- 404 Jonas JB, Fernandez MC, Naumann GOH. Glaucomatous optic nerve atrophy in small discs with low cup-to-disc ratios. *Ophthalmology* 1990; **97**: 1211-1215.
- 405 Tuck MW. Referrals for suspected glaucoma: an International Glaucoma Association survey. *Ophthal Physiol Opt* 1991; **11**: 22-26.
- 406 Tuck MW, Crick R. Testing and referral for chronic glaucoma. *Health Trends* 1989; **21**: 131-134.

- 407 Keltner JL, Johnson CA. Screening for visual field abnormalities with automated perimetry. *Surv Ophthalmol* 1983; **28**: 175-183.
- 408 Trobe JD, Acosta PC, Shuster JJ, Krischer JP. An evaluation of the accuracy of community-based perimetry. *Am J Ophthalmol* 1980; **90**: 654-660.
- 409 Enger C, Sommer A. Recognizing glaucomatous field loss with the Humphrey STATPAC. *Arch Ophthalmol* 1987; **105**: 1355-1357.
- 410 Tuck MW, Crick RP. Efficiency of referral for suspected glaucoma. *BMJ* 1991; **302**: 998-1000.
- 411 Wirtschafter JD, Hard Boberg AL, Coffman SM. Evaluating the usefulness in neuro-ophthalmology of visual field examinations peripheral to 30 degrees. *Trans Am Ophthalmol Soc* 1984; **82**: 329-357.
- 412 Lindblom B, Hoyt WF. High-pass resolution perimetry in neuro-ophthalmology. Clinical impressions. *Ophthalmology* 1992; **99**: 700-705.
- 413 Keltner JL, Johnson CA, Balestrery FG. Suprathreshold static perimetry. Initial clinical trials with the Fieldmaster automated perimeter. *Arch Ophthalmol* 1979; **97**: 260-272.
- 414 Johnson CA, Keltner JL, Balestrery FG. Suprathreshold static perimetry in glaucoma and other optic nerve disease. *Ophthalmology* 1979; **86**: 1278-1286.
- 415 Batko KA, Anctil JL, Anderson DR. Detecting glaucomatous damage with the Friedmann analyzer compared with the Goldmann perimeter and evaluation of stereoscopic photographs of the optic disk. *Am J Ophthalmol* 1983; **95**: 435-447.
- 416 Hicks BC, Anderson DR. Quantitation of glaucomatous visual field defects with the Mark II Friedmann analyzer. *Am J Ophthalmol* 1983; **95**: 692-700.
- 417 Sponsel WE. Visual field quantification in the diagnosis and assessment of chronic open angle glaucoma. M.D. Thesis., University of Bristol, England, 1985.
- 418 Aulhorn E, Karmeyer H. Frequency distribution in early glaucomatous visual field defects. *Doc Ophthalmol Proc Ser* 1977; **14**: 75-83.
- 419 Scott GI. Glaucoma. In: *Traquair's Clinical Perimetry*. London: Henry Kimpton, 1957; 7th edn. 126-152.
- 420 National Academy of Sciences-National Research Council. Recommended standard procedures for the clinical measurement and specification of visual acuity: Report of

- working group 39. *Adv Ophthalmol* 1980; **41**: 103-148.
- 421 Horowitz P, Winfield H. Foundations. In: *The art of electronics*. Cambridge: Cambridge University Press, 1982; 1-49.
- 422 Di Lollo V. Luminous calibration of oscilloscopic displays. *Behav Res Meth Instr* 1979; **11**: 419-421.
- 423 Johnson CA, Keltner JL. Automated suprathreshold static perimetry. *Am J Ophthalmol* 1980; **89**: 731-741.
- 424 Caprioli J. Automated perimetry in glaucoma. In: Walsh TJ, ed. *Visual fields, examination and interpretation*. San Francisco: American Academy of Ophthalmology, 1990; 71-106.
- 425 Hart WM, Yablonski M, Kass MA, Becker M. Multivariate analysis of the risk of glaucomatous visual field loss. *Arch Ophthalmol* 1979; **97**: 1455-1458.
- 426 Parrish RK, Schiffman J, Anderson DR. Static and kinetic visual field testing. *Arch Ophthalmol* 1984; **102**: 1497-1502.
- 427 Ryan BF, Joiner BL, Ryan TA. Departures from assumptions: Non-normality. In: *Minitab Handbook*. Boston: PWS-Kent Publisher, 1985; 2nd edn. 177-179.
- 428 Ryan BF, Joiner BL, Ryan TA. Making inferences from straight-line fits. In: *Minitab Handbook*. Boston: PWS-Kent, 1985; 2nd edn. 229-234.
- 429 Ryan BF, Joiner BL, Ryan TL. Simple regression: Fitting a straight line. In: *Minitab Handbook*. Boston: PWS-Kent, 1985; 2nd edn. 223-227.
- 430 Ryan BF, Joiner BL, Ryan TL. Interpreting residuals in simple and polynomial regression. In: *Minitab Handbook*. Boston: PWS-Kent, 1985; 2nd edn. 249-252.
- 431 Sumbuloglu K. [*Research techniques and statistics in health sciences*](in Turkish). Ankara: Matis, 1978: 197-198.
- 432 Suyama H, Wakakura M. Oculokinetic perimetry for glaucoma. *Jpn J Clin Ophthalmol* 1991; **45**: 179-183.
- 433 Alvarez E, Damato BE, Jay JL, McClure E. Comparative evaluation of oculokinetic perimetry and conventional perimetry in glaucoma. *Br J Ophthalmol* 1988; **72**: 258-262.
- 434 Damato BE, Ahmed J, Allan D, McClure E, Jay JL. The detection of glaucomatous visual field defects by oculo-kinetic perimetry: which points are best for screening? *Eye*

1989; 3: 727-731.

435 Damato BE, Chyla J, McClure E, Jay JL, Allan D. A hand-held OKP chart for the screening of glaucoma: preliminary evaluation. *Eye* 1990; 4: 632-637.

436 Feliuss J, Langerhost CT, van Den Berg TJPT, Greve EL. Oculokinetic perimetry compared with standard perimetric threshold testing. *Int Ophthalmol* 1992; 16: 221-226.

437 Beck RW, Bergstrom TJ, Lichter PR. A clinical comparison of visual field testing with a new automated perimeter, the Humphrey Field Analyzer, and the Goldmann perimeter. *Ophthalmology* 1985; 92: 77-82.

438 Vernon S, Quigley HA. A comparison of the OKP visual field screening test with the Humphrey Field Analyser. *Eye* 1992; 6: 521-524.

439 Wishart PK. Oculokinetic perimetry compared with Humphrey visual field analysis in the detection of glaucomatous visual field loss. *Eye* 1993; 7: 113-121.

440 Chuman H, Nao-i N, Kubota H, Sawada A. Assessment of usefulness of hand-held oculo-kinetic perimetry. In: Mills RP, ed. *Perimetry Update 92/93*. Amsterdam, New York: Kugler-Ghedini, 1993; 305-309.

441 Kato A, Iwase A, Maeda M, Kitazawa Y, Myers S. Clinical evaluation of the oculo-kinetic perimetry glaucoma screener. In: Mills RP, ed. *Perimetry Update 92/93*. Amsterdam/New York: Kugler-Ghedini, 1993; 311-313.

442 Sommer A, Duggan C, Auer C, Abbey H. Analytic approaches to the interpretation of automated threshold perimetric data for the diagnosis of early glaucoma. *Trans Am Ophthalmol Soc* 1985; 83: 250-267.

443 Wilensky JT, Joondeph BC. Variation in visual field measurements with an automated perimeter. *Am J Ophthalmol* 1984; 97: 328-331.

444 Henson DB, Dix SM, Osborne AC. Evaluation of the Friedmann Visual Field Analyser Mark II. Part 1. Results from a normal population. *Br J Ophthalmol* 1984; 68: 458-462.

445 Gutteridge IF. The working threshold approach to Friedmann visual field analyser screening. *Ophthalmic Physiol Opt* 1983; 3: 41-46.

446 Anderson DR. Programmed visual field testing. *Trans Am Ophthalmol Soc* 1982; 80: 326-348.

447 Mutlukan E, Cullen E. Red Colour Comparison Perimetry Chart. *UK Patent Office*

Publications, 2247087A, London, 1992.

448 Mutlukan E, Cullen JF. Perimetry apparatus for the examination of central visual field. UK Patent GB 9202671.4. *UK Patent Office Publications*, London, 1993.

449 Hosokawa H, Nishimura Y, Okumura S. Digital CRT luminance uniformity correction. *SID 87 Digest* 1987; **21**: 412-415.

450 Pennebaker GE, Stewart WC, Stewart JA, Hunt HH. The effects of stimulus duration upon the components of fluctuation in static automated perimetry. *Eye* 1992; **6**: 353-355.

451 Wall M, George D. Visual loss in pseudotumor cerebri. Incidence and defects related to visual field strategy. *Arch Neurol* 1987; **44**: 170-175.

452 Henson DB, Bryson H. Is the variability in glaucomatous field loss due to poor fixation control? In: Mills RP, Heijl A, eds. *Perimetry Update 1990/91*. New York, Amsterdam: Kugler-Ghedini, 1991; 217-220.

453 Heijl A, Lindgren A, Lindgren G. Test-retest variability in glaucomatous visual fields. *Am J Ophthalmol* 1989; **108**: 130-135.

454 Mills RP. A comparison of Goldmann, Fieldmaster 200, and Dicon AP2000 perimeters used in a screening mode. *Ophthalmology* 1984; **91**: 347-354.

455 Mills RP. Evaluation of diagnostic capabilities of interactive test strategies in automated perimetry. *Ophthalmology* 1985; **92**: 1181-1186.

456 Aulhorn E, Harms H, Karmeyer H. The influence of spontaneous eye rotations on the perimetric determination on small scotomas. *Doc Ophthalmol Proc Ser* 1978; **19**: 363-367.

457 Keating D, Mutlukan E, Evans A, McGarvie J, Damato B. A back propagation neural network for the classification of visual field data. *Phys Med Biol* 1993; **38**: 1263-1270.

458 Mutlukan E, Keating D. Visual field interpretation with a personal computer based neural network. *Eye* 1994; **8** (3): 321-323.

459 Herse PR. Factors influencing normal perimetric thresholds obtained using the Humphrey Field Analyzer. *Invest Ophthalmol Vis Sci* 1992; **33**: 611-617.

460 House PH, Drance SM, Schulzer M, Wijsman K. The effect of refractive blur on the visual field using the ring perimeter. *Acta Ophthalmol* 1990; **68**: 87-90.

- 461 Holzl MJ, Lachenmayr BJ, Vivell PM. [Effect of faulty refraction and artificial media opacities on visual acuity perimetry]. *Fortschr Ophthalmol* 1991; **88**: 875-880.
- 462 Atchison DA. Effect of defocus on visual field measurement. *Ophthalmic Physiol Opt* 1987; **7**: 259-265.
- 463 Heuer DK, Anderson DR, Feuer WJ, Gressel MG. The influence of refraction accuracy on automated perimetric threshold measurements. *Ophthalmology* 1987; **94**: 1550-1553.
- 464 Jonas JB, Gusek GC, Fernandez MC. Correlation of the blind spot size to the area of the optic disk and parapapillary atrophy. *Am J Ophthalmol* 1991; **111**: 559-565.
- 465 Haefliger IO, Flammer J. Fluctuation of the differential light threshold at the border of absolute scotomas. Comparison between glaucomatous visual field defects and blind spots. *Ophthalmology* 1991; **98**: 1529-1532.
- 466 Haefliger IO, Flammer J. Increase of the short-term fluctuation of the differential light threshold around a physiologic scotoma. *Am J Ophthalmol* 1989; **107**: 417-420.
- 467 Bek T, Lund Andersen H. The influence of stimulus size on perimetric detection of small scotomata. *Graefes Arch Clin Exp Ophthalmol* 1989; **227**: 531-534.
- 468 Fankhauser F, Haerberlin H. Dynamic range and stray light. An estimate of the falsifying effects of stray light in perimetry. *Doc Ophthalmol* 1980; **50**: 143-167.
- 469 Corbett JJ, Jacobson DM, Maurer RC, et al. Enlargement of the blind spot caused by papilledema. *Am J Ophthalmol* 1988; **105**: 260-265.
- 470 Fletcher WA, Imes RK, Goodman D, et al. Acute idiopathic blind spot enlargement: A big blind spot syndrome without disc edema. *Arch Ophthalmol* 1988; **106**: 44-49.
- 471 Hamed LM, Glaser JS, Gass JDM, et al. Protracted enlargement of the blind spot in multiple evanescent white dot syndrome. *Arch Ophthalmol* 1989; **107**: 194-198.
- 472 Kimmel AS, Folk JC, Thompson HS, et al. The multiple evanescent white-dot syndrome with acute blind spot enlargement. *Am J Ophthalmol* 1989; **107**: 425-426.
- 473 Werner JS, Peterzell DH, Scheetz AJ. Light, vision, and aging. *Optom Vis Sci* 1990; **67**: 214-229.
- 474 Zulauf M, Mandava S, Zeyen T, Caprioli J. Sensitivity and specificity of visual field indices. In: Mills R, ed. *Perimetry Update 92/93*. Amsterdam, New York: Kugler-Ghedini, 1993; 19-23.

- 475 Brabyn JA, Haegerstrom-Portnoy G, Schneck ME, Hennessy D. Attentional visual fields: Age changes and relation to driving. *Invest Ophth Vis Sci (Suppl)* 1994; **35** (4): 1951.
- 476 Owsley C, Ball K, Keeton DM. Relationship between visual sensitivity and target localisation in older adults. *Invest Ophth Vis Sci (Suppl)* 1994; **35** (4): 1953.
- 477 Flanagan JG, Wild JM, Trope GE. Evaluation of FASTPAC, a new strategy for threshold estimation with the Humphrey Field Analyser, in a glaucomatous population. *Ophthalmology* 1993; **100**: 949-954.
- 478 Iwase A, Kitazawa Y, Kato Y. Clinical value of FASTPAC: a comparative study with the standard full threshold method. In: Mills R, ed. *Perimetry Update 92/93*. Amsterdam; New York: Kugler-Ghedini, 1993; 365-367.
- 479 O'Brien C, Poinosawmy S, Wu J, Hitchings R. STATPAC-FASTPAC comparison in glaucoma. In: Mills R, ed. *Perimetry Update 92/93*. Amsterdam, New York: Kugler-Ghedini, 1993; 369-370.
- 480 Casson EJ, Shapiro LR, Johnson CA. Short-term fluctuation as an estimate of variability in visual field data. *Invest Ophthalmol Vis Sci* 1990; **31**: 2459-2463.

APPENDIX

A scientist never really finishes his work, he merely abandons it.
[Paul Valery]

Table 1: Negative contrast (offset) steps available in the ascending threshold program of CAMEC.

Grey Shade Number	Luminance(cd/m ²)		Contrast (Weber's)	
	Background	Stimulus	Percent(%)	Decibel(dB)
37	10.00	10.00	0	~
36	"	9.60	- 4	28
35	"	9.25	- 7.5	22.5
34	"	8.90	- 11	19
33	"	8.55	- 15	17
32	"	8.20	- 18	15
31	"	7.80	- 22	13
29	"	7.20	- 28	11
27	"	6.50	- 35	9
24	"	5.35	- 47	7
20	"	4.15	- 59	5
1	"	2.40	- 76	2.4

Table 2: The blind spot test parameters of Dicon Autoperimeter and CAMEC.

Parameters	Dicon:	CAMEC:
Background Type	Bowl, White	CRT, White
Backgr. Luminance	10 Apostilb	32 Apostilbs
Stimulus Type	Static, onset (diode)	Static, offset
Stimulus Area	2 mm ²	5 mm ²
Stimulus Luminance	500 Apostilb	8 Apostilb
Stimulus Duration	0.3 second	0.3 seconds

Table 3: The amount of plus sphere refraction required to achieve various visual acuity levels.

<u>Visual Acuity</u>	<u>Log Attenuation</u>	<u>Correction(Mean&St.Dev.)</u>
6/6 (20/20; J1)	0.0	3.45 \pm 3.38 Diopter (min. -7.00, max. 0.0)
6/12 (20/40; J3)	0.301	-0.80 \pm 2.90 Diopter (min. -4.00, max. +2.50)
6/24 (20/100; J10)	0.602	+0.05 \pm 3.10 Diopter (min. -3.00, max. +3.50)
6/60 (20/200; J16)	1.00	+0.95 \pm 3.29 Diopter (min. -2.00, max. +5.00)

Table 4: Selection criteria for POAG, OHT and control cases.

	<u>POAG(n=21)</u>	<u>OHT(n=21)</u>	<u>Controls(n=13)</u>
Visual Acuity	\geq 6/6	\geq 6/6	\geq 6/6
Correction	< \pm 7.00 D. spherical eq.	< \pm 7.00 D. spherical eq.	< \pm 7.00 D. spherical eq.
Pupil Size	3-6 mm.	3-6 mm.	3-6 mm.
IOP (highest)	\geq 22 mmHg	\geq 22 mmHg	< 22 mmHg
C/D Ratio	or > 0.5	N/A	\leq 0.5
Visual Field	Abnormal	Normal	Normal

(D:diopeters, IOP:intraocular pressure, C/D=cup to disc ratio, N/A:not applicable)

Table 5: Detection of physiological blind spot according to the number of corresponding test stimuli in OKC.

	Eye		
	Right	Left	Both
Non-Fluctuating Positive			
Chart A	37 (53.6 %)	38 (55.1 %)	75 (54.3 %)
Chart B	54 (80.6 %)	48 (71.6 %)	102 (76.1 %)
Fluctuating Positive			
Chart A	5 (7.2 %)	9 (13.0 %)	14 (10.1 %)
Chart B	5 (7.5 %)	7 (10.5 %)	12 (9.0 %)
False Negative			
Chart A	27 (39.1 %)	22 (31.9 %)	49 (35.5 %)
Chart B	8 (11.9 %)	12 (17.9 %)	20 (14.9 %)
Total			
Chart A	69 (100 %)	69 (100 %)	138 (100 %)
Chart B	67 (100 %)	67 (100 %)	134 (100 %)

Table 6: Stimulus durations which can be obtained with CAMEC software program.

Preset Duration	Actual Mean (sec.)	St. Dev.	Minimum	Maximum
0.1 sec.	0.1655	0.0357	0.10938	0.22266
0.2 sec.	0.2834	0.0600	0.16156	0.39063
0.4 sec.	0.4813	0.0483	0.37891	0.60156
0.6 sec.	0.6617	0.0560	0.55078	0.77344

Table 7: The details of paediatric cases abandoned the test.

Patient#	Age (yrs)	Sex	Eye	Dicon	CAMEC
1	4	F	L	(-)	(-)
2	5	F	L	(-)	(-)
3	4	F	R	(+)	(-)
4	4.5	M	L	(-)	(+)
5	5.5	F	R	(-)	(-)
6	4.5	M	R	(-)	(-)
7	4	M	R	(-)	(-)
8	4	F	L	(-)	(-)

[(+):test completed, (-):test abandoned, M:male, F:female, R:right, L:left]

Table 8: Patients screened for neuro-ophthalmic visual field loss.

<u>Initials</u>	<u>Diagnosis</u>		
		50.MM	Obstructive hydrocephalus
		51.EC	Chiasmal arachnoiditis
1.HC	Pituitary apoplexy	52.EP	Pseudotumor cerebri
2.JG	3rd nerve paresis	53.MM	Multiple sclerosis
3.MD	Occipital lobe infarct	54.HM	Cerebello-pontine angle tumour
4.WS	Arterio-venous malformation	55.JM	Pituitary adenoma
5.AH	Suprasellar meningioma	56.AF	Cerebello-pontine angle tumour
6.MC	Temporo-parietal tumour	57.MS	Pituitary adenoma
7.KW	Migraine	58.GC	Cerebello-pontine angle tumour
8.PC	Pituitary adenoma	59.DB	Arteriovenous malformation
9.LR	Pseudotumor cerebri	60.SC	Head trauma
10.DM	Head Trauma	61.NW	Pituitary adenoma
11.AS	Headache	62.CM	Craniopharyngioma
12.CF	Head Trauma	63.HF	Brainstem tumour
13.JT	Epilepsy	64.WM	Hydrocephalus
14.GM	Head Trauma	65.SR	Migraine
15.EK	Pituitary adenoma	66.JR	Suprasellar tumour
16.ED	Pituitary adenoma	67.AM	Temporal hemianopia
17.JC	Orbital tumour	68.AA	Optic neuritis
18.JS	Pseudotumor cerebri	69.SH	Headache
19.IC	Pituitary Adenoma	70.AL	Mitochondrial myopathy
20.SG	Pseudotumor cerebri	71.AK	Occipital infarct
21.JM	Corpus callosum tumour	72.AM	Arteriovenous malformation
22.FW	Orbital cellulitis	73.GM	Aqueduct stenosis
23.TH	Temporal lobe tumour	74.MM	Head trauma
24.DM	Suprasellar tumour	75.MH	Migraine
25.HA	Sagittal sinus thrombosis	76.MG	Craniopharyngioma
26.JP	Pituitary adenoma	77.DA	Pituitary adenoma
27.SM	Pituitary adenoma	78.CW	Temporo-parietal infarct
28.PB	Parasellar tumour	79.CB	Pituitary adenoma
29.FL	Pseudotumor cerebri	80.GM	Head injury
30.JM	Pituitary adenoma	81.SR	Parieto-occipital infarct
31.JL	Amarosis fugax	82.MB	Ventricular cyst
32.FG	Occipital lobe tumor	83.KM	Parasellar tumour
33.LP	Oculomotor palsy	84.MA	Frontal lobe tumour
34.AC	Pseudotumor cerebri	85.JP	Dysthyroid eye disease
35.AC	Temporal lobe tumor	86.MA	Chiasmal glioma
36.JP	Pituitary adenoma	87.CB	Optic neuritis
37.IV	Craniopharyngioma	88.JH	Empty sella syndrome
38.AC	Hydrocephalus	89.LM	Pseudotumor cerebri
39.JP	Craniopharyngioma	90.WS	Pseudotumor cerebri
40.EH	Hypophysectomy	91.JH	Pituitary adenoma
41.MK	Optic neuritis	92.ET	Suprasellar tumour
42.KR	Brainstem astrocytoma	93.MB	Migraine
43.JA	Pseudotumor cerebri	94.EB	Hydrocephalus
44.TI	Hypothalamic astrocytoma	95.BD	Headache
45.JM	Suprasellar hemangioma	96.VM	Post-traumatic optic atrophy
46.KM	Pituitary adenoma	97.EM	Pseudotumor cerebri
47.IM	Craniopharyngioma	98.ED	Multiple sclerosis
48.CM	Chiasmal glioma		
49.MC	Migraine		

Table 9: Test durations (in seconds) of CAMEC 26-Point screening test in neuro-ophthalmology.

	Mean	St.Dev.	Minimum	Maximum
Unilateral Test:				
Normal (n=5)	514	132	450	750
Abnormal (n=22)	785	218	494	1310
Bilateral Test:				
Both Normal (n=22)	711	97	588	951
One Abnormal (n=13)	778	155	584	1153
Both Abnormal (n=36)	1210	391	638	2126

Table 10: The retinal sensitivity levels in terms of Humphrey decibel units above and below which approximately 70 % of the 'seen' and 'missed' CAMEC responses were given for each dark stimulus contrast and size at different eccentricities in 25 glaucomatous central visual fields.

Eccentricity & Stimulus Area	Stimulus Contrast (Weber's)	Contrast		Below which		Average
		Above which 70% of 'seen'	(n)	70% of 'missed'	(n)	
6 Degrees (2 sq mm)	-10 %	28.7 dB	(n=18)	29.5 dB	(n=14)	29.1 dB
	-22 %	27.8 dB	(n=74)	26.7 dB	(n=26)	27.3 dB
	-37 %	27.5 dB	(n=46)	26.3 dB	(n=6)	26.9 dB
	-76 %	27.0 dB	(n=89)	26.0 dB	(n=11)	26.5 dB
12 Degrees (3 sq mm)	-10 %	27.3 dB	(n=34)	27.7 dB	(n=38)	27.5 dB
	-22 %	26.4 dB	(n=114)	26.6 dB	(n=86)	26.5 dB
	-37 %	26.0 dB	(n=88)	24.5 dB	(n=24)	25.3 dB
	-76 %	24.8 dB	(n=161)	24.0 dB	(n=39)	24.4 dB
18 Degrees (3 sq mm)	-10 %	25.8 dB	(n=60)	26.7 dB	(n=110)	26.3 dB
	-22 %	24.5 dB	(n=255)	24.2 dB	(n=216)	24.4 dB
	-37 %	23.9 dB	(n=185)	23.7 dB	(n=80)	23.8 dB
	-76 %	23.2 dB	(n=325)	23.3 dB	(n=130)	23.3 dB
24 Degrees (5 sq mm)	-10 %	23.7 dB	(n=50)	25.5 dB	(n=130)	24.6 dB
	-22 %	22.8 dB	(n=237)	23.8 dB	(n=263)	23.3 dB
	-37 %	22.5 dB	(n=192)	23.2 dB	(n=88)	22.8 dB
	-76 %	21.6 dB	(n=355)	20.5 dB	(n=125)	21.1 dB
30 Degrees (5 sq mm)	-10 %	23.5 dB	(n=27)	24.5 dB	(n=117)	24.0 dB
	-22 %	22.0 dB	(n=133)	22.5 dB	(n=251)	22.3 dB
	-37 %	21.0 dB	(n=143)	22.0 dB	(n=97)	21.5 dB
	-76 %	20.4 dB	(n=223)	20.5 dB	(n=145)	20.5 dB

Table 11: The retinal sensitivity levels (Humphrey dB) above and below which 70% of the 'seen' and 'missed' responses were recorded for low (-22%) and high (-76%) contrast dark stimuli in 10 glaucomatous visual fields. (Background Luminance= 100 cd/2)

Eccentricity & Stimulus Area	Stimulus Contrast (Weber's)	Above which		Below which	
		70% of 'seen'	70% of 'missed'	70% of 'seen'	70% of 'missed'
6 Degrees (2 sq mm)	-22 %	27.6 dB (n=21)	28.5 dB (n=19)	28.1 dB	28.1 dB
	-76 %	26.1 dB (n=38)	26.1 dB (n=2)	26.1 dB	26.1 dB
12 Degrees (3 sq mm)	-22 %	27.6 dB (n=30)	27.1 dB (n=50)	27.4 dB	27.4 dB
	-76 %	25.6 dB (n=62)	24.0 dB (n=18)	24.8 dB	24.8 dB
18 Degrees (3 sq mm)	-22 %	25.0 dB (n=75)	25.3 dB (n=115)	25.2 dB	25.2 dB
	-76 %	22.8 dB (n=151)	23.6 dB (n=39)	23.2 dB	23.2 dB
24 Degrees (5 sq mm)	-22 %	25.1 dB (n=80)	24.1 dB (n=120)	24.6 dB	24.6 dB
	-76 %	19.2 dB (n=161)	23.2 dB (n=39)	21.4 dB	21.4 dB
30 Degrees (5 sq mm)	-22 %	21.9 dB (n=52)	23.2 dB (n=92)	22.6 dB	22.6 dB
	-76 %	20.5 dB (n=100)	19.5 dB (n=44)	22.3 dB	22.3 dB

Table 12: Offset thresholds at various visual acuity levels (Mean & St.Dev. in dB).

Stimulus Size = 4 mm² (Goldmann III)

Eccentricity	Snellen Acuity			
	<u>6/6</u>	<u>6/12</u>	<u>6/24</u>	<u>6/60</u>
6°	21.8±1.8	21.4±1.7	20.4±2.4	19.2±2.3
12°	21.4±1.7	21.0±2.0	20.8±1.8	18.0±2.9
18°	21.2±1.1	20.4±3.0	18.2±2.4	15.8±3.4
24°	19.4±1.7	17.0±1.0	17.2±1.6	14.0±2.2
30°	16.8±0.4	16.4±1.5	16.0±2.4	14.4±1.5

Stimulus Size = 16 mm² (Goldmann IV)

Eccentricity	Snellen Acuity			
	<u>6/6</u>	<u>6/12</u>	<u>6/24</u>	<u>6/60</u>
6°	23.0±0.0	23.0±0.0	23.0±0.0	22.8±0.5
12°	23.0±0.0	22.2±1.1	22.6±0.9	21.4±1.7
18°	22.0±1.8	22.2±1.8	21.2±2.5	20.6±2.5
24°	21.0±2.0	21.8±1.8	20.8±2.3	20.6±1.7
30°	19.8±2.2	20.4±2.0	19.8±2.3	19.0±2.1

Table 13: Offset stimulus spatial summation coefficient (k) values at and beyond 18 degrees eccentricity at various visual acuity levels (*: k not calculated).

Eccentricity	Snellen Acuity			
	<u>6/6</u>	<u>6/12</u>	<u>6/24</u>	<u>6/60</u>
6°	*	*	*	k=0.30
12°	*	*	*	k=0.28
18°	k=0.07	k=0.13	k=0.25	k=0.4
24°	k=0.13	k=0.40	k=0.18	k=0.55
30°	k=0.25	k=0.33	k=0.32	k=0.38

Table 14: The average results (Mean & Standard Deviation) from the eyes included in the study (POAG=Primary Open Angle Glaucoma, OHT=Ocular Hypertension).

	<u>POAG</u>	<u>OHT</u>	<u>Control</u>
IOP (highest;mmHg)	27.8±5.3 (range 19-36)	27.6±3.1 (range 22-32)	15.6±1.9 (range 13-19)
C/D	0.58±0.14 (range 0.4-0.8)	0.49±0.20 (range 0.2-0.8)	0.42±0.05 (range 0.3-0.5)
Family History	(+):14,(-):7	(+):10,(-):11	(+):0,(-):13
RDVFL	0.80±0.25 (range 0.23-0.99)	0.61±0.37 (range 0.04-0.99)	0.08±0.05 (range 0.02-0.19)
MS _{on} (dB)	26.2±3.3 (range 18.3-30.1)	30.8±1.3 (range 27.4-32.9)	30.7±1.3 (range 28.5-33.0)
MS _{off} (dB)	16.8±2.8 (range 10.0-21.0)	19.8±1.5 (range 17.1-21.9)	20.8±0.7 (range 19.6-21.8)
MD _{on} (dB)	4.3±3.2 (range +0.8_ ₋ +12.5)	0.06±1.19 (range -2.2_ ₋ +2.3)	0.05±0.9 (range -1.35_ ₋ +1.6)
LV _{on} (dB)	35.2±37.3 (range 7.8-136.0)	2.8±1.8 (range 0.5-7.4)	2.8±1.2 (range 0.7-5.2)
MD _{off} (dB)	3.8±2.4 (range -0.1_ ₋ +10.8)	0.8±1.5 (range -1.2_ ₋ +0.3)	-0.2±0.6 (range -0.9_ ₋ +0.8)
LV _{off} (dB)	27.0±22.2 (range 2.0-70.6)	5.4±4.2 (range 1.0-14.4)	1.9±0.6 (range 1.0-2.9)

Table 15: Abnormal test result rate with light onsets and offsets in the glaucoma, OHT and control groups.

	<u>MD_{on}</u>	<u>LV_{on}</u>	<u>MD_{off}</u>	<u>LV_{off}</u>
95% P.L.	0.46 dB	3.15 dB	0.36 dB	2.37 dB
CONTROL	23% (3/13)	23% (3/13)	23% (3/13)	23% (3/13)
OHT	33% (7/21)	33% (7/21)	48% (10/21)	67% (14/21)
GLAUCOMA	100% (21/21)	100% (21/21)	91% (19/21)	95% (20/21)
98% P.L.	0.59 dB	3.22 dB	0.41 dB	2.44 dB
CONTROL	15% (2/13)	15% (2/13)	15% (2/13)	15% (2/13)
OHT	33% (7/21)	33% (7/21)	43% (9/21)	67% (14/21)
GLAUCOMA	100% (21/21)	100% (21/21)	91% (19/21)	91% (19/21)
99.9% P.L.	1.56 dB	5.23 dB	0.83 dB	2.92 dB
CONTROL	0% (0/13)	0% (0/13)	0% (0/13)	0% (0/13)
OHT	5% (1/21)	14% (3/21)	43% (9/21)	62% (13/21)
GLAUCOMA	86% (18/21)	100% (21/21)	86% (18/21)	91% (19/21)

Table 16: The test durations and total number of stimulus presentations with the light onset stimuli using bracketing technique, and with the light offset stimuli using ascending single crossing method. Short term fluctuation could not be calculated for the offsets because of lack of repeat thresholding at selected locations (ASC=Ascending Single Crossing; BT=Bracketing Technique; STF=Short Term Fluctuation).

	<u>POAG</u>	<u>OHT</u>	<u>CONTROL</u>
<u>Test Time (seconds)</u>			
BT	747±100 (range 600-943)	653±89 (range 516-915)	655±76 (range 520-870)
ASC	1249±358 (range 608-1890)	832±260 (range 392-1337)	683±133 (range 480-888)
<u>Number of Trials</u>			
BT	389±52 (range 319-501)	340±14 (range 315-365)	342±12 (range 316-359)
ASC	145±12 (range 69-231)	99±32 (range 56-159)	76±13 (range 58-96)
<u>STF (dB)</u>			
BT	1.7±0.8 (range 0.9-4.5)	1.4±0.4 (range 0.8-2.1)	1.3±0.3 (range 0.7-1.9)
ASC	N/A	N/A	N/A

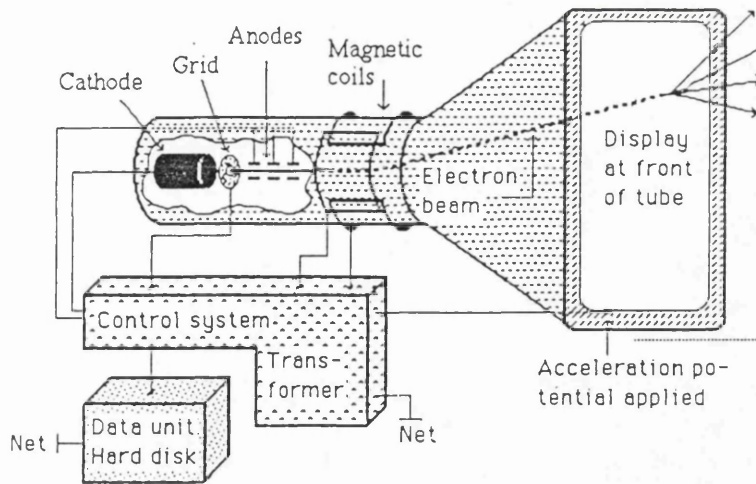


Figure 1: Schematic drawing of the principle of a CRT as utilised in video-display terminals (From: The Man-Machine Interface, Raufs JA,ed:., The MacMillan Press Ltd,1991).

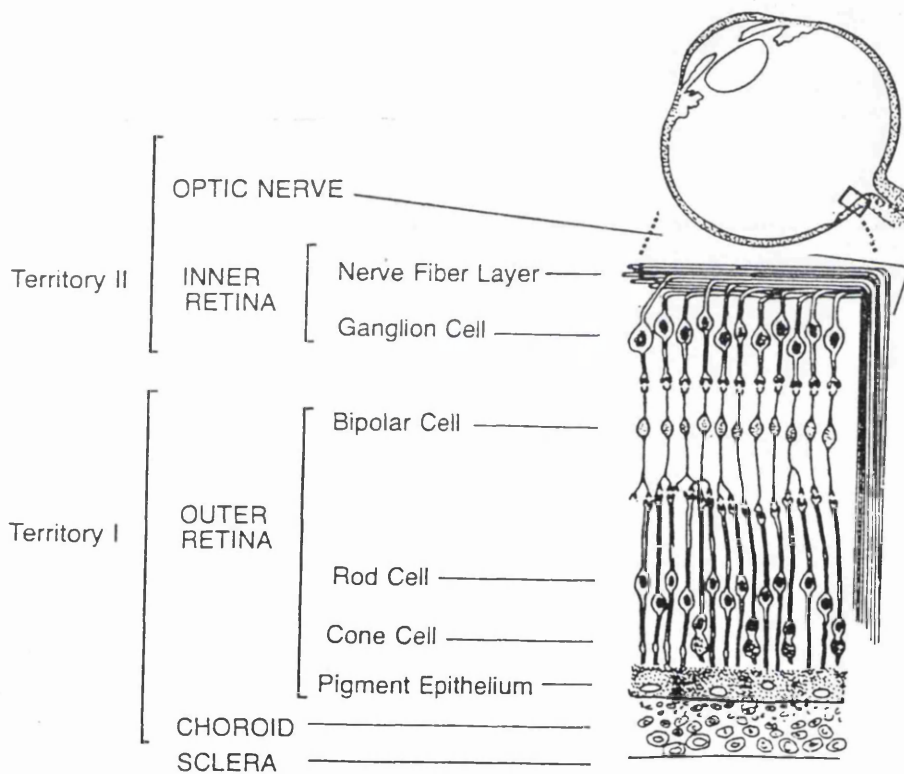


Figure 2: The retina transmits visual information into the optic nerve (From: The Visual Fields Manual, Trobe J.D., Glaser, J.S., Triad Publishing, 1983).

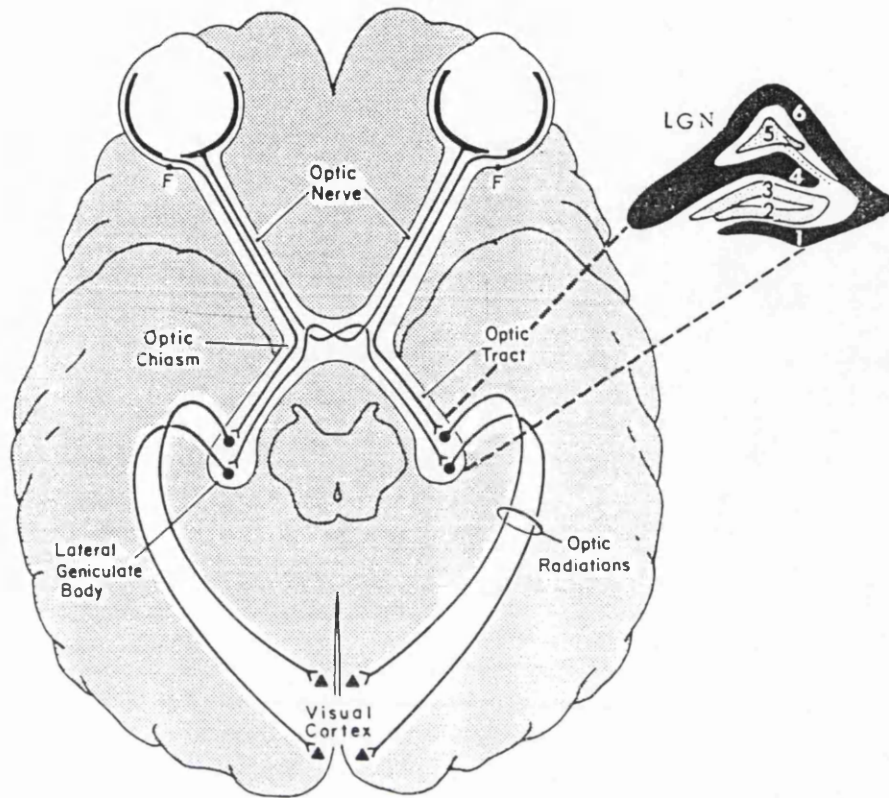


Figure 3: The retino-cortical neural visual pathway. LGN=Lateral Geniculate Nucleus (From: The Visual Fields Manual, Trobe J.D., Glaser, J.S., Triad Publishing, 1983).

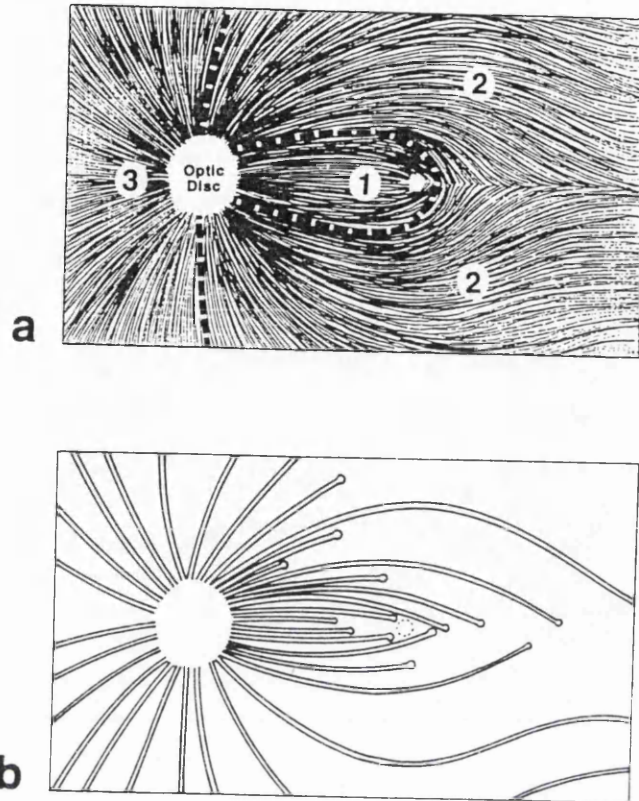


Figure 4: The organisation of the retinal nerve fiber layer.

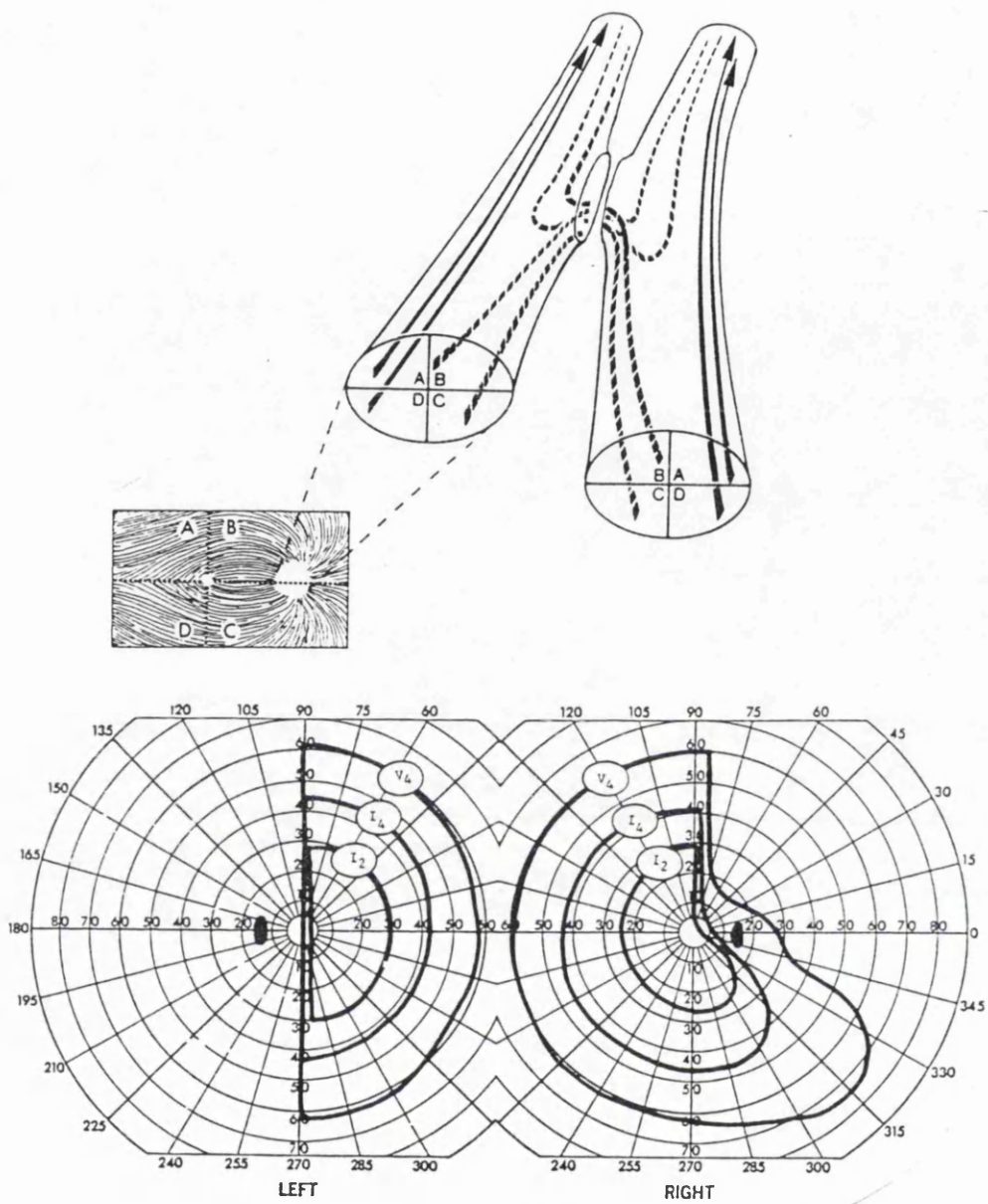


Figure 5: a. The optic chiasm, b. Hemianopic field loss in chiasmatic lesion (From: The Visual Fields Manual, Trobe J.D., Glaser, J.S., Triad Publishing, 1983).

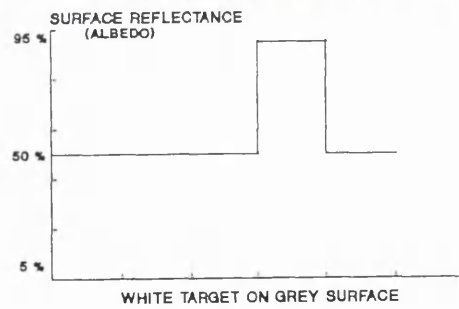
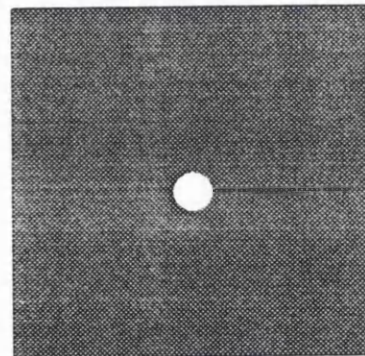
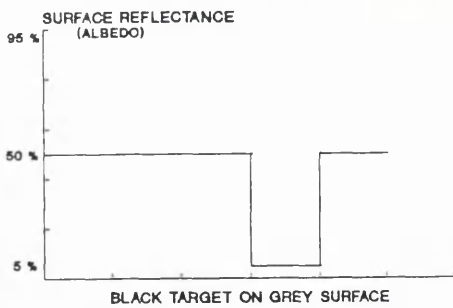
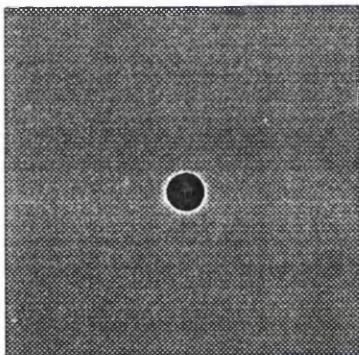
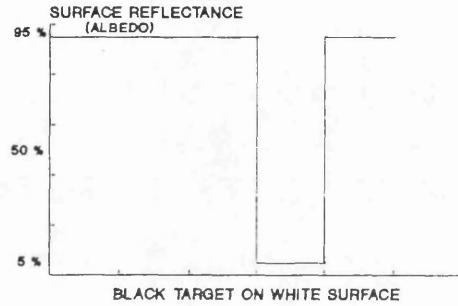
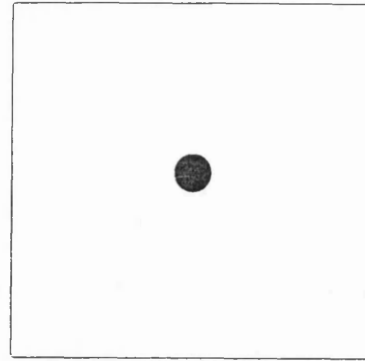
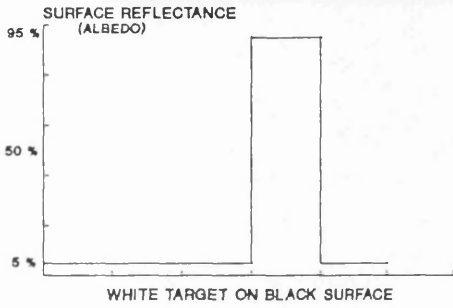
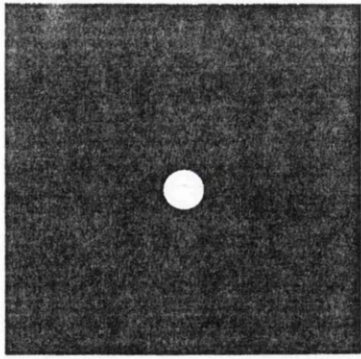
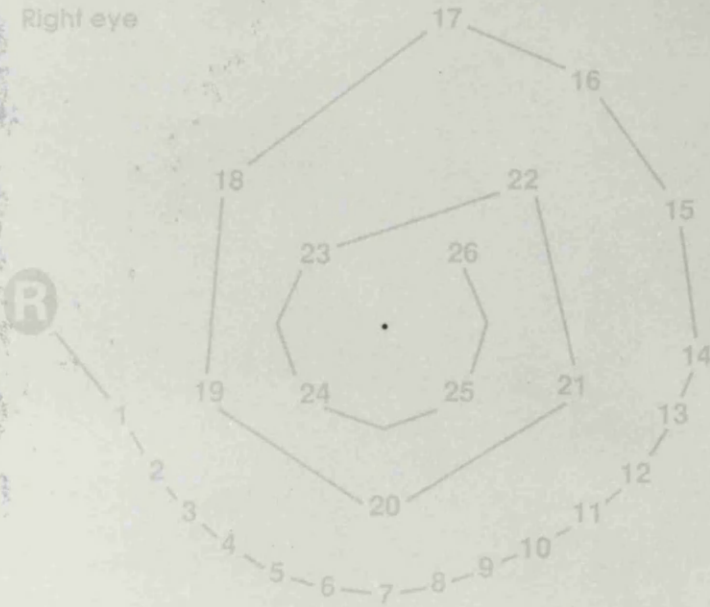


Figure 6: Luminance profiles of light increments (onsets) and decrements (offsets) introduced by black and white stimuli on opposite as well as grey backgrounds.

OKP GLAUCOMA SCREENING TEST

Glaucoma can cause peripheral blindness that begins in the periphery. The screening test may help you discover an abnormality in your peripheral vision which might be caused by the condition.

Right eye



INSTRUCTIONS

You will need a pen, a record sheet and a good light shining from above.



- 1 Fold the patch inwards and hold it over the closed left eye, using the left hand, as shown in the illustration.
- 2 Support the lower edge of the chart on a table or on your lap and with the right hand hold the chart upright. The black spot should be about 16 inches (40cm) directly in front of the right eye.
- 3 Proceed with the test only if the numbers are clearly seen.
- 4 Look at the letter R. If you are in the correct position the black spot should disappear into your normal blind spot.
- 5 Look at the number 1 for about one second. Without moving your eye away from the number, ask yourself whether the spot can be seen out of the corner of your eye. Remember to keep the eye very still when looking at the number and do not look directly at the spot.
- 6 Repeat this procedure with each number in turn from 1-26. When you have finished, confirm your results by performing the examination a second time.
- 7 If any numbers consistently make the spot disappear, cross out the corresponding numbers on the record sheet.

If any number repeatedly makes the spot disappear you are advised to have a full eye examination. Turn the chart over to test the left eye.

Figure 7: The Oculo-Kinetic Campimetry Chart.

Figure 8: A. Oculo-Kinetic Campimetry Chart A. B. OCU Chart A.

Chart A

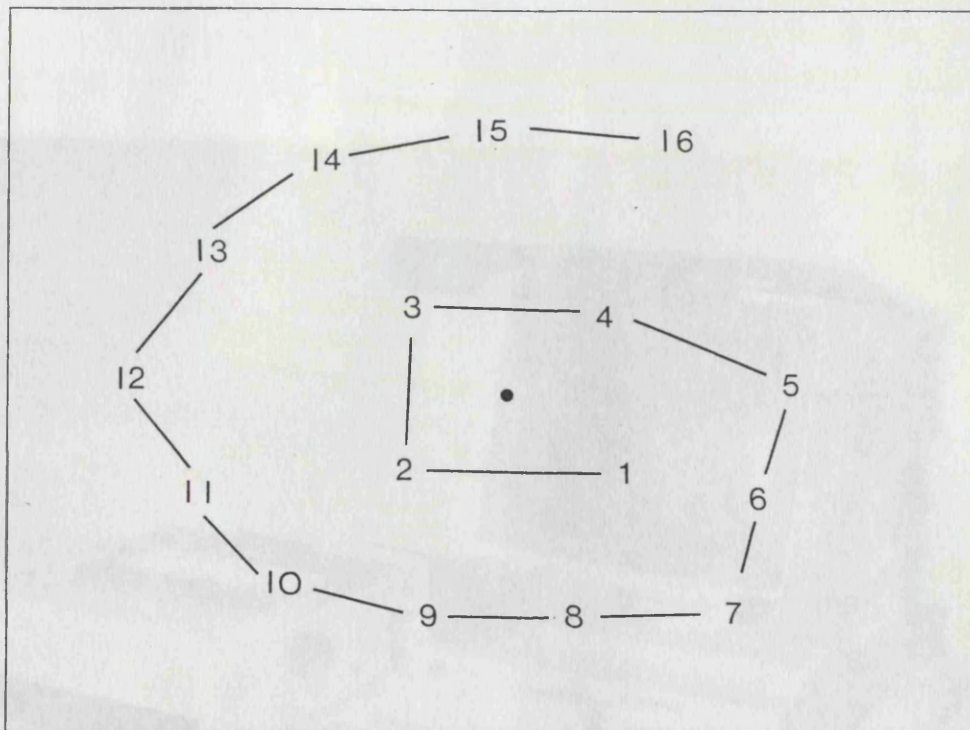


Chart B

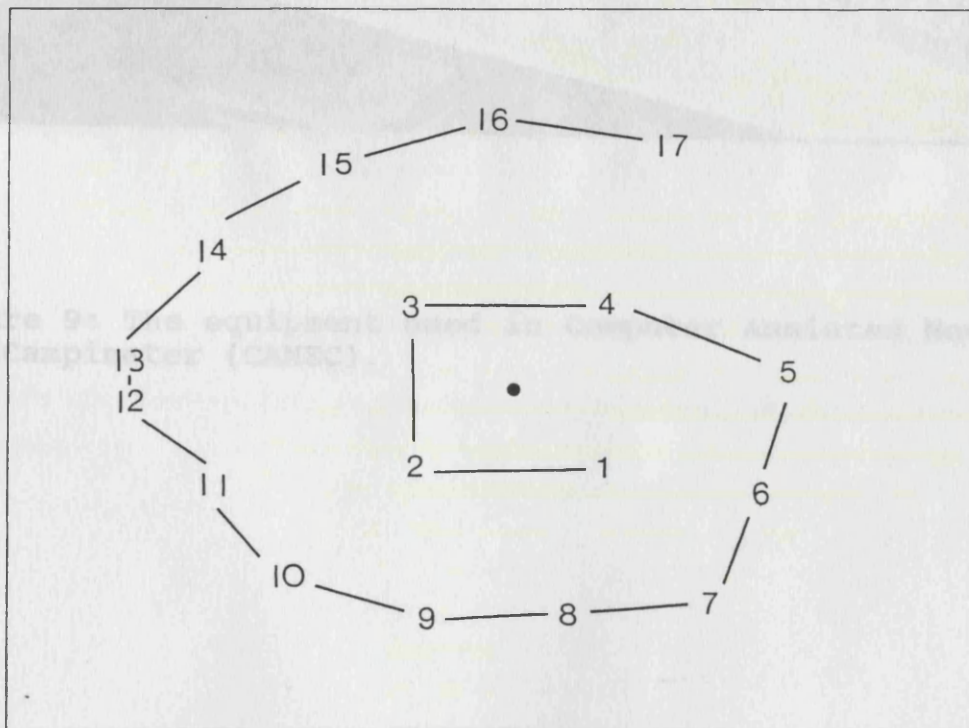


Figure 8: a. Oculo-Kinetic Campimetry Chart A; b. OKC Chart B.

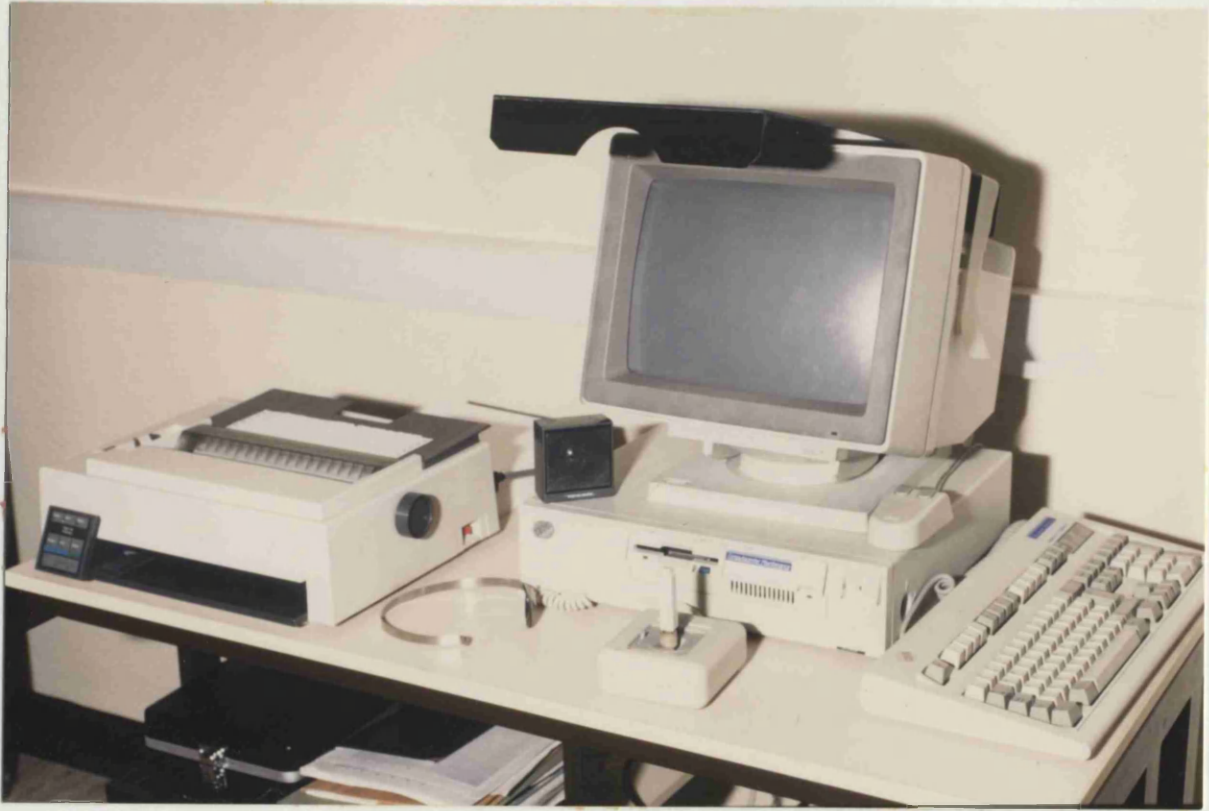


Figure 9: The equipment used in Computer Assisted Moving Eye Campimeter (CAMEC).

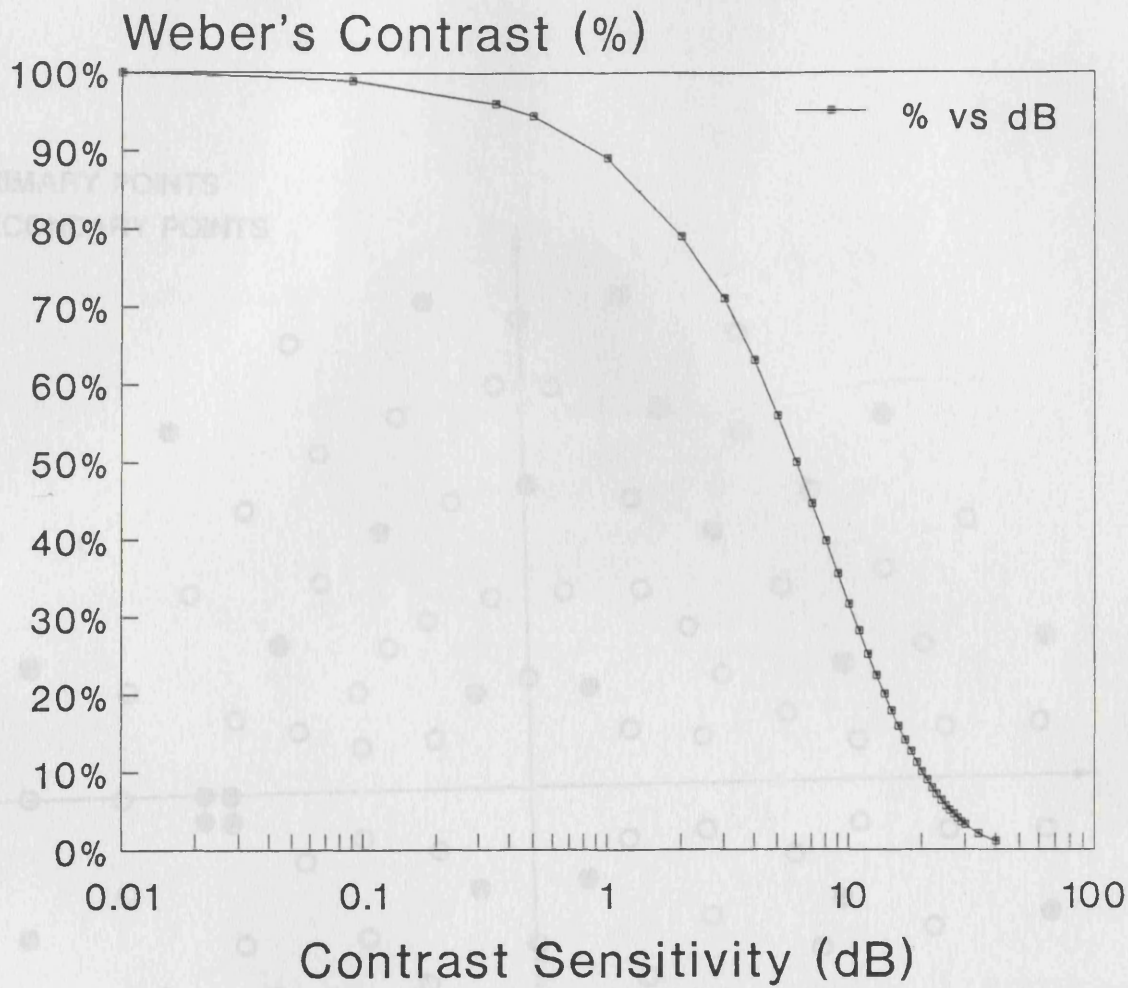


Figure 10: Conversion of percentage and decibel contrast values for stimuli.

Figure 11: The test grid for CMHC 25 Point Detecting Pattern (Filled circles: Primary test locations; Empty circles: Secondary test locations).

● PRIMARY POINTS
○ SECONDARY POINTS

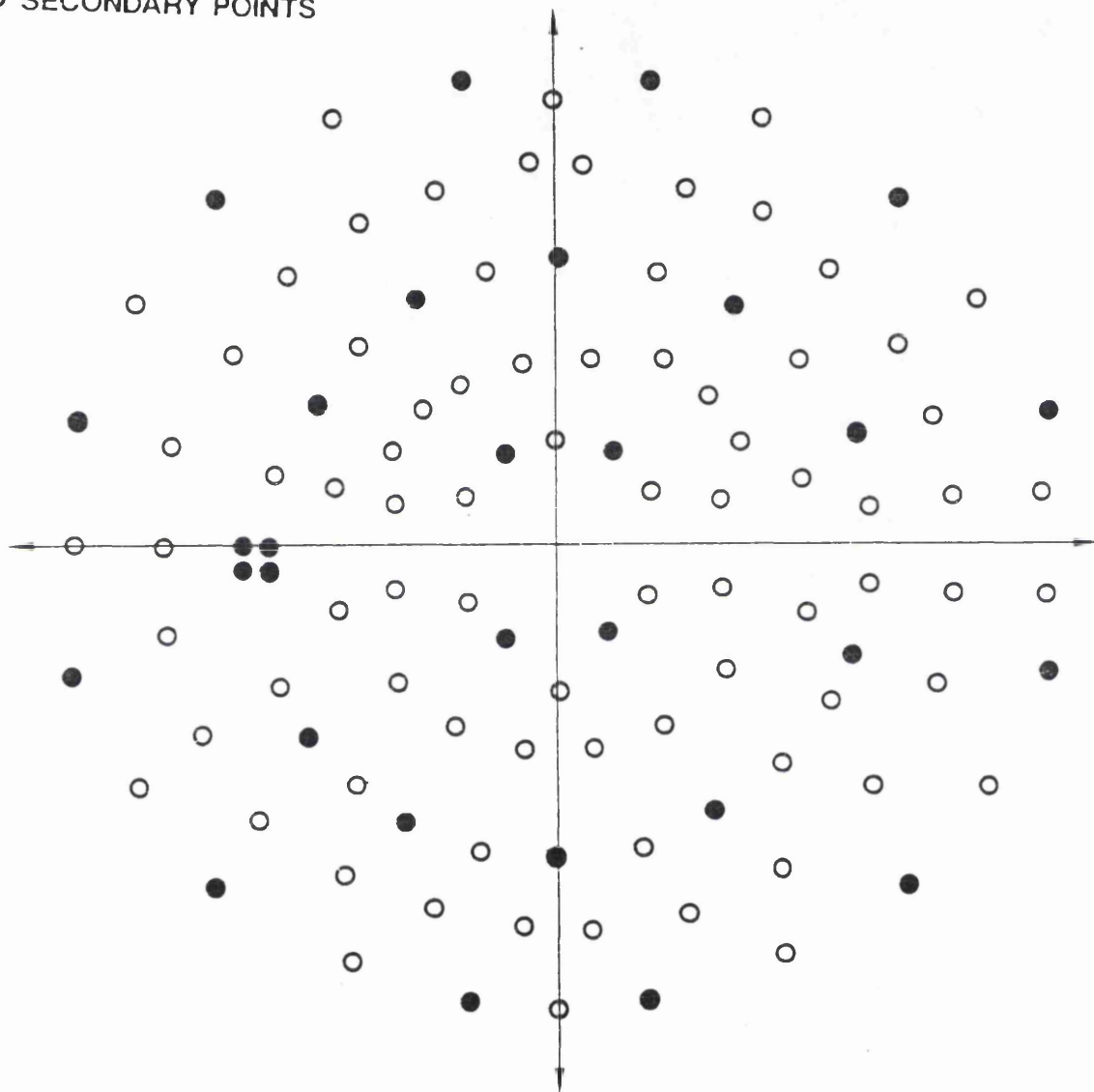


Figure 11: The test grid for CAMEC 26 Point Screening Program (Filled circles: Primary test locations; Empty circles: Secondary test locations).

Age Distribution of Children
Seen with CAMEC and DICON
(n = 32)

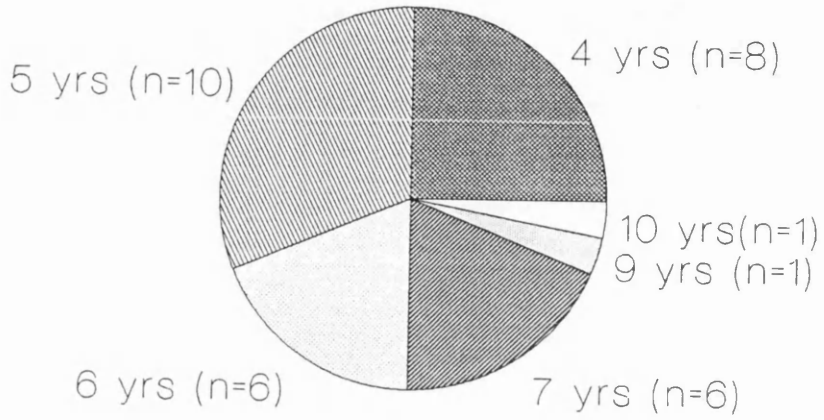


Figure 12: Age distribution of the children tested with CAMEC and Dicon Autoperimeter Blind Spot Test Programs.

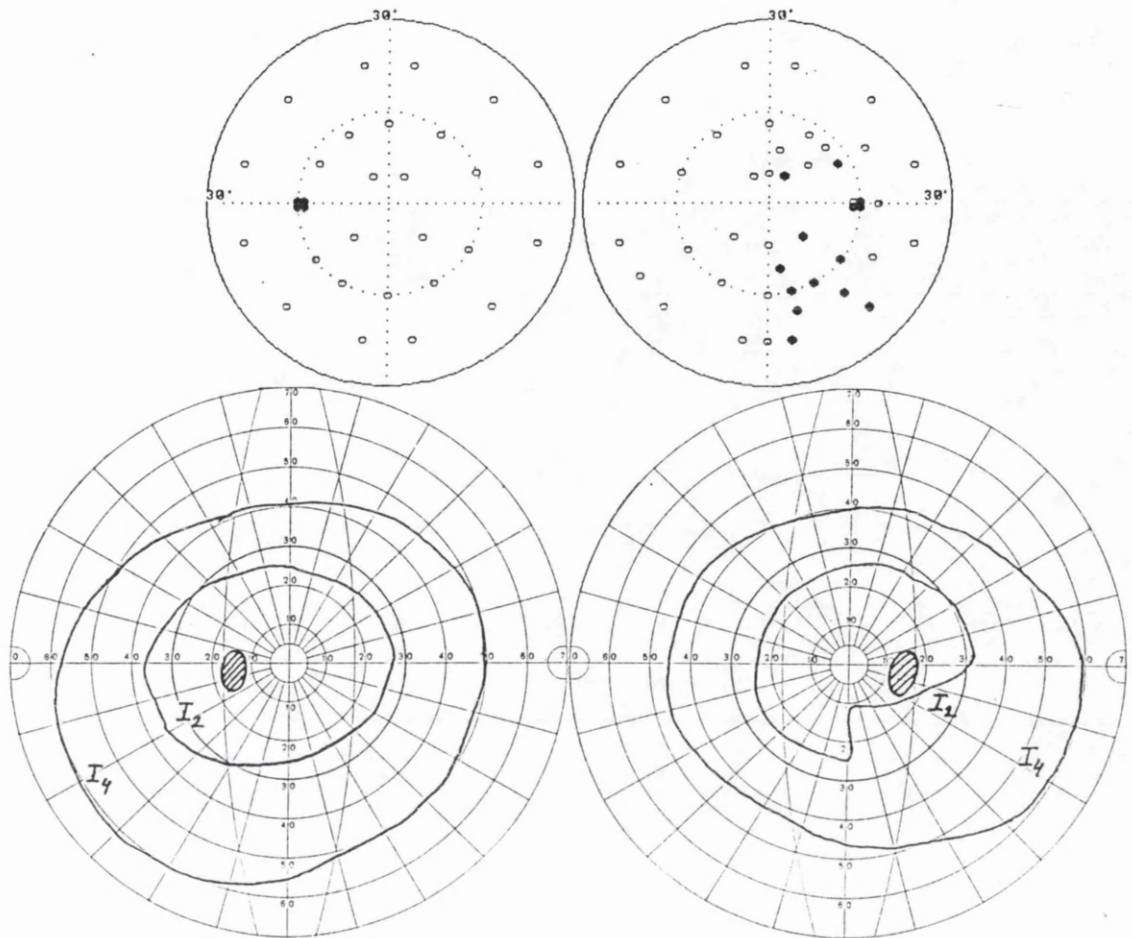


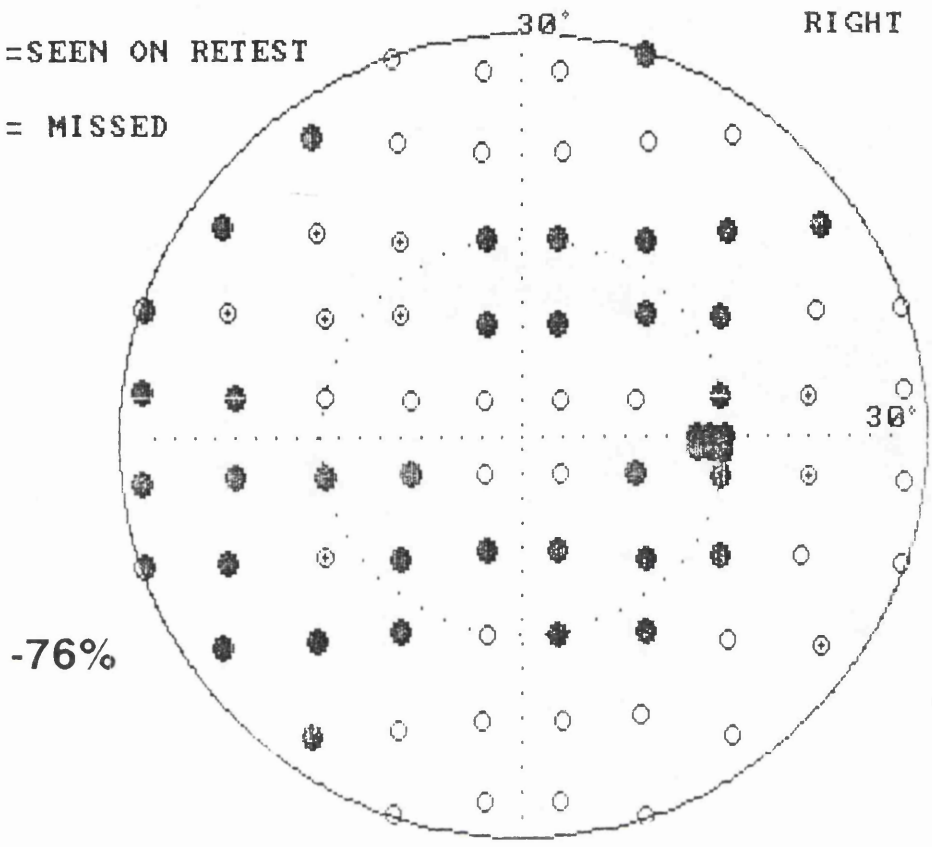
Figure 14: Primary test locations in the normal left visual field and secondary test locations added automatically in the abnormal right field of a 66 year old male with right optic atrophy secondary to craniopharyngioma. Field defect is represented with filled circles. The spatial resolution of the test grid is higher along the borders of detected scotoma due to the addition of the secondary stimuli. No secondary stimuli were used in the normal left eye.

CAMEC2 VISUAL FIELD PLOT MJ, M, 58 YRS

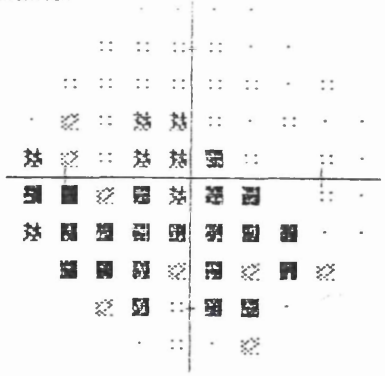
○ = SEEN

⊕ = SEEN ON RETEST

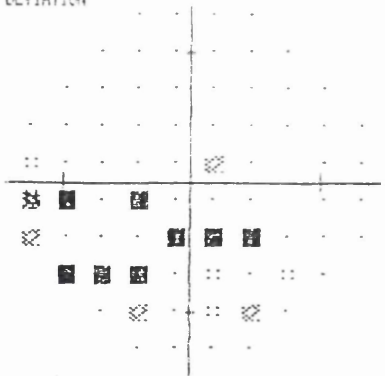
● = MISSED



TOTAL
DEVIATION

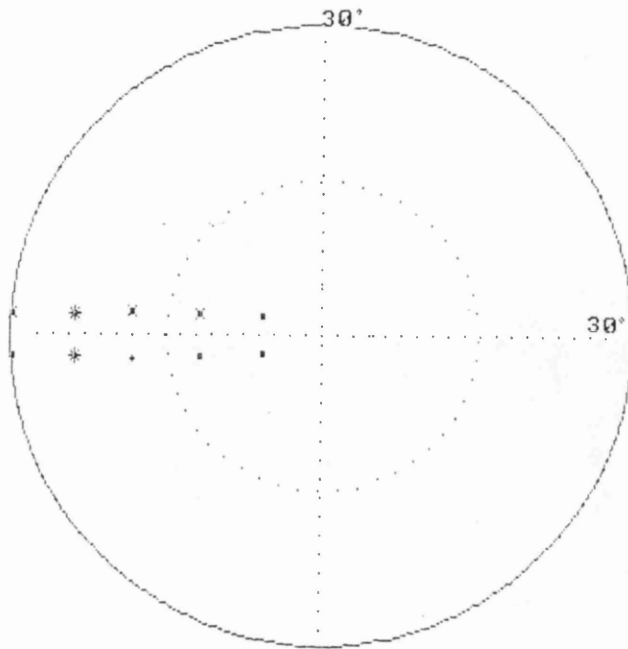


PATTERN
DEVIATION



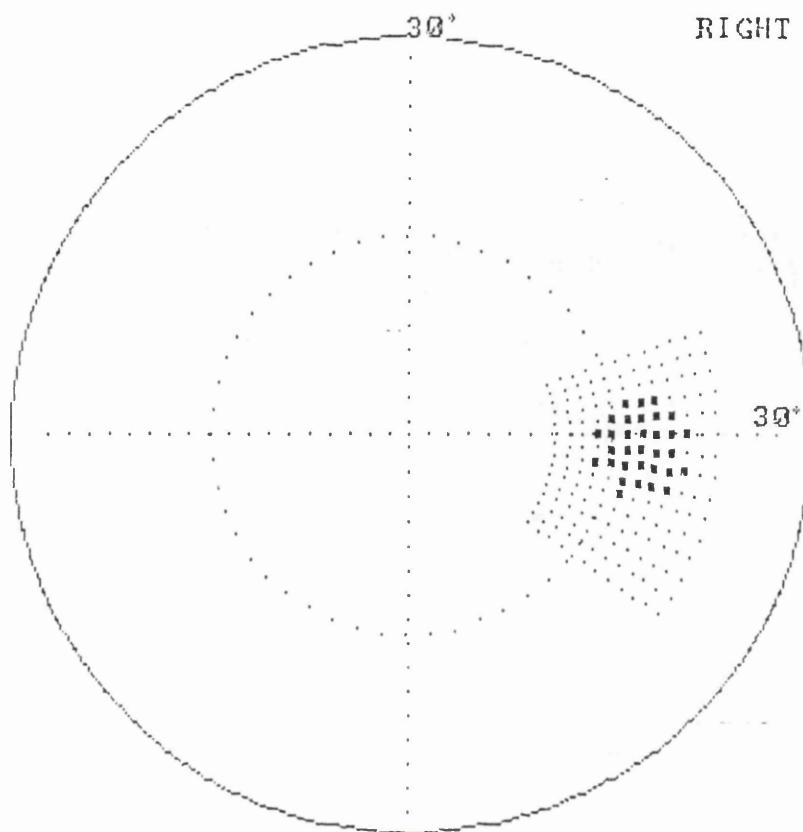
PROBABILITY SYMBOLS
 ○ P < 5%
 ⊕ P < 2%
 ● P < 1%
 ■ P < 0.5%

Figure 15: The stimulus locations of CAMEC 76 Point Screening Test, showing double arcuate scotomas in a glaucomatous eye tested with single intensity (-76%) offset stimuli.



KEY							
·	28 DB	·	22 DB	·	19 DB	·	17 DB
×	15 DB	*	13 DB	⊕	11 DB	⊗	9 DB
⊗	7 DB	⊕	5 DB	⊗	3 DB	⊗	< 3 DB

Figure 16: The offset stimuli test locations along the nasal horizontal meridian. The vertical and horizontal separation between the stimuli were 4 and 6 degrees respectively.



	LEFT	RIGHT	Stimulus Duration (s)
No. Seen	0	148	0.20 + 2.00
No. Missed	0	32	Test time (s)
False +ves	0	0	745
False -ves	0	5	

Figure 17: The blind spot test grid of CAMEC had one-degree resolution.

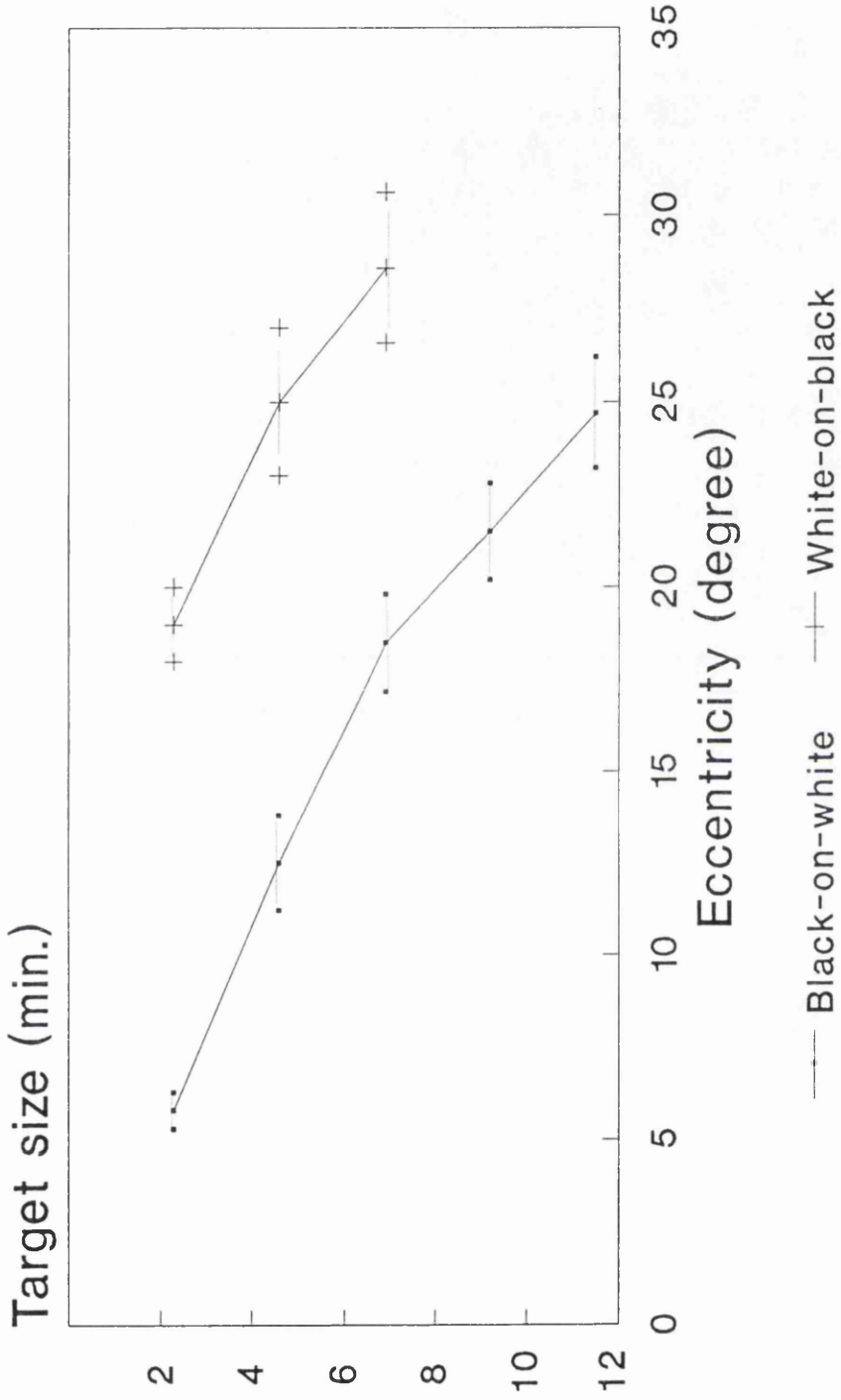


Figure 18: 'Hill of Vision' to black-on-white and white-on-black stimuli.

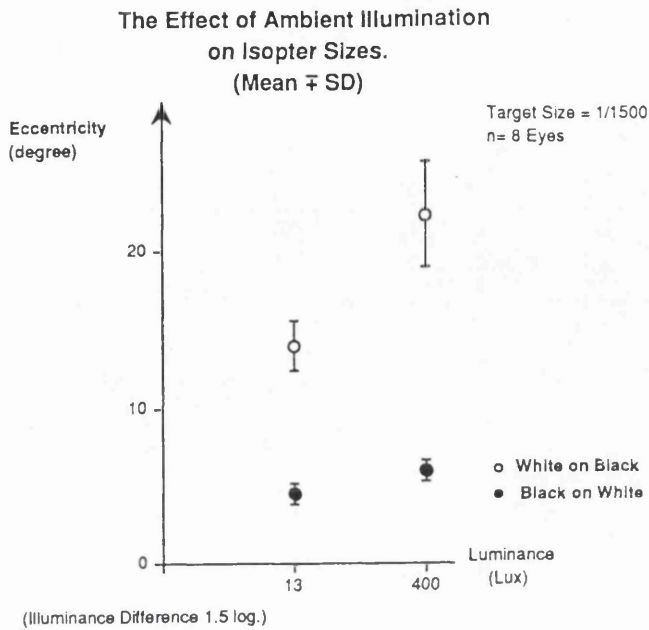


Figure 19: The effect of ambient illumination on black-on-white and white-on-black stimuli.

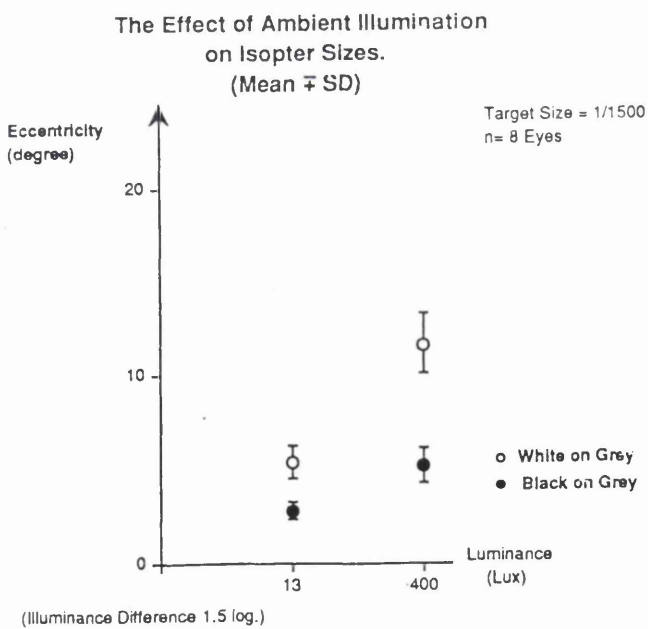


Figure 20: The effect of ambient illumination on black-on-grey and white-on-grey stimuli.

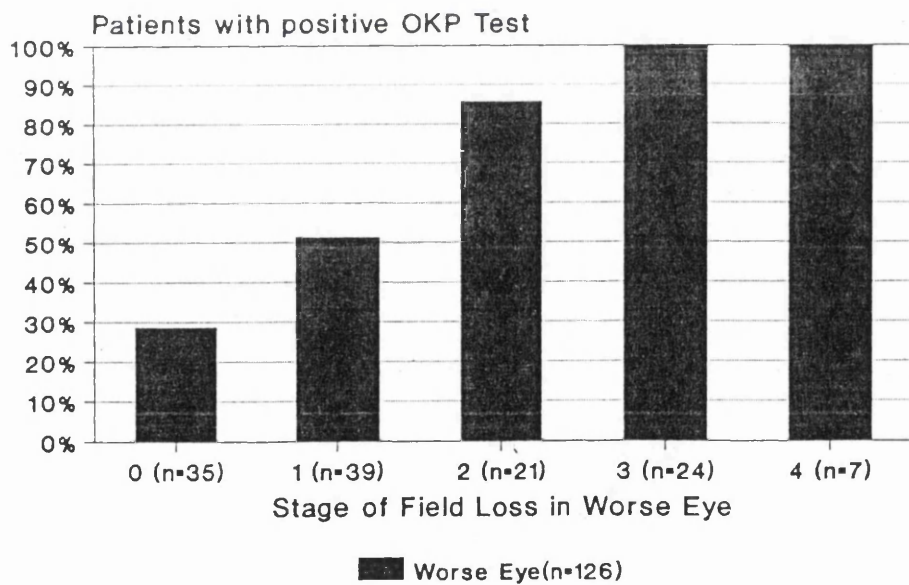
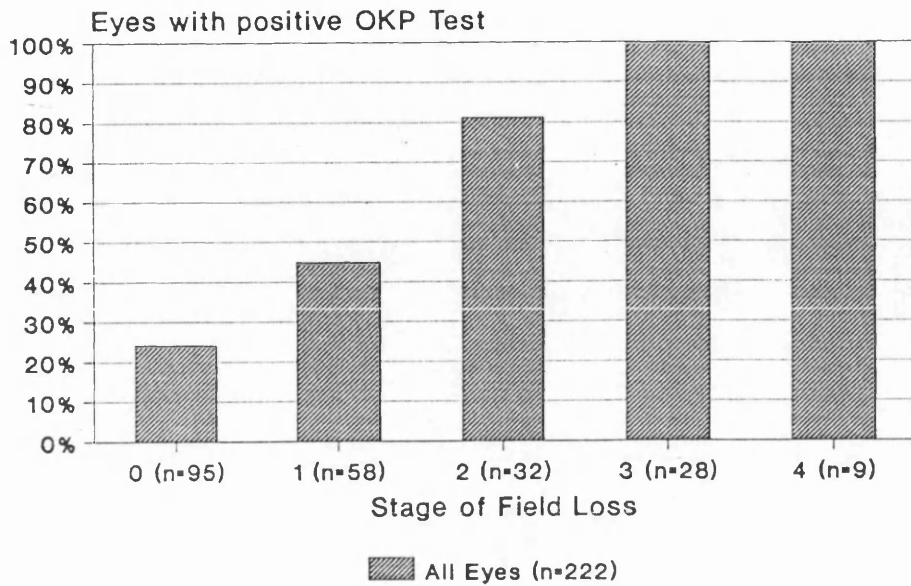


Figure 21: OKC positive result rate according to the stage of glaucomatous visual field loss in all eyes (top) and worse eye of each patient (bottom).

Controls

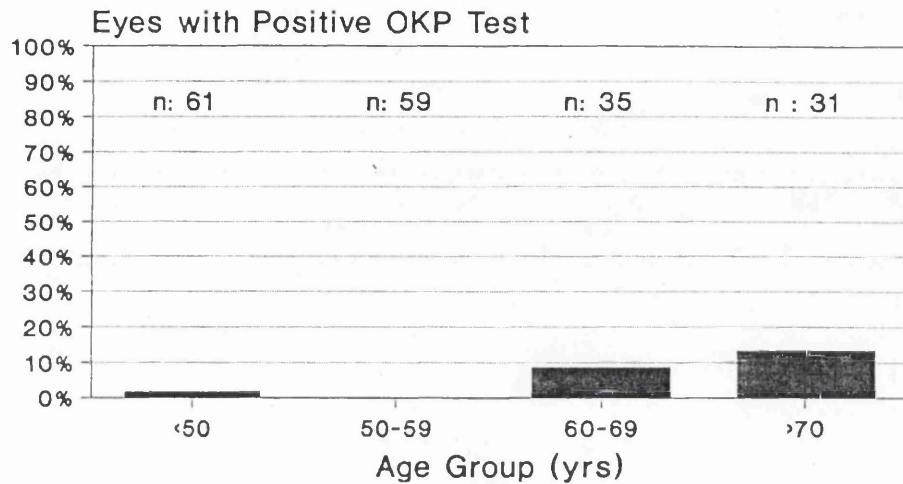


Figure 22: OKC positive result rate according to the age of control cases.

Suspects

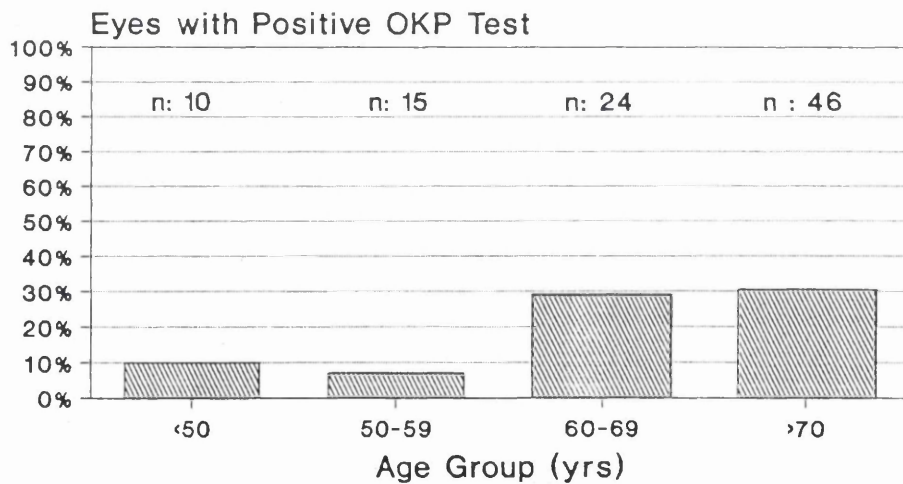


Figure 23: OKC abnormality in glaucoma suspect eyes of various age groups.

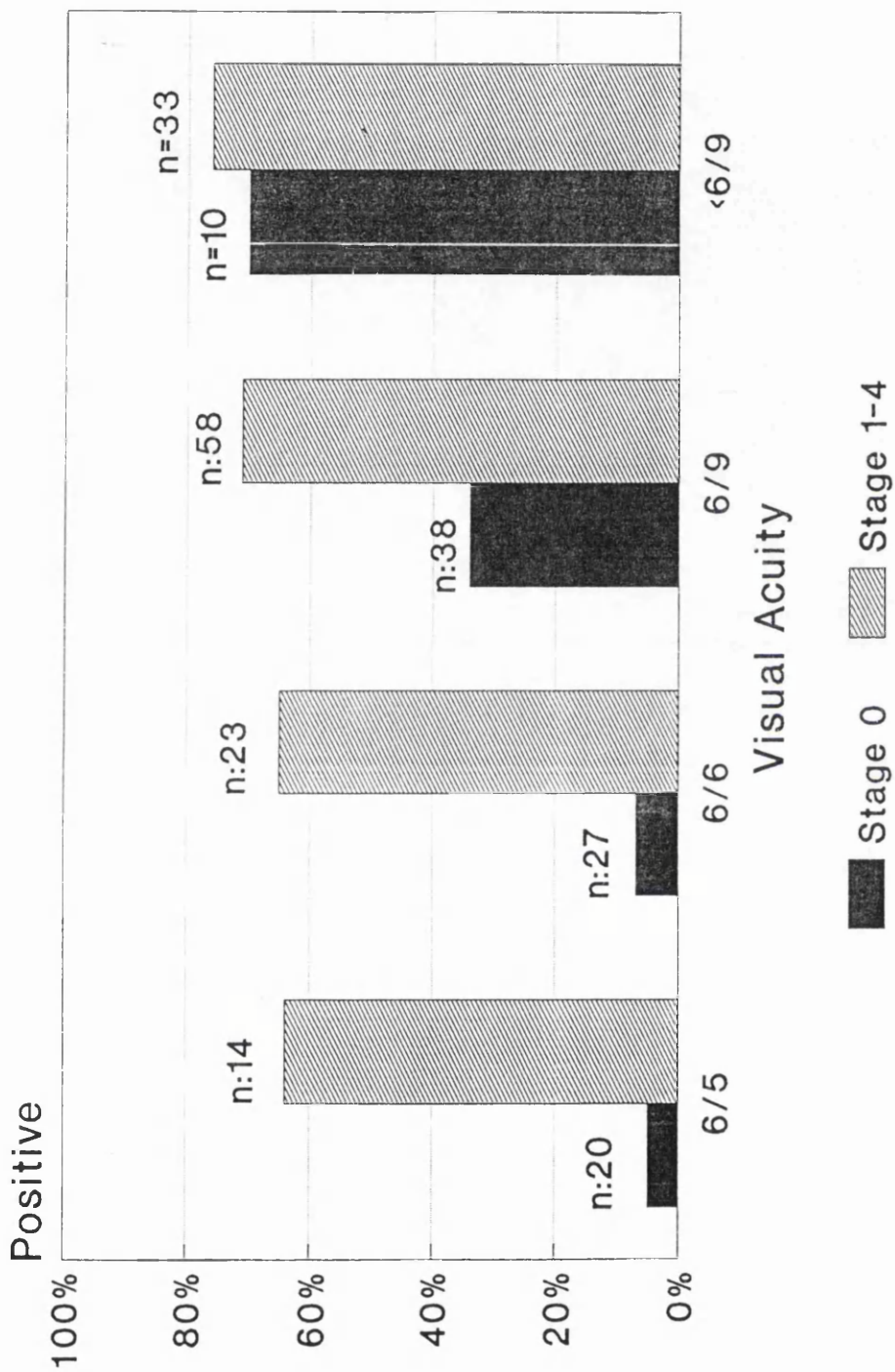


Figure 24: Positive OKC result rate according to the level of visual acuity.

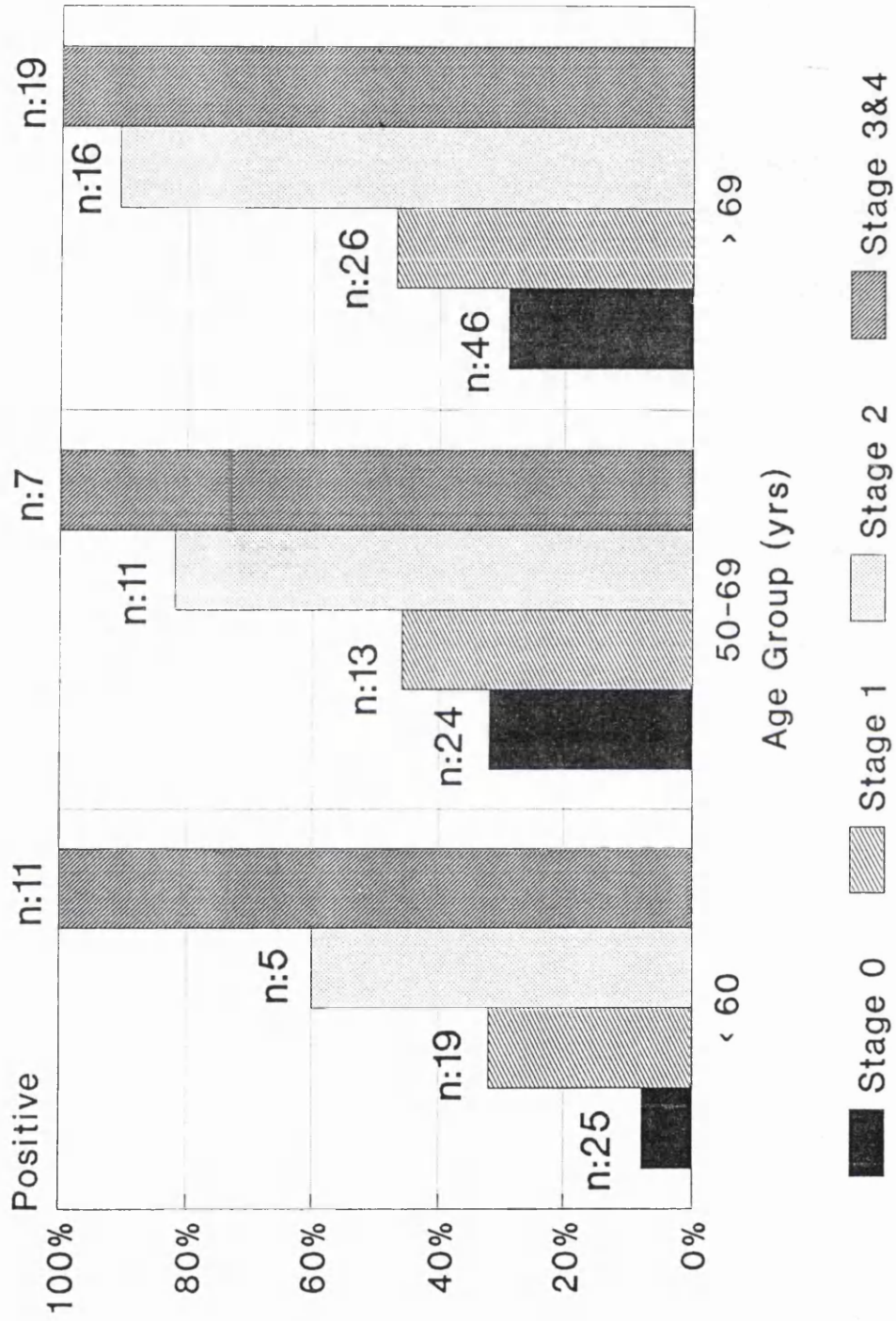


Figure 25: OKC results in different age groups.

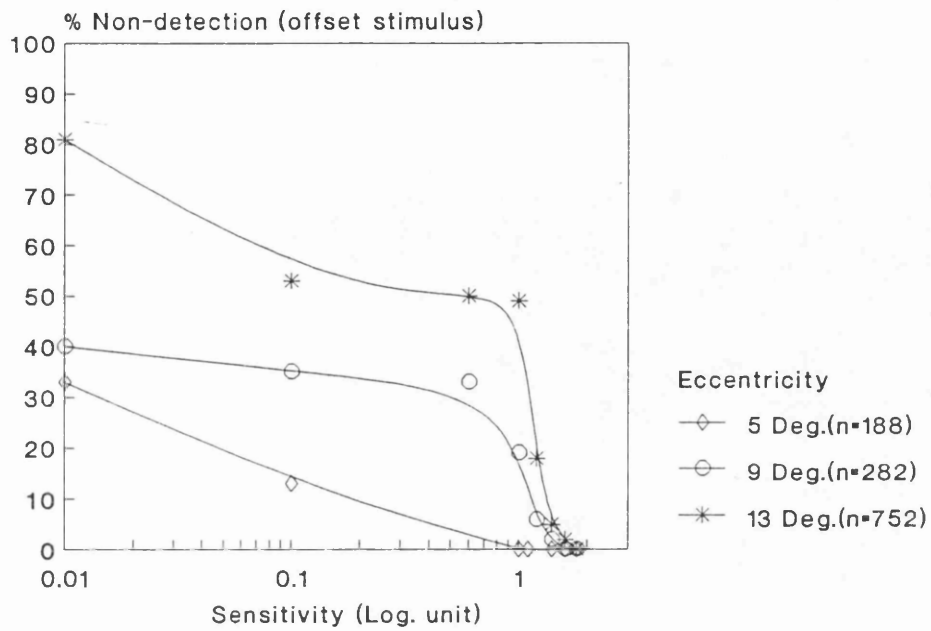
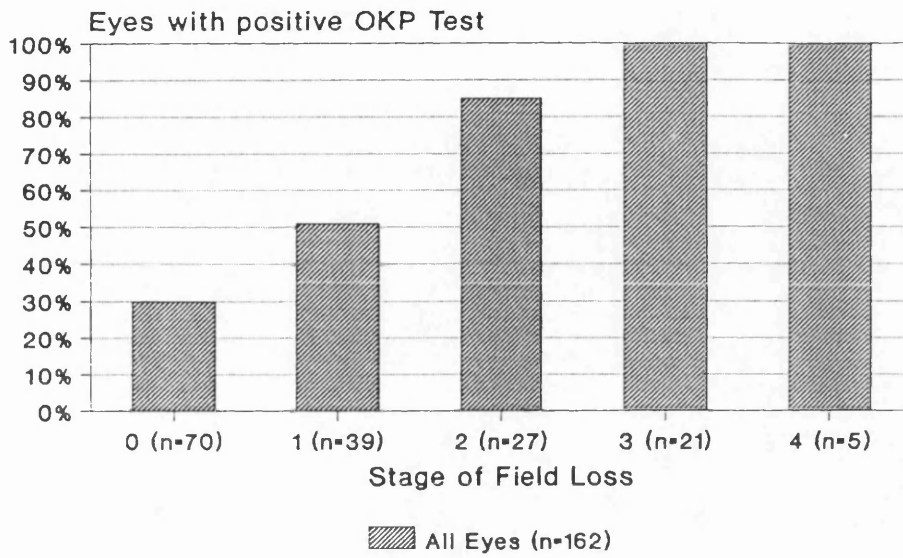


Figure 26: Equivalent Friedman Analyser light sensitivity required for 50% detection of 1.5 mm diameter offset (black-on-white) stimulus of OKC.

1.5 mm Stimulus
Above Age 60



3 mm Stimulus
Above Age 60

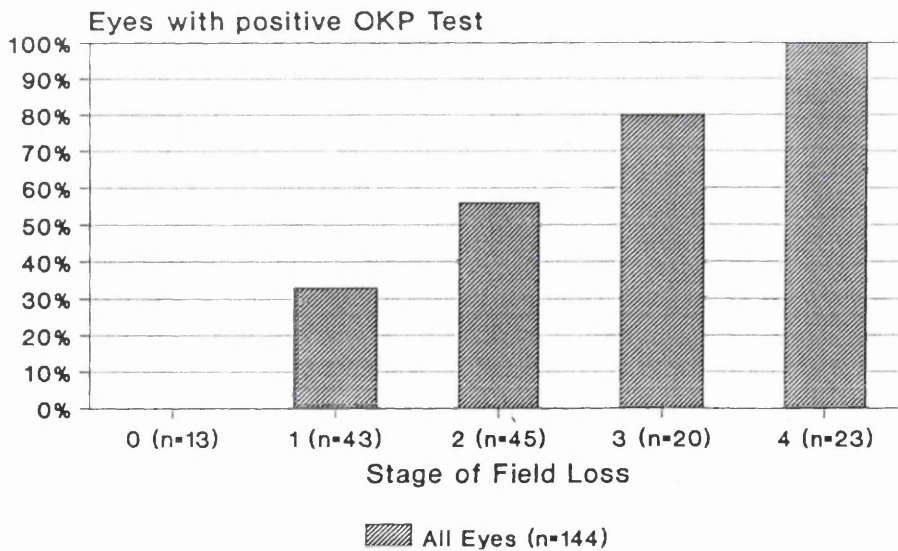


Figure 27: OKC results above the age of 60 years, using 1.5 mm (top) and 3.0 mm (bottom) black-on-white stimulus.

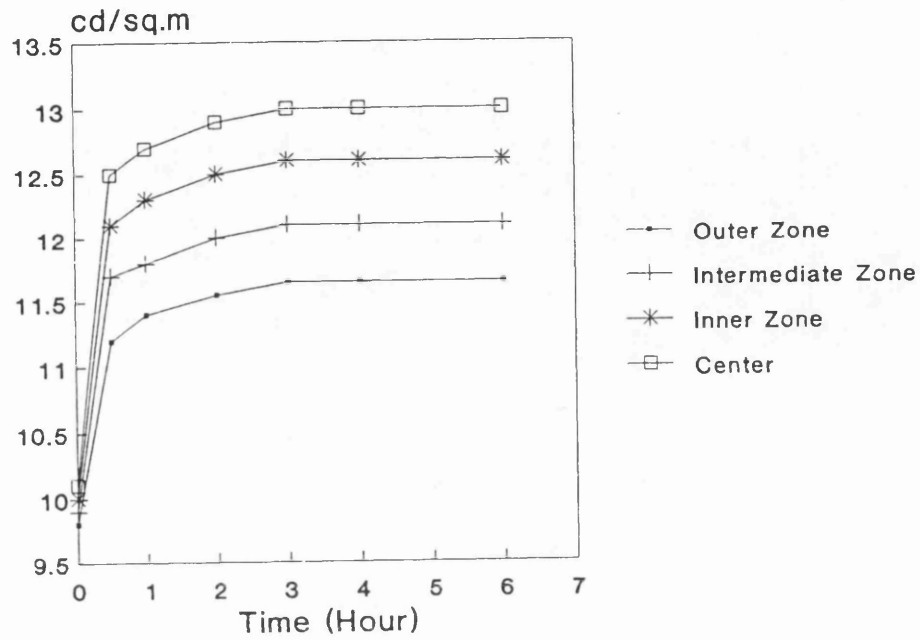


Figure 28: The average luminance of the concentric zones on CRT surface against time (in hours).

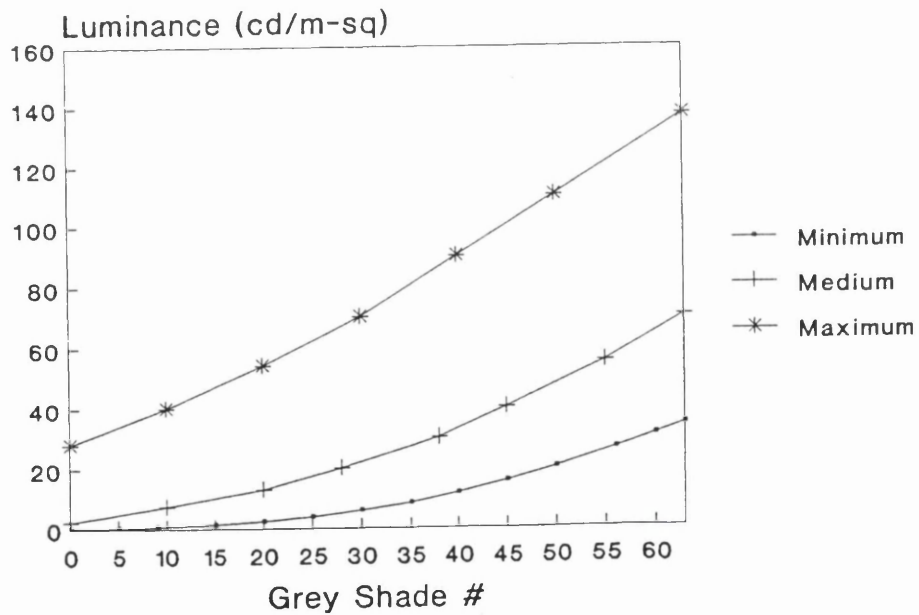


Figure 29: The effect of various (ie, minimum, medium, maximum) screen 'Brightness' setting on the luminosity of 64 shades of grey.

Figure 30: Top: The average luminance of 64 shades of grey as uniform screen background. Bottom: The average luminance obtained with small grey patches (shades 1-40) as foreground on 10 cd/m² background.

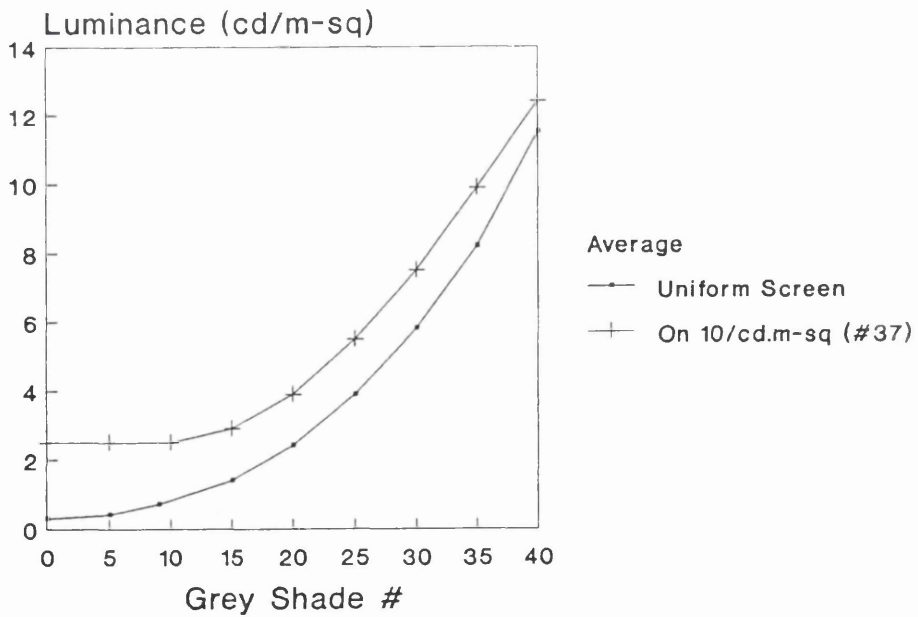
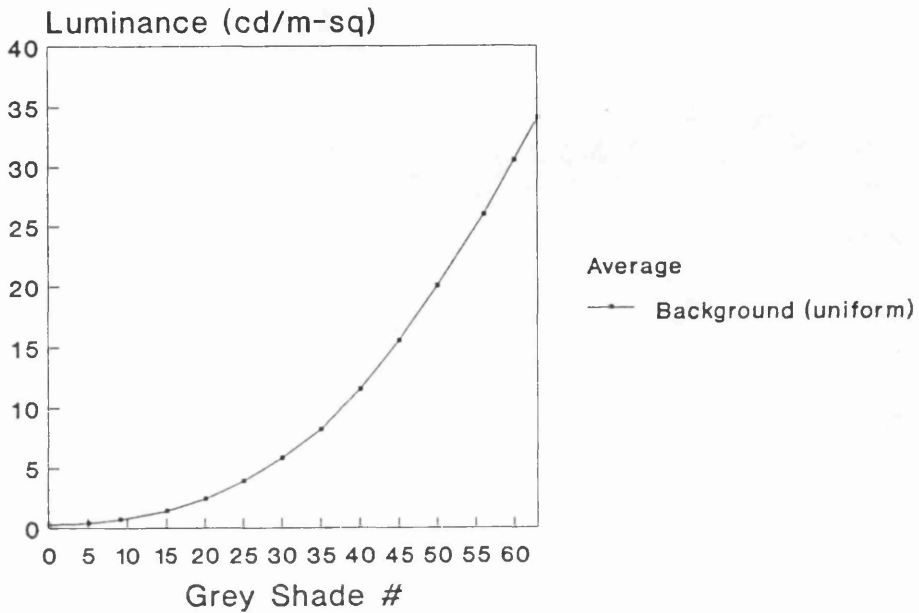
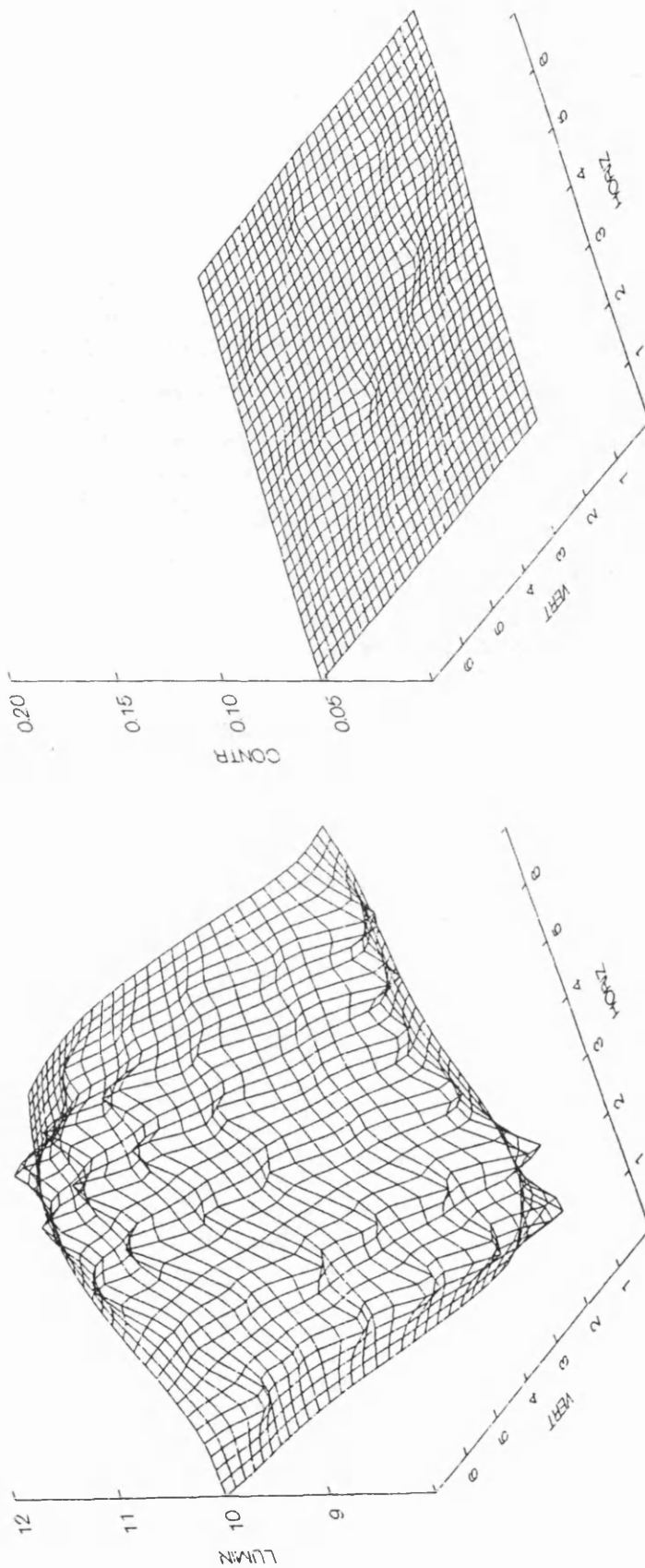


Figure 31: The variation in CRT screen luminance at 36 locations (6x6) on the monitor used for tests (left). The topographical non-uniformity of the background applies equally to the stimulus intensity and provides stability to the stimulus contrast (right).



Fixation Quality
Percentage Stimuli Missed in Blind Spot

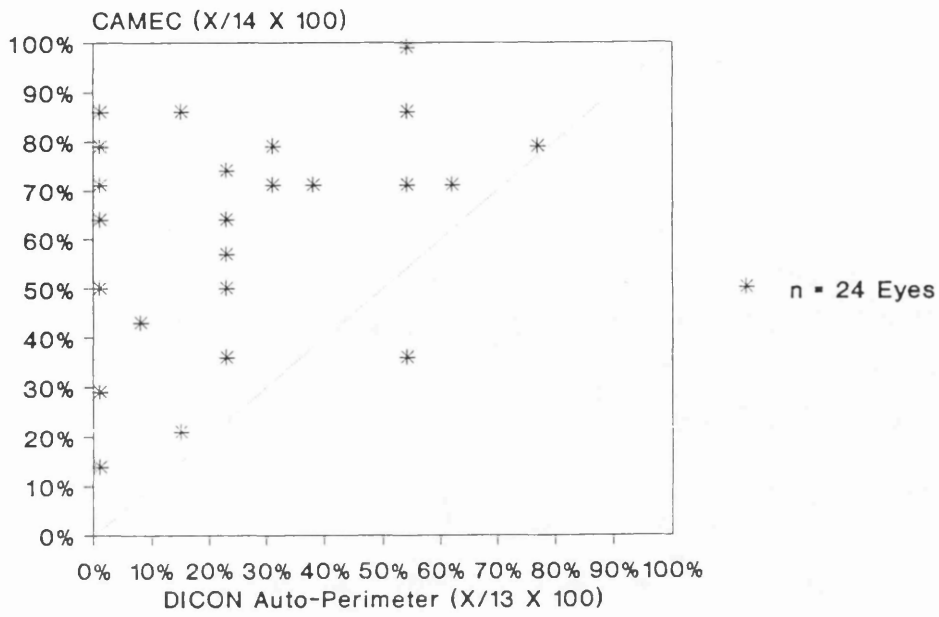


Figure 32: The scores obtained in each eye by the blind spot tests of CAMEC and Dicon Autoperimeters.

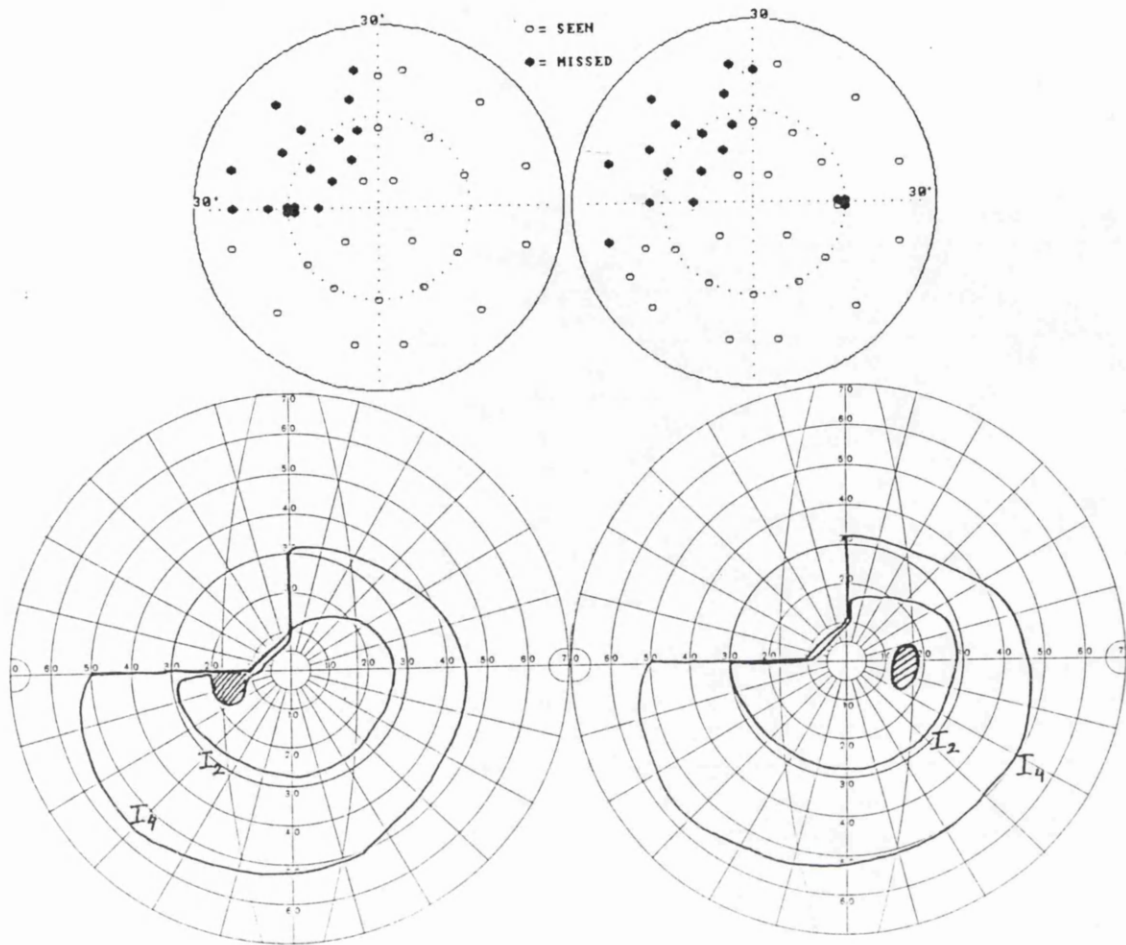


Figure 33: Left homonymous superior quadrantanopia to light offsets (top) and Goldmann perimeter (bottom) caused by a right intracranial temporo-parietal lobe tumor.

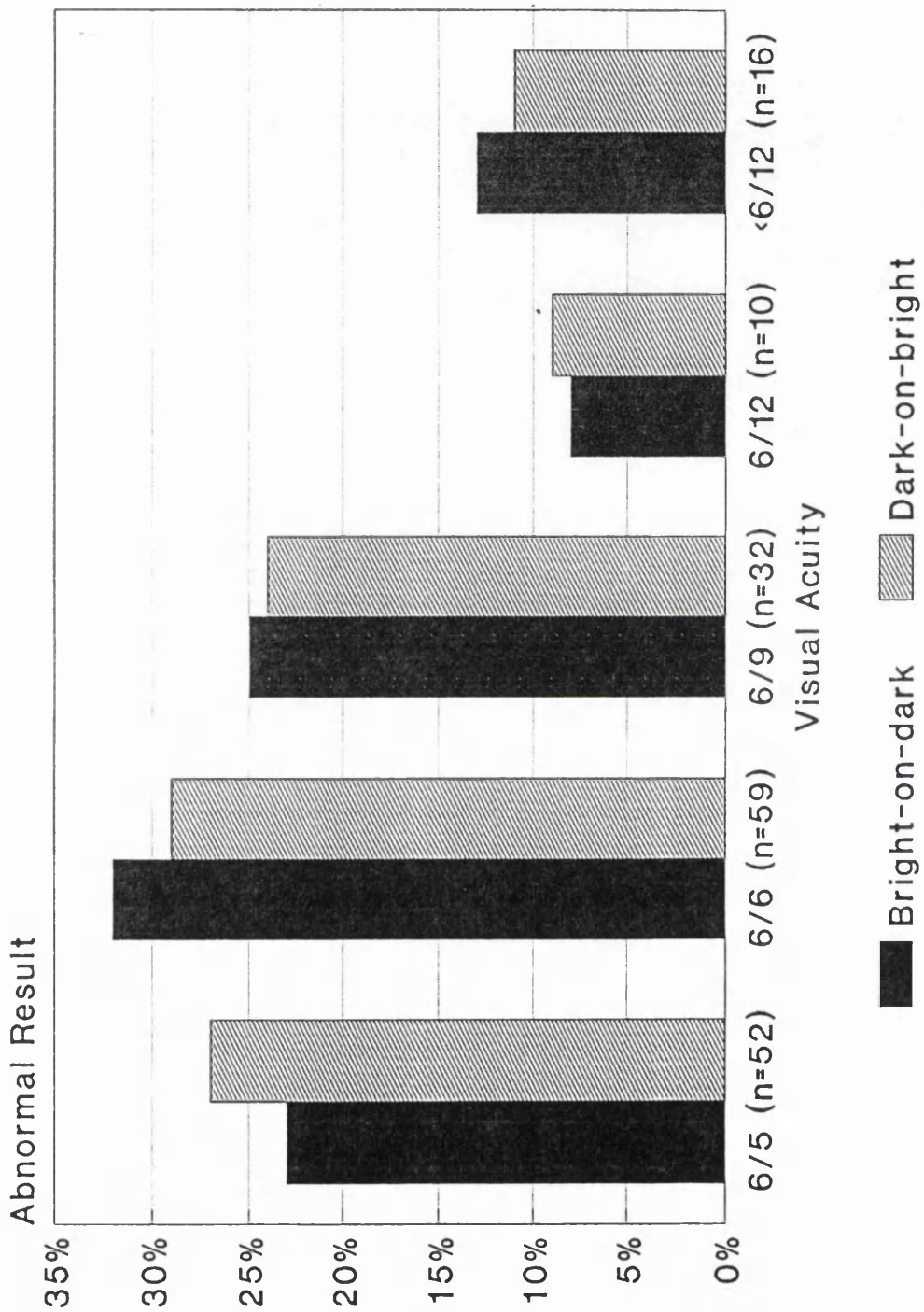


Figure 34: Positive (abnormal) result rate with CAMEC and Goldmann tests according to different visual acuity levels.

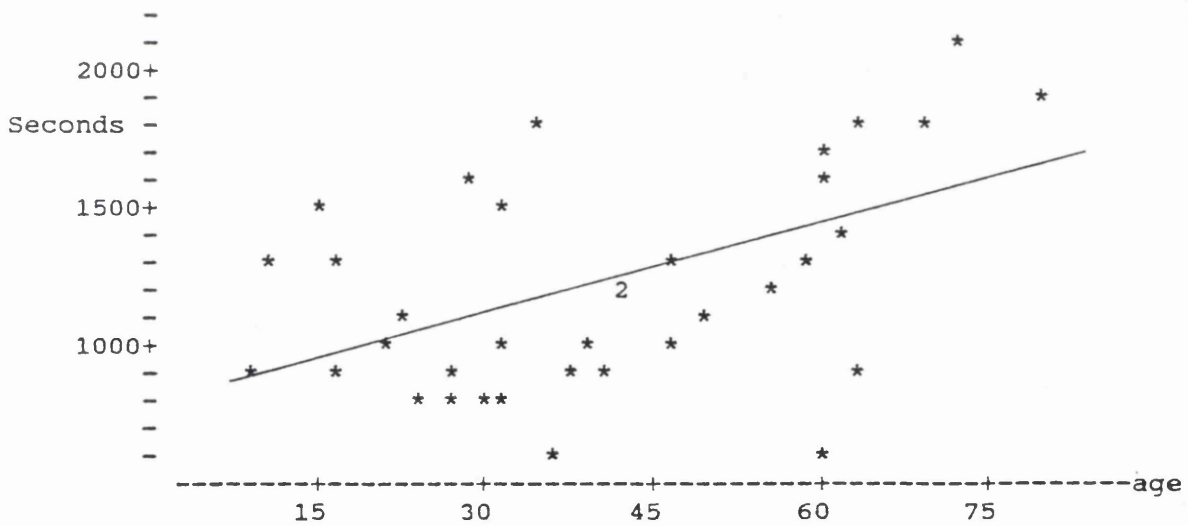
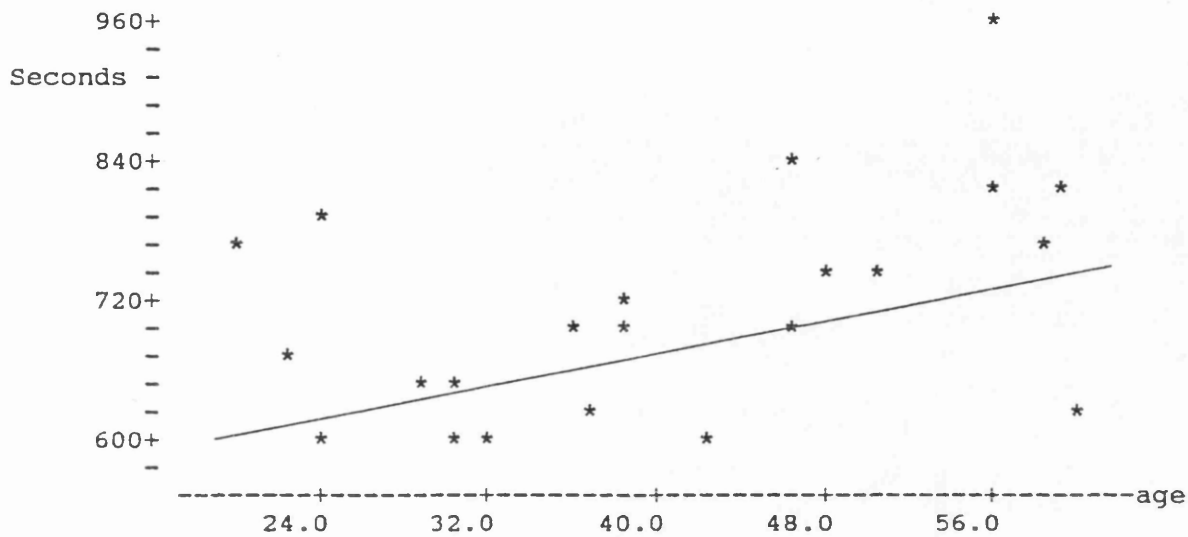
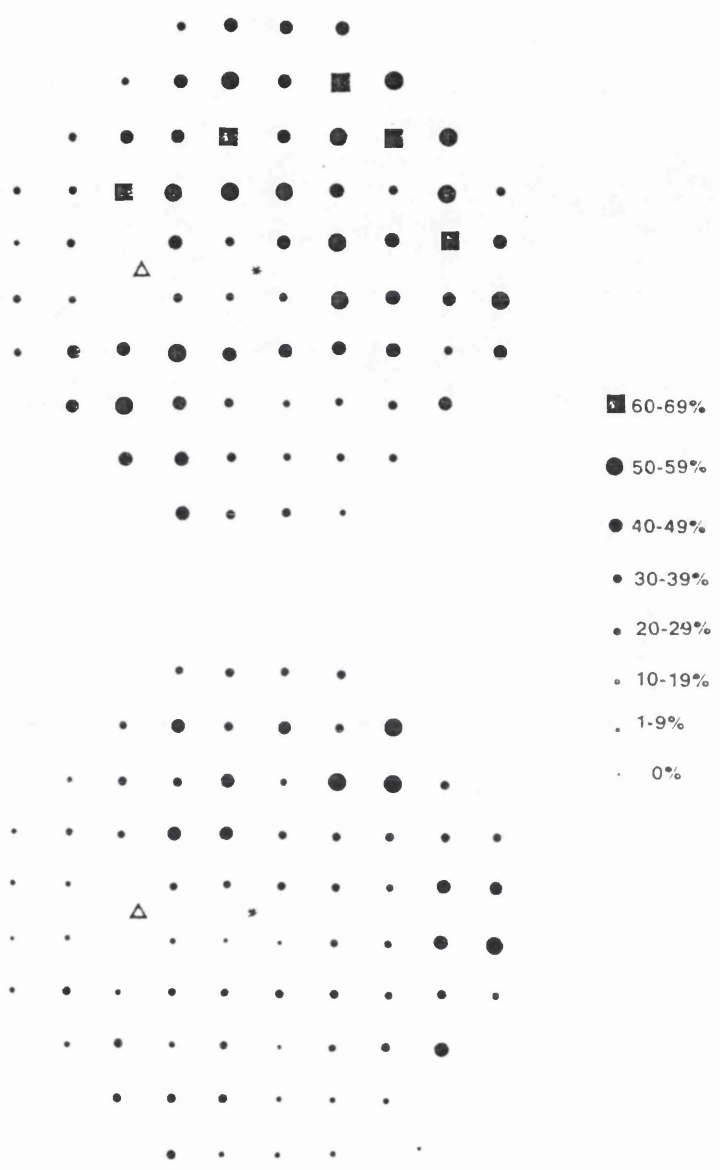


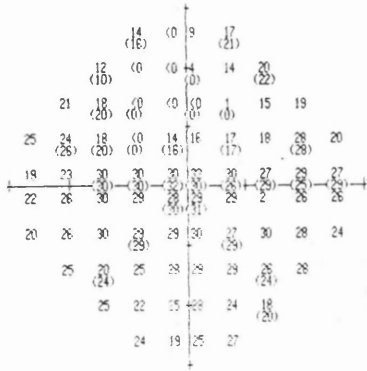
Figure 35: Regression analysis of CAMEC test duration (in seconds) versus patient age (in years) in bilaterally normal (top) and abnormal fields (bottom).



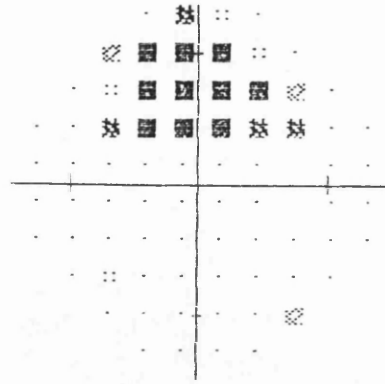
OUTSIDE 95% CONFIDENCE INTERVAL

Figure 36: The frequency of abnormality at each test location on STATPAC Total Deviation (top) and Pattern Deviation (bottom) results.

Right
 Age 69
 Questions asked 566
 Fixation losses 3/28
 False pos errors 1/14
 False neg errors 1/15
 Test time 00:17:23



Pattern
 deviation



CAMEC2 VISUAL FIELD PLOT

SP, F, 69 YRS

○ = SEEN
 ⊙ = SEEN ON REIEST
 ● = MISSED

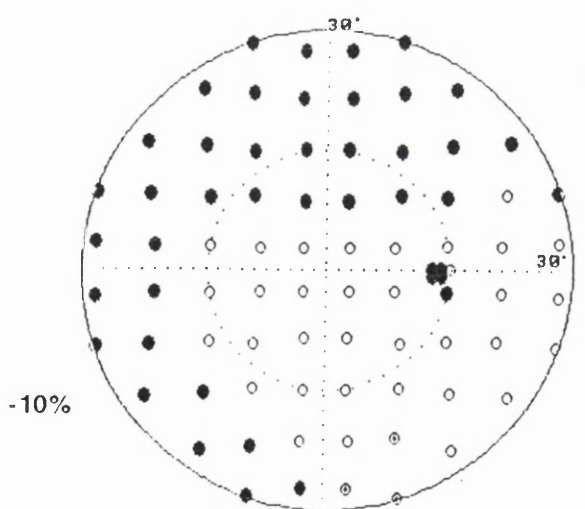
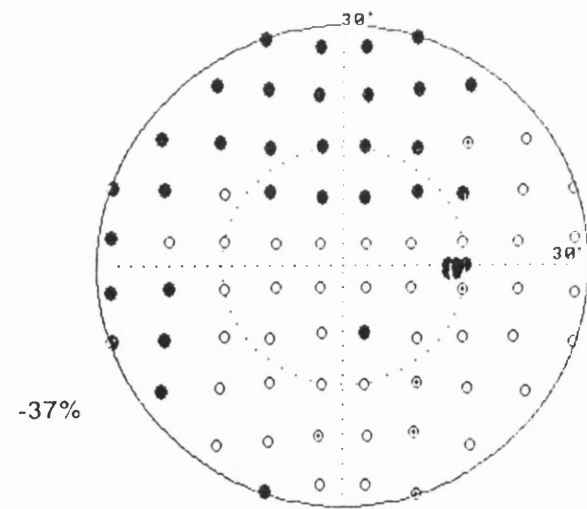
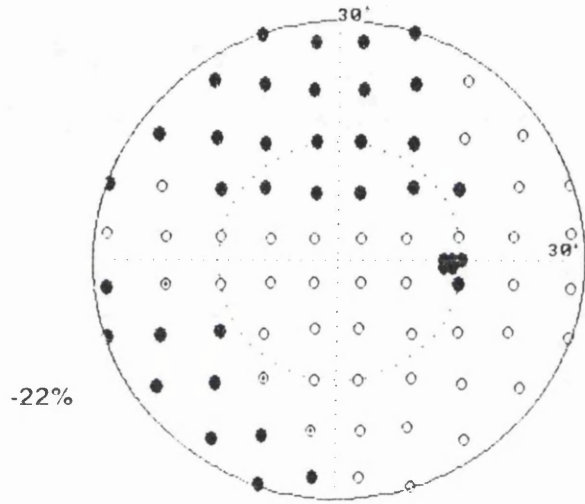
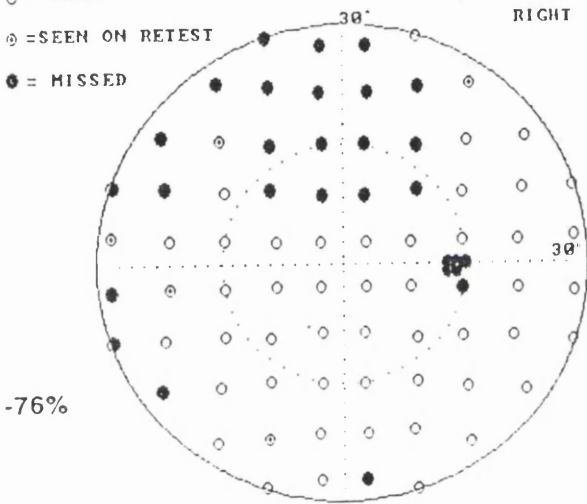
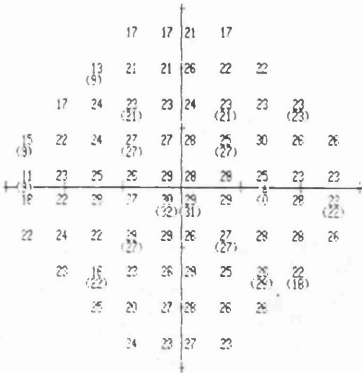


Figure 37: A superior Bjerrum scotoma to Humphrey VFA on STATPAC (top row) and CAMEC with four different single intensity offset stimulus contrasts (middle and bottom rows). Offset stimuli were not age adjusted and the normal portions of the diseased central visual field served as the control for the detectability of offset stimuli. No age-matched controls with completely normal eyes were employed.

Right
 Age 71
 Questions asked 502
 Fixation losses 6/26
 False pos errors 0/12
 False neg errors 3/22
 Test time 00:14:40



Pattern deviation



CAMEC2 VISUAL FIELD PLOT

VN, F, 71 YRS

- = SEEN
- ⊙ = SEEN ON RETEST
- = MISSED

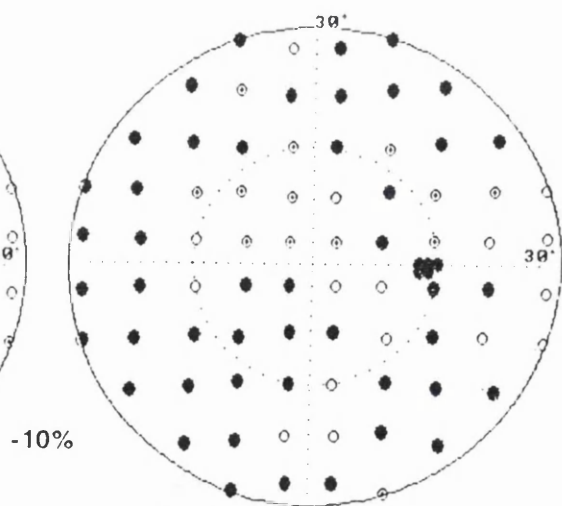
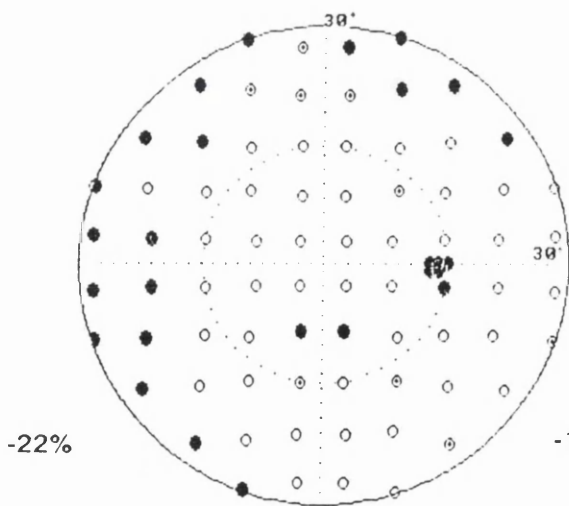
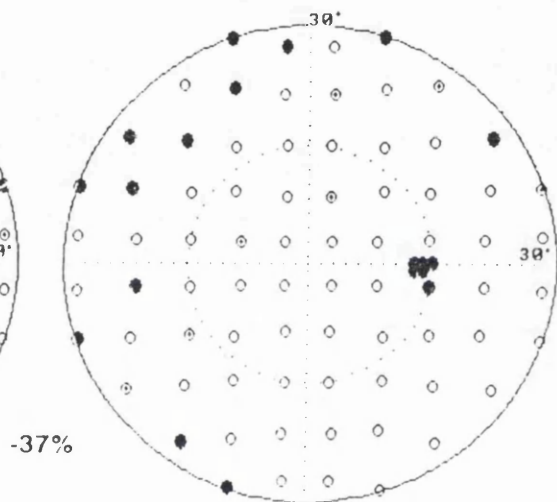
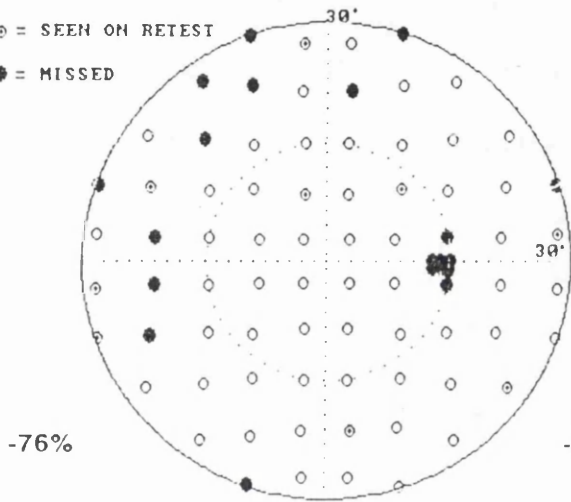


Figure 38: The nasal field loss on STATPAC result appeared more extensive when compared with lowest contrast (-10%) offset stimuli which also revealed double arcuate scotomas. Single intensity offset stimulus contrasts were not age adjusted and selected arbitrarily. Normal portions in the field serve as the control for the diseased parts in each tested eye.

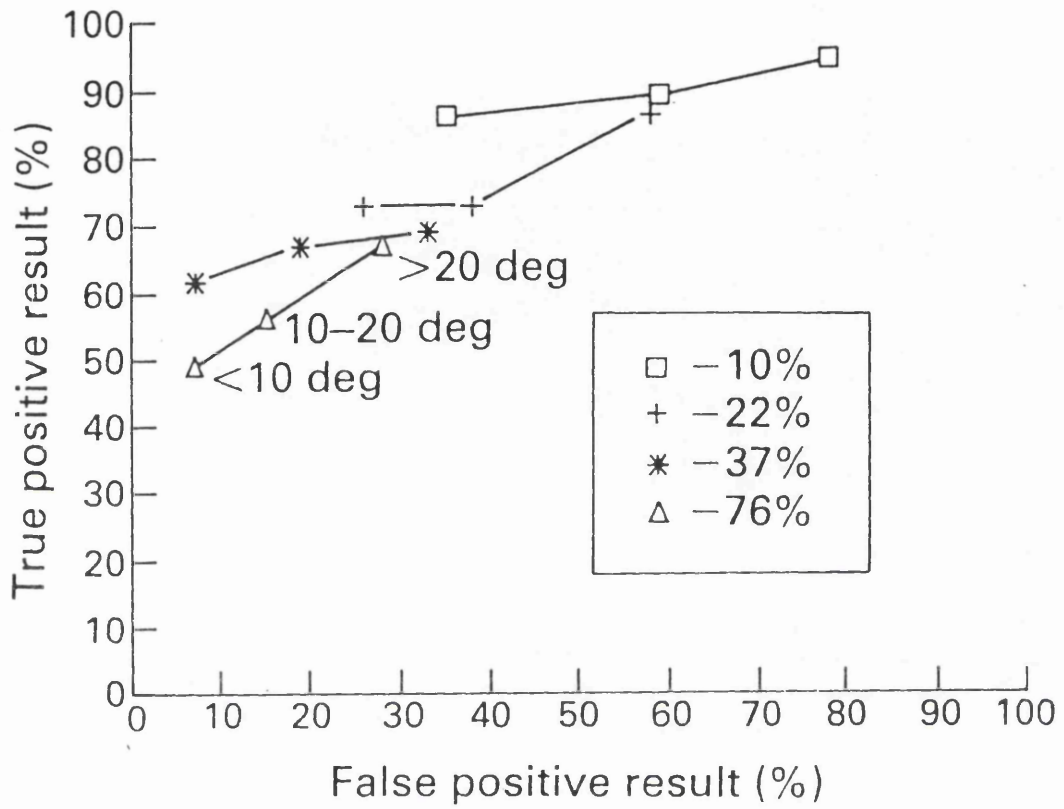


Figure 39: The true and false positive result rates with offset stimuli against STATPAC Pattern Deviation results at all test points in three annuli eccentricity bands.

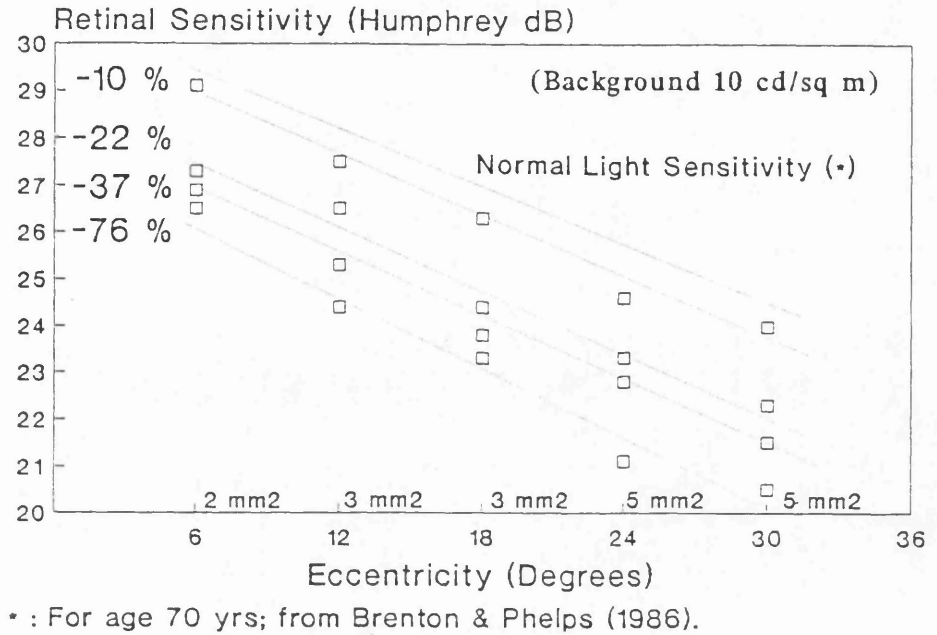


Figure 40: Equivalent Humphrey threshold levels required for the detection of light offsets on 10 cd/m² background.

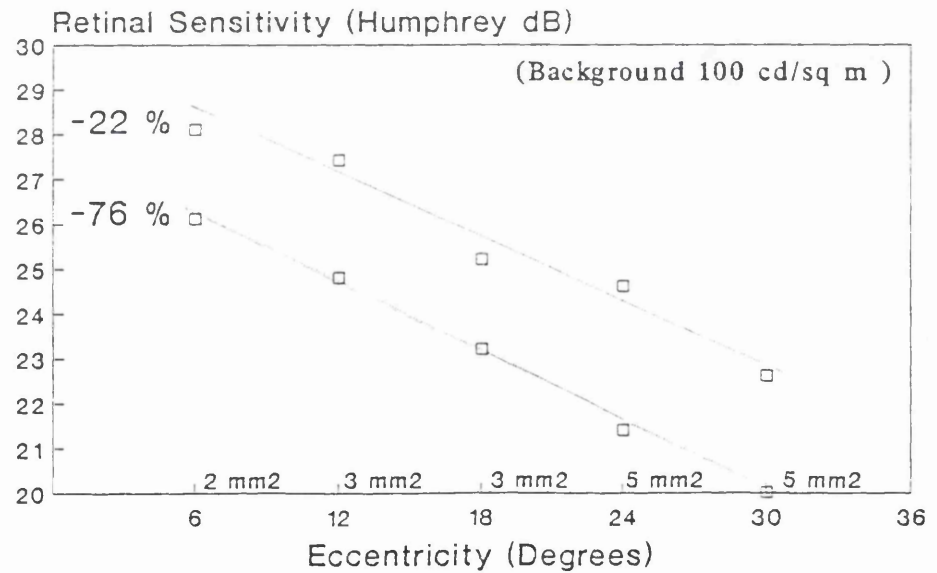


Figure 41: Equivalent Humphrey threshold levels required for the detection of light offsets on 100 cd/m².

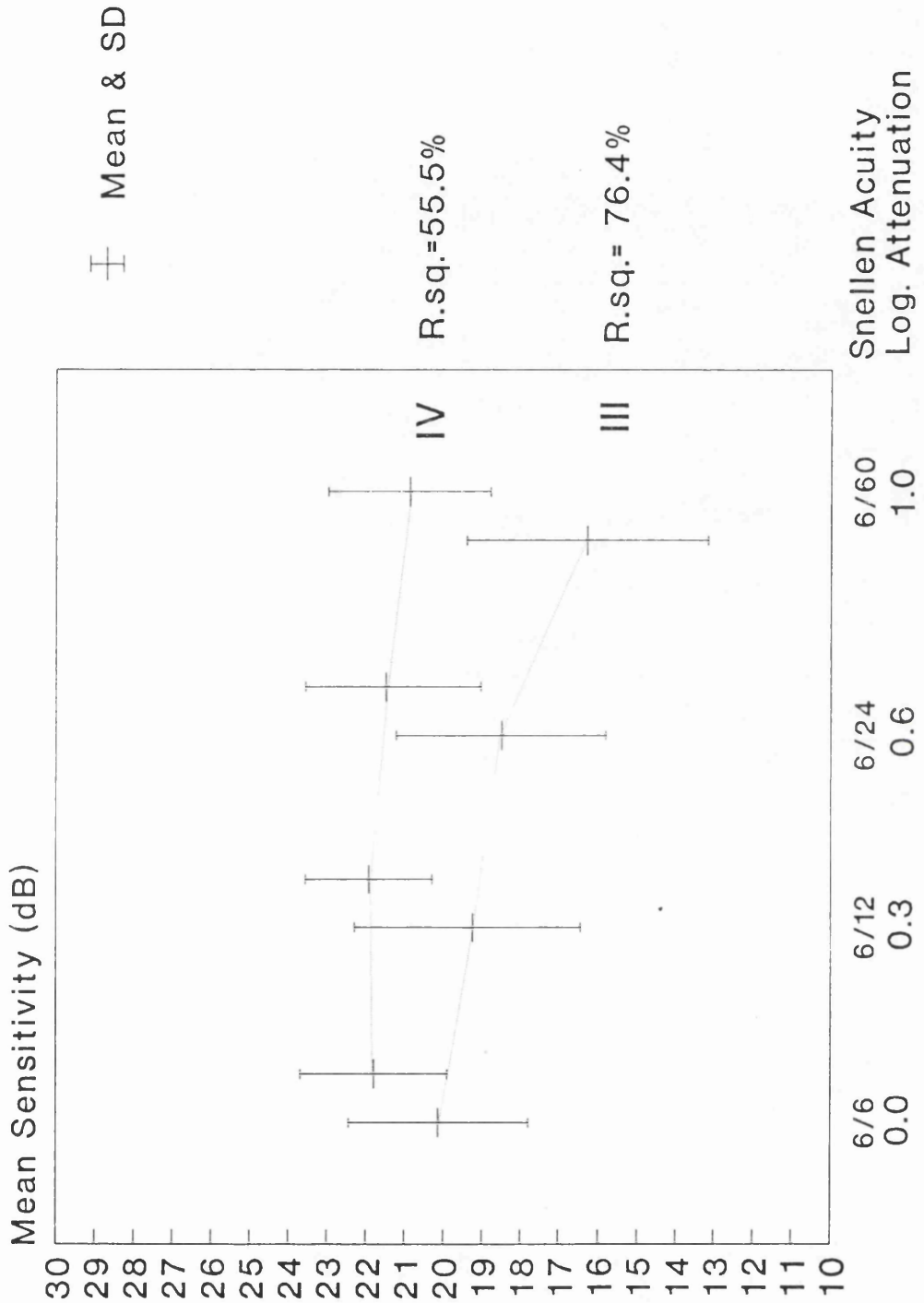


Figure 42: The effect of visual acuity on detection thresholds to light offsets.

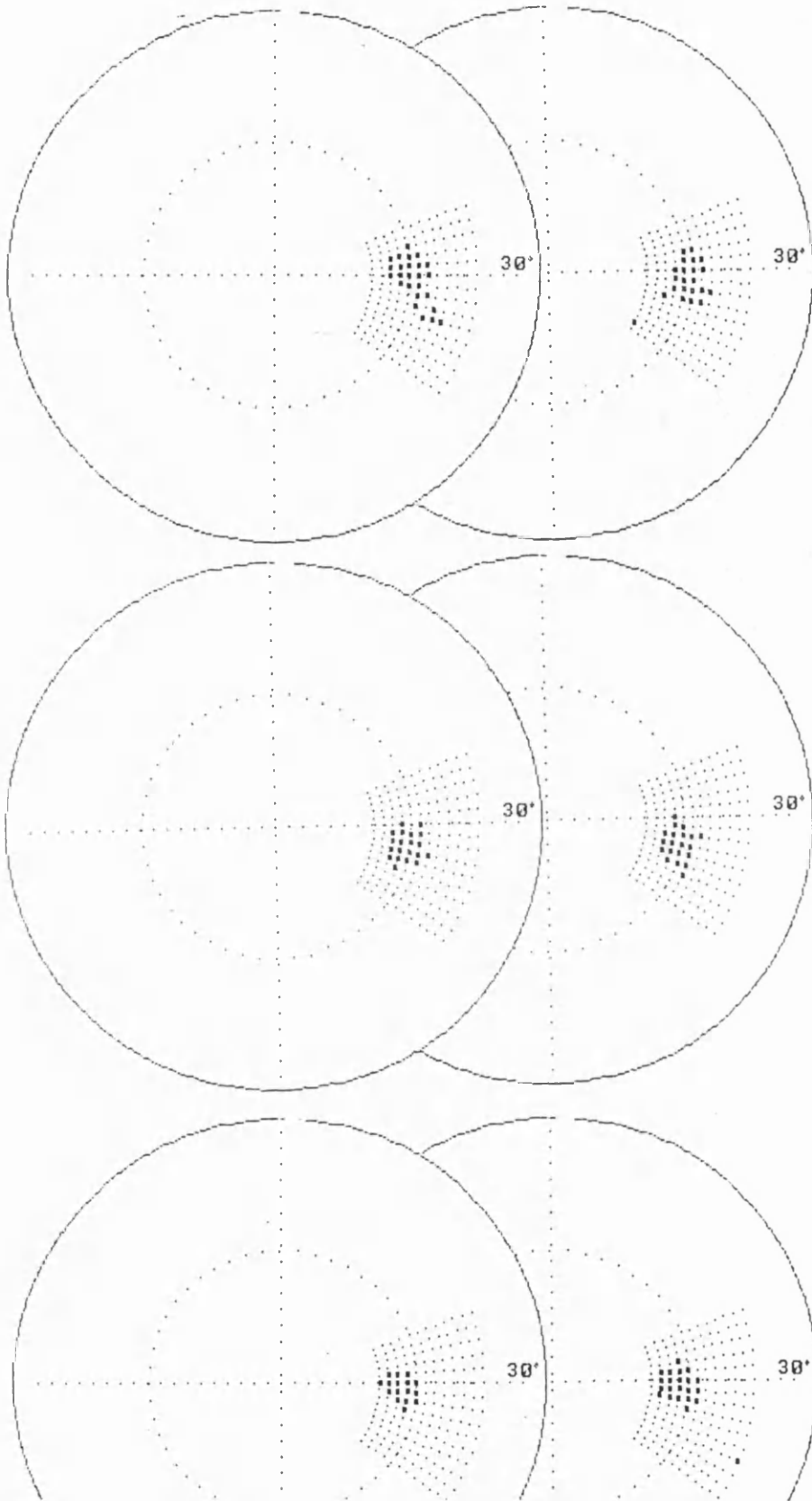
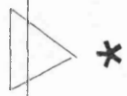


Figure 43: Topographical reproducibility of blind spot mapping varied between 64% (top) to 80% (middle) with an average of 73% (bottom).

Figure 44: Mean±Standard Deviation offset detection sensitivity (in decibels) at each test location in the central visual field.

19.4±1.7	20.4±2.2	19.7±2.1	19.2±2.8
19.9±1.4	21.3±1.3	21.5±1.1	20.5±1.8
19.2±1.8	21.3±1.3	21.8±0.8	21.3±1.3
18.5±2.1	20.2±1.8	22.0±0.0	22.0±0.0
19.2±2.0	20.1±1.5	22.0±0.0	22.0±0.0
19.6±1.8	21.4±1.6	21.5±1.1	21.3±1.3
19.7±2.1	20.6±1.6	21.1±1.4	20.5±2.0
18.1±2.2	19.8±1.9	19.8±1.9	20.1±2.0
		21.1±1.4	20.2±1.8
		21.5±1.1	20.2±1.8
		21.8±0.8	21.5±1.1
		22.0±0.0	21.1±1.4
		22.0±0.0	20.5±1.8
		22.0±0.0	20.1±2.0



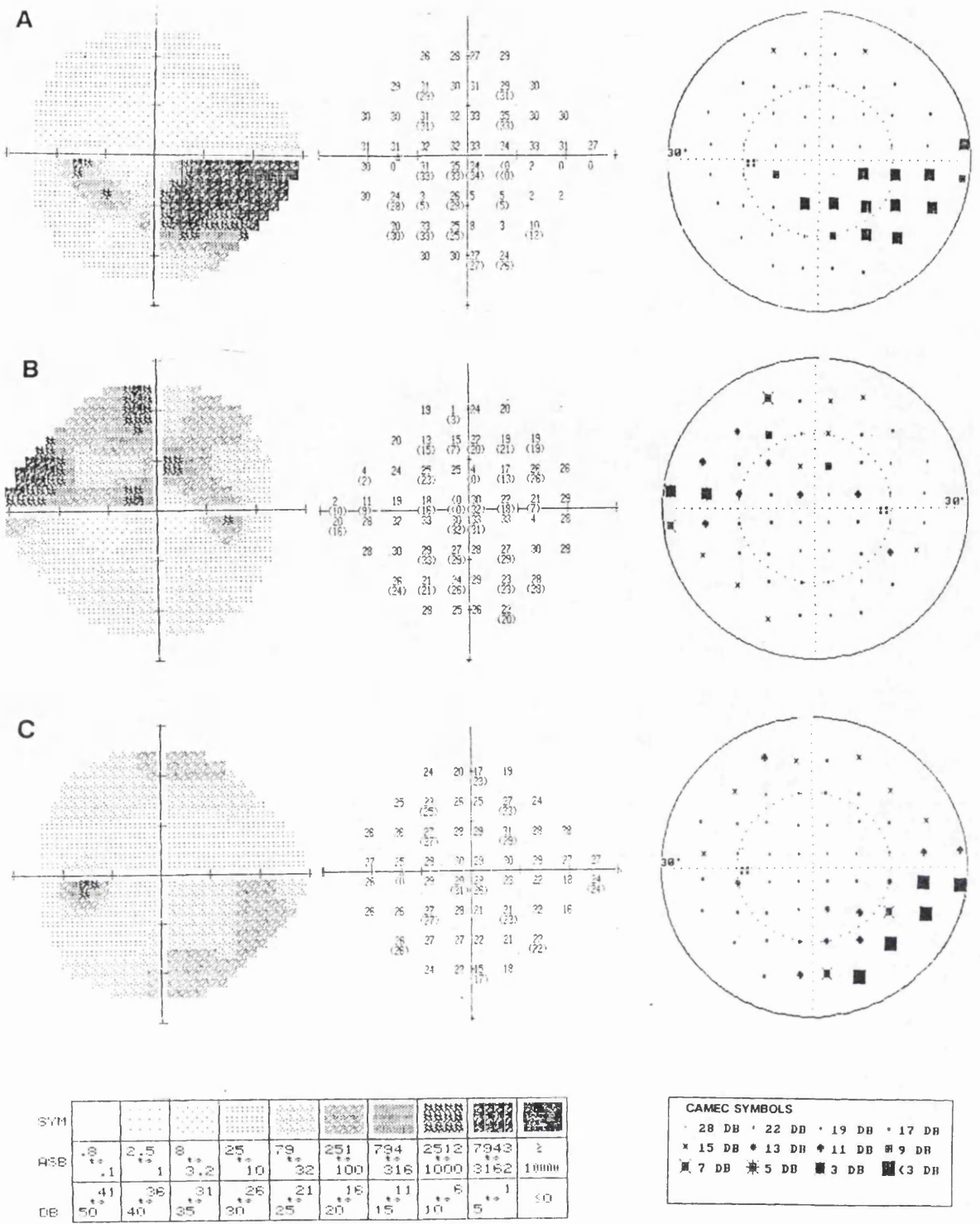


Figure 45: CAMEC and Humphrey VFA results in three glaucomatous eyes showing similar defects.

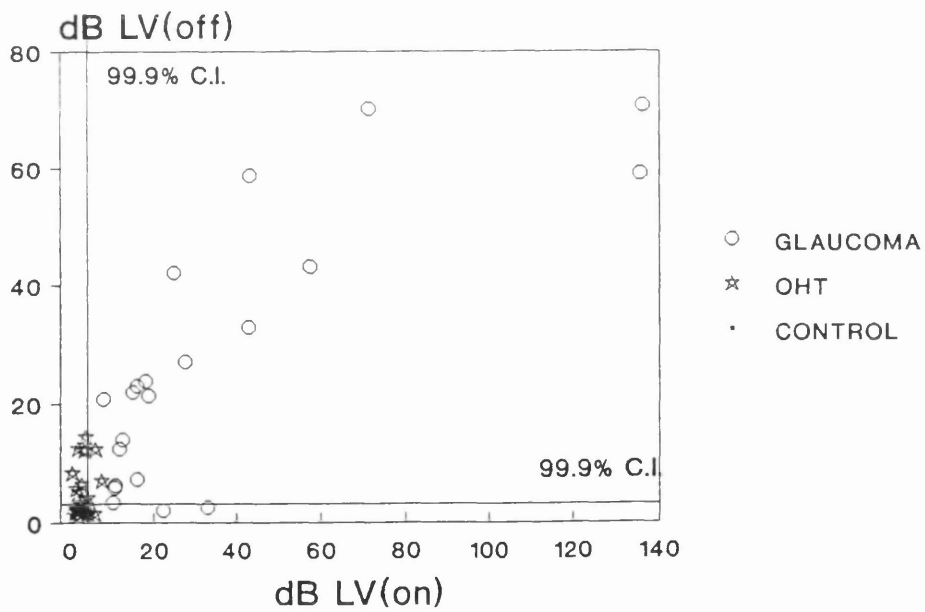
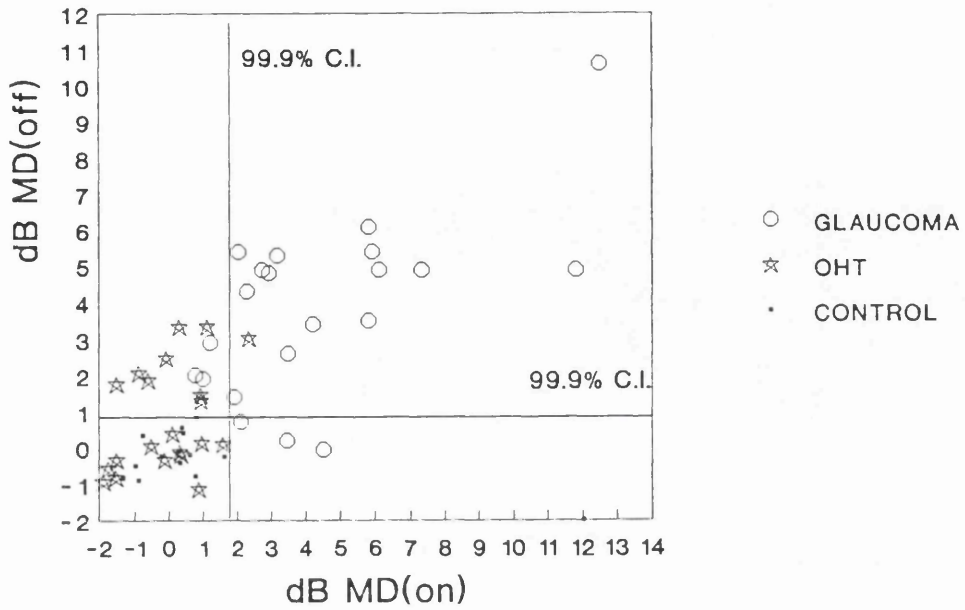
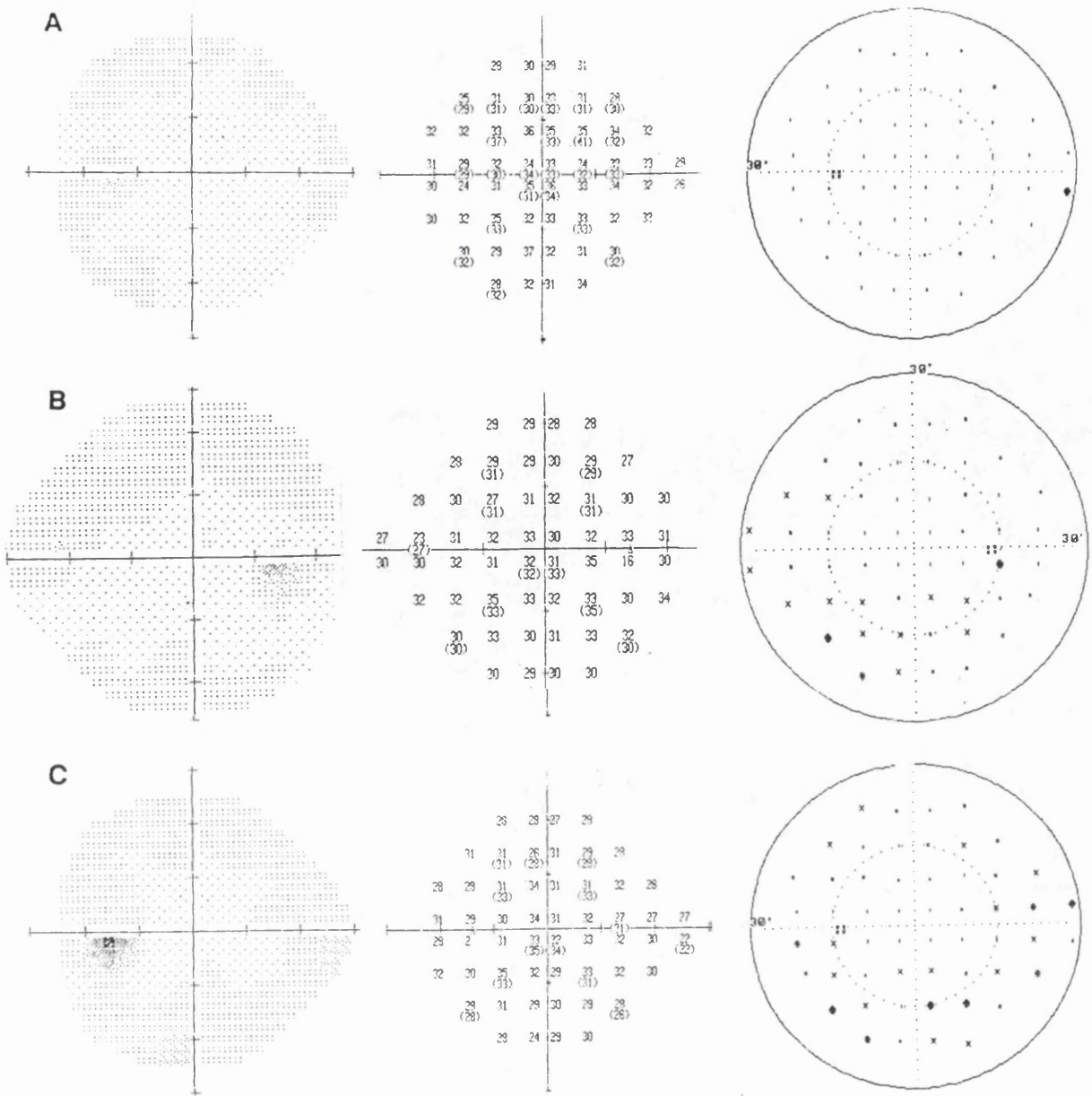


Figure 46: Global field indices obtained with offset and onset stimuli.



SYM									
ASB	.8	2.5	8	25	79	251	794	2512	7943
	.1	1	3.2	10	32	100	316	1000	3162
DB	41	38	31	26	21	16	11	8	5
	50	40	35	30	25	20	15	10	5

CAMEC SYMBOLS			
○	28 DB	•	22 DB
◊	19 DB	◊	17 DB
×	15 DB	◊	13 DB
◊	11 DB	◊	9 DB
◊	7 DB	◊	5 DB
◊	3 DB	◊	<3 DB

Figure 47: The field results from three ocular hypertensives. The normal field of the right eye of a 69 year old male with IOP of 25 mmHg and symmetrical CDR of 0.2 (Top); In a 63 yr old male, offset stimuli showed an inferior Bjerrum scotoma in the right eye with IOP of 32 mmHg (20 mmHg in the left eye) and CDR of 0.7 (0.4 in the left eye) (Middle); Superior nasal step and inferior Bjerrum scotoma to offsets in the left eye of a 69 year old female with IOP of 32 mmHg and CDR of 0.6 (27 mmHg and 0.5 in the right eye respectively) (Bottom).

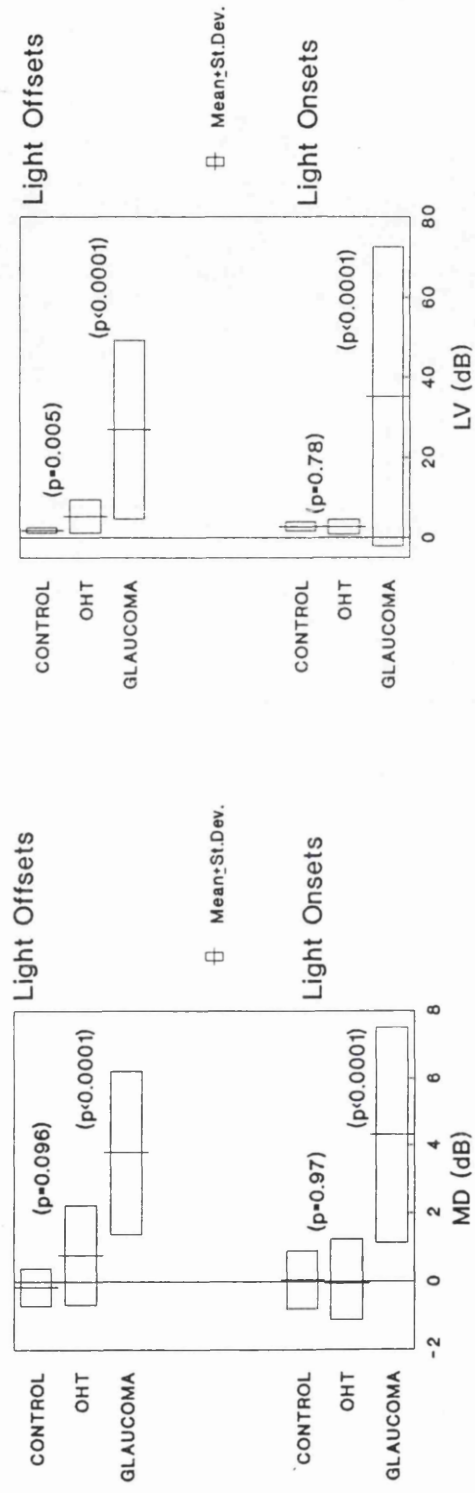
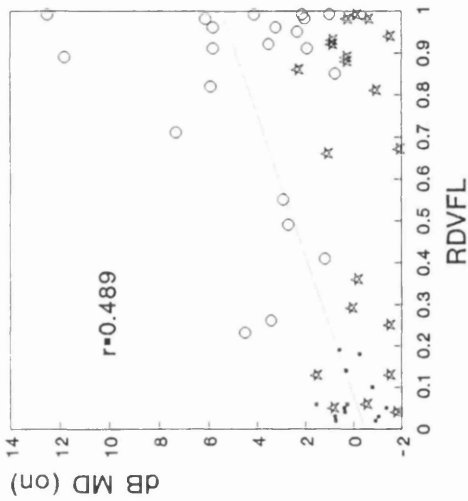
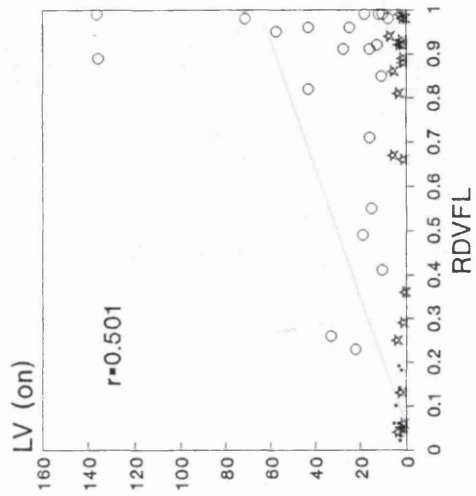


Figure 48: Average global field indices obtained with onset and offset stimuli.

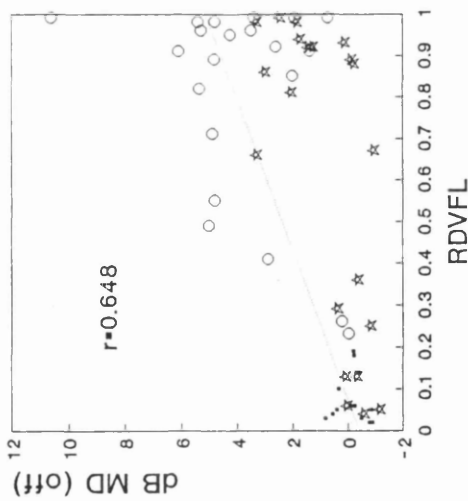
Figure 49: The correlation between the global visual field indices and the risk of developing visual field loss (RDVFL) in all eyes.



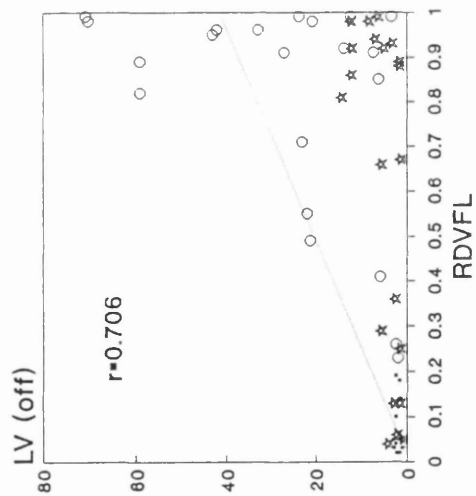
○ GLAUCOMA
 ☆ OHT
 · CONTROL



○ GLAUCOMA
 ☆ OHT
 · CONTROL



○ GLAUCOMA
 ☆ OHT
 · CONTROL



○ GLAUCOMA
 ☆ OHT
 · CONTROL

Figure 50: The correlation between the global visual field indices and the level of intra-ocular pressure (IOP) in all eyes.

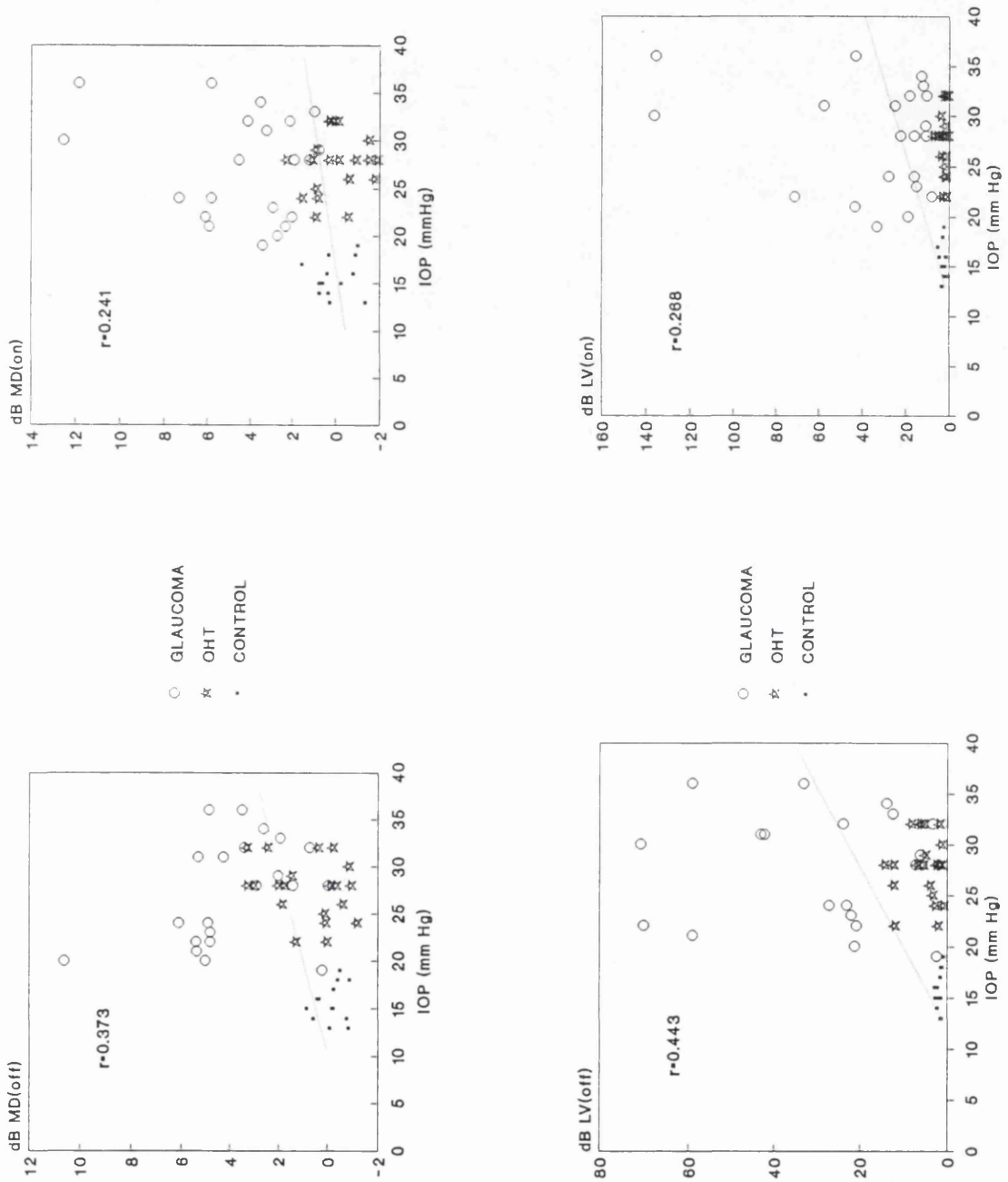
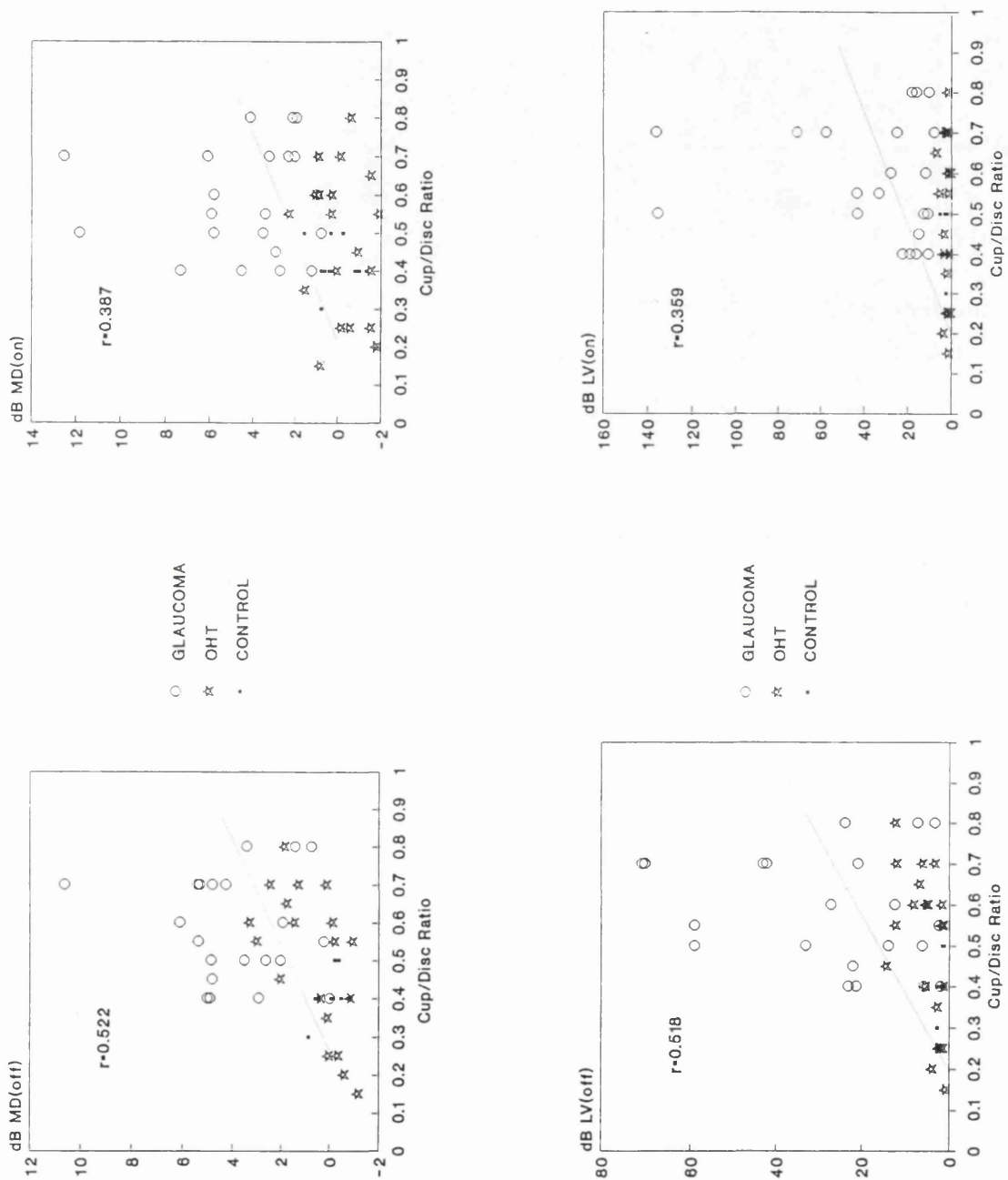


Figure 51: The correlation between the global visual field indices and the cup-to-disc ratio (CDR) in all eyes.



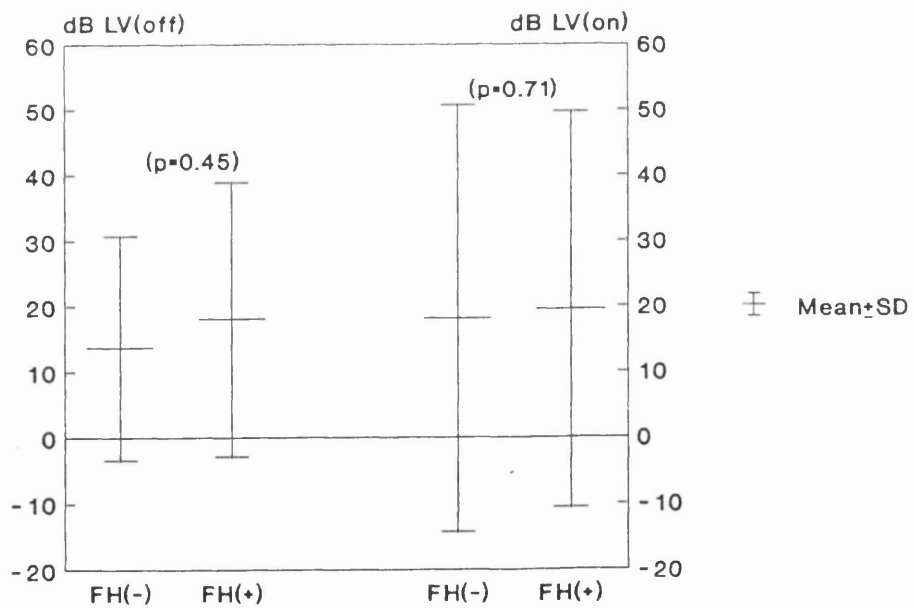
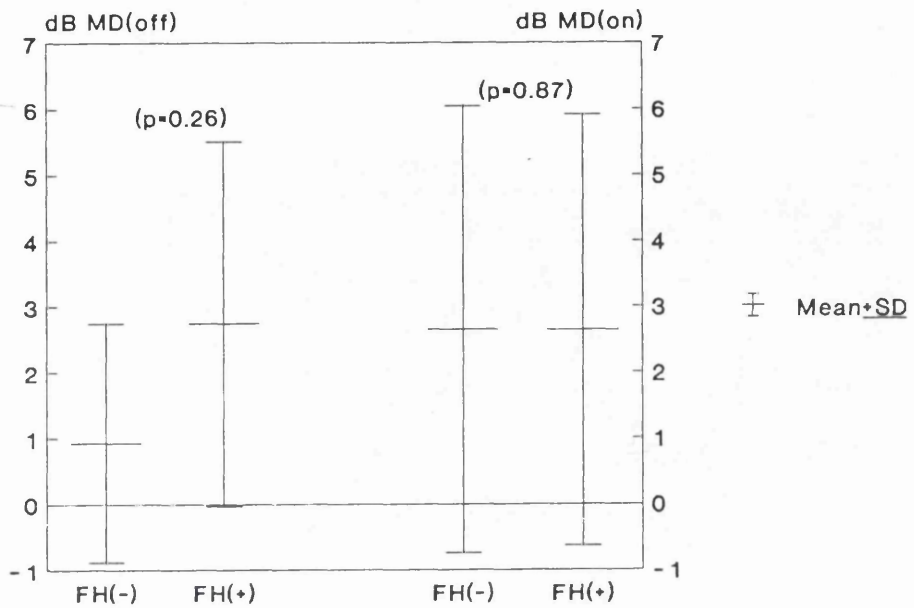


Figure 52: Family history had no significant effect on average field scores obtained with onset and offset stimuli.

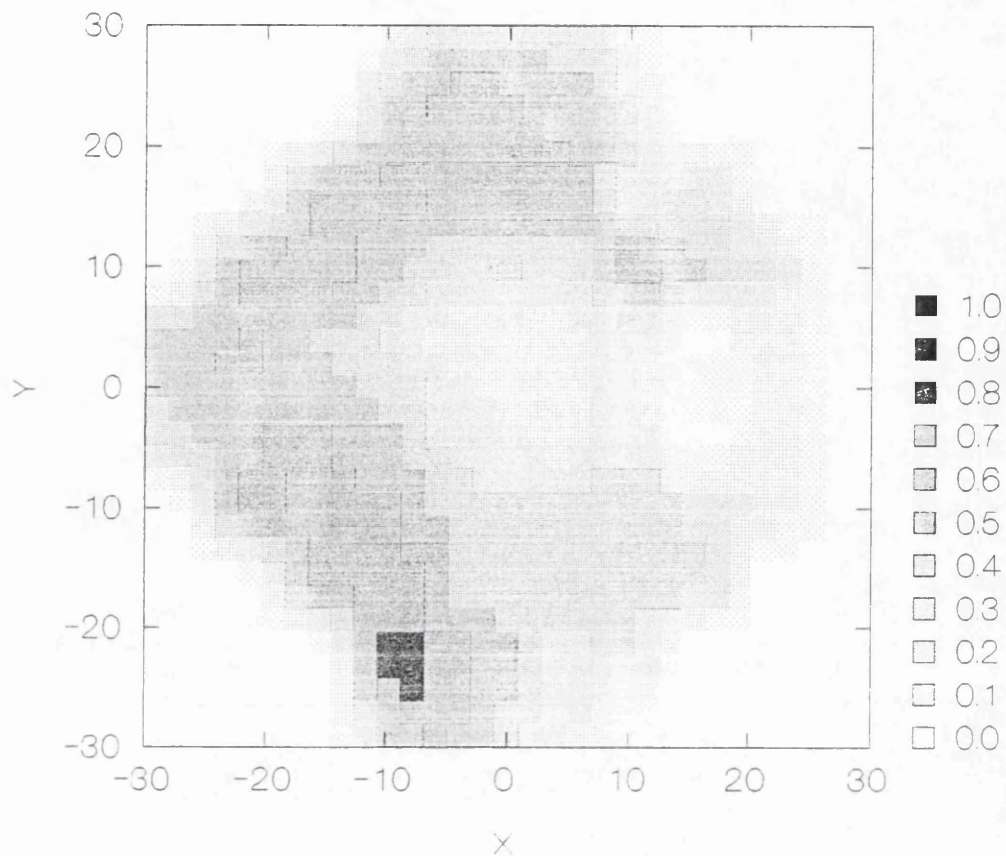


Figure 53: Topographical frequency distribution of visual field defects to onset stimuli of Humphrey VFA in POAG.

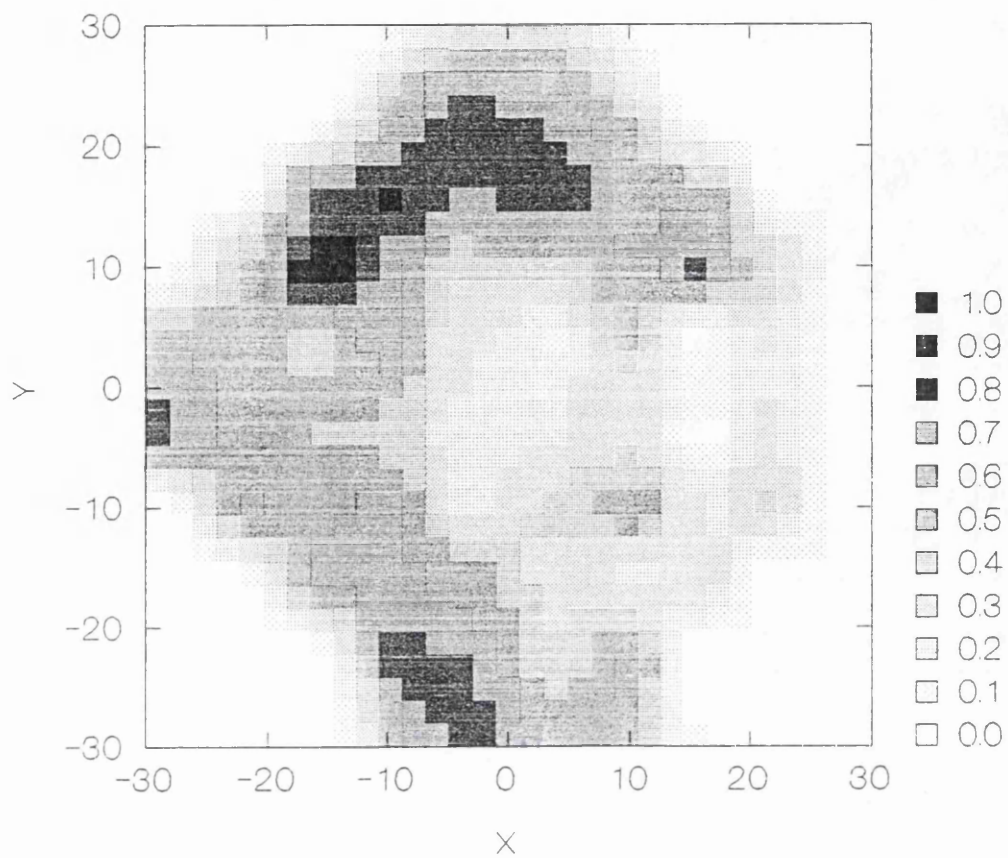


Figure 54: Topographical frequency distribution of visual field defects to offset stimuli of CAMEC in POAG.

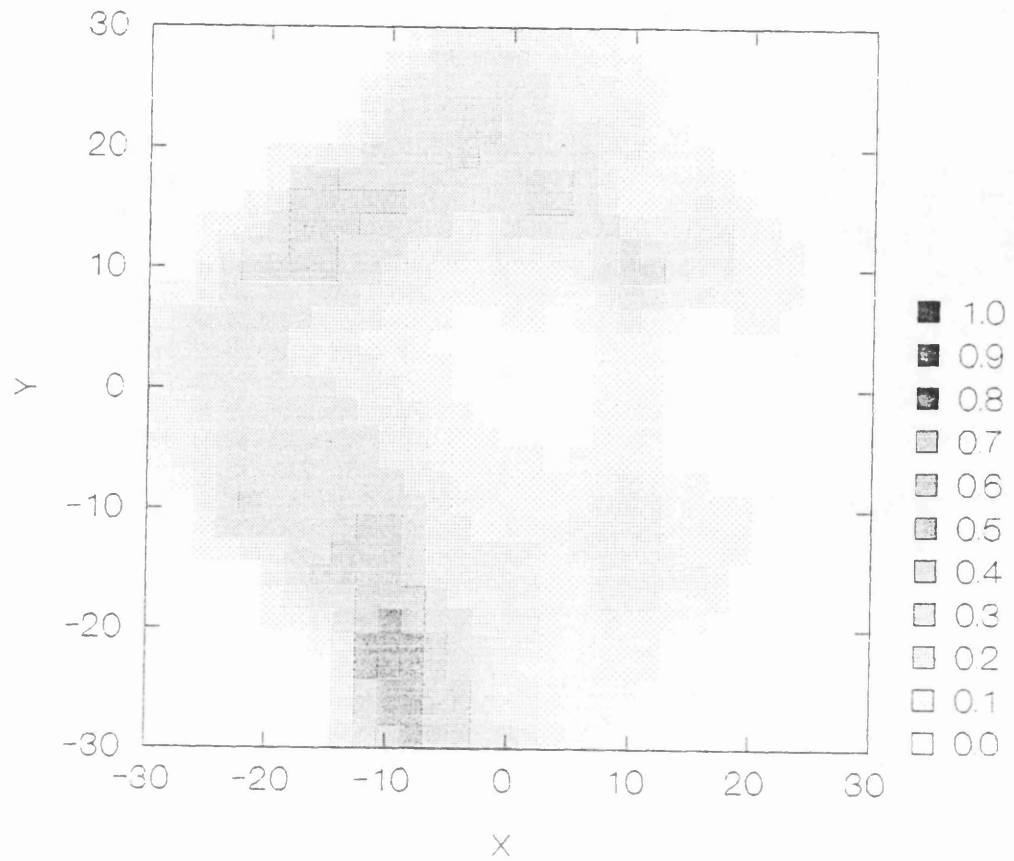
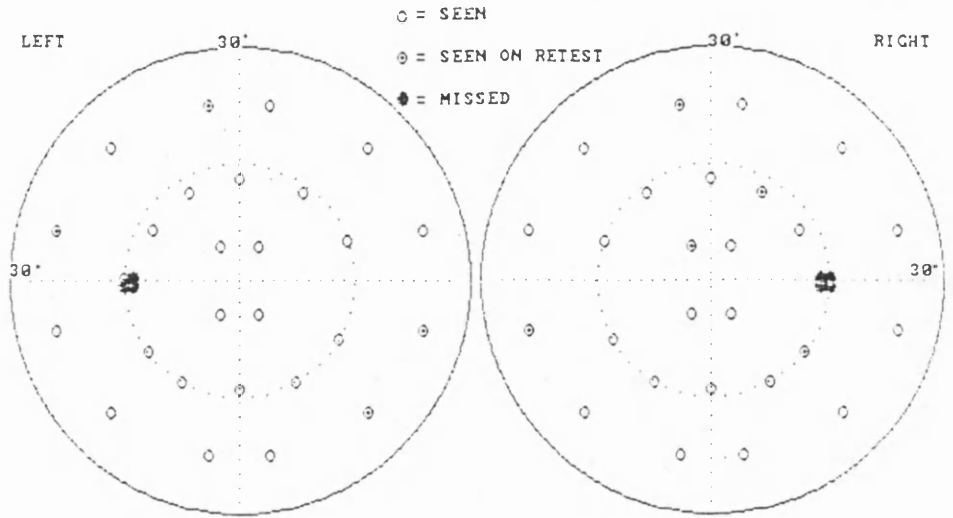


Figure 55: Topographical frequency distribution of visual field defects to offset stimuli of CAMEC in OHT.

CAMEC2 VISUAL FIELD PLOT



No. Seen: 26
 No. Missed: 0
 False Negatives: 4
 False Positives: 0
 Stimulus Size (mins of arc): 12
 Stimulus Duration(s): 0.30

No. Seen: 26
 No. Missed: 0
 False Negatives: 5
 False Positives: 0
 Stimulus Size (mins of arc): 12
 Stimulus Duration(s): 0.30

Name: Age: Date: 27-03-1992 Test time(s): 603

FIXATION LOSSES: 0/11
 FALSE POS ERRORS: 0/3
 FALSE NEG ERRORS: 0/1

TEST TIME: 00:02:106
 HFA S/N: 840-2423

• = POINTS SEEN: 39/40
 X = RELATIVE DEFECTS: 1/40
 ■ = ABSOLUTE DEFECTS: 0/40
 ▲ = BLIND SPOT

LEFT RIGHT

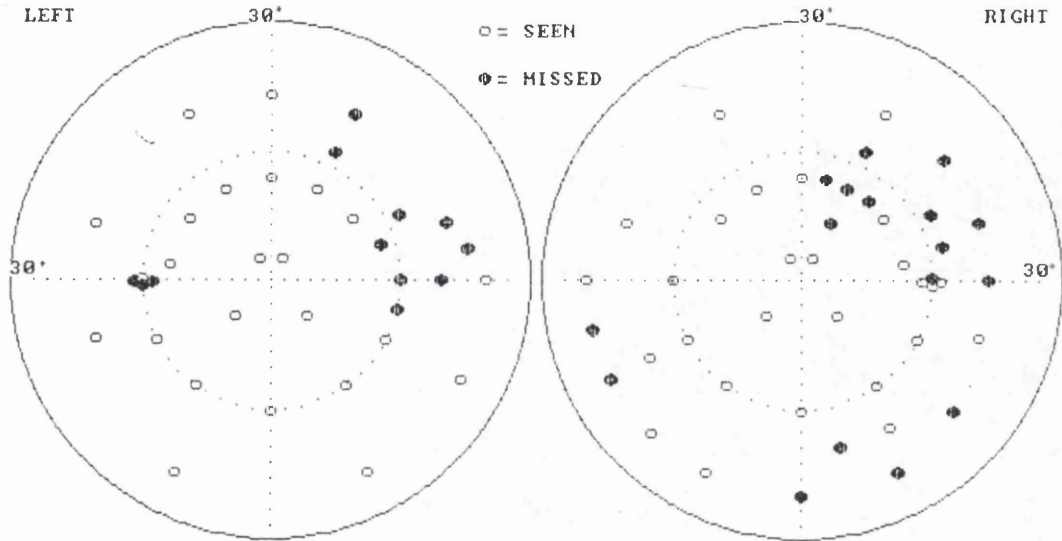
FIXATION LOSSES: 0/11
 FALSE POS ERRORS: 0/3
 FALSE NEG ERRORS: 0/3

TEST TIME: 00:03:1

• = POINTS SEEN: 39/40
 X = RELATIVE DEFECTS: 0/4
 ■ = ABSOLUTE DEFECTS: 0/4
 ▲ = BLIND SPOT

Figure 56: Normal visual fields of an 8 year-old to CAMEC and Humphrey tests.

CAMEC2 VISUAL FIELD PLOT



No. Seen: 23
No. Missed: 9
False Positives: 5
Guesses: 1
Stimulus Size (mins of arc): 12
Stimulus Duration(s): 0.40

Name: Age:

No. Seen: 24
No. Missed: 16
False Positives: 2
Guesses: 1
Stimulus Size (mins of arc): 12
Stimulus Duration(s): 0.40

Date: 05-07-1991 Test time(s): 1443

Figure 57: Right homonymous supero-temporal partial quadrantanopia caused by left temporal lobe lesion in a 5 1/2 year old girl who could be tested with CAMEC only.

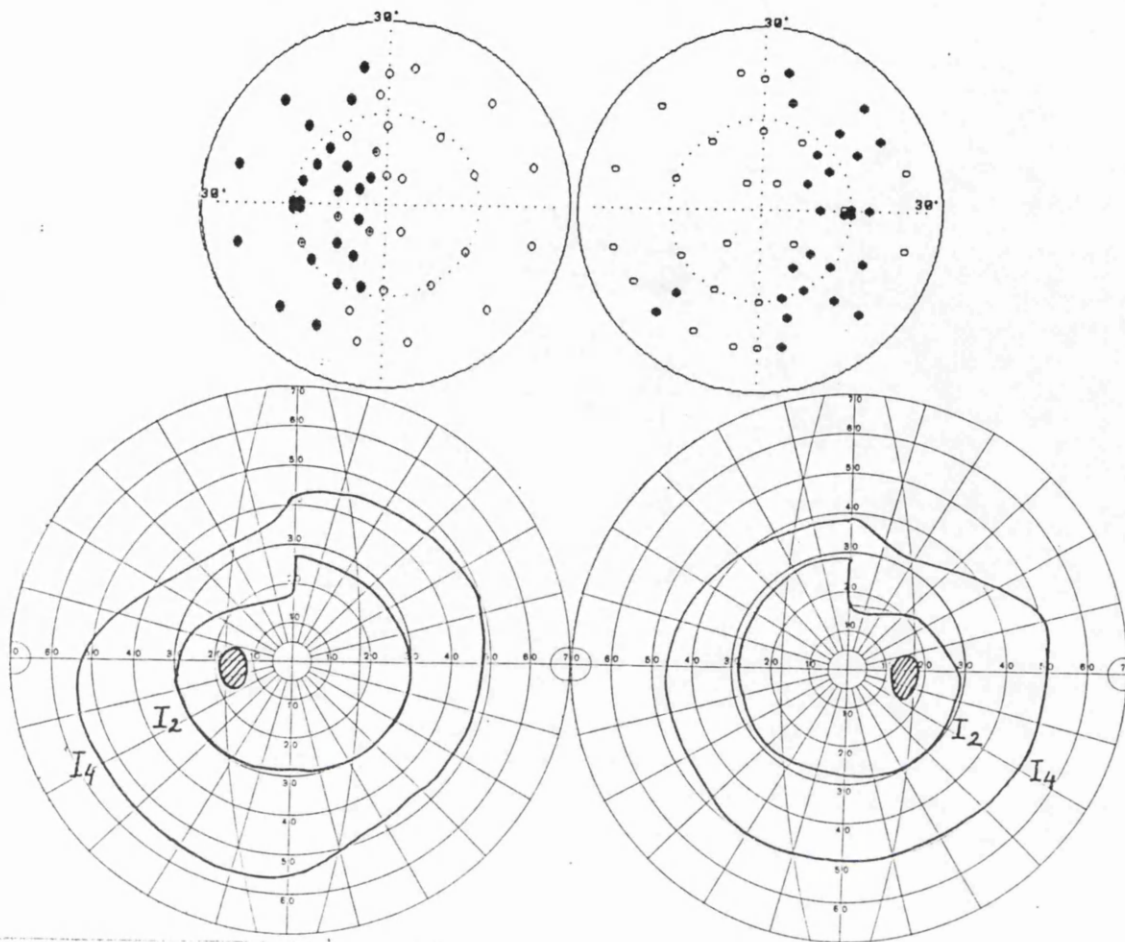


Figure 58: Complete bitemporal hemianopia to the offset stimuli of CAMEC in a 50 year old male with pituitary adenoma. The hemianopic defects were partial, involving only the upper temporal quadrants, when tested with conventional Goldmann perimetry.

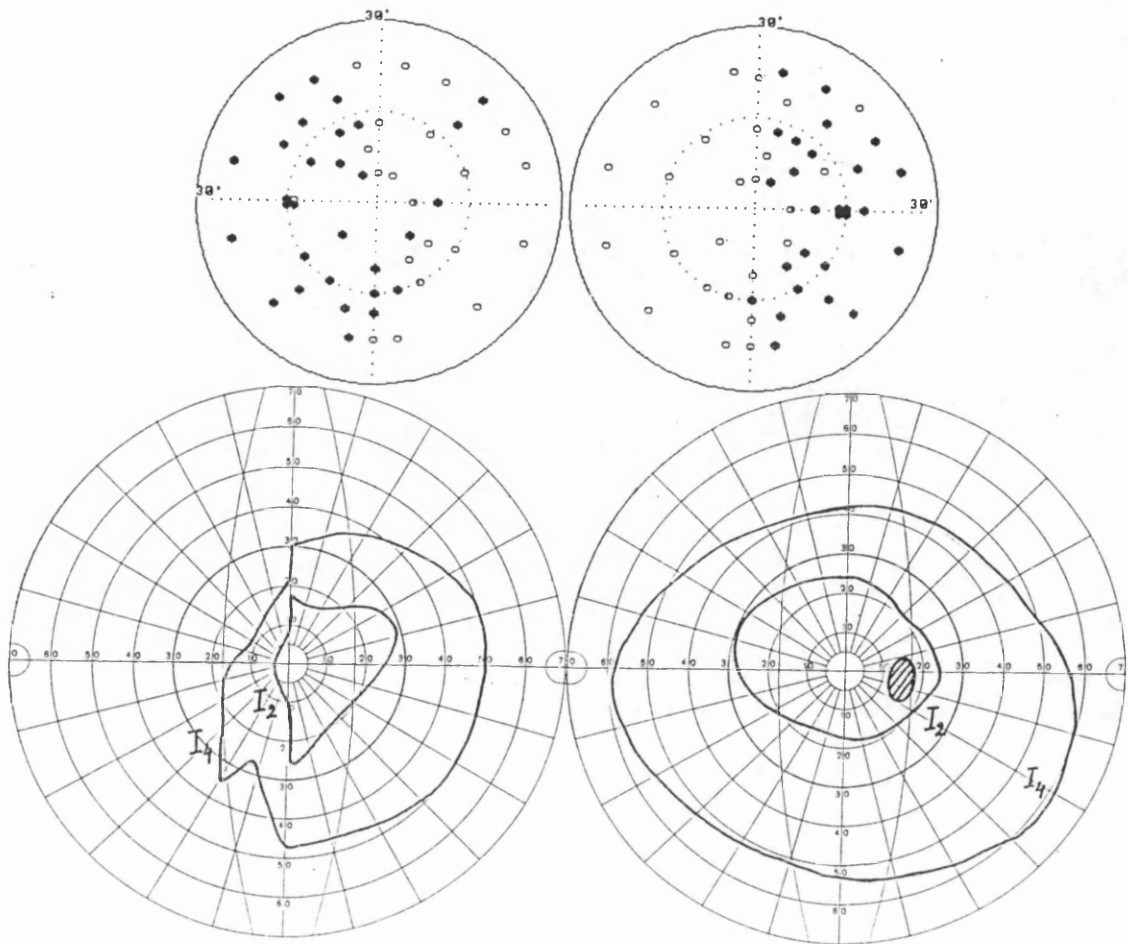


Figure 59: Bitemporal hemianopia to the offset stimuli of CAMEC in craniopharyngioma. The complete hemianopic defect to the offset stimuli was underestimated by Goldmann perimetry in the right eye.



RNIB
challenging blindness

Royal National Institute for the Blind

224 Great Portland Street
London W1N 6AA
Telephone 071-388 1266
Central Fax 071-388 2034

Our Ref: ZW/pc

7 June 1994

Dr E Mutiukan
Neuro-Ophthalmology
Henry Ford Hospital
2799 West Grand Boulevard
Detroit
Michigan
48202-2689
USA

Dear Dr Mutlukan

**RE: COMPUTER ASSISTED MOVING EYE CAMPIMETRY IN
THE DETECTION AND MANAGEMENT OF GLAUCOMA.**

Thank you very much for submitting your final report on the above project and associated papers and poster. Your report was very well received by our committee when it was considered at the Prevention of Blindness Sub Committee on 11 May 1994.

Yours sincerely

Mrs Zoë Wavell
Research Grants Co-ordinator
RNIB Health Services Unit



RNIB
challenging blindness

Royal National Institute for the Blind

224 Great Portland Street
London W1N 6AA
Telephone 071-388 1266
Central Fax 071-388 2034

Our Ref: ZW/pc

15 March 1994

Dr E Mutlukan
Neuro-Ophthalmology Unit
Henry Ford Hospital
2799 West Gland Boulevard
Detroit
Michigan
48202 USA

Dear Dr Mutlukan

**RE: FINAL REPORT - EVALUATION OF CHAMEC IN THE
DETECTION AND MANAGEMENT OF GLAUCOMA.**

Thank you for submitting your final report on the above project which was discussed by RNIB Prevention of blindness Research Sub Committee when it met on 9 February. Members were impressed with the content of the report and asked that their congratulations be extended to all those concerned.

Yours sincerely

Zoë Wavell
Research Grants Co-ordinator
RNIB Health Services Unit



Royal National Institute for the Blind

224 Great Portland Street
London W1N 6AA
Telephone 071-388 1266 Fax 071-388 2034

Our Ref: ZW/jm

21 October 1992

Dr Erkan Mutlukan, BSc, MD
Tennent Institute of Ophthalmology
University of Glasgow
38 Church Street
Glasgow
G11 6NT.

Dear Dr Mutlukan

Re: RNIB Research Grant

Title: Computer Assisted Moving Eye Campimetry

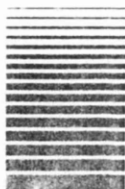
Thank you very much for your report on the above research project. When it met on 7 October our Prevention of Blindness Research Sub-committee was extremely impressed by the results you have achieved and have asked me to extend their congratulations to you.

Further to your letter of 31 August I am afraid that RNIB is unable to offer you any assistance with your travelling scholarship to Japan. I do hope you will be successful in finding funding from elsewhere and have a successful and enjoyable conference.

Yours sincerely

A handwritten signature in cursive script that reads 'Zoe Wavell'.

Zoe Wavell
Prevention of Blindness Development Officer
RNIB Health Services Unit



PATRONS: Her Majesty the Queen, Her Majesty Queen Elizabeth the Queen Mother
PRESIDENT: His Grace the Duke of Westminster DL
CHAIRMAN: John A Wall MA (Oxon)
VICE CHAIRMAN: Colin M Low MA
HON FINANCIAL ADVISER: The Rt Hon the Lord Catto
HON TREASURERS: A F Morton, Jack A Dunn FCIB
DIRECTOR GENERAL: Ian Bruce BSocSc FBIM
DIRECTOR OF FINANCE AND ADMINISTRATION: B T Gifford ACIS

Incorporated by Royal Charter. Registered in accordance with the National Assistance Act 1948 and the Charities Act 1960 Reg. No. 226227



The Royal Society of Medicine
1 Wimpole Street, London, W1M 8AE

Tel. 071 408 2119 Fax 071 355 3197

Erkan Mutlukan BSc MD
Tennent Institute of Ophthalmology
University of Glasgow
G11 6NT

30 June 1993

Dear Mr Mutlukan

Thank you for applying for an Ophthalmology Section Travelling Fellowship. I am delighted to let you know that the Council have decided to award you a fellowship of £500. Please find the cheque enclosed.

You may be asked to attend a Section meeting and report on your trip to Florida.

Yours sincerely

Mrs S Greshoff
SECTIONS OFFICER

THE W. H. ROSS FOUNDATION (Scotland)
FOR THE STUDY OF PREVENTION OF BLINDNESS

Chairman Advisory Committee
Dr J.F. CULLEN, F.R.C.S.

Reply to Secretary
43A HIGH STREET,
LINTHGHOW EH49 7ED
TELEPHONE: 0506 842736

Dr. Erkan Mutlukan
Tennent Institute of Ophthalmology
38 Church Street
Glasgow G11 6NT

3rd December 1991

Dear Dr. Mutlukan

I have pleasure in confirming the Trustees' approval for an award of £2,244 for your project 'The Dark Perimetric Stimulus in Detection of Visual Field Loss'.

Please let me know how you wish this to be paid.

Yours sincerely,

Margaret Millar
Margaret Millar
Secretary



IGA

International Glaucoma Association

KINGS COLLEGE HOSPITAL, DENMARK HILL, LONDON SE5 9RS ENGLAND

Telephone: 071-737 3265 or 071-274 6222 Ext. 2934 Registered Charity No.274681
Fax: 071-737 3265

Chairman: Ronald Pitts Crick FRCS
Association Secretary: Mrs Betsy Wright
Membership Secretary: John Wright ACP F.Col.P.

Patrons:
Sir John Wilson CBE
Lady Martin

20th August 1992.

Dr. Mutlukan,
Tennent Institute of Ophthalmology
University of Glasgow,
38 Church Street,
Glasgow
G.11. 6NT

Dear Dr. Mutlukan,

It was a pleasure to support your application for the I.G.A. Research Grant at the Glaucoma Group Grants Committee's recent meeting in Oxford and as you know it was successful.

A cheque for the £2,500 is enclosed at the request of Dr. Nagasubramanian, Secretary of the Glaucoma Group, with our congratulations. You are already aware of the general regulations regarding I.G.A. grants which we note with satisfaction you have always scrupulously observed. We shall follow the progress of your work with great interest.

Yours sincerely,

R. PITTS CRICK FRCS
CHAIRMAN



IGA

International Glaucoma Association

KINGS COLLEGE HOSPITAL, DENMARK HILL, LONDON SE5 9RS ENGLAND

Telephone: 071-737 3265 or 071-274 6222 Ext. 2934

Registered Charity No.274681

Fax: 071-737 3265

Chairman: Ronald Pitts Crick FRCS

Association Secretary: Mrs Betsy Wright

Membership Secretary: John Wright ACP F.Col.P.

Patrons:

Sir John Wilson CBE

Lady Martin

RPC/VG

11th March 1993

Dr E. Mutlukan
University of Glasgow
Tennent Institute of Ophthalmology
Western Infirmary
38 Church Street
Glasgow G11 6NT

Dear Dr Mutlukan

We are very pleased to assist you with a travel grant for the ARVO meeting and enclose our cheque.

I am sure A.N.N.S. will prove very useful for visual field assessment.

Should the organisers be willing for you to show some IGA literature at a table where participants will see it, as at the I.P.S. meeting in Kyoto, we should be most grateful both to you and to them.

With best wishes for an excellent meeting

Yours sincerely

MR R. PITTS CRICK FRCS
CHAIRMAN



INTERNATIONAL PERIMETRIC SOCIETY

August 7, 1992

Via FAX 041-339 7485

Erkan Mutlukan, MD
Research Fellow
Tennent Institute of Ophthalmology
38 Church Street
Glasgow G11 6NT
UNITED KINGDOM

Dear Dr. Mutlukan:

Congratulations. You have been selected as one of three recipients of an IPS travel grant in the amount of US \$1,000. In addition, your registration fee to the meeting will be waived. Please note that travel expenses in excess of US \$1,000 cannot be covered by the Society, nor can the costs of the optional social events at the meeting.

One or more of your abstracts has been accepted for the meeting. Notification of presentation as a paper or poster, and presentation time on the program are being sent by airmail to corresponding authors today.

By copy of this letter, I am notifying Dr. Fritz Dannheim, Treasurer of the IPS, who will be in contact with you regarding your preferred method of receiving this travel grant (e.g. bank transfer, cheque, currency type).

I look forward to seeing you in Kyoto.

Yours sincerely,

Richard P. Mills, MD
IPS Secretary

cc: Fritz Dannheim, MD
Yoshiaki Kitazawa, MD
Anders Heijl, MD

RPM/sc



UNIVERSITY
of
GLASGOW

Ext: 4238

AKS/AH/5.5/pg-schol

25 May 1993

Mr Erkan Mutlukan
3rd Year PhD Student
Department of Ophthalmology
Western Infirmary
Glasgow

Dear Mr Mutlukan

I am pleased to inform you that at the recent meeting of the Scholarships Committee you were awarded a travelling scholarship of £250.

A cheque will be sent to you at Medical Faculty Office in approximately two weeks from the date of this letter.

Yours sincerely

Mrs A K Spurway
Administrative Assistant

FACULTY OF MEDICINE

University of Glasgow, Glasgow G12 8QQ

Dean: Professor B. Whiting Clerk: Dr F. Miller

Administrative Assistants: Mrs A. K. Spurway (Higher Degrees) Ext 4238 Mrs J. Allan (Undergraduate) Ext 4239

Miss L. Blackwood (Undergraduate Admissions) Direct Line 041-330 4424

Telephone: 041-330 8855 Fax: 041-330 5440



UNIVERSITY
of
GLASGOW

Ext: 4238

AKS/AH

27 May 1992

Mr Erkan Mutlukan
Research Assistant
Department of Ophthalmology
Western Infirmary
Glasgow

Dear Mr Mutlukan

I am pleased to tell you that at the recent meeting of the Scholarship Committee you were awarded a travelling scholarship for £500.

A cheque will be sent to you at your Department shortly.

Yours sincerely

Mrs A K Spurway
Administrative Assistant

FACULTY OF MEDICINE

University of Glasgow, Glasgow G12 8QQ

Dean: Professor B. Whiting Clerk: Dr F. Miller

Administrative Assistants: Mrs A. K. Spurway (Higher Degrees) Ext 4238 Mrs J. Allan (Undergraduate) Ext 4239

Miss L. Blackwood (Undergraduate Admissions) Direct Line 041-330 4424

Telephone: 041-339 8855 Fax: 041-330 5440

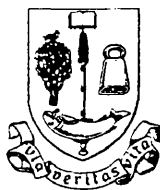
UNIVERSITY OF GLASGOW

Dean: Professor Donald Campbell, C.B.E.

Clerk: Fiona Miller. Ph.D.

Telephone: 041-339 8855

Telex: 777070 UNIGLA



Faculty of Medicine,
University of Glasgow
Glasgow G12 8QQ

Fax: 041-330 5440

Ext: 4238

AKS/AH

3 July 1991

Mr Erkan Mutlukan
c/o Department of Ophthalmology
Western Infirmary
Glasgow

Dear Mr Mutlukan

I am pleased to inform you that it has been agreed by the adjudicators that you be awarded the Dr Mary Hawthorne Prize for your essay.

The Senate Office is responsible for arranging payment of the prize (£300) and I have informed them today of the award. The essay should now be bound and lodged in the University archive.

May I add my congratulations to you on your success.

Yours sincerely

Handwritten signature of Mrs A K Spurway.

Mrs A K Spurway
Administrative Assistant

cc Professor C M Kirkness

UNIVERSITY OF GLASGOW

Serial no: 143

Senate Office
University of Glasgow
Glasgow G12 8QQ

July 18, 1991

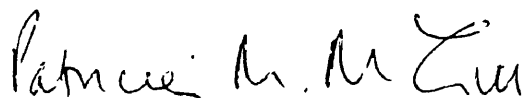
Dear Erkan Mutlukan

**MARY HAWTHORNE PRIZE
MEDICAL OPHTHALMOLOGY ESSAY - £ 300**

I am pleased to inform you that on the recommendation of the Senate, you have been granted the above-named award.

I am asked by the Senate to congratulate you on your success and to send a cheque for the amount of the award.

Yours sincerely



Miss Patricia M McGill
Clerk to the Senate Office

E. H. Webster
W. M. Christie
A. M. Donaldson
J. A. M. Cuthbert
A. J. Campbell
D. A. R. Ballantine

D. B. Reid
N. J. Mackenzie
I. C. Ferguson
S. G. Fraser
W. M. C. Grant
C. Dunbar

MITCHELLS ROBERTON

SOLICITORS

Consultants:
N.W. McMillan
R.Y. Henderson

Associates:
M.M. Inglis
I. Nicolson

George House, 36 North Hanover Street, Glasgow G1 2AD. Telephone: 041-552 3422 Facsimile: 041-552 2935 RE Box GW77.

1st Class

Dr E Mutlukan
Western Infirmary Eye Department
38 Church Street
Glsow G11 6NT

Our Ref: EHW MM-MCC00901

Your Ref:

15th September 1992

Dear Dr Mutlukan

William McCunn's Trust

We refer to your Application for a Travelling Scholarship to travel to the Xth International Perimetric Society Meeting in Japan in October. We are pleased to advise you that after consideration of your Application the Trustees have awarded you a grant of £250 towards your expenses.

We enclose herewith a receipt for £250 and on return of the signed receipt we shall forward our cheque.

Yours faithfully



enc



E. H. Webster
W. M. Christie
A. M. Donaldson
J. A. M. Cuthbert
A. J. Campbell
D. A. R. Ballantine

D. B. Reid
N. J. Mackenzie
I. C. Ferguson
S. G. Fraser
W. M. C. Grant
C. Dunbar

MITCHELLS ROBERTON

SOLICITORS

Consultants:
N.W. McMillan
R.Y. Henderson

Associates:
M.M. Inglis
I. Nicolson

George House, 36 North Hanover Street, Glasgow G1 2AD. Telephone: 041-552 3422 Facsimile: 041-552 2935 RE Box GW77.

1st Class

Dr Erkan Mutlukan
Tennent Institute of Ophthalmology
38 Church Street
Glasgow G11 6NT

Our Ref: EHW MM-MCC00901

Your Ref:

6th March 1992

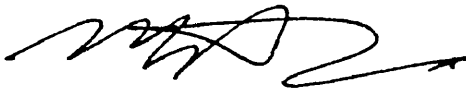
Dr Dr Mutlukan

William McCunn's Trust

We refer to your Application for a Travelling Scholarship to present papers at the IXth Congress of the European Society of Ophthalmology, Brussels, Belgium. We are pleased to advise you that after consideration of your Application the Trustees have awarded you a grant of £300 towards your expenses.

We enclose herewith a receipt for £300 and on return of the signed receipt we shall forward our cheque.

Yours faithfully

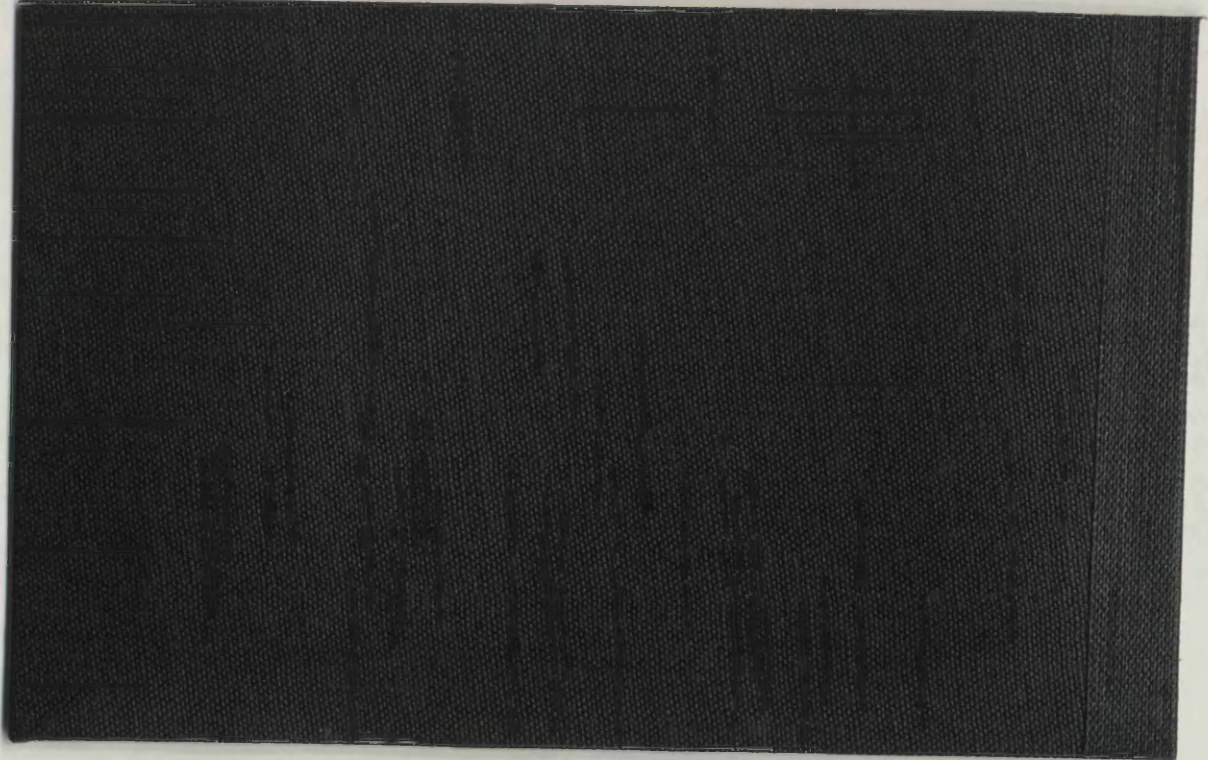


enc

Please be aware that computer discs which are used in several machines run a high risk of corruption, especially as a result of infection by a virus. You are strongly recommended, if you intend to use the disc(s) enclosed, to ensure that your computer is protected with appropriate software for the detection of known viruses, and for the repair of damage they may cause.

Please refer any problems to the Library Enquiry Desk (ext 6704/5).

GUL 96.40



GLASGOW
UNIVERSITY
LIBRARY



30114006317187